

HYDROCLIMATIC VARIABILITY IN NORTHEAST TURKEY: IDENTIFYING
CLIMATE AND RIVER FLOW DYNAMICS AND CONTROLS

by

FAIZE SARIŞ

A thesis submitted to The University of Birmingham for the degree of DOCTOR OF
PHILOSOPHY

School of Geography, Earth and Environmental Sciences

College of Life and Environmental Sciences

The University of Birmingham

July 2011

UNIVERSITY OF
BIRMINGHAM

University of Birmingham Research Archive

e-theses repository

This unpublished thesis/dissertation is copyright of the author and/or third parties. The intellectual property rights of the author or third parties in respect of this work are as defined by The Copyright Designs and Patents Act 1988 or as modified by any successor legislation.

Any use made of information contained in this thesis/dissertation must be in accordance with that legislation and must be properly acknowledged. Further distribution or reproduction in any format is prohibited without the permission of the copyright holder.

ABSTRACT

The East Black Sea (EBS) and the Çoruh River basins (ÇRB) of northeast Turkey have a number of challenging water related issues of socio-economic and ecological importance. This PhD thesis aims to understand hydroclimatological variability across Turkey taking a large-scale perspective by defining precipitation regimes and extremes and then focussing on the climatic and basin drivers of river flow variability in northeast Turkey region. At the national-scale, Turkey exhibits six precipitation regime regions of which three characterise northeast region. The northeast and southwest coastal regions of Turkey are characterised by the highest frequency of extreme precipitation events. The mountainous area of the EBS is defined by May-June Peak river flow regime, while ÇRB is characterised by April-May Peak flow regime. Intra-annual variability in the timing of river flow over northeast Turkey is controlled mainly by the regional climatic variability. Spring rainfall maxima together with the contribution of snowmelt generate high river flow amounts for the ÇRB. The May-June river flow peak in the EBS is linked to snowmelt. Important changes are detected in temperature extremes, also in precipitation and river flow for some cases. Regional precipitation and temperatures for September-May period have an important influence on river flow extremes. Temperature variability across northeast Turkey is closely linked to seasonal indices of East-North Atlantic teleconnection patterns, especially during winter and the significant results demonstrate a spatially coherent pattern across the region. This study provides important new data for the assessment of management of available water resources as well as future water resource stress.

ACKNOWLEDGEMENTS

I would like to thank the following persons and institutions that contributed to make this PhD study become true:

I sincerely thank my supervisors, Dr. David M. Hannah and Dr. Warren J. Eastwood (from School of Geography, Earth and Environmental Sciences (GEES) at the University of Birmingham) for their continual guidance, careful supervision, support and friendship throughout my PhD. They were always encouraging me and gave fruitful ideas and suggestions on my work. I also thank to my external supervisor Prof. Hafzullah Aksoy (from Department of Civil Engineering at the Istanbul Technical University (ITU)) for his valuable advices on my work and guidance for getting data.

I am grateful to the Higher Education Council of Turkey and the Çanakkale Onsekiz Mart University (ÇOMU) for the financial support during the last four years and for the opportunity that I was funded to do my PhD at the University of Birmingham.

I acknowledge the following institutions that provided data used in this study: Department of Geography at ÇOMU for kindly providing the precipitation data, the State Meteorological Service at Ankara for providing all daily meteorological datasets for northeast region of Turkey, and local offices of the State Hydraulic Works and the Electrical Power Resources Survey and Development Administration (in Trabzon, Rize, Artvin, Gümüşhane and Erzincan) for sharing the local information of stations. I am also grateful to Selami Yıldırım for providing metadata of meteorology stations and explaining the procedure for data quality assessment, and Dr. Ebru Eriş (Department of Civil Engineering, ITU) for kindly sharing river flow data of her PhD project. GEES and ÇOMU are thanked for providing some financial support to get river flow data. Digital land use data were provided from Geographical Information Systems (GIS) Department of Ministry of Environment and Forest

at Ankara. Dr. Cengiz Akbulak (Department of Geography, ÇOMU) is thanked for his efforts on getting this data and guidance to use it.

A travel grant was provided from British Institute of Archaeology at Ankara (BIAA) for the fieldwork in northeast Turkey between 26 July and 06 August 2008. The “*Climate, vegetation and landscape change in northern Turkey: a multi-indicator approach from coupled lake/peat and speleothem records*” project which was granted by BIAA and led by Dr. Warren J. Eastwood greatly supported this fieldwork and also given financial support to contribute obtaining the river flow data. I am very thankful to the project team for their collaboration in order to achieve this fieldwork. I am also thankful to the BIA at Ankara for the logistic support while we were in Turkey.

Kevin Burkhill and Anne Ankcorn (GEES, University of Birmingham) are thanked for cartographic assistance. I sincerely thank to Çetin Şenkul (Department of Geography, Afyon Kocatepe University) and Cihan Bayrakdar (Department of Geography, Istanbul University) for their invaluable contributions on the GIS work of this study.

I am very thankful to my friends and my beloved family for their infinite support during the last four years.

TABLE OF CONTENTS

LIST OF ILLUSTRATIONS

LIST OF TABLES

LIST OF ABBREVIATIONS

| | |
|--|----|
| 1. INTRODUCTION | 1 |
| 1.1. Problem and research gap..... | 1 |
| 1.2. Aim and objectives..... | 4 |
| 1.3. Thesis structure | 6 |
| 1.4. Chapter summary | 7 |
| 2. LITERATURE REVIEW..... | 8 |
| 2.1. Hydroclimatological research context: links and space-time dynamics | 8 |
| 2.2. Hydroclimatic research in Turkey..... | 12 |
| 2.2.1. Climatic variability and changes in Turkey..... | 14 |
| 2.2.2. Climatic variations linked to atmospheric patterns..... | 17 |
| 2.2.3. River flow variability in Turkey and links to climate | 19 |
| 2.3. Chapter Summary..... | 23 |
| 3. RESEARCH DESIGN, DATA AND METHODS..... | 24 |
| 3.1. Research Design..... | 24 |
| 3.2. Data | 25 |
| 3.3. Methods approaches..... | 31 |
| 3.4. Chapter summary | 40 |
| 4. SPATIAL VARIABILITY OF PRECIPITATION REGIMES OVER TURKEY..... | 42 |
| 4.1. Introduction..... | 42 |
| 4.2. Study area | 45 |
| 4.3. Data and methodology..... | 47 |
| 4.3.1. Precipitation data..... | 47 |
| 4.3.2. Regime classification methodology | 48 |
| 4.4. Results and discussions | 50 |
| 4.4.1. Precipitation regime shape..... | 50 |
| 4.4.2. Precipitation regime magnitude | 55 |
| 4.4.3. Composite (shape and magnitude) precipitation regimes..... | 58 |
| 4.5. Conclusion | 61 |
| 4.6. Chapter summary | 64 |
| 5. LONG-TERM TRENDS IN PRECIPITATION EXTREMES ACROSS TURKEY (1963-2002) | 65 |
| 5.1. Introduction..... | 65 |
| 5.2. Data and methods..... | 68 |
| 5.2.1. Precipitation data..... | 68 |
| 5.2.2. Methods | 69 |
| 5.2.2.1. Extreme indices calculations | 69 |
| 5.2.2.2. Cluster analysis | 70 |
| 5.2.2.3. Mann-Kendall rank correlation..... | 71 |
| 5.3. Patterns in precipitation extremes | 72 |
| 5.3.1. Seasonality and magnitude characteristics of precipitation extremes..... | 72 |
| 5.3.2. Extremely heavy precipitation days | 75 |
| 5.3.3. Regional characteristics of precipitation extremes..... | 76 |
| 5.4. Trend analysis..... | 78 |

| | |
|--|-----|
| 5.4.1. Trends in precipitation extremes..... | 78 |
| 5.4.2. Trends precipitation percentiles..... | 78 |
| 5.4.3. Inter-annual fluctuations and change points..... | 82 |
| 5.5. Discussion and conclusion..... | 83 |
| 5.6. Chapter summary..... | 86 |
| 6. DEFINING CLIMATIC REGIONS AND VARIABILITY IN NORTHEAST TURKEY (1981-2007)..... | 87 |
| 6.1. Introduction..... | 87 |
| 6.1.1. Background on eastern Mediterranean and Turkish climate..... | 90 |
| 6.2. Study area and data..... | 92 |
| 6.2.1. Data..... | 94 |
| 6.3. Methods..... | 97 |
| 6.3.1. Climate regime classification..... | 98 |
| 6.3.2. Water budget calculations..... | 99 |
| 6.3.3. Time series analysis..... | 100 |
| 6.4. Results..... | 102 |
| 6.4.1. Climate regimes regions of northeast Turkey..... | 102 |
| 6.4.2. Annual water balance and climate types..... | 106 |
| 6.4.3. Temporal variability of climate series..... | 109 |
| 6.5. Discussion and conclusion..... | 112 |
| 6.6. Chapter summary..... | 115 |
| 7. RIVER FLOW REGIMES OF NORTHEAST TURKEY: SPACE-TIME VARIABILITY AND LINKS WITH LOCAL CLIMATE..... | 116 |
| 7.1. Introduction..... | 116 |
| 7.2. Study area and data..... | 121 |
| 7.2.1. Study area..... | 121 |
| 7.2.1.1. East Black Sea Basin..... | 121 |
| 7.2.1.2. Çoruh River Basin..... | 123 |
| 7.2.1.3. Climate and vegetation..... | 124 |
| 7.2.1.4. Land use properties and changes..... | 125 |
| 7.2.2. Data..... | 128 |
| 7.3. Methods..... | 134 |
| 7.3.1. Cluster analysis..... | 134 |
| 7.3.2. Homogeneity and trend tests..... | 135 |
| 7.3.3. Multiple linear regression..... | 136 |
| 7.4. Results and discussion..... | 137 |
| 7.4.1. River flow regimes..... | 137 |
| 7.4.1.1. Flow regime shape..... | 137 |
| 7.4.1.2. Flow regime magnitude..... | 141 |
| 7.4.1.3. Regime stability (year-to-year regime dynamics)..... | 145 |
| 7.4.2. Temporal variability of river flows..... | 149 |
| 7.4.3. Relationship between seasonal river flow and regional climate..... | 151 |
| 7.5. Conclusion..... | 156 |
| 7.6. Chapter summary..... | 159 |
| 8. DETECTING CHANGING FREQUENCY AND LONG-TERM TRENDS IN PRECIPITATION, TEMPERATURE AND RIVER FLOW EXTREMES FOR NORTHEAST TURKEY..... | 160 |
| 8.1. Introduction..... | 160 |

| | |
|---|-----|
| 8.2. Data and study area | 165 |
| 8.2.1. Data sets..... | 165 |
| 8.2.2. Study area | 166 |
| 8.3. Methods | 168 |
| 8.3.1. Extreme indices calculations..... | 168 |
| 8.3.2. Trend test | 168 |
| 8.3.3. Multiple linear regression | 170 |
| 8.4. Results and discussion..... | 171 |
| 8.4.1. Spatial patterns in river flow, precipitation and temperature extremes..... | 171 |
| 8.4.2. Long-term trends in precipitation, temperature and river flow extreme events | 174 |
| 8.4.3. Assessing the influence of climatic variability on frequency of extreme events | 183 |
| 8.5. Conclusion | 189 |
| 8.6. Chapter summary | 191 |
| 9. TELECONNECTION AND SURFACE HYDROCLIMATOLOGY OF NORTHEAST TURKEY | 192 |
| 9.1. Introduction..... | 192 |
| 9.2. Study area | 199 |
| 9.2.1. Temperature, precipitation and river flow characteristics of the study basins | 199 |
| 9.3. Data | 200 |
| 9.4. Method..... | 204 |
| 9.4.1. Pearson's correlation | 204 |
| 9.5. Results and discussion..... | 205 |
| 9.5.1. Relationship between the teleconnection indices and temperature..... | 206 |
| 9.5.2. Relationship between the teleconnection indices and precipitation..... | 211 |
| 9.5.3. Relationship between the teleconnection indices and river flow | 216 |
| 9.6. Conclusion | 218 |
| 9.7. Chapter summary | 220 |
| 10. SYNTHESIS AND FURTHER RESEARCH..... | 221 |
| 10.1. Key conclusions | 221 |
| 10.2. Implications | 224 |
| 10.3. Recommendations for further research | 225 |

APPENDIX I: *Hydrological Sciences Journal* paper

APPENDIX II: *Hydrological Sciences Journal Red Book* paper

APPENDIX III: *Selected photographs of river gauging stations over the East Black Sea Basin*

APPENDIX IV: *Selected photographs of river gauging stations over the Çoruh River Basin*

LIST OF REFERENCES

LIST OF ILLUSTRATIONS

| | |
|--|----|
| Figure 1.1: Northeast region of Turkey | 2 |
| Figure 3.1: A schematic illustration to conceptualize the scope of the thesis | 25 |
| Figure 3.2: Selected meteorological monitoring stations located in northeast Turkey | 26 |
| Figure 3.3: Changing in the number of (opened-O and closed-C) river gauging stations in northeast Turkey region | 29 |
| Figure 3.4: Selected river gauging stations | 31 |
| Figure 4.1: Maps of the previous climate regions from other studies..... | 44 |
| Figure 4.2: Major geographic regions and elevation of Turkey | 45 |
| Figure 4.3: Schematic diagram of air masses influencing winter and summer climate of the eastern Mediterranean region..... | 47 |
| Figure 4.4: Standardized (z -scores) monthly values for all stations within the precipitation regime shape regimes | 50 |
| Figure 4.5: Spatial distribution of precipitation regime shape across Turkey..... | 51 |
| Figure 4.6: Summary of spatial patterns for (a) shape, (b) magnitude, and (c) composite regimes across Turkey | 53 |
| Figure 4.7: Spatial distribution of precipitation magnitude regimes across Turkey.... | 56 |
| Figure 4.8: Spatial distribution of composite (shape and magnitude) precipitation regimes across Turkey | 59 |
| Figure 4.9: Simplification of precipitation regimes of Turkey into coastal, transitional and inland regions..... | 60 |
| Figure 5.1: Intra-annual variability in percentage of moderate wet (R75), very wet (R95) and extremely wet days (R99) among the precipitation regime regions..... | 72 |
| Figure 5.2: Box and Whiskers plots of precipitation regime regions for extreme precipitation threshold values..... | 74 |
| Figure 5.3: The intra-annual variability of the extremely heavy precipitation events. | 76 |
| Figure 5.4: Spatial distribution of extreme precipitation magnitude regime classes across Turkey..... | 77 |
| Figure 5.5: Spatial distribution of the long-term trends of annual precipitation extremes across the Turkey: (a) R75, (b) R95 and (c) R99 | 80 |
| Figure 5.6: Spatial distribution of the long-term trends of annual precipitation percentiles across the Turkey: (a) P75, (b) P95 and (c) P99 | 81 |
| Figure 5.7: Year to year variations (—◆—) in annual precipitation for 75% percentile series at selected representative stations of precipitation regime regions..... | 83 |
| Figure 6.1: Basic characteristics of study area and locations of meteorological stations | 89 |
| Figure 6.2: Flow chart illustrating the approach for regime classification procedure . | 99 |

| | |
|--|-----|
| Figure 6.3: Annual climate regime classification map..... | 101 |
| Figure 6.4: Line plots illustrating seasonality of climate variables (Lines are defined as; (A:-■-) Bayburt, Gümüşhane, Ispir, Oltu and Tortum; (B:-▲-) Giresun, Akçaabat; Trabzon and Artvin; (C:-●-) Rize, Hopa and Pazar) | 103 |
| Figure 6.5: Box plots illustrating variability in magnitude of climate variables | 104 |
| Figure 6.6: Graphs illustrating annual water balance in selected stations..... | 108 |
| Figure 6.7: Spatial variability of the significant increasing trends for temperature series observed the period between July and October..... | 110 |
| Figure 6.8: Year by year deviations from average temperature series at 75 th percentile for August series of coastal stations | 112 |
| Figure 7.1: Physiographic (a) and river network (b) maps of study area..... | 120 |
| Figure 7.2: Geological characteristics of the northeast Turkey | 122 |
| Figure 7.3: Slope characteristics of the northeast Turkey | 123 |
| Figure 7.4: Land cover map of the study area for 2006 | 127 |
| Figure 7.5: Basin delineation map of the study area (a) and location of the stations (b) | 131 |
| Figure 7.6: Standardized long-term regimes for all stations within each of the river flow shape class | 138 |
| Figure 7.7: Box and Whiskers plots of station mean and maximum river flow for magnitude classes of long (a,b) and short (c,d) classifications | 143 |
| Figure 7.8: Spatial distribution of stations within river flow regime shape classes .. | 144 |
| Figure 7.9: Interannual regime variability: Standardized average regimes of all station-years within each shape class for annual river flow | 145 |
| Figure 7.10: Box-plots showing the stability of regime shape and regime sequencing at stations (a) number of regime classes, (b) number of regime couplets | 147 |
| Figure 7.11: Basin frequencies of flow regime shape and magnitude | 148 |
| Figure 7.12: Seasonal composite river flow, precipitation and temperature..... | 155 |
| Figure 8.1: Location of stations evaluated for extreme analyses..... | 164 |
| Figure 8.2: Sample magnitude characteristics of selected annual extremes | 172 |
| Figure 8.3: Results of M-K test for seasonal river flow and precipitation percentiles | 179 |
| Figure 8.4: Results of M-K test for spring-summer precipitation and temperature percentiles..... | 180 |
| Figure 8.5: Results of M-K test for summer-autumn precipitation and temperature percentiles..... | 181 |
| Figure 8.6: Seasonal composite river flow, precipitation and temperature percentile series for selected stations of the ÇRB | 187 |
| Figure 8.7-1: Seasonal composite river flow, precipitation and temperature percentile series for selected stations of the EBS Basin | 188 |

| | |
|---|-----|
| Figure 8.7-2: Seasonal composite river flow, precipitation and temperature percentile series for selected stations for the EBS Basin | 189 |
| Figure 9.1: Location of stations evaluated for teleconnection analyses..... | 197 |
| Figure 9.2: Annual temperature, precipitation and river flow regime characteristics | 198 |
| Figure 9.3: Comparison of time series for the annual value of the NAO, EA, EA/WR, POL and SCAND indices..... | 203 |
| Figure 9.4: Year by year departures in standardized index values and temperature series for selected stations showing the correlation between seasonal temperature and the EA and EA/WR patterns | 207 |
| Figure 9.5: Associations between seasonal temperature and various large-scale atmospheric patterns | 209 |
| Figure 9.6: Year by year departures in standardized index values and river flow series at selected stations showing the correlation between seasonal precipitation-river flow and EA/WR, EA and POL patterns..... | 213 |
| Figure 9.7: Associations between seasonal precipitation and various large-scale atmospheric patterns | 214 |
| Figure 9.8: Associations between seasonal river flow and various large-scale atmospheric patterns | 215 |

LIST OF TABLES

| | |
|---|-----|
| Table 3.1: List of obtained meteorological from DMI for northeast Turkey | 27 |
| Table 3.2: Basic information on available river gauging stations across the northeast Turkey | 30 |
| Table 4.1: Metadata of selected precipitation stations across Turkey | 48 |
| Table 4.2: Precipitation regime shape class frequencies in the main geographical regions | 52 |
| Table 4.3: Average values of precipitation indices for stations within the five regime magnitude classes | 55 |
| Table 4.4: Precipitation regime magnitude class frequencies in the main geographical regions | 55 |
| Table 4.5: Precipitation regime composite class frequencies in the main geographical regions | 58 |
| Table 5.1: Definitions of the indices used for identifying precipitation extremes..... | 70 |
| Table 5.2: The percentage of events defined with extremely heavy precipitation amounts | 75 |
| Table 5.3: Average values of thresholds for extreme precipitation indices within the four regime magnitude classes..... | 77 |
| Table 5.4: Results of trend analysis for extreme precipitation indices among the precipitation regime regions | 79 |
| Table 5.5: Results of trend analysis for precipitation percentile amounts among the precipitation regime regions | 79 |
| Table 6.1: Long-term averages of meteorological variables for selected stations | 94 |
| Table 6.2: Percentages of significant results obtained from K-W (a), runs (b) and M-K (c) tests for monthly series of meteorological variables | 96 |
| Table 6.3: Shape, magnitude and composite climate regime classification results... | 101 |
| Table 6.4: Climate type classification of northeast Turkey stations according to Thornthwaite method based on moisture index..... | 106 |
| Table 6.5: Percentages of significant results showing the increasing trends for monthly temperature percentile series | 111 |
| Table 7.1: Main hydrological characteristics of river gauging stations (A, B) and basic climatic information of meteorological stations (C) evaluated in this chapter | 130 |
| Table 7.2: Average values for the runoff indices for all basins within the flow regime magnitude classes | 142 |
| Table 7.3: Inter-annual regime (a) magnitude and (b) shape variability for river flow | 146 |
| Table 7.4: Results of trend test: summarizing table for monthly flows (a), test statistics of selected stations (b) and seasonal river flow series (c)..... | 150 |

| | |
|--|-----|
| Table 7.5: Significant results of MLR analysis | 152 |
| Table 8.1: Main properties of climate and river gauging stations selected for analysis | 165 |
| Table 8.2: Definitions of selected extreme indices..... | 169 |
| Table 8.3: Annual extreme threshold values of stations | 170 |
| Table 8.4: Proportion of significant trends detected in annual extremes..... | 174 |
| Table 8.5: Proportion of significant trends detected in seasonal extremes | 177 |
| Table 8.6: Results of regression analysis for ÇRB | 183 |
| Table 8.7: Results of regression analysis for EBS Basin..... | 185 |
| Table 9.1: Basic information about data source used in correlation analysis | 200 |
| Table 9.2: List and definitions of evaluated atmospheric patterns | 201 |
| Table 9.3: Percentage of significant correlation results detected for monthly relationships..... | 205 |
| Table 9.4: Percentage of significant correlation results detected for monthly relationships..... | 210 |

LIST OF ABBREVIATIONS

| | | |
|--------|---|--|
| AFPU | : | Artvin Forest Planning Unit |
| AOI | : | Arctic Oscillation Index |
| CA | : | Cluster Analysis |
| CLIVAR | : | Climate Variability And Predictability |
| CPC | : | Climate Prediction Center |
| cP | : | Continental Polar Air Mass |
| cT | : | Continental Tropical Air Mass |
| ÇRB | | Çoruh River Basin |
| DEM | : | Digital Elevation Model |
| DFA | : | Discriminant Function Analysis |
| DMI | : | Turkish State Meteorological Service (Turkish) |
| DSI | : | State Hydraulic Works (Turkish) |
| DTR | : | Diurnal Temperature Ranges |
| EA | : | East Atlantic Pattern |
| EA/WR | : | East Atlantic/Western Russia Pattern |
| EBS | : | East Black Sea |
| ECHAM4 | : | European Center HAMburg 4 |
| EIE | : | Electrical Power Resources Survey And Development Administration (Turkish) |
| ENSO | : | El Niño Southern Oscillation |
| GIS | : | Geographical Information Systems |
| GPS | : | Global Positioning System |
| HadCM3 | : | Hadley Centre Coupled Model, Version 3 |
| IPCC | : | Intergovernmental Panel on Climate Change |
| K-W | : | Kruskal-Wallis Test |
| M-K | : | Mann-Kendall Rank Correlation Test |
| MLR | : | Multiple Linear Regression |
| MoEF | : | Ministry of Environment and Forestry |
| mP | : | Marine Polar Air Mass |
| mT | : | Marine Tropical Air Mass |
| NAO | : | North Atlantic Oscillation |
| NAOI | : | North Atlantic Oscillation Index |

| | | |
|---------|---|--|
| NCAR | : | National Center For Atmospheric Research |
| NCEP | : | National Center For Environmental Prediction |
| NOAA | : | National Oceanic And Atmospheric Administration |
| PC | : | Principal Component |
| POL | : | Polar/Eurasia Pattern |
| RPCA | : | Rotated Principal Components Analysis |
| SCAND | : | Scandinavia Pattern |
| SHI | : | Surface Humidity Index |
| SI | : | Sensitivity Index |
| SO | : | Southern Oscillation |
| SST | : | Sea Surface Temperature |
| TAR | : | Third Assessment Report |
| WMO | : | World Meteorological Organisation |
| WMO-CCL | : | World Meteorological Organization–Commission For Climatology |

1. INTRODUCTION

1.1. Problem and research gap

Water is the most important natural source for humanity due to its crucial role in the sustainability of life (World Water Assessment Programme, 2009). In addition to this, water is also a resource with critical importance of providing energy, food and other resources for societies. Due to increasing energy demands, hydroelectric is a clean and alternative energy resource for some countries, although most hydroelectric schemes have some environmental implications. Turkey is one such country that has a considerable number of hydroelectric power units (Akpınar and Komurcu, 2011); however, there are still many gaps in the current knowledge and understanding of the effect of hydroelectric schemes on river ecosystems, regional river flow regimes together with the intra-annual and year to year variability of regional and local climates. Protecting the ecological variability of aquatic ecosystems as well as attempts to mitigate the effects and impacts of anthropogenic pressures on freshwater environments are some of the goals associated with the European Water Framework Directive to which Turkey has a draft plan for implementation of this directive (Sümer, 2011).

The northeast region of Turkey is characterised by relatively high annual precipitation totals and river flow (Atalay and Mortan, 2003); and it is a mountainous region with high ecological status (Berkun, 2010). This mountainous region is of prime interest to the energy sector; however, the ecological richness of this region must be protected and water resources must be exploited sustainably.

Mountainous regions exhibit many different climate types, thus support many different ecosystems and have among the highest species richness at a global scale (*Fourth Assessment Report, FAR*). The FAR identified mountain regions as having experienced above-average warming during the 20th century: a trend that is likely to continue (Fischlin *et al.*, 2007). Related impacts include an earlier and shortened snow-melt period, with more rapid water release and possible downstream flooding which, in combination with reduced glacier extent, could cause water shortage during the growing season (Fischlin *et al.*, 2007).

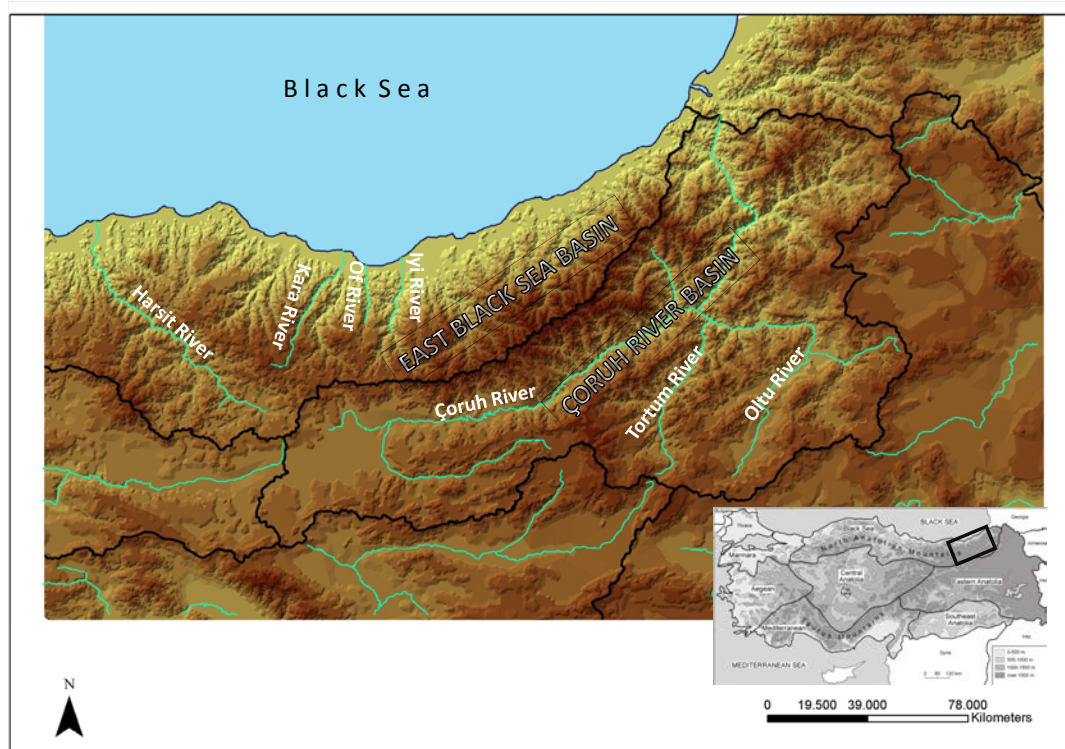


Figure 1.1 Northeast region of Turkey.

Predictions for warming trends in subtropical zones, where Turkey is located, are between 1-2 C° for 1900-2050 (Türkeş, 2003b), together with the increases in the length and intensity of warmer and drier periods. The most important impact of predicted changes in temperature increases is an increase in flood events in terms of the melting of permanent snow fields and glaciers in mountain regions, such as northeast Turkey. In fact, the existence of mountain

glaciers together with considerable amounts of precipitation in the form of snow suggests that the northeast region of Turkey is vulnerable to the climatic changes. This region comprised two major basins namely the East Black Sea Basin (EBS, located to the north side of the Black Sea Mountains) and the Çoruh River Basin (ÇRB, located to the south) (Figure 1.1). Indeed, there is a pressing need to research the regional hydroclimatology because the consequences of the variable climatic conditions are most likely to have an adverse effect on water resources and hence the socio-economy of the region, with Turkey-wide repercussion (Türkeş, 2010).

Since 1995 the number of research studies that have focused on the climatology and hydrology of Turkey has increased markedly (See Section 2.2); although these studies have generally focused on the hydroclimatology of Turkey at a national scale (e.g. Türkeş 1996, 1998, Türkeş *et al.*, 2009; Kadioglu 2000, Kahya *et al.*, 2008a, 2008b; Kalayci and Kahya 2006). Generally, these climatological and hydrological studies have employed statistical modelling techniques to analyse the nature and magnitude of the trends in the time series. Some of these studies also have investigated possible relationships with different atmospheric patterns and have attempted to explain important linkages with Northern Hemisphere teleconnection patterns. However, simulation models for Turkey neither adequately explain local variability nor can they be applied at regional or local (river basin) scales, especially for large, diverse regions such as northeastern Turkey (Tatli *et al.*, 2004). Very few climatology (Reis, 2008) or hydrology (Aksoy *et al.*, 2006) studies have been undertaken for northeast Turkey, although some studies have begun to assess the hydropower potential of river basins in northeast Turkey (Akpınar *et al.*, 2009, 2011).

Thus, previous studies yielded much needed information on the broad scale, national characteristics of climatology and hydrology in Turkey. But there is a paucity of regional scale studies to increase the knowledge and understanding of sub-regional and basin scale hydroclimatological changes in Turkey. Indeed, there is not any previous research identifying hydroclimatological variability across the northeast Turkey region. Hence, important research gaps exist for hydroclimatology research in this region:

- 1) The climate and river flow regimes of northeast Turkey have not been characterised systematically across the region.
- 2) There is a lack of knowledge on the spatiotemporal variability of hydroclimatological extremes across the region.
- 3) There is a lack of knowledge on the impact of Northern Hemisphere (Atlantic/Eurasian) teleconnection patterns on the temperature, precipitation and river flow of northeast Turkey.

It is crucial to increase the knowledge and understanding of the finer-scale intricacies of the influence that climate variability has on river flow in northeast Turkey. Research into regional hydroclimatology will help to establish the key processes causing hydroclimatological change in northeast Turkey, and identify key factors of variability, to detect similarities in response among stations, and to contribute to sustainable management of freshwaters in the context of climate change and variability.

1.2. Aim and objectives

This thesis aims to undertake the first comprehensive research on the hydroclimatology of northeast Turkey within a large perspective that examines precipitation, temperature and river flow interactions in the two major basins of northeast Turkey (East Black Sea Basin (EBS) and Çoruh River Basin (ÇRB)).

A variety of methods are employed to analyse variability in climate and river flow, trends and driving factors and thus, achieve a robust explanation of regional and intra-regional hydroclimatic variability of northeast Turkey. Prior to regional scale analyses and assessment, the precipitation regime regions and extreme precipitation variability over the whole Turkey will also be explained (Chapter 4 and 5). These significant contributions to precipitation climatology knowledge of Turkey support the hypotheses of this thesis claiming that northeast Turkey has a specific and unique hydroclimatological character and so it must be investigated by using more comprehensive data network. To achieve the research aim and address the key research gaps the objectives of this thesis are:

- 1) To redefine the precipitation regime regions across Turkey by characterizing the intra-annual precipitation behaviour and annual precipitation characteristics (Chapter 4).
- 2) To define spatiotemporal variability in precipitation extremes by analysing extreme wet days and high precipitation totals for Turkey (Chapter 5).
- 3) To identify climate regime characteristics of northeast Turkey and to examine long-term (inter-annual) trends in climatological variables (Chapter 6).
- 4) To classify river flow regimes considering their seasonality (shape), size (magnitude) and year to year stability; and to quantify driving climatic factors on river flow variability over northeast Turkey (Chapter 7).
- 5) To define temperature, precipitation and river flow extreme characteristics of northeast Turkey, observed trends in calculated extreme series and quantify the regional climate impact on river flow extremes (Chapter 8).
- 6) To elucidate the teleconnections between surface hydroclimatology (temperature, precipitation and river flow) of northeast Turkey and North/East Atlantic atmospheric oscillations (Atlantic/Eurasia part of Northern Hemisphere indices) (Chapter 9).

1.3. Thesis structure

This thesis contains ten chapters which are organised as follows:

- Chapter 1 (this chapter) provides a brief overview on the research context and outlines the research problem, motivation, research gaps, the aim and objectives of the thesis.
- Chapter 2 provides the evidence base and overarching research rationale for the thesis by literature review.
- Chapter 3 outlines the overall research design of the thesis. A discussion of common data sources, data selection procedure and an outline of methods applied are provided.
- Chapter 4 provides a new classification approach for Turkish annual precipitation regimes and redefines precipitation regions across Turkey within a large-scale perspective by interpreting the emergent precipitation regime regions based on regional atmospheric circulation and the main physiographic features modifying precipitation climatology. This chapter has been published in Hydrological Sciences Journal (2010:55/2) and a copy of the paper is provided in the Appendices (Appendix I).
- Chapter 5 identifies the spatiotemporal variability in precipitation extremes across Turkey by elucidating extreme precipitation magnitude and timing characteristics and detecting year by year trends and highlighting significant change points of extreme precipitation time series.
- Chapter 6 characterises systematically the climatology of northeast Turkey. The climatic regimes and time-based changes for five climate component are analysed. This chapter provides new fundamental knowledge on the climate of northeast Turkey and yields a framework for subsequent climate-related analyses.
- Chapter 7 identifies variability in river flow regimes, and trends in monthly and seasonal (minimum, mean and maximum) flow series for northeast Turkey. The role of regional climate controls and basin properties on river flow are investigated. This chapter concludes

by synthesising climate and land use changes with variability in river flow regimes across the region.

- Chapter 8 discusses the observed variability in extreme temperature, precipitation and river flow events across northeast Turkey. Extreme event characteristics based on specific indices are defined, trends in calculated extreme temperature, precipitation and river flow time series are detected and, finally, the role of precipitation and temperature on extreme river flow character are quantified.
- Chapter 9 elucidates the connections between Northern Hemisphere teleconnection indices and surface hydroclimatic components (monthly and seasonal temperature, precipitation and river flow series) over northeast Turkey by analysing the magnitude and nature of the association and establishing the regional and/or basin scale influence of atmospheric oscillations. Preliminary result of this chapter has subsequently been published in IAHS Red Book (2010:340) and a copy of the paper is provided in the Appendices (Appendix II).
- Chapter 10 concludes by drawing together the key findings of this research and making suggestions for further research. Notably, synthesis across chapters is given to demonstrate how the main elements of each data chapter fit together and to show how research objectives were achieved.

1.4. Chapter summary

This chapter has provided background on the hydroclimatological research context for this thesis. The need for a climate-hydrology research in northeast Turkey has been explained and yields rationale for the aim of this PhD research. The research gaps and the objectives to address have been justified and stated. Chapter 2 provides the literature review which explains the hydroclimatology of Turkey and develops further the research rationale.

2. LITERATURE REVIEW

This chapter undertakes a literature review to identify research gaps for investigation. The review is split into two parts: (i) a summary of the international hydroclimatological research context and (ii) hydroclimatological research in Turkey, particularly climate and river flow relationships. The chapter ends by presenting the research gaps identified and the corresponding objectives to be addressed in the thesis.

2.1. Hydroclimatological research context: links and space-time dynamics

Hydrological systems are vulnerable to climatic changes and are affected by a range of processes that include fluctuations in the volume, timing and intensity of river flow, the type of precipitation (whether it falls as snow or rain) and the timing and intensity of snowmelt (Kundzewicz *et al.*, 2007). Data reflecting these key components need to be collated, analysed and evaluated in order to more fully understand the main characteristics of the hydroclimatology of a region or a basin spatially and how these characteristics change through time in order to detect the main drivers and processes acting both locally, regionally and hemispherically. Hydroclimatological research also provides vital information to government and other responsible authorities and institutions so that informed management practices and good governance can be implemented for the sustainable use of water sources for future.

Many hydroclimatological-based research studies focus on the interaction between hydrology

and climatology and range from global to basin scales; however, most recently many of studies have also considered the effects and impacts that variability in hydroclimatological systems has upon freshwater ecology (Hannah *et al.*, 2007a, Hannah *et al.*, 2007b). Investigations into detecting possible relationships between various climate parameters and river flow can be assessed in a variety of approaches that include: the classification of flow regimes, trend analyses of river flows, snowmelt and/or glacier melt hydrological process, frequency analysis of extreme events and the study of larger scale atmospheric processes and hydroclimatological variability.

The classification of river flows is very important not only to describe annual cycle (seasonality) of flows, but also to identify homogenous regions in order to more fully understand spatial variability of flows. Multivariate techniques such as Cluster Analysis (CA), Rotated Principal Components Analysis (RPCA) and Empirical Orthogonal Function Analysis are widely used to specify objective regions for each seasonality type. One classification method, devised by Hannah *et al.* (2000) and adapted by Harris *et al.* (2000) has been successfully used for identifying large-scale patterns in climate and river flow regimes. Bower *et al.* (2004) developed this further and examined between-year stability within identified regimes. They proposed a novel sensitivity index (SI) that assesses river flow regimes and climatic sensitivity that influences river flow. This classification technique was subsequently and successfully applied in Nepal, by Kansakar *et al.* (2004) and Hannah *et al.* (2005a) and identified the underlying spatial structure of precipitation and flow regimes. These studies identified the shape (i.e., the timing of peak) and magnitude (low, intermediate and high) characteristics of precipitation and compared these to flow regime data in an extreme physical environment where hydroclimatological patterns are complex and relatively understudied.

Using long-term data for hydroclimatology research is another important aspect to be able to plan a successful management of water resources. Methods for detecting trends in hydroclimatic variables are quite important to elucidating impacts of human-induced climate change. Such studies attempt to determine the potential effect of global warming at a range of temporal and spatial scales; observed trends may then have a significant impact on decision-making for water resource planning. Thus, time series analysis is a very important strand of hydroclimatological research; the major components being the analysis of trend, cyclical, peak and persistence. One of the main objectives in hydroclimatological research is the signal to noise ratio, therefore, irregular signals in the time series is most probably 'noise', while 'random fluctuations' can be smoothed using appropriate techniques in order to detect the underlying nature of the series. Generally, non-parametric trend tests are used to detect secular changes in time series (Whitfield, 2001; Yue *et al.*, 2003; Yang *et al.*, 2004; Oguntunde *et al.*, 2006; Zhang *et al.*, 2006; Dixon *et al.*, 2006; Wilson *et al.*, 2010). These methods, which are distribution free means that they are the most appropriate to analyse climatic and hydrologic data. On the other hand, temporal autocorrelation within a time series and cross-correlation between sites can both affect the ability of the trend test (Burn and Hag Elnur (2002), Yue and Wang (2002), Yue and Pilon (2004)). Removing serial correlation prior to trend analysis has been suggested as a means to eliminate the possible effects of high autocorrelation caused by the increasing possibility of significant trends. Regression methods can also be applied in order to reveal possible relationships between tributaries, different rivers or basins and climatic parameters for specific time periods (Kletti and Stefan, 1997; Regonda *et al.*, 2005, Laize & Hannah, 2010). For example, Kletti and Stefan (1997) investigated the relationship between various climate parameters (e.g., air temperature, rainfall, snowfall, dew point temperature, wind and runoff) as independent variables for three

Minnesota streams through linear regression analysis. Regonda *et al.* (2005) examined cause-and-effect relationships between the timing of snowmelt in mountain basins in western United States and trends in associated hydroclimatic variables.

Rare weather events that occur in a particular place and for a particular time period are known as extreme events. When a pattern of extreme weather persists for some time, such as a season, it may be classed as an *extreme climate event*, especially if it yields an average or total that is itself extreme (e.g., drought or heavy rainfall over a season) (Climate Change, 2007). It has been suggested that the increase in extreme weather events can be linked to global warming (Rosenzweig *et al.* 2001). However, extreme events either associated with global warming or natural climate variability need to be analysed in order to detect the driving mechanisms and processes leading to these events which have the potential to inform on effective decision making to manage risk and mitigate the effects of natural hazards. The observed increase in precipitation intensity and other observed climate changes, e.g., an increase in westerly weather patterns during winter over Europe, leading to very rainy low-pressure systems that often trigger floods. Flood magnitude and frequency are likely to increase in most regions, and volumes of low flows are likely to decrease in many regions (Kundzewicz *et al.*, 2007). Trends in maximum flows for major river basins globally have been investigated by many researchers (e.g., Robson *et al.*, 1998; Douglas *et al.*, 2000; Svensson *et al.*, 2005; Mudelsee *et al.*, 2003; Hannaford and Marsh, 2007). Results suggest that long-term persistence of low flow conditions (hydrological drought) indicates that the variation of low flows is more evident for Europe since the 1970 (Douglas *et al.*, 2000; Zaidmann *et al.*, 2001; Hodginks *et al.*, 2005; Fleig *et al.*, 2006).

Some modes of variability in climate and hydrological systems are strongly linked with

various large-scale atmospheric phenomena (Hurrell 1995, Hurrell and VanLoon 1997, Wanner *et al.* 2001, Kutiel *et al.* 2002, Trigo *et al.* 2005, Xoplaki, Luterbacher and Gonzalez-Rouco 2006, Kingston *et al.* 2006a, 2006b, 2007, Nesterov 2009). Variability of atmospheric circulations includes weather patterns at a variety of temporal scales: days (e.g. frontal systems); weeks (e.g. mid-summer wet periods); months (e.g. cold winters); years (e.g. periods of hot summers and droughts); centuries (e.g. climate change). Teleconnection patterns refer to recurring and persistent, large-scale pattern of pressure and circulation anomalies that span vast geographical areas. These large scale circulation anomalies are a naturally occurring aspect of planet earth's chaotic atmospheric system and can arise primarily as a reflection of internal atmospheric dynamics. It is generally accepted that global warming caused by human-induced climate change may serve to cause reorganisations of these large scale teleconnection patterns and these reorganisations may have detrimental effects on the climatology of specific regions.

2.2. Hydroclimatic research in Turkey

A large number of research studies have outlined the effects of climate change on the hydroclimatology of Turkey showing unequivocally changes in trends on surface variables. These have subsequently been synthesised by The Ministry of Environment and Forestry (MoEF) which outlines future projections and adaptation strategies to climate change in the First National Communication of Turkey on Climate Change (Apak and Ubay, 2007). Firstly, a synopsis of climate changes over the last several years will be outlined and this will be followed by a short discussion on climate changes as predicted by model outputs for Turkey. The most prominent feature of the collated data is the widespread increase in summer temperatures mostly for western and south-western regions of Turkey. However, a general decreasing trend in winter temperatures can also be discerned; these recorded climatic

changes have been more significant for coastal regions. For the transition seasons (autumn and spring), regions with significant trends do not show any spatially coherent behaviour (Apak and Ubay, 2007). Significant trends were detected for both winter and autumn precipitation totals. Winter precipitation in the western provinces of Turkey has decreased significantly in the last five decades, while autumn precipitation, on the other hand, has increased at stations that are located mostly in the northern parts of Central Anatolia. For spring and summer, only a few stations record data showing statistically significant changes (Apak and Ubay, 2007). Future model simulations have been performed which suggest that winter temperatures will increase higher for the eastern half of the country, while for summer, this pattern is reversed with the western half of the country experiencing temperature increases up to 6°C against an area-averaged annual mean temperature increase for the entire of country estimated to be around 2-3°C. Winter and spring precipitation is predicted to decrease along the Aegean and Mediterranean coasts and increase along the Black Sea coast of Turkey with the severest reductions in precipitation predicted to be for the south western coastal regions, while the Black Sea coastal region is expected to receive substantially more precipitation. A slight increase in precipitation totals is predicted for autumn in Turkey nationally, summer precipitation totals are predicted to remain the same (Apak and Ubay, 2007).

Model simulations also predict changes in snow water equivalent with reductions of up to 200 mm in the high plains regions of eastern Anatolia and the eastern part of the Black Sea Mountains with concomitant effects on river flows for river basins in this region of Turkey. Coastal erosion and flooding along Turkish shorelines is a major problem of national significance, particularly in northern Turkey along the Black Sea coast, the northern Aegean and eastern Mediterranean regions (Apak and Ubay, 2007); changes in the annual amounts

and distribution of snow and rainfall may exacerbate this problem. Clearly, there is much heterogeneity in Turkey with pronounced regional differences in terms of fluctuations and trends of the climatic system. The effect of climate change on river flow and groundwater recharge varies regionally and between model scenarios; however, these largely follow the projected changes in precipitation (Kundzewicz *et al.*, 2007). Indeed, different catchments respond differently to the same changes in climate drivers, these depending largely on the physiogeographical and hydrogeological characteristics for each individual catchment (Topaloğlu, 2006b).

2.2.1. Climatic variability and changes in Turkey

An increasing trend in temperature series has been detected by Türkeş *et al.* (1995, 1996) who show that mean temperatures for winter and spring have experienced an increasing trend annually, whereas the data indicate that maximum summer and autumn temperatures have experienced a significant cooling trend for the period 1930-1993. Mean minimum temperatures have also increased markedly for all seasons for the majority of regions. Kömüştü (1998) carried out time series analysis of fluctuations in long-term annual mean air temperature series for Turkey and for most series no cyclicality could be determined. However, Kömüştü (1998) further revealed that the Black Sea region was characterised by lower annual mean temperatures that reached 12°C with the data showing a cooling period until the early 1950s in contrast to the warming observed for other regions. Türkeş *et al.* (2002a) found that summer and particularly autumn mean temperatures have decreased over northern and continental inner regions. Annual, winter, spring and summer maximum temperature data indicate a positive trend for many stations for only some stations located in the Eastern Anatolia region. The data also indicate a general negative trend in winter and autumn minimum temperatures for some parts of the Marmara, Black Sea and Eastern Anatolia

regions, while a general positive trend can be discerned for much of Turkey and significant trends in the Mediterranean region of the country. Diurnal temperature ranges (DTR) have also significantly decreased at most of the urbanised and rapidly urbanizing stations (most of the stations may have been affected by the urban heat island effect as a result of land-use changes and rapid urbanisation) for all seasons except partly in winter over Turkey (Türkeş *et al.*; 2002a, Tayanç *et al.* 1997). Daytime maximum temperatures have shown weak warming and cooling in comparison with significant warming of night-time minimum temperatures for many regions of Turkey and for most seasons (Türkeş and Sümer, 2004). A general cooling trend can also be observed for much of the Black Sea region in annual, winter and spring series with a significant cooling trend observed for autumn. The lowest increase was in the Black Sea region.

Turkish precipitation data indicate a significant decreasing trend, especially for southern parts of Turkey with drier than normal conditions recorded since 1970 (Türkeş, 1996). For the period 1930-1993, Türkeş (1996, 1998) found that annual and winter precipitation series for many stations decreased over a considerable part of Turkey since the early 1970s. Generally wetter conditions occurred during the 1940s, 1960s, late 1970s, early 1980s and mid-late 1990s, whereas generally drier conditions dominated during the early-mid 1930s, early-mid 1970s, mid-late 1980s, early 1990s, and 1999/2000 over most of Turkey (Türkeş, 1998, 2003). Kadioglu *et al.* (1999a) and Kadioglu (2000) analysed the precipitation climatology of Turkey with Harmonic and Principal Component analyses, respectively and found that maximum (minimum) precipitation records are recorded for December or January (August or July) for all of Turkey (Kadioglu *et al.*, 1999a). As the coefficient of variation value approaches 100, by definition more precipitation events occur with local orographic or convective effects and become more pronounced compared to synoptic scale frontal

precipitation events. It has been found that only the first and the second harmonics are sufficient to explain more than 90% of the climatological variations in Turkey (Kadioglu *et al.*, 1999a), while the second harmonic indicates a decreasing regional trend from eastern to more western parts of Turkey. For Turkey it appears that this harmonic indicates the orographic precipitation features. Equally it may reflect the dominance of convective precipitation in the north eastern and eastern continental parts of Turkey (Kadioglu *et al.*, 1999a). Kadioglu (2000) identified that the first PC axis represented the synoptic systems over the Turkey. The influences of continentality towards more interior regions of Anatolia and the effect of mountains in eastern Turkey are shown by the second PC axis. The third PC axis appears to explain the marine influence of the surrounding season precipitation (Türkeş *et al.*, 2009). Sen and Habib (2000) developed an optimum interpolation method for the spatial analysis of monthly precipitation in Turkey and found that maximum precipitation occurs in the southwestern part of the country from November to April; whereas from May to October continuously maximum precipitation occurs in the north and northeastern parts of Turkey. Türkeş *et al.* (2002b) also investigated persistence and periodicity components in annual and seasonal precipitation anomaly series for 91 stations in Turkey and found considerable inter-regional differences and inter-seasonal contrasts in terms of periodicity and persistence characteristics of precipitation series. Precipitation series are characterised by a negative serial correlation coefficient. Statistically significant negative relationships between precipitation anomalies and 500 hPa geopotential height anomalies in winter and autumn showed an apparent spatial coherence over most of Turkey. Normalised winter precipitation series indicate persistence at many stations, except those in the Black Sea rainfall region. Tatli *et al.* (2004) applied a new downscaling method for regional climate process. Their results show that precipitation regimes for the coastal regions of Turkey (Mediterranean, Aegean, Marmara and Western Black Sea) are controlled mainly by the large scale pressure systems. They also

emphasised that the local characteristics (namely topography and rain-shadows) can determine the probability of precipitation intensity in addition to large scale processes, while local scale processes are more effective than large scale processes for interior regions. Partal and Kahya (2006) identified some significant trends, especially in the annual means for January, February, and September precipitation. A noticeable decrease in the annual mean precipitation was observed mostly for western and southern Turkey, as well as along the coastal region of the Black Sea. Regional average series also displayed trends similar to those for individual stations.

2.2.2. Climatic variations linked to atmospheric patterns

Following studies have investigated the synchronization between precipitation, temperature and large scale variations in terms of ENSO (*El Niño Southern Oscillation*) and La Niña events, North Atlantic Oscillation and Arctic Oscillation in order to elucidate their impacts on Turkish climate. In particular, Kadioglu *et al.* (1999b) investigated the potential effects of the ENSO warm extreme on Turkish monthly precipitation totals. Distinct effects of high ENSO index months were found indicating that a large part of the month-to-month variability may be attributed to El Niño events. Spatially coherent and statistically significant precipitation responses to El Niño were also shown for some regions of Turkey (Türkeş (1998). Karabork and Kahya (2003) detected coherent and significant precipitation responses to both the extreme phases of the SO in two core regions of Anatolia, namely western Anatolia and eastern Anatolia. For western Anatolia, the April-July wet period during El Niño events is the season when the teleconnection is strongest and consistent. For eastern Anatolia, the February-June wet period during El Niño events was found to be the signal season having higher rates of coherence and consistency. Finally, Karabork *et al.* (2007) analysed empirically the determined shifts in the observed probability distribution of precipitation data

in association with SO extremes. Their results confirm the wet responses of Turkish precipitation to El Niño events, whereas those for La Niña events seem to be masked by sampling variations within the study period.

Variations in Turkish precipitation have a significant correlation with NAO phases. Türkeş and Erlat (2003a, 2005a, 2005b and 2006) studied the precipitation changes together with possible linkages to NAO for different time periods and found a close correlation between year-to-year and longer time-scale variability of the NAOIs (*North Atlantic Oscillation Index*) and the extreme NAO phases and the spatial and temporal variations and anomaly patterns in the precipitation of Turkey. A close association is also reported between the spatial distribution and magnitude of the negative correlation coefficients for the NAOIs and the precipitation series, spatial distribution patterns and severity of wetter (drier) conditions with the negative (positive) NAOI phase both annually and also for winter and autumn seasons (Türkeş and Erlat, 2003a). Variability of winter precipitation at most stations in Turkey (western regions) is significantly correlated with variability of the three NAOIs. Composite precipitation analyses exhibit an apparent opposite anomaly pattern for the majority of stations between the weak and strong phases of the NAOIs. Widespread severe droughts in 1943, 1957, 1973, 1974, 1983, 1989, 1990, 1992, 1993 and 1994, and widespread strong wet conditions in 1940–1942, 1956, 1963, 1966, 1969 and 1970 were linked to the extreme high- and low-index events of at least two NAOIs, respectively (Türkeş and Erlat, 2005a and 2005b). They also emphasised that, annual, winter, spring, autumn and partly summer composite precipitation means are mostly characterised by wetter than long-term average conditions during negative NAOI phases, whereas positive NAOI responses mostly exhibit drier than long-term average conditions annually and in all seasons except summer. Spatially coherent and statistically significant changes in the precipitation amounts during the extreme

NAOI phases are more apparent in the west and mid Turkey (Türkeş and Erlat, 2006).

More recently, Türkeş and Erlat (2008) investigated the observed changes and variability in winter mean temperature series for 70 stations in Turkey and the circulation types at 500-hPa geopotential height level to explain atmospheric controls of temperature variations during the extreme and normal phases of the Arctic Oscillation Index (AOI). Negative relationships were found for year-to-year variability of normalised winter (seasonal and monthly) temperatures and the AOI winter indices for all stations. Coherent large-scale and marked changes in winter temperatures occurred during extreme winter AOI phases. Winter temperatures tended to increase significantly during the negative AOI phase, while they tended to decrease significantly during the positive winter AOI phase. During strong phases of the AOI, strong anticyclonic anomaly circulation dominates over the northeast Atlantic and Europe, including Turkey and the Mediterranean basin, while negative anomalies dominate over the region of the Icelandic low. As a result of these anomaly patterns, enhanced northerly and northeasterly airflows from Polar Regions dominate over the Black Sea, Turkey and the eastern Mediterranean regions.

The contextualisation of previous climatology research has highlighted that Turkey climate is largely variable both spatially and temporally. Precipitation and temperature of Turkey have exhibited significant trends for the 20th Century; also the climatic variables are sensitive to the large-scale atmospheric patterns.

2.2.3. River flow variability in Turkey and links to climate

Studies on the investigation of variability patterns in river flows of Turkish rivers have been evaluated. River flow regionalisation over Turkey was undertaken by Kahya *et al.*, (2008a

and 2008b) by applying PCA, CA and Harmonic analyses. Kahya *et al.* (2008a) evaluated monthly river flow data from 78 gauging stations for the period 1964–1994 by using PCA with a varimax orthogonal function. They identified 7 river flow regions correlated well with the climate zones for Turkey as defined by the recent study by Ünal *et al.* (2003) which was based on cluster analysis of temperature and precipitation data. An annual cycle analysis of seasonal river flow using Harmonic vectors was also carried out by Kahya *et al.* (2008a) in order to identify seasonal variation of river flow. Seven annual cycle types were identified; spatial variability in annual cycle of river flow showed that for the mountainous areas of northeast Turkey in particular, the timing of peak flows was designated as May or June (reflecting a December-February dry period for this region). Kahya *et al.* (2008b) undertook a river flow regionalisation study using hierarchical CA on the data from 80 river flow stations across Turkey in order to objectively classify river flow data into similar regions. The identified river flow pattern zones were correlated the homogenous river flow zones of Turkey determined by the rotated principal component analysis (Kahya *et al.* (2008a). A comparison of all twelve monthly cluster patterns together were also achieved by Kahya *et al.* (2008b) to characterise hydrologic regionalization of Turkish river flow patterns. 6 clusters were considered for each month. For northeast Turkey in particular, Kahya *et al.* (2008b) showed that the East Black Sea Basin can be divided into two sub-regions based upon the analysis of river flow patterns for the following months: January, April, May, June and July.

The NAO-river flow link was also investigated. Cullen and deMenocal (2000) who investigated the association of river flow changes in the Tigris and Euphrates Rivers with the NAO. They accomplished this through the development of composite indices of Turkish winter temperature and precipitation to capture the inter-annual–decadal climate variability for the Tigris–Euphrates headwater region. Their data showed that these indices were

significantly correlated with the NAO, with 27% of the variance in precipitation accounted for by this natural mechanism. They also demonstrated that the Euphrates river flow exhibits $\sim\pm 40\%$ variability about the 35-year mean value ($663 \text{ m}^3/\text{s}$) teleconnected with NAO extreme. Karabork *et al.* (2005) documented the influences of the NAO and the SO on a range of Turkish climatic variables (precipitation, stream flow, maximum and minimum temperatures) and found that the NAO appeared to have a significant influence on precipitation and river flow patterns for winter months. Lag-correlation results also indicated a prediction potential for both precipitation and stream-flow variables in connection with the NAO. However, simultaneous and time-lag correlations between the climatic variables and the SO index indicated weaker relationships in comparison with those for the NAO. Kahya and Karabork (2001) analysed El Niño and La Niña signals in river flow data for Turkey and detected two core regions for possible associations with these anomalies: namely northwestern and eastern Anatolia. Kahya and Kalaycı (2004) applied Mann- Kendall test on monthly mean river flow data for 56 of the 83 stations for Turkey and found a generally downward trend for the 31 year period 1964 to 1994 with only significant trends observed for the western part of Turkey.

Ciğizoğlu *et al.* (2005) investigated the existence of trends in maximum, mean, and low flows of Turkish rivers for the last 30–60 yr. Significant decreasing trend existence was detected for the majority of rivers in western and southern Turkey and in some parts of central and eastern Turkey in mean and low flows which was a parallel trend pattern with Turkish precipitation. Topaloğlu (2006a) investigated the regional significance of trends for annual and monthly river flows for 75 stations in Turkey for the period 1968-1997 and found significant decreasing trends only for the Marmara, Aegean, Mediterranean and Central Anatolia regions for the period 1968-1997. Topaloğlu (2006b) further analysed river flow data for 84 stations in 26 river basins in Turkey in order to identify changes through time in monthly, mean,

minimum and maximum river flows. Significant decreasing trends could be detected for basins in western Turkey, whereas very little evidence of significant change could be detected for the rest of the country. An important result of this study was evidence of an increasing trend in maximum river flows for the East Black Sea and Çoruh River basins. In a further study, Ödemiş and Evrendilek (2007) analysed hydrological data for 38 rivers in Turkey in order to detect spatial and temporal trends in water quality (water temperature, PH and chemical compound) and quantity (river flow rate) characteristics for the period 1995-2002. They found that basins in Turkey experienced a generally decreasing trend of 16% in flow rates and of 5% increase in river water temperature, with considerable spatial variation. They suggested that reductions in flow rate can be attributed to increased evapotranspiration, decreased precipitation, or a combination of both, which will be influenced by global climate change.

For the northeast Turkey region in particular, Aksoy *et al.* (2006) analysed instantaneous maximum flows for eleven river gauging stations in the Eastern Black Sea basin for the period 1963-1990 in order to detect randomness, jump, trend, and probability distribution function. The maximum instantaneous river flow time series of the region was considered to be natural after the random structure of the time series was determined. Only two stations were found with a trend while no trends were detected for the majority of stations. No jumps were linked to stations at all.

However, important regional hydroclimatic knowledge could be derived from national-scale studies showing the dissimilarities across Turkey; a particular research gap currently exists for increasing understanding on regional scale dynamics of hydroclimatic change. It is crucial to investigate the influence that climate variability has on river flow with respect to the physical

geography of a particular region like northeast Turkey. This region is a climatically-sensitive location where the extant glaciers exist in Kaçkar Mountains on the north. Increasing the understanding on river flow regimes, river flow-climate interaction, river flow extremes and river flow link to teleconnection patterns will help to increase understanding the regional dynamics and changing mechanism and the role of future climate changes in determining water resources in this region. In addition to this, such knowledge will provide a new insight to implementing of projects for hazard management and hydropower plants.

2.3. Chapter summary

This chapter has evaluated the overall research context, and has examined in detail the hydroclimatological background of Turkey (Each 'Introduction' section within the following six chapters also provides an evaluation of previous studies as to scope of the particular chapter). The next chapter presents the research design and explains the data and methods used in this thesis.

3. RESEARCH DESIGN, DATA AND METHODS

3.1. Research design

This section outlines the overarching research design of the thesis and highlights how all the aspects of the research fit together. Figure 3.1 provides a schematic illustration that conceptualizes the scope of the thesis. The next six chapters deal with each aspect of hydroclimatological research in Turkey and northeast Turkey in particular. Chapter 4 examines the spatial variability of precipitation across Turkey and defines the precipitation seasonality and magnitude regimes. Chapter 5 follows and identifies extreme precipitation variability over Turkey, thus chapters 4 and 5 not only provide new large-scale aspects of hydroclimatic variability of Turkey, but also highlight the uniqueness of the northeast region of Turkey compared to other regions. Chapter 6 introduces the climate regimes of the northeast region of Turkey in order to lay the foundations of and explain the variability of climate in this region. Chapter 7 then defines the river flow regimes, evaluates long-term trends in maximum, mean and minimum river flow series and aims to quantify the relationship between river flow against various parameters of the regional climate. This chapter provides a comprehensive regime classification of river flows within the northeast region of Turkey and examines the spatiotemporal variability in river flows alongside analyses of climate. Thus, this chapter forms the basis in understanding hydroclimatological process within the region. Chapter 8 analyses the extreme characteristics and variability in hydroclimatic time series and discusses the climatic factors behind extreme variability. Thus this chapter aims to addresses the pressing and highly important issue related to climate

change impacts on water resource availability for the region. Chapter 9 quantifies the relationship between regional hydroclimatology of northeast Turkey region and northern hemisphere atmospheric indices and shows how teleconnection patterns affect temperature, precipitation and river flow variability in the region. Chapter 10 is the conclusion chapter and synthesizes the key findings, and how this has increased the knowledge and understanding on hydroclimatology of northeast Turkey as well as suggestions for future work.

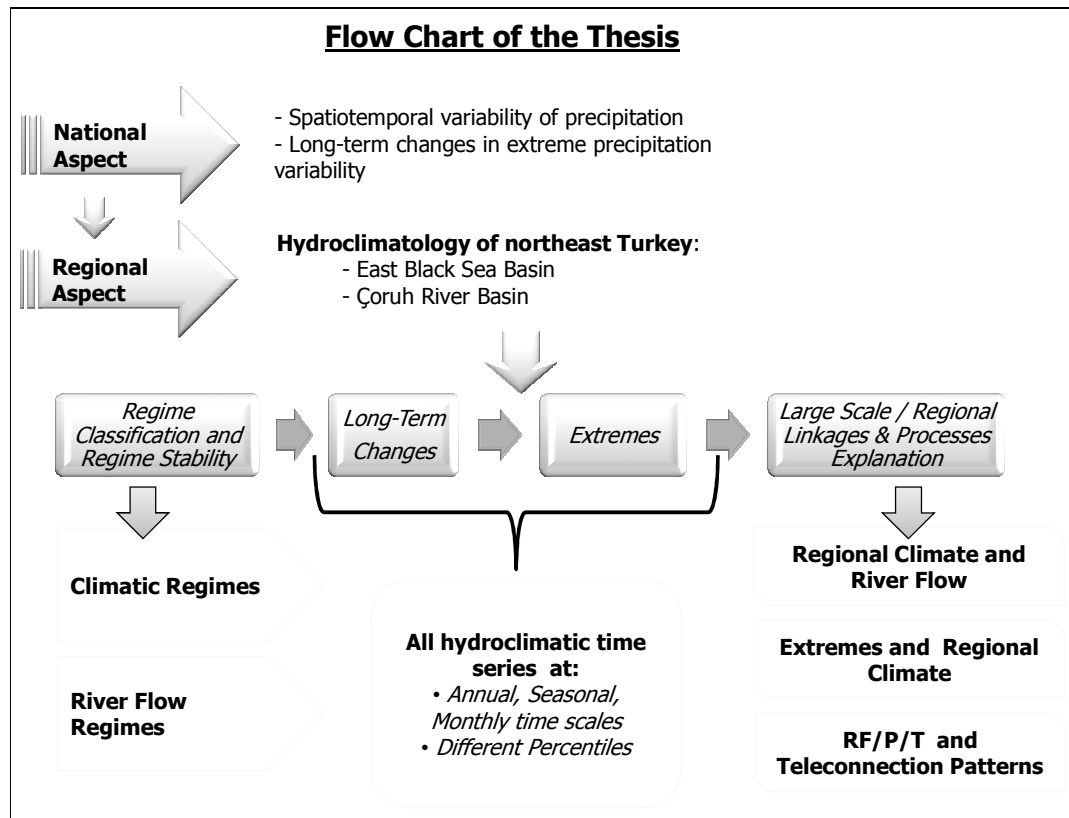


Figure 3.1 A schematic illustration to conceptualize the scope of the thesis.

3.2. Data

Various climate and river flow data are evaluated in this study. Monthly precipitation totals for 107 Turkish State Meteorological Service (Turkish Abbreviation DMI) stations are used for analysing precipitation regimes and extremes for Turkey. These stations have a 40-year overlapping record period (1963–2002) and generally provide an optimum spatial coverage for the country. For the regional scale studies, daily station data for mean temperature,

minimum temperature, maximum temperature, precipitation, relative humidity, cloudiness, and evaporation parameters for 16 meteorological stations located in northeast Turkey region were obtained for the period 1975 to 2007 (Figure 3.2).

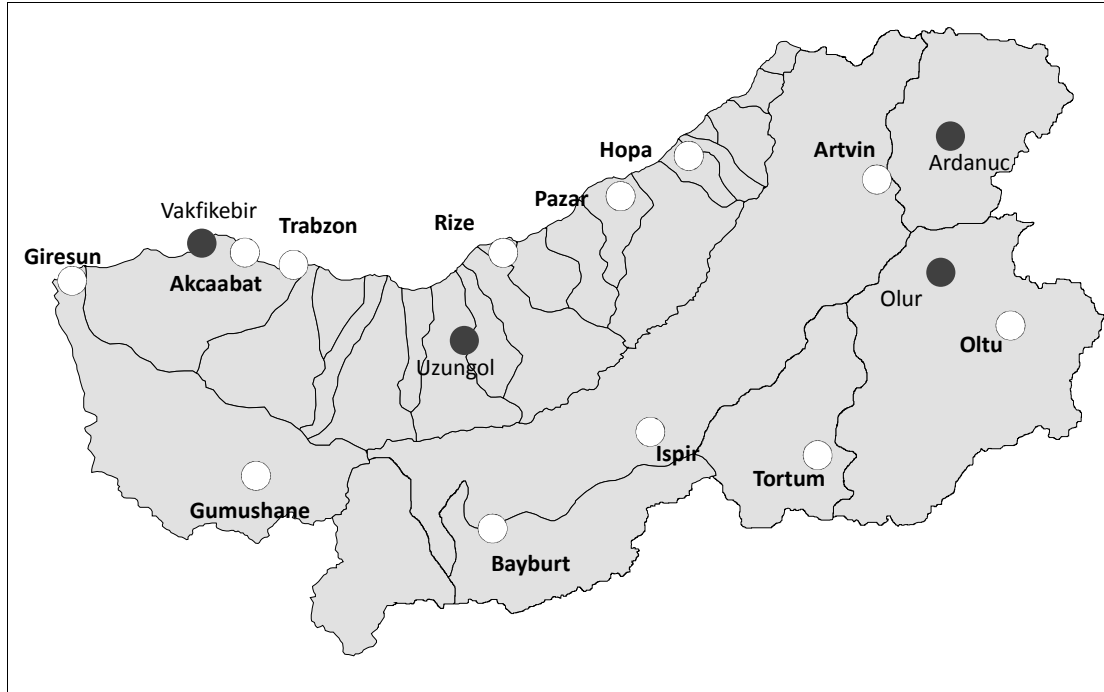


Figure 3.2 Selected meteorological monitoring stations located in northeast Turkey (Grey dots represent small climate stations with incomplete data).

The data records for the period 1975-2007 were scanned for data quality by DMI. DMI did not provide data before 1975 because it has not yet been quality assured and controlled for use by researches. In addition to this, long-term average monthly data for rainy days, storm days (thunderstorm), snow depth and snow period data were also obtained. However, daily time series for the main climatic indicators of the 7 parameters include a considerable amount of missing data for four small climate stations within the study area (Table 3.1 which shows the available years of climatic time series). Notably, the Uzungöl station in the EBS basin is important in terms of representing the highlands (1400 m height). But, there is a significant amount of missing data. Finally, 12 meteorology stations out of a total of 16 were selected for analyses (Figure 3.2) providing maximum length of observation and continuous records.

Therefore the period 1981 to 2007 is evaluated by multivariable climatic analyses for monthly mean, minimum and maximum temperature, total precipitation, mean cloudiness and mean relative humidity variables. However, in order to undertake joint analyses of river flow data with selected climate variables (e.g., temperature, precipitation and evaporation), series are arranged for the period spanning from 1976-2005. Data selection and arrangement procedures are explained in detail at the data section of each chapter.

Table 3.1 List of obtained meteorological data from DMI for northeast Turkey.

| <i>Station Type</i> | <i>Stations</i> | <i>Period</i> | <i>Latitude (N)</i> | <i>Longitude (E)</i> | <i>Elevation</i> |
|--------------------------|-----------------|-----------------|---------------------|----------------------|------------------|
| Small Climate St. | 1166-Ardanuç | 1976-83.96-2007 | 41.13 | 42.05 | 520 |
| | 1302-Vakfikebir | 1984-89.2001-07 | 41.05 | 39.28 | 5 |
| | 1651-Olur | 1989-2007 | 40.83 | 42.13 | 1300 |
| | 1962-Uzungöl | 1991-2007 | 41.62 | 40.28 | 1450 |
| Large Climate St. | 17089-Bayburt | 1975-2007 | 40.25 | 40.23 | 1584 |
| | 17626-Akçaabat | 1975-2007 | 41.03 | 39.56 | 6 |
| | 17628-Pazar | 1975-2007 | 41.03 | 40.90 | 79 |
| | 17666-Ispir | 1975-2007 | 40.48 | 41.00 | 1222 |
| | 17668-Oltu | 1975-2007 | 40.55 | 42.00 | 1322 |
| | 17688-Tortum | 1975-2007 | 40.30 | 41.53 | 1572 |
| Synoptic St. | 17034-Giresun | 1975-2007 | 40.92 | 38.40 | 37 |
| | 17037-Trabzon | 1975-2007 | 41.00 | 39.72 | 30 |
| | 17040-Rize | 1975-2007 | 41.03 | 40.52 | 9 |
| | 17042-Hopa | 1975-2007 | 41.40 | 41.43 | 33 |
| | 17045-Artvin | 1975-2007 | 41.18 | 41.82 | 628 |
| | 17088-Gümüşhane | 1975-2007 | 40.47 | 39.47 | 1219 |

Daily river flow data were obtained from the Electrical Power Resources Survey and Development Administration (Turkish Abbreviation EIEI) and the State Hydraulic Works (Turkish Abbreviation DSI) of Turkey. Since 1938, 60 stations in the East Black Sea (EBS) Basin and 44 stations in the Çoruh River Basin (ÇRB) have been established. Although the spatial representativeness of river gauging stations seems quite well, the number of stations with long period observation (at least more than 10 years) is quite few. The temporal changes in the number of open and closed stations for the EBS and Çoruh River basins are shown by a

graph in Figure 3.3. Unfortunately, the availability of stations having long-period, complete records with 'good' quality data are very few in number. Therefore, a compromise must be achieved between data quality, length and the continuity of the record; thus the research strategy of this thesis aimed to minimise data gaps by selecting the most continuous and longest data sets of stations with overlapping periods. The location of stations on the river networks, the observation period and the distances between each station were also considered in overall station selection. Each station is also considered as a representative for sub-basins as well. River flow data for 32 stations in total were obtained from authorised institutions (Table 3.2). However, 10 of the 32 stations (those that are shaded in Table 3.2) do not have continuous records for more than 5 sequential years. The optimum data set consists of 12 stations that have 25 years of continuous data; this is acceptable for time series analysis (Figure 3.4). For joint analyses of climatic parameters, 8 river gauging stations (4 stations per basin) are evaluated; these have continuous data for the period 1976-2005. Monthly mean river flow data for 22 stations for the period 1992-2001 [i.e., for 10 years] were assessed in the analysis of river flow regime classification was undertaken in order to achieve a more representative spatial pattern. Thus, longer term data (12 stations) were used to understand the temporal heterogeneity of the hydroclimatology of northeast Turkey, but also shorter term data (22 stations) were evaluated to achieve a greater understanding of the spatial heterogeneity of the hydroclimatology of northeast Turkey.

The metadata for both the meteorological and river gauging stations were further interrogated in order to learn more about station history, specific measuring techniques and also to determine important instrumental or locational change details. The metadata assessment (data preparation and quality procedure) of the obtained hydrometeorological records is outlined in each chapter prior to every analysis.

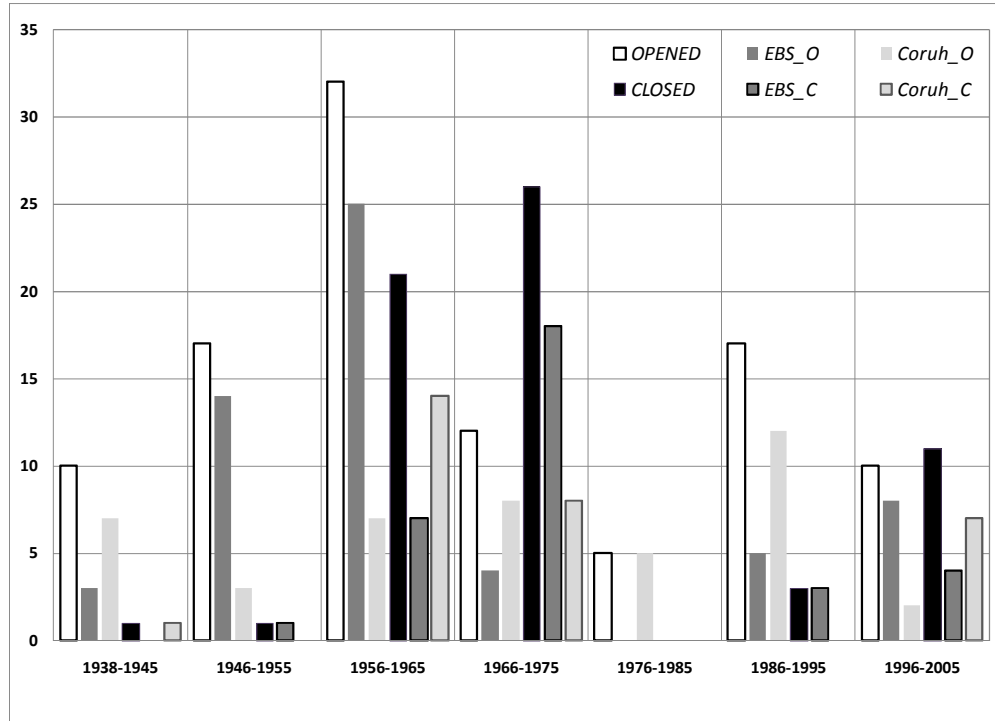


Figure 3.3 Changing in the number of (opened-O and closed-C) river gauging stations in northeast Turkey region.

Data sets for the monthly standardised selected Northern Hemisphere teleconnection indices (*North Atlantic Oscillation (NAO)*, *East Atlantic Pattern (EA)*, *Scandinavia Pattern (SCAND)*, *East Atlantic/Western Russia Pattern (EA/WR)* and *Polar/Eurasia Pattern (POL)*) were evaluated to test correlation between teleconnection patterns and surface hydroclimatology of northeast Turkey. The index data were provided by the Climate Prediction Center (CPC) of National Oceanic and Atmospheric Administration (NOAA).

Digital hydrographic data and land use data (2000 and 2006) were provided by Geographical Information Systems (GIS) Departments of DSI and MoEF in Turkey, respectively. Geology, landslide, land use and soil maps were obtained from General Directorate of Mineral Research and Exploration in printed 1/500000 scale format.

Table 3.2 Basic information on available river gauging stations across the northeast Turkey.

| | Station Code | River | Station Name | Period (years) | Latitude (N) | Longitude (E) | Elevation (m) |
|----------------------|------------------|----------------|--------------|----------------|--------------|---------------|---------------|
| East Black Sea Basin | 2202 | Karadere | Ağnas | 64 | 40.01 | 40.85 | 78 |
| | 2215 | Çamlidere | Dereköy | 43 | 40.6 | 40.73 | 942 |
| | 2218 | İydere | Şimşirli | 52 | 40.49 | 40.82 | 338 |
| | 2232 | Fırtına Deresi | Topluca | 44 | 41.01 | 41.07 | 237 |
| | 2233 | Tozköy Deresi | Tozköy | 43 | 40.58 | 40.67 | 1296 |
| | 2234 | Yanbolu | Findikli | 29 | 40.83 | 39.97 | 100 |
| | 2240 | Harsit | Eymür | 30 | 40.85 | 38.87 | 120 |
| | 2244 | Karadere | Aytas | 29 | 40.68 | 39.88 | 500 |
| | 2252 | Solaklı | Ulucami | 28 | 40.75 | 40.25 | 275 |
| | 2257 | Ögene | Açak | 28 | 40.67 | 40.20 | 650 |
| | 2258 | Görelle | Cücen | 27 | 40.87 | 39.03 | 300 |
| | 2259 | Kalyon | Çiftdere | 27 | 40.83 | 39.70 | 250 |
| | 2262 | Hemşin | Konaklar | 23 | 41.03 | 41.00 | 300 |
| | 2264 | Pazar | Kovanlık | 27 | 40.75 | 38.15 | 550 |
| | 2266 | Maki | Cevizlik | 26 | 40.85 | 40.40 | 300 |
| | 2272 | Arılı | Arılı | 25 | 41.20 | 41.18 | 175 |
| | 2274 | Hemşin | Çat | 25 | 40.87 | 40.93 | 1100 |
| Çoruh River Basin | 2282 | Salarha | Komurculer | 22 | 40.92 | 40.53 | 250 |
| | 2285 | Senoz | Kaptanpasa | 20 | 40.97 | 40.78 | 400 |
| | 2301 | Berta Çayı | Berta | 33 | 40.78 | 38.08 | 310 |
| | 2304 | Çoruh Nehri | Bayburt | 65 | 40.23 | 40.26 | 1545 |
| | 2305 | Çoruh Nehri | Peterek | 65 | 41.48 | 40.74 | 654 |
| | 2315 | Çoruh Nehri | Karşıköy | 38 | 41.71 | 41.45 | 57 |
| | 2316 | Çoruh Nehri | İspir Köp. | 42 | 40.96 | 40.46 | 1170 |
| | 2321 | Parhal Deresi | Dutdere | 35 | 41.53 | 40.89 | 705 |
| | 2322 | Çoruh Nehri | Altınsu | 29 | 41.89 | 41.16 | 201 |
| | 2323 | Oltu Suyu | İşhan Köp. | 44 | 41.70 | 40.78 | 572 |
| | 2325 | Oltu Suyu | Aşağı Kumlu | 33 | 42.13 | 40.63 | 1129 |
| 2326 | Meydancık Deresi | Dutlu | 25 | 42.29 | 41.37 | 875 | |
| 2328 | Ardanuc Deresi | Ferhatlı | 25 | 42.02 | 41.14 | 365 | |
| 2330 | Çamlıkaya Deresi | Çamlıkaya | 25 | 41.18 | 40.64 | 995 | |

River gauging stations were appraised and assessed during fieldwork in northeast Turkey between 26 July and 06 August 2008. Gauging stations were visited in order to examine the ‘integrity’ of the meteorological and river gauging stations. The geomorphology, biogeography and hydrological structure and land use characteristics surrounding each gauging station was assessed; more specifically physical and anthropogenic factors in close proximity to gauging sites that might affect measurements were noted. Local departments of DSI and EIE were also visited in order to ascertain relevant information on data collecting,

preparation and service techniques and protocol as well as any data quality control procedures. GPS measurements for each gauging sites were carried out and several photographs were taken in order to examine pertinent features of the drainage basins of the study area. In Chapter 7, a general assessment of fieldwork and useful and critical information derived from field observations is presented.

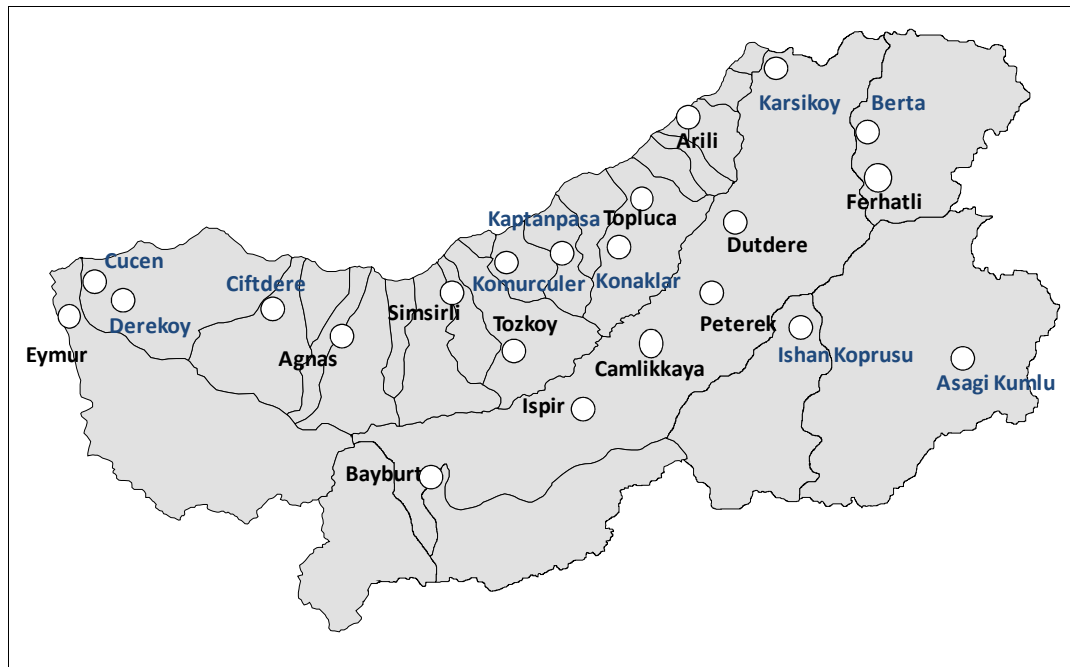


Figure 3.4 Selected river gauging stations (Black (blue) captions show the stations with long-period (short-period)).

3.3. Methods approaches

In this thesis, a wide range of statistical techniques is applied to meteorological and hydrological secondary data to analyse and explain hydroclimatological variability both in space and time. Both univariate and multivariate methods are employed in order to more fully explain variability modes of climatic and basin drivers and their interaction with each other and large-scale circulations. The following approaches are adopted: (1) *Controlling data homogeneity and randomness*; (2) *Thornthwaite water budget and moisture index calculations* (3) *Identifying regime regions*; (4) *Detecting correlation and trends in time*

series; (5) *Defining extreme events*; (6) *Process explanation and* (7) *Mapping*. Brief information on the adopted methodologies for studying the mean hydroclimatology of northeast Turkey are provided below:

1- Controlling data homogeneity and randomness (Chapters 4, 6 and 7): Kruskal-Wallis Homogeneity test is used to control data against any inhomogeneity.

The distribution-free Kruskal-Wallis (K-W) test was used based on the approach in Sneyers (1990), and in Türkeş (1996, 1998) and Türkeş *et al.* (2009) for Turkish climatic series of observations to statistically decide whether climatic and river flow time series are homogeneous or not. For calculating the K-W test statistic (X_K), observations of each sub-period (or each series) are firstly replaced by their ranks r_{ij} as occupied in total ordered sample series. If k is the number of sub-periods (or independent series); n_j , $j = 1, 2, \dots, k$ is the sample size of the sub-periods j , then test statistic (X_K) is written as

$$X_K = \left[\frac{12}{n(n+1)} \sum_{j=1}^k \frac{R_j^2}{n_j} \right] - 3(n+1) \quad [3.1]$$

where

$$R_j = \sum_{i=1}^{n_j} r_{ij} \quad \text{and} \quad [3.2]$$

$$n = \sum_{j=1}^k n_j \quad [3.3]$$

Under the null hypothesis of homogeneity of the determined sub-period's averages, the test statistic X_K is distributed approximately as χ^2 with $(k-1)$ degrees of freedom. The homogeneity of variances was also verified by using the same test. Sample size of sub-periods and the significance level were taken as $n_j = 5$ and the $\alpha = 0.05$, respectively. Then, a subjective assessment for each statistically significant result was executed by making use of the additional information available with plotted daily time-series graphs and a station history

file based on the official documents of the DMI.

Non-parametric runs test is applied in order to check the randomness of data with using their own serial correlation which appears as persistence in time series. The persistence in time series means that a value or event continues to happen (repeat itself) for longer than expected. Runs tests can be used to test the randomness of a distribution, by taking the data in the given order and marking with “+” the value greater than the median, and with “-” the value less than the median. The sequential elements in a data set, which are marked as “+” or “-” are called a ‘run’. The number of runs is defined as (R). Distribution function ($E(R)$) and ($var(R)$) are calculated and the standardised test statistics Z is obtained (WMO, 1966).

$$E(R) = n/2 + 1 \quad [3.4]$$

$$Var(R) = (n-1)/4 \quad [3.5]$$

$$Z = (R - E(R)) / \sqrt{var(R)} \quad [3.6]$$

The null hypothesis is rejected for high values of Z at a one-sided distribution. The probability value (α), which is provided from a cumulative standard normal distribution table, may be accepted or rejected according to the significance level of the test (WMO, 1966). Test statistics which are above the 5% and 1% significance levels ($\alpha \leq 0.05$ and 0.01 ; two-tailed test) are accepted as significant.

2- Thornthwaite water budget and moisture index calculations (Chapter 6): Thornthwaite’s water budget and climate classification were calculated by considering the approach used in the WATBUG program (Water-Budget Interactive Modelling Program) which was developed and described by Willmott (1977).

A modified version of the algorithm was also discussed by Willmott *et al.* (1985). According to the Thornthwaite (1948), WATBUG is a useful tool to calculate monthly (or daily) climatic

water budgets, from air temperature and precipitation data. WATBUG produces outputs such as unadjusted potential evapotranspiration (*UPE*), adjusted *PE* (*APE*), soil moisture storage (*ST*), actual evapotranspiration (*AE*), soil moisture deficit (*DEF*) and soil moisture surplus (*SURP*) in mm. Thornthwaite's Moisture Index (1948) is calculated as follows:

$$L_m = (100S - 60D)/PE \quad [3.7]$$

where, *S* is annual water surplus and *D*, deficit (mm); *PE* is annual potential evapotranspiration (mm). Negative values of the moisture index indicate dry climates, while positive values are found in moist climates. Climate types of northeast Turkey were determined using this index calculation.

3- Identifying regime regions (Chapter 4, 6 and 7): Hierarchical Cluster Analysis (CA)

Ward's method is employed in order to identify climate and river flow regimes. Discriminant Function Analysis (DFA) is used to assess whether the original grouped cases were correctly classified or not (Bower *et al.*, 2004).

The aim of CA is to group stations into homogeneous groups that are manageable in number, while maximising the differences between them (Griffith and Amrhein, 1997). Hierarchical CA progressively joins stations that are most similar using an algorithm which starts with each station in a separate cluster and combines the clusters until all stations are in the same cluster. Several regionalisation studies involve CA (e.g. Mosley, 1981; Gottschalk, 1985; Haines *et al.*, 1988; Gustard and Gross, 1989; Stahl and Demuth, 1999; Hannah *et al.*, 2000; Harris *et al.*, 2000; Bower *et al.*, 2004 and Kansakar *et al.*, 2005). There are several subjective decisions that need to be made when using CA (Bower, 2004):

- Whether to use standardised or unstandardised input variables,

- The cluster method (options include; single linkage, average linkage, centroid clustering, and Ward's method),
- The distance or similarity measure to be used in clustering (e.g. Euclidian distance, Pearson correlation),
- The numbers of clusters.

In this study, an approach developed by Hannah *et al.*, (2000) and Harris *et al.*, (2000) is adopted which aims to depict differences in both the timing (shape) and magnitude (size) of the climate and flow regime data using separate analyses. The outcomes of the two separate classifications are then be combined together to yield a composite regime classification. Detailed information on regime classification approach and identification of the procedure for precipitation, climate and river flow regime classifications are explained in methodology sections of Chapter 4, 6 and 7, respectively.

DFA is a method which has been used following CA to reorganise groups (e.g. Mosley, 1981) and, thus, results in the re-classification of some stations. DFA can only be used to increase homogeneity of the groups through re-organisation but is unsuitable to provide an initial classification (Griffith and Amrhein, 1997). However, DFA has been used on predefined group criteria as known from Bower (2004).

4- Detecting correlation and trends in time series (Chapter 5, 6, 7, 8 and 9): Mann-Kendall rank and Pearson serial correlation tests are used to analyse time-based changes in the time series and hydroclimatic links with teleconnections.

Mann-Kendall rank correlation (M-K) tests are employed to detect trends and change points in the time series. Trend component reflects the long-term progression of the series. M-K is a

non-parametric and rank-based test which is the most appropriate for hydroclimatological datasets used as part of this study, which do not conform to assumptions underlying other correlation tests (e.g. normal distribution). M-K test is preferred, it (i) allows easier interpretations of results, and (ii) provides the basis for other tests commonly used in climatology and hydrology.

In M-K test, the original observations of x_i are initially replaced by their corresponding ranks k_i , such that each term is assigned a number ranging from 1 to N reflecting its magnitude relative to magnitudes of all other terms (Türkeş *et al.*, 2009). Then, for each element, k_i , number n_i of elements k_j preceding it ($i > j$) is calculated with ($k_i > k_j$): value of the first term of the series k_1 is compared with the values of all the later terms in the series from 2nd to N th; number of later terms whose values exceed k_1 is counted up, and then this number is denoted as n_1 . Then, the value of the 2nd term k_2 is compared with the values of all the later terms; the number of later terms exceed k_2 is counted and it is denoted as n_2 . This procedure is continued for each term of the series to k_{N-1} and its corresponding number n_{N-1} for each station's snowfall data. P statistic is then obtained by,

$$P = \sum_{i=1}^{N-1} n_i \quad [3.8]$$

$M-K$ rank correlation statistic τ is derived from N and P by following equation:

$$\tau = \frac{4P}{N(N-1)} - 1 \quad [3.9]$$

Distribution function of τ is the Gaussian for all N larger than about 10, with an expected value of zero and variance (τ_{var}) equal to

$$\tau_{var} = \frac{(4N+10)}{9N(n-1)} \quad [3.10]$$

and the significance test (τ)_t is then calculated with

$$(\tau)_t = 0 \mp t_g \sqrt{\tau_{\text{var}}} \quad [3.11]$$

where, t_g is the desired probability point of the Gaussian distribution with a two-sided test, which is equal to 1.960 and 2.58 for five and one percent levels of significance, respectively. The null hypothesis for absence of any trend in the series is rejected for large values of the test statistic $|\tau_t|$ for the desired level of significance. The selected data sets (monthly, seasonal, annual and different percentiles series derived from daily time series) are documented in the Data and Methodology section of the relevant chapters (Chapters 5, 6 and 7) which use the M-K test for detecting trends.

Pearson serial correlation test is employed in order to detect the significance between two variables and is a useful technique to determine the nature and magnitude of the correlation. In this study, Pearson's correlation coefficient is used to detect the linear relationship between atmospheric indices and temperature, precipitation and river flow series (Chapter 9). The Pearson's correlation coefficient is a common measure of the degree of linear correlation between two variables X and Y :

$$\rho_{xy} = \frac{1}{n} \sum_{i=1}^n \left(\frac{x_i - \mu_x}{\sigma_x} \right) \left(\frac{Y_i - \mu_y}{\sigma_y} \right) \quad [3.12]$$

where μ_x (μ_y) and σ_x (σ_y) are the mean and the standard deviation of X (Y) respectively. The results obtained are equivalent to dividing the covariance between X and Y by the product of their standard deviation σ_x and σ_y . The correlation value ρ_{xy} ranges from -1 to $+1$. A correlation of -1 (1) means that there is a perfect (negative) positive relationship between X and Y (Helsel and Hirsch, 2002). Using a two-tailed test, the correlation is attributed as significant for large values of coefficient at 0.05 and 0.01 levels.

The non-parametric (K-W, runs, M-K and Pearson) tests used in this study follow a similar overall procedure: firstly null and alternative hypotheses are defined; secondly, a test statistic is evaluated, the magnitude of which generally increases with the strength of the relationship or distinction being tested and finally, the null hypothesis is rejected (or accepted) on the basis of the probability. The latter step is often completed by comparing the observed test statistic to critical values corresponding to specific probabilities of a type-I error (rejecting the null hypothesis when it is, in fact, true), denoted α . Typical values of α selected for hypothesis testing range from 0.01 to 0.05, depending on the level of conservatism adopted (Fleming, 2004).

5- Defining extreme events (Chapters 5 and 8): Indices of the World Meteorological Organization–Commission for Climatology (WMO–CCL) and the Research Programme on Climate Variability and Predictability (CLIVAR) are adopted for identifying hydroclimate extreme characteristics (Peterson *et al.*, 2001 and Klein-Tank and Können, 2003).

Four Temperature and five precipitation indices are initially selected. A further analysis used four and three more extreme temperature and precipitation indices (based on threshold percentiles). All the river flow indices are adapted from precipitation indices by taking into account the nature of river flow extremes. Definitions of the selected and derived indices of temperature, precipitation and river flow series are presented in the relevant chapters (Chapters 5 and 8). Daily records were used in order to calculate time series of extremes at annual and seasonal scales. The values of the percentile thresholds were determined empirically from the observed station series for the period 1963-2002 for the national scale study (Chapter 5) and for the period 1976-2005 for the regional study of northeast region of Turkey. The percentiles were calculated using wet days $P > 1$ mm, which indicates those days

having equal to or more than 1 mm precipitation. This is mostly accepted as wet day criteria for climate studies (Klein-Tank and Können, 2003). DMI measure and record the precipitation amount between less than 1 mm and higher than 0.1 mm.

6- Process explanation (Chapters 7 and 8): Multiple linear regression (MLR) analysis is selected to quantify the relationship between mean and extreme river flow series and regional climatic drivers.

Regression analyses refer to a complete process of studying the causal relationship between dependent variable and a set of independent, explanatory variables. Linear regression analysis begins by assuming that a linear relationship exists between the dependent variable (y) and independent variables (x). It then proceeds by fitting a line to the set of observed data; the nature of the fit informs upon the interpretation of the analysis (the effects of x variables on y). An important outcome of regression analysis is an equation that allows the prediction of values of y from values of x (Rogerson, 2001). In short, regression analysis is used to specify and test the functional relationship between variables and the process often leads the researcher to suspect that two or more variables are associated in some form of cause and effect relationship. Once it can be demonstrated how the variables are related, models can be developed, which may be thought of as a simplification of reality. Regression analysis provides: (a) a simplified view of relationships between variables, (b) a way of fitting a model with data, and (c) a means for evaluating the importance of the variables and the correctness of the model (Rogerson, 2001).

In MLR, with p independent explanatory variables, the regression equation is

$$\hat{y} = a + b_1x_1 + b_2x_2 + \dots + b_px_p \quad [3.13]$$

where \hat{y} is the predicted value of the dependent variable. With a given set of observations on the dependent (y) and independent (x) variables, the problem is to find the values of the parameters a and b_1, b_2, \dots, b_p . The solution is found by minimizing the sum of squared residuals:

$$\min_{\{a, b_1, \dots, b_p\}} (y - a - b_1 x_1 - \dots - b_p x_p)^2 \quad [3.14]$$

Since the problem and solution is identical with bivariate regression, there are more parameters to estimate and the geometric interpretation is carried out in a higher-dimensional space because more than one predictor must be found. For example, if $p=2$, and there is a need to find a, b_1 and b_2 a plane is fitted through the set of points plotted in a three-dimensional space where the axes are represented by y variable and two x variables assuming that there is no multicollinearity among the independent variables. This means that the correlation among the explanatory x-variables should not be high.

7- Mapping: ArcMAP, Global Mapper and ArcGIS GIS packages were used to produce DEM (Digital Elevation Model), slope, drainage, sub-basin delineation and land use maps. The sub-delineation map for the EBS and Çoruh River basins were plotted manually by considering the DEM and drainage map. Maps showing spatial variability of precipitation regimes and extremes across Turkey were carried out in MapInfo GIS package based on the base map used in Sariş (2006).

3.4. Chapter summary

The selected statistical procedures in this thesis are robust quantitative methods that have been used widely in other hydroclimatic research. A full justification for the methods employed is provided in the results chapters (4-9). In brief, the main strengths of the methods are producing physically interpretable results and detecting distinct patterns and characteristics

among the data. The limitations regarding spatial and temporal resolution of the data might affect the performances of the statistical methods.

This chapter has presented the research design of the thesis to show how the chapters fit together. Data and statistical methods used in the analyses are summarised. The next chapter provides new classification approach for Turkish annual precipitation regimes and redefine precipitation regions across Turkey.

4. SPATIAL VARIABILITY OF PRECIPITATION REGIMES OVER TURKEY

4.1. Introduction

Spatial variability of precipitation regimes has profound effects on water resources, aridity and desertification conditions (e.g. Frederick & Major, 1997; Kansakar *et al.*, 2004; Xoplaki *et al.*, 2004). The spatial structure of precipitation requires robust analysis to elucidate dominant patterns of variability, to regionalize areas with similar precipitation patterns, and to understand the factors and process driving emergent distributions. Therefore, the existent understanding of precipitation variability should be improved by new research and analytical method development for large countries, such as Turkey, which are characterised by climatic and physiographic complexity.

For Turkey, Türkeş (1996) explored seasonal variability in spatial patterns of mean annual rainfall totals and identified geographical factors influencing these distributions. This work divided Turkey into seven rainfall regions, based primarily on an index of seasonality (i.e. calendar season percentage of annual total rainfall). Türkeş (1998) refined the rainfall climatology of Turkey, showing: (a) the Mediterranean coast with a marked seasonal regime and peak winter rainfall; (b) the Black Sea coast with rainfall relatively uniform across the year; (c) the continental interior with spring rainfall maxima; and (d) Northeast Anatolia with peak rainfall in spring-summer (Figures 4.1(a)). Kadioglu *et al.* (1999a) and Kadioglu (2000) investigated precipitation patterns across Turkey using harmonic and principal component

analyses, respectively. Kadioglu *et al.* (1999a) found the first and second harmonics explained >90% of the variation in precipitation and suggested maximum (minimum) precipitation occurs in December or January (August or July) across all of Turkey (*cf.* Türkeş, 1996, 1998). Kadioglu (2000) used principal components (PCs) to identify spatial patterns and controls of precipitation. Retained PCs were interpreted to represent: (PC1) synoptic weather systems influencing all of Turkey; (PC2) continentality in Anatolia and the effect of mountains in eastern Turkey; and (PC3) maritime influence around the coasts. Sen & Habib (2000) developed an optimum spatial interpolation method for monthly precipitation data across Turkey, which detected two regional trends not identified previously: (1) maxima in the southwest during November to April, and (2) maxima in the north and northeast during May–October. Most recently, Ünal *et al.* (2003) applied cluster analysis to monthly average, maximum and minimum temperature and monthly total precipitation records to define homogeneous climate regions of Turkey (Figures 4.1(b) and (c)). This research compared five clustering algorithms; each algorithm yielded seven climate zones, but with considerable differences in regional boundaries between algorithms. However, no physical interpretation of these regions was provided by Ünal *et al.* (2003).

Hence, previous research on pan-Turkey precipitation patterns has yielded somewhat inconsistent findings, due, at least in part, to the application of a range of methods to different data sets (in terms of spatial coverage and time span). To date, analysis of spatial patterns has focused on year-to-year variation in annual totals or seasonal indices, or used monthly data to identify timing of precipitation maxima or minima. Thus, there is a need for detailed study of the intra-annual cycle (regime) of precipitation across Turkey, which investigates systematically (and jointly) spatial variation in both magnitude and timing of precipitation. Such research is necessary to provide finer-scale information of onset and cessation of wet

and dry periods and a basis for more robust regionalization of spatial structure in precipitation regime, which in turn will advance understanding of the complexity in, and processes driving, the precipitation climatology of Turkey.

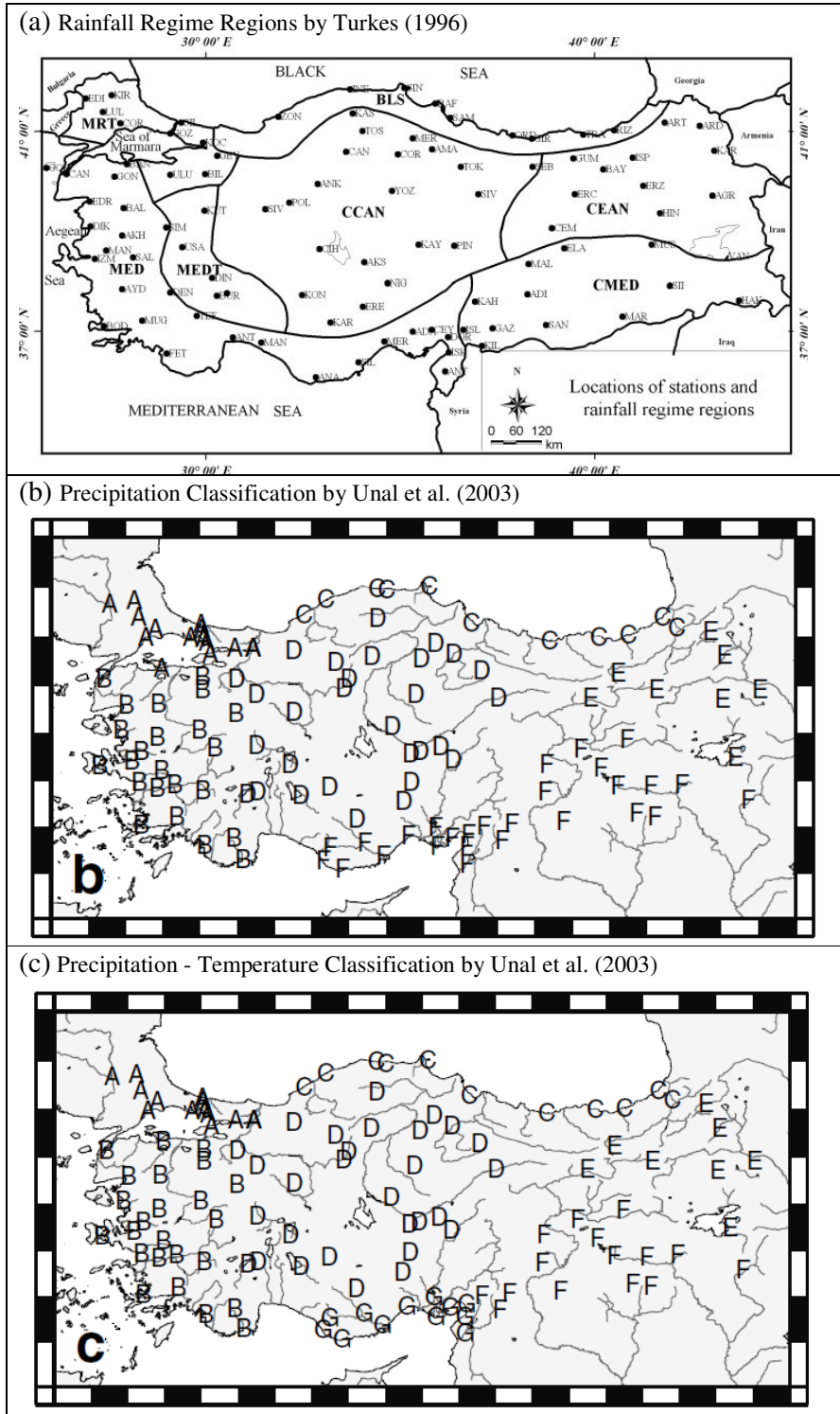


Figure 4.1 Maps of the previous climate regions from other studies.

This chapter aims to characterize the nature and dynamics of precipitation regimes across Turkey and, thus, to elucidate the key controlling factors upon spatial patterns in intra-annual precipitation behaviour. This aim is achieved through the following specific objectives: (1) to test a classification scheme that identifies the shape (timing) and magnitude (size) of annual precipitation regimes; (2) to identify precipitation regime regions across Turkey; and (3) to interpret of the emergent precipitation regime regions based on regional atmospheric circulation and the main physiographic features modifying precipitation climatology.

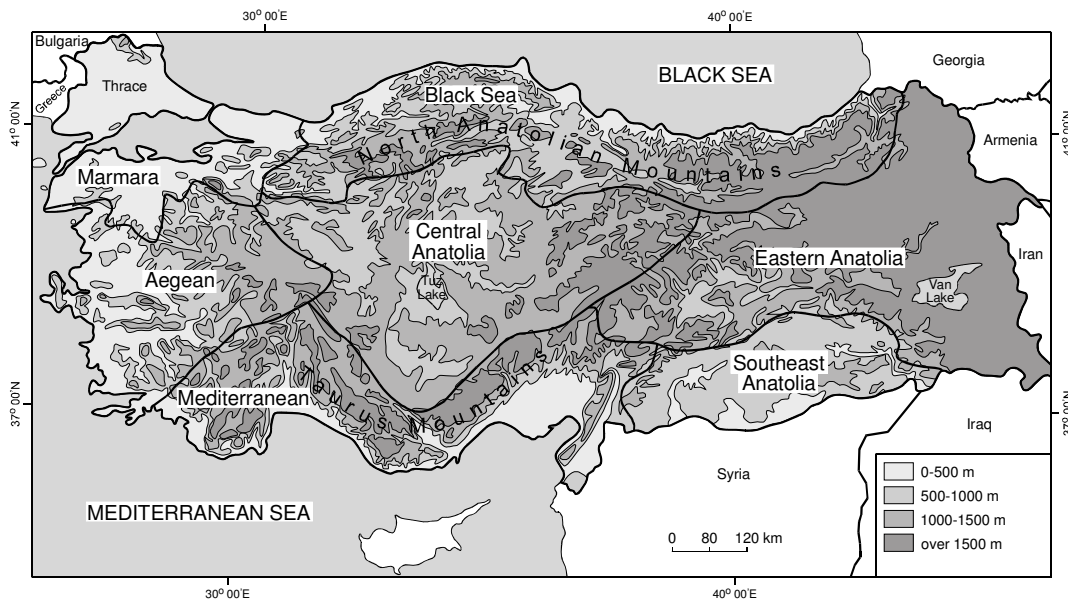


Figure 4.2 Major geographic regions and elevation of Turkey.

4.2. Study area

Turkey extends more than 1600 km west to east and nearly 800 km north to south with an average elevation of 1132 m (Figure 4.2). Turkey is part of the greater Alp-Himalayan belt with a complex geological structure (Atalay & Mortan, 2003). Elevation increases towards the east, where the two mountain ranges (North Anatolian and Taurus) converge to form the East Anatolia Region (mean elevation >1500 m) (Atalay & Mortan, 2003).

Turkey is located mainly in the subtropical zone between the humid mid-latitude zone and dry/hot tropical zone, so experiences subtropical highs in summer and prevailing westerlies in winter (Figure 4.3). A Mediterranean macroclimate of extended, warm, dry summers with occasional thunderstorms and cool, wet winters is experienced (Xoplaki, 2002; Harding, 2006). The Turkish climate is strongly influenced by the coupled pressure systems that occur over Iceland (low) and the Azores (high) (Figure 4.3). To the east, the dominant pressure system is the Siberia (high) to the north and Monsoon (low) to the south (Akcar *et al.*, 2007). In winter, the prevailing air flows over Turkey are controlled by the large-scale Siberia anticyclone and polar front cyclones, and Mediterranean depressions (Tatli *et al.*, 2004). Westerly-northwesterly and easterly-northeasterly air flows are the product of polar front depressions and the Siberia anticyclone, respectively. Southwesterly and southerly air flows are the product of Mediterranean frontal depressions (Tatli *et al.*, 2004).

Turkey is affected by Polar and Tropical air masses in winter and summer, respectively. The cP (continental-Polar) is a continental, cold and dry air mass that originates from Siberia (Figure 4.3), and which causes orographic rains if it becomes saturated while crossing the Black Sea (Akcar *et al.*, 2007). The mP (marine-Polar) air mass originates from the Atlantic Ocean and travels across Europe and the Balkans. It becomes unstable over Turkey and causes rainfall in coastal areas (Black Sea and Marmara) and snowfall at higher elevations and in the interior. The transport of mP air into the Mediterranean basin by the Polar jet-stream, its lifting (by changes in relief), and subsequent warming (by the Mediterranean Sea) is a major underlying mechanism of both Mediterranean cyclogenesis and the creation of the “Mediterranean air mass”. The Mediterranean trajectory of mP is more effective than the Atlantic trajectory in terms of generating rainfall (Tatli *et al.*, 2004).

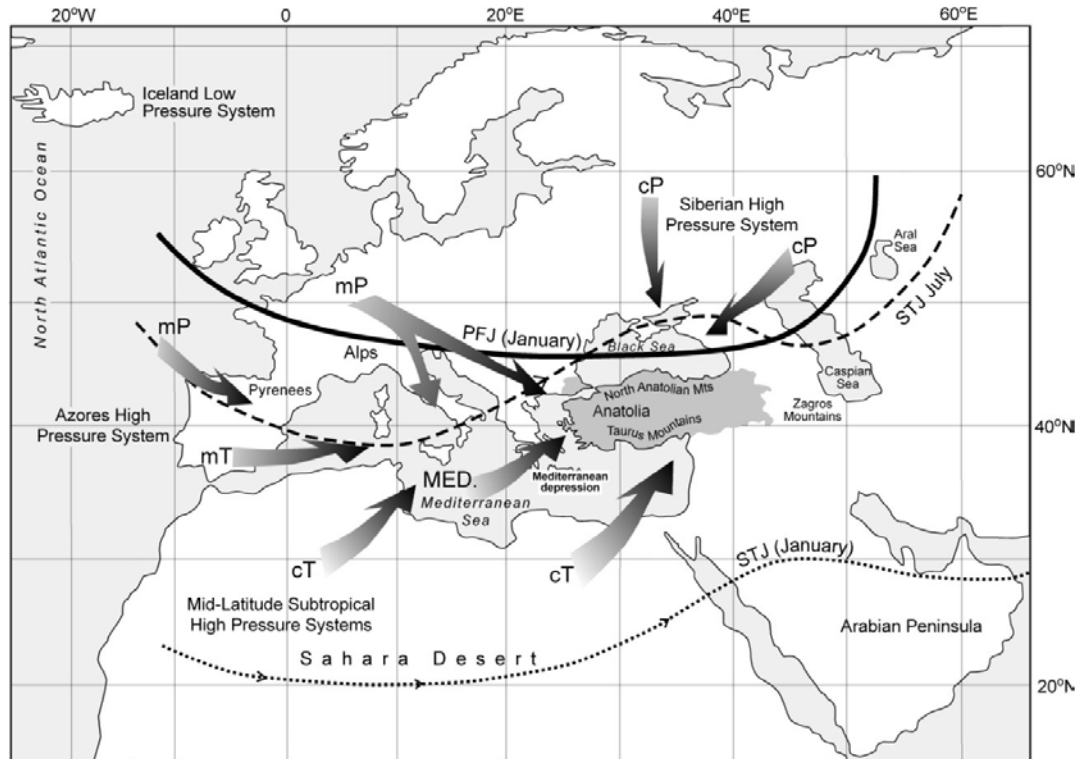


Figure 4.3 Schematic diagram of air masses influencing winter and summer climate of the eastern Mediterranean region (MED: Mediterranean Air Mass; mP: Marine Polar Air Mass; cP: Continental Polar Air Mass; mT: Marine Tropical Air Mass; cT: Continental Tropical Air Mass; PFJ: Polar Front Jet; STJ: Sub-tropical Jet).

4.3. Data and methodology

4.3.1. Precipitation data

Monthly precipitation totals for 107 (DMI) stations are used. Table 4.1 provides basic metadata for stations. These stations were selected based on record length, and for providing optimum spatial coverage across the country. Records range from 40 to 72 years; the average time span is 64 years, with the earliest record starting in 1930. A 40-year overlapping record period was identified as 1963–2002. Homogeneity of time-series was checked for all 107 stations using the Kruskal-Wallis (K-W) test. For 107 stations, statistical inhomogeneities were identified in precipitation for winter months. However, these statistically significant inhomogeneities are related to long-term variations and significant trends, not step changes in the time-series (Sariş, 2006; Türkeş *et al.*, 2009).

Table 4.1 Metadata of selected precipitation stations across Turkey.

| Station name | Station number | Data length (years) | Latitude (°N) | Longitude (°E) | Altitude (m) | Station Name | Station number | Data length (years) | Latitude (°N) | Longitude (°E) | Altitude (m) |
|--------------|----------------|---------------------|---------------|----------------|--------------|----------------|----------------|---------------------|---------------|----------------|--------------|
| Adana | 17351 | 73 | 37.00 | 35.33 | 27 | Ipsala | 17632 | 46 | 40.93 | 26.40 | 10 |
| Adiyaman | 17265 | 65 | 37.75 | 38.28 | 672 | Iskenderun | 17370 | 63 | 36.58 | 36.17 | 4 |
| Ağrı | 17099 | 65 | 39.72 | 43.05 | 1632 | Ispir | 17666 | 50 | 40.48 | 41.00 | 1222 |
| Akhisar | 17184 | 66 | 38.92 | 27.85 | 93 | Izmir | 17220 | 65 | 38.43 | 27.17 | 25 |
| Aksaray | 17834 | 64 | 38.38 | 34.08 | 965 | Kahramanmaraş | 17255 | 49 | 37.60 | 36.93 | 572 |
| Amasya | 17085 | 67 | 40.65 | 35.83 | 412 | Karaman | 17932 | 66 | 37.18 | 33.22 | 1025 |
| Anamur | 17320 | 59 | 36.08 | 32.83 | 4 | Kars | 17098 | 73 | 40.62 | 43.10 | 1775 |
| Ankara | 17130 | 73 | 39.95 | 32.88 | 891 | Kastamonu | 17074 | 73 | 41.37 | 33.78 | 800 |
| Antakya | 17984 | 62 | 36.20 | 36.17 | 100 | Kayseri | 17196 | 66 | 38.73 | 35.48 | 1093 |
| Antalya | 17300 | 73 | 36.88 | 30.70 | 54 | Keskin | 17730 | 46 | 39.68 | 33.62 | 1140 |
| Ardahan | 17630 | 65 | 41.12 | 42.72 | 1829 | Kirklareli | 17052 | 70 | 41.73 | 27.23 | 232 |
| Artvin | 17045 | 57 | 41.18 | 41.82 | 628 | Kizilcahamam | 17664 | 46 | 40.47 | 32.65 | 1033 |
| Aydin | 17234 | 72 | 37.85 | 27.85 | 56 | Kilis | 17978 | 71 | 36.72 | 37.12 | 638 |
| Bafra | 17622 | 50 | 41.57 | 35.92 | 20 | Kocaeli | 17066 | 65 | 40.78 | 29.93 | 76 |
| Bandırma | 17114 | 57 | 40.35 | 27.97 | 58 | Konya | 17244 | 73 | 37.73 | 32.48 | 1031 |
| Bayburt | 17686 | 73 | 40.25 | 40.23 | 1584 | Kuşadası | 17232 | 45 | 37.87 | 27.25 | 22 |
| Bilecik | 17122 | 70 | 40.15 | 29.98 | 539 | Kütahya | 17725 | 73 | 39.42 | 29.97 | 969 |
| Bingöl | 17203 | 43 | 38.88 | 40.48 | 1177 | Lüleburgaz | 17600 | 65 | 41.40 | 27.35 | 46 |
| Bodrum | 17290 | 66 | 37.05 | 27.43 | 26 | Malatya | 17199 | 72 | 38.35 | 38.32 | 948 |
| Burdur | 17238 | 63 | 37.72 | 30.28 | 967 | Malazgirt | 17780 | 48 | 39.15 | 42.53 | 1565 |
| Ceyhan | 17960 | 70 | 37.03 | 35.82 | 30 | Manavgat | 17954 | 57 | 36.78 | 31.43 | 38 |
| Cihanbeyli | 17800 | 51 | 38.65 | 32.93 | 968 | Manisa | 17186 | 73 | 38.62 | 27.43 | 71 |
| Çanakkale | 17112 | 66 | 40.15 | 26.42 | 6 | Mardin | 17275 | 64 | 37.30 | 40.73 | 1050 |
| Çankiri | 17080 | 55 | 40.60 | 33.62 | 751 | Mersin | 17340 | 73 | 36.80 | 34.60 | 3 |
| Çemişgezek | 17768 | 64 | 39.07 | 38.92 | 953 | Merzifon | 17083 | 68 | 40.87 | 35.33 | 755 |
| Çermik | 17874 | 40 | 38.13 | 39.45 | 700 | Muğla | 17292 | 73 | 37.22 | 28.37 | 646 |
| Çorlu | 17054 | 66 | 41.17 | 27.80 | 83 | Muş | 17204 | 53 | 38.73 | 41.48 | 1320 |
| Çorum | 17084 | 73 | 40.55 | 34.95 | 776 | Niğde | 17250 | 68 | 37.97 | 34.68 | 1211 |
| Denizli | 17237 | 55 | 37.78 | 29.08 | 425 | Ordu | 17033 | 52 | 40.98 | 37.90 | 4 |
| Dikili | 17180 | 62 | 39.07 | 26.88 | 3 | Pınarbaşı | 17802 | 51 | 38.72 | 36.40 | 1500 |
| Dinar | 17862 | 65 | 38.07 | 30.17 | 864 | Polatlı | 17728 | 73 | 39.58 | 32.15 | 886 |
| Divriği | 17734 | 48 | 39.37 | 38.12 | 1225 | Rize | 17040 | 73 | 41.03 | 40.52 | 9 |
| Dört Yol | 17962 | 73 | 36.85 | 36.22 | 28 | Salihli | 17792 | 63 | 38.48 | 28.13 | 111 |
| Dursunbey | 17700 | 46 | 39.58 | 28.63 | 639 | Samsun | 17030 | 73 | 41.28 | 36.30 | 44 |
| Edirne | 17050 | 73 | 41.67 | 26.57 | 51 | Siirt | 17210 | 72 | 37.92 | 41.95 | 896 |
| Edremit | 17696 | 40 | 39.60 | 27.02 | 21 | Silifke | 17330 | 73 | 36.38 | 33.93 | 15 |
| Elazığ | 17201 | 72 | 38.67 | 39.23 | 990 | Simav | 17748 | 42 | 39.08 | 28.98 | 809 |
| Ereğli | 17248 | 52 | 37.50 | 34.05 | 1044 | Sinop | 17026 | 71 | 42.02 | 35.17 | 32 |
| Erzurum | 17096 | 73 | 39.92 | 41.27 | 1758 | Sivas | 17090 | 73 | 39.75 | 37.02 | 1285 |
| Fethiye | 17296 | 64 | 36.62 | 29.12 | 3 | Sivrihisar | 17726 | 73 | 39.45 | 31.53 | 1070 |
| Gaziantep | 17261 | 64 | 37.07 | 37.38 | 855 | Şanlıurfa | 17270 | 66 | 37.13 | 38.77 | 549 |
| Geyve | 17662 | 73 | 40.52 | 30.30 | 1000 | Şebinkarahisar | 17682 | 42 | 40.30 | 38.42 | 1300 |
| Giresun | 17034 | 73 | 40.92 | 38.40 | 37 | Şile | 17610 | 63 | 41.18 | 29.37 | 83 |
| Gökçeada | 17110 | 65 | 40.20 | 25.90 | 72 | Tefenni | 17892 | 49 | 37.32 | 29.77 | 1142 |
| Gönen | 17674 | 53 | 40.10 | 27.65 | 37 | Tokat | 17086 | 70 | 40.30 | 36.57 | 608 |
| Göztepe | 17062 | 73 | 40.97 | 29.08 | 33 | Tosya | 17650 | 51 | 41.02 | 34.03 | 870 |
| Gümüşhane | 17088 | 45 | 40.47 | 39.47 | 1219 | Trabzon | 17037 | 65 | 41.00 | 39.72 | 30 |

4.3.2. Regime classification methodology

The hierarchical, agglomerative cluster analysis is adopted to separately classify annual precipitation regimes according to their “shape” (timing) and “magnitude” (size) (devised by Hannah *et al.*, 2000; adapted by Harris *et al.*, 2000; evaluated by Bower *et al.*, 2004; Kansakar *et al.*, 2004; and Hannah *et al.*, 2005a).

The shape classification identifies stations with a similar form of annual regime, regardless of

the absolute magnitude. In this application, the magnitude classification is based upon four indices (i.e. the mean, minimum, maximum and standard deviation of mean monthly precipitation observations total) for each station, regardless of their timing. This approach has the advantage that these two important regime attributes may be interpreted separately as well as jointly by simply combining shape and magnitude classes for each station to yield a “composite” classification.

To classify precipitation regime shape independently of magnitude, the 12 monthly observations for each station were standardised separately using z -scores (mean = 0, standard deviation = 1) prior to clustering. The four magnitude indices were derived for the long-term regime for each station; it was necessary to standardize between indices (to control for differences in their relative values) by expressing each index as z -scores across the 107 stations.

For both shape and magnitude, classification was achieved by hierarchical, agglomerative cluster analysis using Ward’s method. Ward’s method was selected because it typically outperforms other algorithms in terms of separation to give relatively dense clusters with small within-group variance (Yarnal, 1992; Griffith & Amrhein, 1997; Bower *et al.*, 2004). Ward’s method has been widely and successfully used in the climatological studies (e.g. Stone, 1989). The structure of the cluster dendrogram and breaks of slope in the agglomeration schedule (scree) plot were used to determine the appropriate number of clusters (Griffith & Amrhein, 1997). Thus, each of the 107 stations was grouped by both regime shape and magnitude, which also permitted composite shape and magnitude classification. The spatial distribution of the shape, magnitude and composite classes allowed precipitation regime regions to be identified.

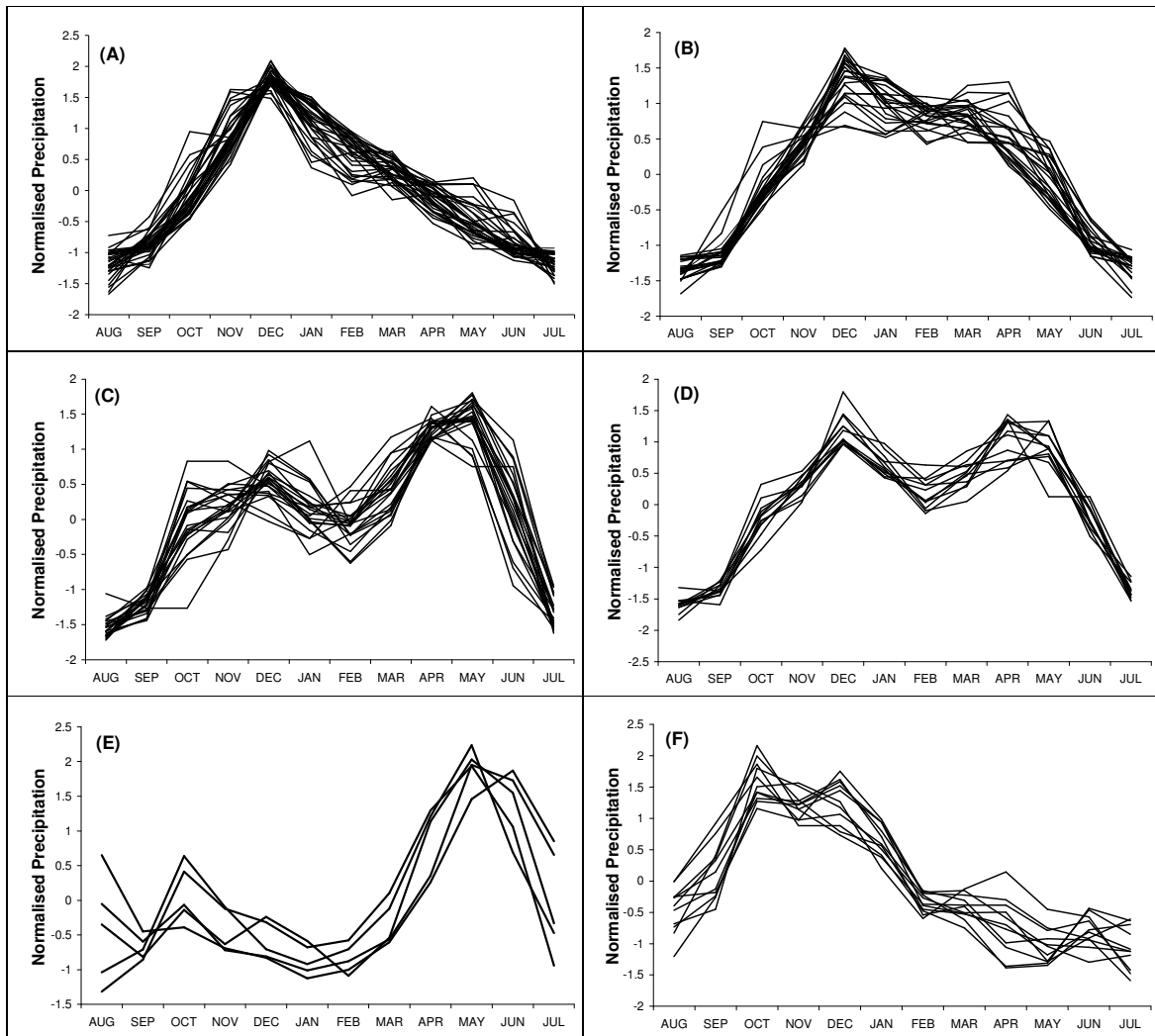


Figure 4.4 Standardised (z-scores) monthly values for all stations within the precipitation regime shape regimes.

4.4. Results and discussions

4.4.1. Precipitation regime shape

Six precipitation regime shape classes were identified (Figure 4.4):

- Regime A. December peak with rapid onset of wet winter and gradual cessation into dry summer (33 stations).
- Regime B. December peak with extended wet winter followed by marked decline in spring to dry summer (24 stations).
- Regime C. May peak with a gradual onset (wet spring), secondary winter (December) peak and short dry summer (22 stations).

- Regime D. April–May peak with gradual onset, main rainy period in spring with marked cessation in June, and secondary winter (December) peak (12 stations).
- Regime E. May peak with rapid onset, short wet spring, relatively dry summer, secondary autumn (October) peak and dry winter (five stations).
- Regime F. October peak with rapid onset, and wet autumn-winter (11 stations).

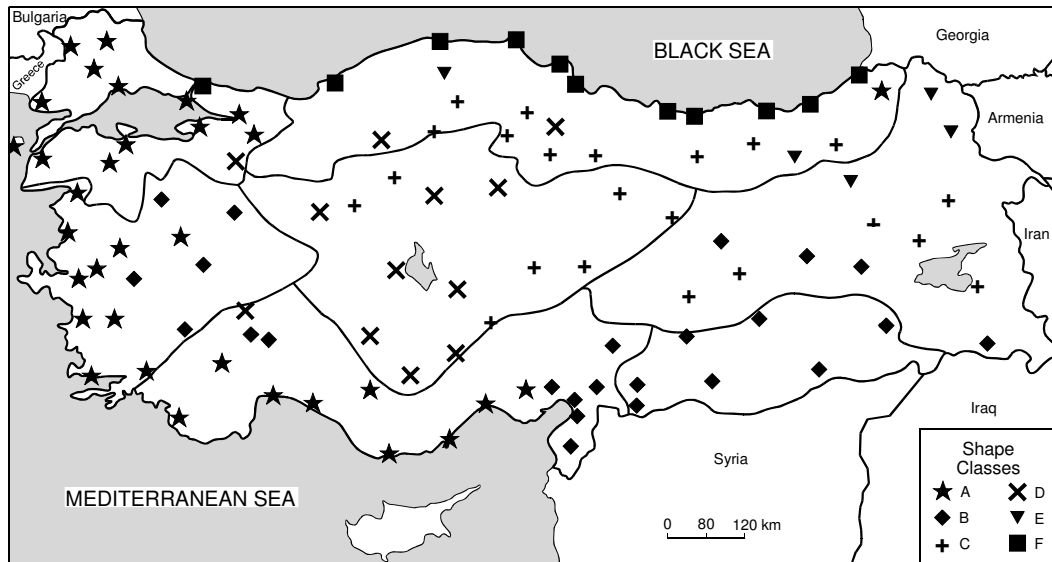


Figure 4.5 Spatial distribution of precipitation regime shape across Turkey.

The spatial distribution of precipitation regime shape classes is shown in Figure 4.5. The geographical regions of Turkey (based on the major physiographic units in Figure 4.2) are overlain on this map; these regions provide a convenient framework to help structure discussion of spatial precipitation patterns. Briefly, the Black Sea region is characterised by the North Anatolian Mountain range and the Mediterranean region by the Taurus Mountains. The Southeast Anatolia region represents the southeastern part of the Taurus Mountains, while the Central Anatolia and Eastern Anatolia are characterised by plateau and high plateau topography, respectively. To the west, the Marmara and Aegean regions form low-altitude plains.

Table 4.2. Precipitation regime shape class frequencies in the main geographical regions (Percentage of regimes in each region is given in parentheses.).

| Shape regime | Black Sea | Marmara | Aegean | Mediterranean | Central Anatolia | Eastern Anatolia | Southeast Anatolia |
|--------------|-----------|---------|---------|---------------|------------------|------------------|--------------------|
| A | 1 (4) | 13 (86) | 10 (67) | 9 (50) | - | - | - |
| B | - | - | 5 (33) | 8 (44) | - | 4 (31) | 7 (100) |
| C | 9 (38) | - | - | - | 7 (47) | 6 (46) | - |
| D | 2 (8) | 1 (7) | - | 1 (6) | 8 (53) | - | - |
| E | 2 (8) | - | - | - | - | 3 (23) | - |
| F | 10 (42) | 1 (7) | - | - | - | - | - |

The spatial distribution of regimes becomes more complex from west to east and from coast to interior regions. Table 4.2 and Figure 4.6(a) present the frequency distribution and summary of distribution of the shape regimes by region. Marmara (86%), coastal Aegean (67%) and Mediterranean (50%) are dominated by Regime A. Regime B is found along the southeast Mediterranean coast (Amanos Mountains–Iskenderun Gulf, 44%), and interior of the Aegean (33%). The uniquely homogeneous (Regime B) region is Southeast Anatolia. Regime C dominates inland regions: Central Anatolia (47%), Eastern Anatolia (46%) and the southern interior of the Black Sea (38%). In Central Anatolia, the dominant regime is D (53%). Regime E is observed only for a few stations in the northeast part of the Eastern Anatolia region, while Regime F is confined to the coastal zone of the Black Sea (42%).

The distribution of precipitation regimes with a December peak (A and B) may be explained by winter rainfall supplied from mid-latitude (northeast Atlantic) and Mediterranean depressions which are most active during winter (Türkeş, 1998; Kostopoulou & Jones, 2007). The interior of the Aegean, southeast Mediterranean and southwest Anatolia regions (Regime B) are differentiated from coastal regions by an extended period of winter–spring precipitation. For Regime B, the rainier spring most probably reflects convective activity (Türkeş, 1998).

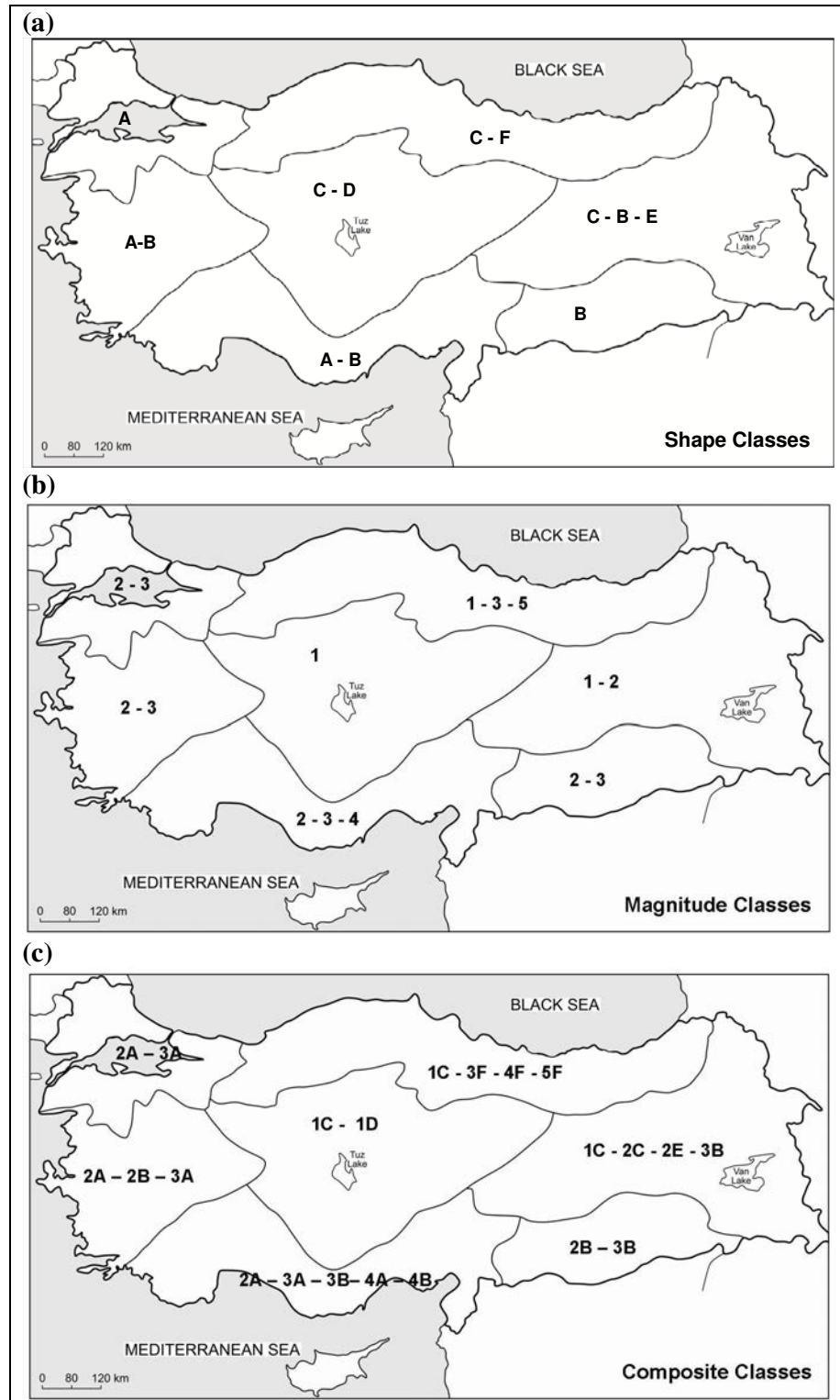


Figure 4.6 Summary of spatial patterns for (a) shape, (b) magnitude, and (c) composite regimes across Turkey.

Winter is the wettest period across Turkey, except in Eastern and Central Anatolia where spring is rainiest. May and April–May peaks (Regime C and D) are most probably caused by convective rainfall rather than frontal systems. Precipitation formation is modified by local topography in continental Anatolia (i.e. Central Anatolia, Eastern Anatolia and the southern part of the Black Sea region) (Kutiel & Türkeş 2005). The April–May rainfall peak in Central Anatolia is commonly referred to as the “Kırkikindi yağmurları” (40-afternoon rains), which indicates its convective origins. The timing of precipitation peaks for Regime C and D are similar; but there are clear differences in the length of the rainy season. Central Anatolia (D) is influenced by frontal systems during winter; whereas Eastern Anatolia and the southern Black Sea (C) experience drier winters due to small-scale high-pressure centres caused by localised thermal effects. The occurrence of Regime E (dry winter and marked May peak) in the northeast Eastern Anatolia is due to the combined effect of high topography and continentality and the Siberian High to the east, which tends to reduce winter precipitation. Indeed, the eastern part of Turkey receives much less precipitation in winter than other parts of the country (Türkeş, 1998). The occurrence of an October peak precipitation regime (Regime F) along the Black Sea coast can be explained by the frequent northeastern Atlantic originating depressions in autumn (Karaca *et al.*, 2000; Trigo *et al.* 1999). In comparison, southern regions of Turkey do not receive much autumn rain because the dominant atmospheric systems are located at northerly latitudes and the Mediterranean depression is relatively weak at this time.

In summary, intra-annual variability in the timing of precipitation (i.e. regime shape) over Turkey is controlled mainly by the North Atlantic and Mediterranean depressions which are influential in winter. However, local factors cause modification of cyclone trajectory and, hence, the timing of precipitation (peak in spring) especially for interior and high elevation

regions. The October rainfall peak for the northern Black Sea coast may be explained by prefrontal depression systems, which are only effective in northern Anatolia during the autumn.

4.4.2. Precipitation regime magnitude

Five regime magnitude classes can be identified that may be ordered with respect to the four precipitation magnitude indices (Table 4.3):

- Regime 1. Low with the lowest values for all indices (32 stations).
- Regime 2. Intermediate with the second lowest values for all indices (32 stations).
- Regime 3. Moderately-high with third highest values for all indices (35 stations).
- Regime 4. High with the second highest values for all indices (six stations).
- Regime 5. Very-high with the highest values for all indices (two stations).

Table 4.3 Average values of precipitation indices for stations within the five regime magnitude classes (1: low; 2: intermediate; 3: moderately high; 4: high; 5: very high).

| Precipitation Magnitude index | Regime average | | | | | Average (All stations) |
|------------------------------------|----------------|-------|--------|--------|--------|---------------------------|
| | 1 | 2 | 3 | 4 | 5 | |
| Mean (mm month ⁻¹) | 33.97 | 46.81 | 64.40 | 96.62 | 183.57 | 54.07 |
| Max (mm month ⁻¹) | 49.11 | 71.99 | 100.35 | 150.83 | 251.66 | 82.20 |
| Min. (mm month ⁻¹) | 0.00 | 0.00 | 0.01 | 0.01 | 0.35 | 0.01 |
| Std dev. (mm month ⁻¹) | 8.77 | 12.32 | 16.98 | 25.70 | 46.12 | 14.17 |
| No. of stations | 32 | 32 | 35 | 6 | 2 | 107 |

Table 4.4 Precipitation regime magnitude class frequencies in the main geographical regions (Percentage of regimes in each region is given in parentheses.).

| Magnitude Regime | Black Sea | Marmara | Aegean | Mediterranean | Central Anatolia | Eastern Anatolia | Southeast Anatolia |
|---------------------|-----------|---------|--------|---------------|---------------------|---------------------|-----------------------|
| 1 | 10 (42) | 1 (6) | – | 2 (11) | 14 (93) | 5 (39) | – |
| 2 | 3 (13) | 7 (47) | – | 4 (22) | 1 (7) | 5 (39) | 3 (43) |
| 3 | 7 (29) | 7 (47) | 5 (33) | 9 (50) | – | 3 (22) | 4 (57) |
| 4 | 2 (8) | – | 1 (7) | 3 (17) | – | – | – |
| 5 | 2 (8) | – | – | – | – | – | – |

Figure 4.7 illustrates the spatial distribution of magnitude regimes based on a simplified scheme, as shown in Figure 4.6(b). The frequency distribution of regimes is summarised in Table 4.4. Regime 1 clearly dominates in Central Anatolia (93%), but also predominates in

Eastern Anatolia (39%) and the inland parts of the Black Sea region (42%). Thrace (47%), the Aegean (60%), Southeast Anatolia (43%) and Eastern Anatolia (39%) are mainly characterised by intermediate regimes (Regime 2). Regime 3 is distributed across Anatolia (Table 4.4). The Anatolian part of the Marmara region (also known as South Marmara, 47%), the Black Sea coast (29%) and Mediterranean coast (50%) also have high occurrence of moderately-high regimes. Regime 4 is only detected for six stations. Southwest Turkey (17%) is represented by Regime 4. Antakya (southeast Mediterranean coast), Zonguldak and Giresun (Black Sea coast, 8%) also experience high precipitation regimes. Very-high precipitation regimes (Regime 5) are only recorded for Rize and Hopa (northeast Black Sea region, 8%).

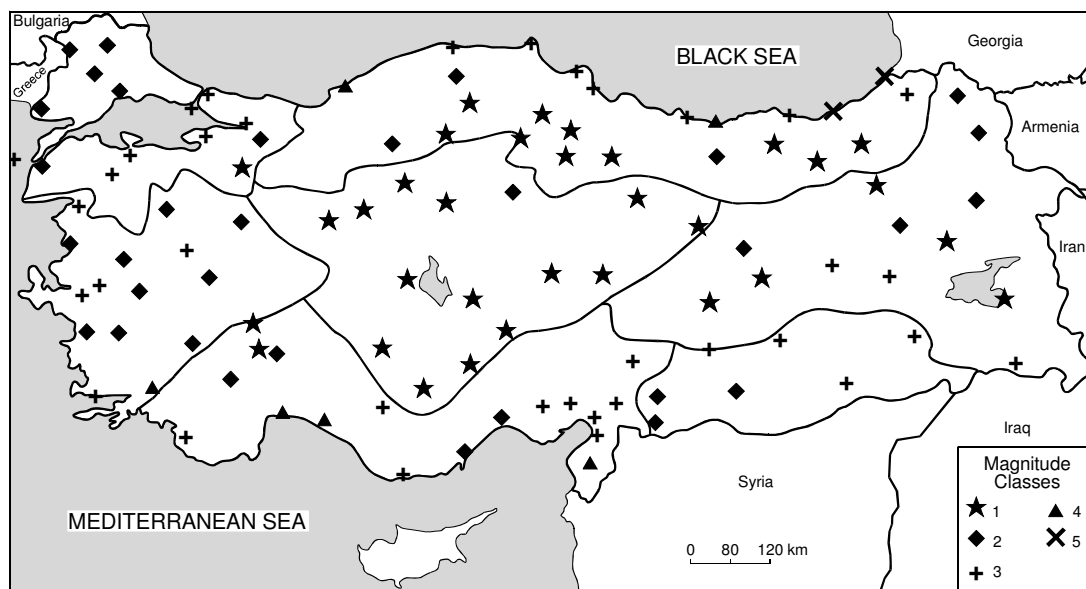


Figure 4.7 Spatial distribution of precipitation magnitude regimes across Turkey.

The Central Anatolia region is characterised by the lowest magnitude regime. Dry sub-humid climatic conditions prevail here, with the Konya Plain having a semi-arid climate (Türkeş, 1999). Central Anatolia is a formation area for thermal lows and experiences continentality, thus the region has propensity for precipitation deficits (Spanos *et al.*, 2003). The transition zone between central and Eastern Anatolia are also dominated by Regime 1. The southwest part of the Black Sea region is in a rain shadow of the western Black Sea Mountains and so

receives limited rainfall. The Aegean region has an intermediate regime due to a combination of maritime influence and topography. The predominantly horst and graben topography of western Turkey, which is perpendicular to the coast, does not obstruct airflow, while the Aegean Sea is the major winter–spring cyclone source areas at the sub-synoptic scale (Trigo *et al.*, 1999). Regime 2 also dominates Thrace; this area is influenced by polar front and Balkan-originated air flows (Kutiel *et al.*, 2001). Moderately-high regimes are observed for South Marmara, and coastal regions of the Aegean, Mediterranean, Southeast Anatolia and Black Sea regions (Figure 4.6(b)). Relatively high precipitation for these coastal locations is the combined result of frontal and orographic rains. For example, the Taurus Mountains trim the Mediterranean coast and form a barrier to moist air. One of the most notable features of this new precipitation regionalization is the extension of moderately-high regimes toward Southeast Anatolia (previously defined as dry, semi-arid, e.g. Türkeş, 1999). Regime 3 is concentrated along the physiographic transition between the Mediterranean and Southeast Anatolia region; this zone is influenced by the Mediterranean cyclones. These weather systems are sourced from the Cyprus Low, which is an important driver of eastern Mediterranean cyclogenesis (Trigo *et al.*, 1999). The highest precipitation regimes are divided into two regimes (4 and 5) with a limited number of stations (Table 4.4).

In summary, precipitation regime magnitude across Turkey appears to depend on the strength of influence of mid-latitude and Mediterranean cyclones, and probably local factors. Interior regions are characterised by low (mainly convective, see Section 4.1) rainfall while coastal regions are predominantly affected by frontal and orographic precipitation. Local topography appears to be a modifier of regime magnitude: enhancing precipitation on windward slopes and reducing precipitation penetration to cause rain shadows.

Table 4.5 Precipitation regime composite class frequencies in the main geographical regions (Percentage of regimes in each region is given in parentheses.).

| Composite Regime | Black Sea | Marmara | Aegean | Mediterranean | Central Anatolia | Eastern Anatolia | Southeast Anatolia |
|------------------|-----------|---------|--------|---------------|------------------|------------------|--------------------|
| 1B | - | - | - | 1 (6) | - | - | - |
| 1C | 8 (33) | - | - | - | 7 (47) | 4 (31) | - |
| 1D | 1 (4) | 1 (7) | - | 1 (6) | 7 (47) | - | - |
| 1E | 1 (4) | - | - | - | - | 1 (8) | - |
| 2A | - | 7 (46) | 4 (27) | 3 (16) | - | - | - |
| 2B | - | - | 5 (33) | 1 (5) | - | 1 (8) | 3 (43) |
| 2C | 1 (4) | - | - | - | - | 2 (15) | - |
| 2D | 1 (4) | - | - | - | 1 (6) | - | - |
| 2E | 1 (4) | - | - | - | - | 2 (15) | - |
| 3A | 1 (4) | 6 (40) | 5 (33) | 4 (22) | - | - | - |
| 3B | - | - | - | 5 (28) | - | 3 (23) | 4 (57) |
| 3F | 6 (25) | 1 (7) | - | - | - | - | - |
| 4A | - | - | 1 (7) | 2 (11) | - | - | - |
| 4B | - | - | - | 1 (6) | - | - | - |
| 4F | 2 (9) | - | - | - | - | - | - |
| 5F | 2 (9) | - | - | - | - | - | - |

4.4.3. Composite (shape and magnitude) precipitation regimes

A composite precipitation classification may be achieved by combining shape and magnitude regimes, which permits standardised seasonal responses to be scaled by precipitation amount (Table 4.5, Figure 4.8). Of the 30 possible, 16 composite regimes can be observed across 107 stations. December peak regimes (A and B) combine with intermediate and moderately-high magnitude (2 and 3). Regime 2A, 2B, 3A and 3B account for 49% of all stations. Regime A and B also combine with high magnitude, but only in three cases. April and May peak regimes (C and D) join mainly with low magnitude, and on two occasions intermediate. Overall, 1C is the most common single regime (18%). No composite regimes are found for April and May peaks with higher magnitudes (3, 4 or 5). Regime E (May peak) combines with low and intermediate magnitude in one (1E) and four (2E) instances, respectively. October peak (F) combines only with moderately-high, high and very high regimes.

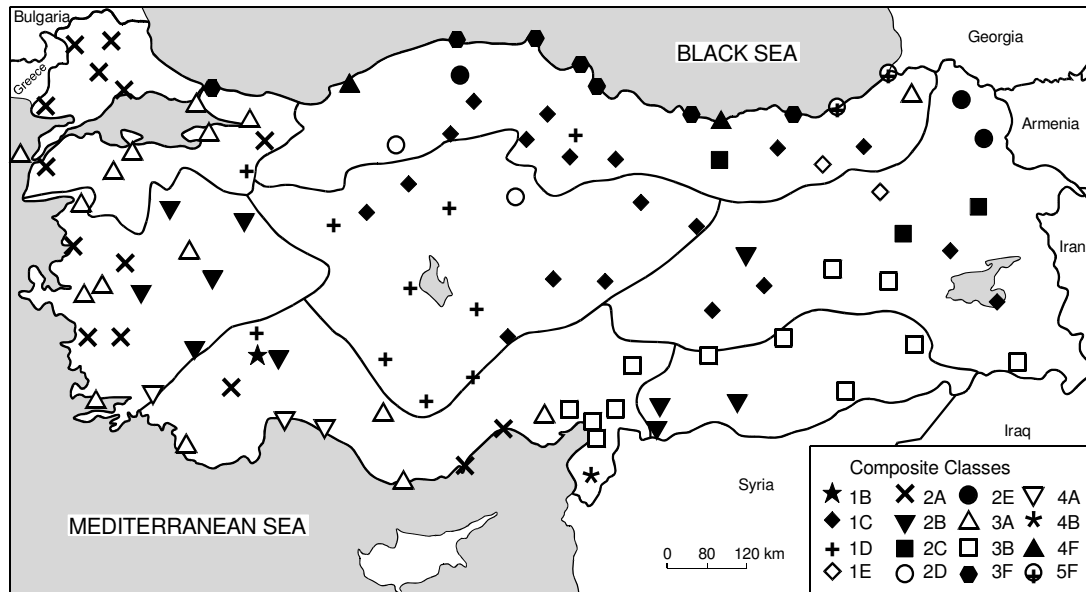


Figure 4.8 Spatial distribution of composite (shape and magnitude) precipitation regimes across Turkey.

The underlying spatial structure is summarised in Figure 4.6(c). The coastal Aegean, Mediterranean and Marmara regions are characterised by 2A (27%, 16%, 46%), and 3A (33%, 22%, 40%), respectively. 4A was found only at one station in the Aegean and at two stations in the Mediterranean regions. The transitional areas of the Aegean and the Mediterranean are dominated by 2B (33%) and 3B (28%). Southeast Anatolia represents another transitional zone, with regimes 2B (43%) and 3B (57%). Central Anatolia is dominated by two regimes (1C = 47%; 1D = 47%). Regime 1C is specific to Eastern Anatolia (31%); this region is also characterised by 3B (23%). Regimes 3F, 4F and 5F are observed solely along the Black Sea coast, in order from west to east. There is a marked shift in regimes between the coast (3F) and the interior parts (1C) of the Black Sea region in both precipitation timing (April–October) and declining magnitude due to the rain shadow effect of the North Anatolian Mountains (sections 4.1 and 4.2).

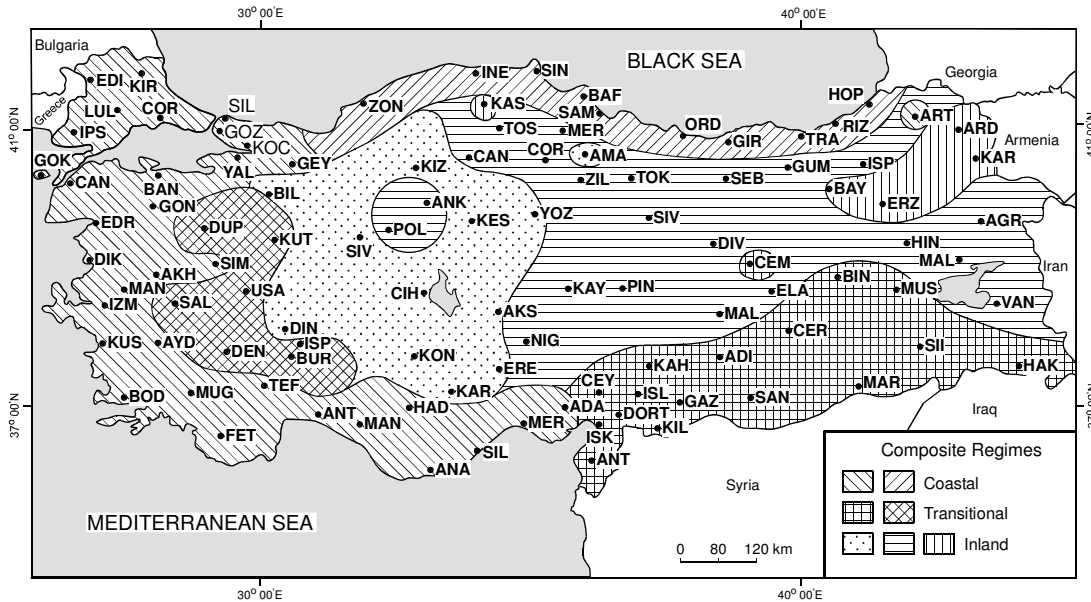


Figure 4.9 Simplification of precipitation regimes of Turkey into coastal, transitional and inland regions.

Figure 4.9 simplifies the complex patterns identified above to illustrate spatially coherent regions that summarize key climate and physiographic controls on precipitation regimes across Turkey. The boundaries of regions map onto physiographic divides; they are indicative, not conclusive. According to Figure 4.9, composite regimes may be classified into three groups:

- *Coastal Regimes*: Regimes 2A, 3A, 4A (clear December peak with intermediate, moderately high and high magnitudes) and 3F, 4F and 5F (marked October peak with moderately high, high and very high magnitudes). This group signifies all coastal areas of Turkey, which are under the consistent control of cyclogenesis and also affected by orographic rains.
- *Transitional Regimes*: Regimes 2B and 3B (December peak and extended rainy period to spring with intermediate and moderately high magnitude). Southeast Anatolia (which was defined as continental Mediterranean rainfall region by Türkeş (1996) and interior west Anatolia (which was defined as Mediterranean Transitional rainfall region by Türkeş, 1996) are classified as transitional regimes because they are controlled by the coupled

effects of frontal and convective rainfall.

- *Inland Regimes*: Regimes 1C, 2C, 1D, 1E and 2E (May peak with low and intermediate magnitude). Continental Anatolia defines this group with a marked rainy spring period and characteristic convective rains.

In summary, the distribution of composite precipitation regimes over Turkey exhibits spatial structure with clear zoning in coastal regions and more complex patterns in transitional zones, interior and high relief regions (except Central Anatolia and Southeast Anatolia) (Figure 4.9).

4.5. Conclusion

This chapter analyses the nature and structure of precipitation regimes across Turkey and, in so doing, provides finer-scale information on intra-annual precipitation dynamics and a more robust regionalization of precipitation regimes. The study refines and extends the existing classifications of Turkish precipitation climatology. Furthermore, this research demonstrates the utility of the novel classification methodology in providing a more objective approach to categorizing two important regime attributes: timing (shape) and magnitude. The emergent regime classes yield the most detailed and systematically joint analyses of spatial variation in magnitude and timing of precipitation across Turkey to date.

Precipitation shape regimes (seasonality) exhibit clear spatial structure from coast to interior. Marked December peak regimes (Regime A) characterise Marmara, coastal Aegean and Mediterranean regions. December peak with extended wet winter (Regime B) is dominant in the interior of Aegean and Mediterranean and Southeast Anatolia regions. The Black Sea coast experiences an October peak (Regime F) while the interior of this region is dominated by a May peak (Regime C). In Central Anatolia, the west experiences an April–May peak

(Regime D) and the east is dominated by a May peak (Regime E). Eastern Anatolia show greatest complexity being characterised by Regime B in the low altitude south, Regime C in the higher altitude east and Regime E in the northeast.

In terms of magnitude, five different regimes are identified: (1) low, (2) intermediate, (3) moderately high, (4) high, and (5) very high. Low magnitude precipitation (Regime 1) occurs across Central Anatolia and the interior parts of the Black Sea and Mediterranean regions. Regime 2 typifies Thrace and Aegean regions. Regime 3 is most evident in Southeast Anatolia, South Marmara, along the Black Sea coast and in the southeast Mediterranean region. Regime 4 is observed at four stations along the south coast of the Mediterranean region and two stations on the Black Sea coast. Very high magnitude precipitation (Regime 5) is restricted to the northeast Black Sea coast.

Composite regimes scale standardised seasonal precipitation response (shape) by size (magnitude), which is necessary to yield a climatologically informative regionalization. The composite classification indicates low magnitude combined with April and May peak regimes characterize inlands areas, namely Central Anatolia and Eastern Anatolia. Intermediate magnitude with December peak regimes dominate in Thrace, the interior Aegean and Southeast Anatolia. These areas may be defined as transitional zones and specify the modified Mediterranean climate regime. Moderately high to very high magnitude occur only for Marmara, Aegean and Mediterranean coasts (December peak) and Black Sea coast (October peak) regimes.

These intra-annual regime classifications indicate the key controls upon spatial patterns in Turkish precipitation to be: (1) large-scale atmospheric circulation during the winter months

for coastal regions of Marmara, Black Sea, Aegean and Mediterranean regions and (2) convectonal rainfall for interior regions that experience a rainy spring. The physiography of Turkey has a major influence on precipitation regimes. High relief and continentality play an important role in causing rainfall deficit for interior regions; and, where mountains are located along the coast, high precipitation occurs, particularly in winter. Eastern Anatolia experiences the most intricate precipitation patterns of any region, which is linked to complex mountainous terrain. The number of gauges for the Eastern Anatolia region is not adequate to fully determine the spatial pattern in precipitation over this region. Likewise, precipitation data for the mountainous regions of the Black Sea and Mediterranean are restricted, since long-term stations are located at <700 m.

This study has refined and extended the understanding of the spatial structure in precipitation regimes over Turkey. These findings are not only of climatological interest; they have practical implications for the assessment and prediction of water resources, particularly given the growing population of Turkey. Indeed, potable water scarcity has been a significant problem for Turkey's major cities in recent years (Beler Baykal *et al.*, 2000). The regimes identified herein show clear spatiality in intra-annual timing and amount of precipitation delivery, which may potentially be used as a basis to inform sustainable water resource management. Moreover, given present concerns about future climate variability, it is important to extend this research on long-term average conditions to understand the year-to-year variability in precipitation and river flows to assess current and potential future water resource stress.

4.6. Chapter summary

In this chapter, the spatial variability of monthly precipitation across Turkey was examined and the precipitation seasonality and magnitude regimes were identified. Coastal, transitional and inland regime types were also divided different type of precipitation regimes within themselves. Chapter 5 will follow the context of this chapter and identifies the extreme precipitation variability across Turkey.

5. LONG-TERM TRENDS IN PRECIPITATION EXTREMES ACROSS TURKEY (1963-2002)

5.1 Introduction

A large proportion of the global land area was affected increasingly by a significant change in frequency of climatic extremes during the second half of the 20th century such as more frequent heavy rainfall events (Frich *et al.*, 2002). These globally observed, widespread and significant increases in precipitation extremes imply a tendency toward wetter conditions throughout the 20th century (Alexander *et al.*, 2006). For the Mediterranean region, the daily extreme precipitation totals (95th percentile) produce significant increasing trends not only for the duration of the rainy season, but also for the period 1950-2000 (Narrant and Douguédroit, 2006).

For Mediterranean countries, several studies were carried out to determine the variability in extreme precipitation events at different spatial scales. For example in Italy, Brunetti (2004), found that the number of wet days showed a negative trend nationally; but northern regions of Italy were characterised by significant increasing trends for daily precipitation intensity during the 20th Century. In northeast Spain for the period 1923 - 2002, Ramos and Martínez-Casasnovas (2006) analysed changes in precipitation concentration during the year by evaluating several indices. They detected an overall increase in precipitation in all indices for winter and summer. The total number of wet days per year increased, which also implies an increase for the extreme events for winter and autumn. Pujol *et al.* (2007) investigated the

changes in monthly and annual maximum series of 92 precipitation gauges in the French Mediterranean region. Their results indicated that monthly maxima have been steadily decreasing for March and increasing for April, which means a shift of rainy days by one month. Significant increases were also detected in annual maxima and in monthly maxima for October, in the southern part of the Massif Central. Houssos and Bartzokas (2006) studied extreme precipitation events in Greece by analysing daily precipitation totals during the period 1970-2002. Although they only considered days with precipitation amounts above 35mm (5% upper limit), a statistically significant minimum frequency of extreme precipitation events was identified for the period 1986–1991 that is linked to a high positive NAO index. Furthermore, important changes were also observed in daily precipitation totals for Greece exceeding various thresholds such as 10, 20, 30 and 50 mm. The increasing trend in the percentage of wet days exceeding specific thresholds is more evident and statistically significant since the decade of 1970 to present (Nastos and Zerefos, 2007). Bartholy and Pongrácz (2007) documented an increase in the regional intensity and frequency of extreme precipitation events, while the total precipitation has decreased for the Carpathian region. For the Middle East, Zhang *et al.* (2005) explain the trends in extreme precipitation events and temperature indices for 15 countries for the period 1950-2003. Trends in precipitation indices show that the number of days with precipitation and the average precipitation intensity together with maximum daily precipitation events, are weak in and do not show any spatial coherence. Although, different seasonality and intensity patterns have been observing in precipitation extremes, it appears the frequency of extreme precipitation events increases while the total precipitation decreases, especially for eastern Mediterranean Basin.

For Turkey, it has been demonstrated by several researchers that the monthly, seasonal and annual precipitation totals indicate significant changes both in space and time (Türkeş 1996

and 1998; Sen and Habib; 2000; Kadioglu *et al.*, 1999a; Tatli *et al.*, 2004; Partal and Kahya 2006; Türkeş *et al.*, 2009; Sariş *et al.*, 2010). Important decreasing trends in annual and winter precipitation totals are highlighted over western and southern coastal regions of Turkey. An earlier study by Tümertekin and Cöntürk (1958), which analysed the maximum daily precipitation totals per year for 223 stations, showed that the daily average maximum precipitation amount ranges from 20 to 150 mm. Continental Anatolia was characterised by 30-40 mm of daily maximum precipitation (10-15% of the annual total), while coastal regions exhibited very high amounts of daily maximum precipitation (90-150 mm). The highest amount of daily precipitation was recorded for sites along the northeast Black Sea coast and for sites located in coastal regions along the southwest Mediterranean coast. However, the changing patterns in precipitation proportion, especially the contribution of high and extreme precipitation events have not yet been analysed in detail for Turkey.

The Mediterranean region is one of the most sensitive areas regarding the predicted precipitation extreme conditions for future climate, since it lies in the transitional zone between the mid-latitudes and sub-tropical zones (Oikonomou *et al.*, 2008). The region is dominated by regular aridity during summer, recurrent periods of drought and extreme precipitation events during rainy seasons (Oikonomou *et al.*, 2008). The observed trends in intensity and frequency of extreme precipitation events must be taken into account in order to achieve a better management of water resources (World Water Assessment Programme, 2009). Therefore, is highly important to evaluate the past changes in extreme precipitation events and to present further regional studies to obtain a clear pattern of climatic extremes.

This chapter aims to present a comprehensive study about the spatiotemporal variability in precipitation extremes by analysing changing patterns in the extreme wet days and for days

with high precipitation totals across Turkey. The following approach is adopted to clarify characteristics of extremes and to elucidate patterns and trends for the period 1963-2002. In particular, for each station (i) the number of wet days per year above the thresholds for 75%, 95% and 99% percentiles and the number of extremely heavy precipitation days which have 60 mm/day precipitation are calculated; (ii) the characteristics of (seasonality and magnitude) extreme precipitation events and regional distinctions based on the precipitation regime regions (Sariş *et al.*, 2010) are identified; and (iii) the amount of precipitation per year for the 75%, 95% and 99% percentiles and number of wet days above the thresholds for 75%, 95% and 99% are analysed to detect long-term trends and change points.

5.2 Data and methods

5.2.1 Precipitation data

Daily precipitation totals for 107 Turkish State Meteorological Service stations were used, selection was based upon record length and to the need provide an optimum spatial coverage across Turkey. A 40-year overlapping record period from 1963 to 2002 was used. This data set was arranged by Sariş (2006) as seasonal series and tested by running *Kruskal-Wallis Homogeneity Test* to control the inhomogeneities in data. For 107 stations, statistical inhomogeneities were identified for winter months of few stations. However, these statistically significant inhomogeneities are related to long-term variations and significant trends (Sariş, 2006; Türkeş *et al.*, 2009). The most recent study on quality control and homogeneity of Turkish precipitation data was carried out by Göktürk *et al.* (2008) who achieved outlier trimming and homogeneity checking and correction on the monthly precipitation totals of 267 stations throughout Turkey (including all stations used in this study). According to the results of this study, the precipitation data for most of the stations were found to be homogeneous against any non-climatic changes. Therefore, the period 1963-

2002 is reliable for time series analysis.

The locations of stations and the precipitation regime regions of Turkey are illustrated in Figure 4.9. In this map, the precipitation regimes of Turkey were classified into three groups: (a) *coastal regimes* (clear December and October peak with moderately high and high precipitation magnitudes), (b) *transitional regimes* (December peak and extended rainy period to spring with intermediate and moderately high precipitation magnitude), and (c) *inland regimes* (May peak with low and intermediate precipitation magnitude).

5.2.2 Methods

5.2.2.1 Extreme indices calculations

The indices of the World Meteorological Organization–Commission for Climatology (WMO–CCL) and the Research Programme on Climate Variability and Predictability (CLIVAR) were adopted for identifying precipitation extreme characteristics (Peterson *et al.*, 2001 and Klein-Tank and Können, 2003). The selected indices of precipitation extremes for analysis were shown in Table 5.1. Daily records were used in order to calculate time series of precipitation extremes at annual scale. The values of the percentile thresholds were determined empirically from the observed station series for the period 1963-2002. The percentiles were calculated using wet days $P > 1$ mm.

For the R75, R95 and R99 indices, the number of wet days that precipitation exceeds the 75, 95 and 99 percentiles is calculated per each year for the period 1963-2002. This specific threshold was calculated from the average of the entire record for each station for the 75th (R75%), 95th (R95%) and 99th (R99%) percentiles. The user defined precipitation days index is calculated by evaluating the number of day's precipitation more than 60 mm/day at a single

station (also suggested by Karagiannidis *et al.* 2009).

Table 5.1 Definitions of the indices used for identifying precipitation extremes.

| Indices of precipitation extremes | | | |
|--|---------------------------------|--|---|
| Index | Description | Formula | Interpretation |
| R75% | Moderately wet days | No. of days RR > 75ptile calculated for wet days | Day count. Percentile threshold of amounts on wet days only |
| R95% | Very wet days | No. of days RR > 95ptile calculated for wet days | Day count. Percentile threshold of amounts on wet days only |
| R99% | Extremely wet days | No. of days RR > 99ptile calculated for wet days | Day count. Percentile threshold of amounts on wet days only |
| R60mm | User defined precipitation days | No. of days precipitation > 60 mm | Day count. Fixed threshold |

In addition to the extreme precipitation indices, the precipitation amounts for each year at the 75th (P75%), 95th (P95%) and 99th (P99%) percentiles were calculated. Thus, the annual x -percentile P_x of the precipitation was obtained to analyse the long-term changes in heavy precipitation amounts.

5.2.2.2 Cluster analysis

Cluster analysis was applied in order to classify precipitation extremes by considering their magnitude (developed by Hannah *et al.*, 2000; adapted by Harris *et al.*, 2000; evaluated by Bower *et al.*, 2004, Kansakar *et al.*, 2004, Hannah *et al.*, 2005a, and Sariş *et al.*, 2010). The magnitude classification is achieved by using long-term average threshold values for the three indices (i.e. the R75, R95 and R99) for each station, regardless of their timing. It was also necessary to standardise between the indices (to control for differences in their relative values) by expressing each index as z -scores across the 107 stations.

The magnitude classification was performed by using Ward's method. The structure of the cluster dendrogram and breaks of slope in the agglomeration schedule (*scree*) plot were used

to determine the appropriate number of clusters (Griffith and Amrhein, 1997). Thus, each of the 107 stations was grouped by magnitude of precipitation extremes and the classification of extreme precipitation magnitude was provided.

5.2.2.3 Mann-Kendall rank correlation

Trend test was employed to the time series of the number of wet days and time series of precipitation percentile amounts [$P_x(i)$, where $i = 1, \dots, t$ years] (Dixon *et al.*, 2006; Osborn *et al.*, 2000). Trends in wet days above a specific threshold (R75, R95 and R99) were analysed in order to understand the inter-annual variability in the number of (1) moderately wet, (2) very wet and (3) extremely wet days. Trends in high precipitation percentiles were also detected for delineating the long-term change of precipitation intensity. Three precipitation percentiles (P75), (P95) and (P99) was determined which indicate (i) high precipitation; (ii) very high precipitation, (iii) extreme precipitation, respectively.

Long-term trends in extreme precipitation series were detected by using the M-K rank correlation test (WMO, 1966). The M-K is a distribution-free test and is suitable for non-normally distributed data, which are frequently encountered in hydrometeorological time series (WMO, 1966). Its non-linearity together with it being a non-parametric test of a significance for a trend should be considered, because series of climatic observations mostly do not have the Gaussian distribution or other specific form of distribution (e.g., Student t , Gamma, etc.) and therefore do not show linear-type long-term variations. Test statistics which are above the 5% and 1% significance levels ($\alpha \leq 0.05$ and 0.01 of two-tailed test) were accepted as significant.

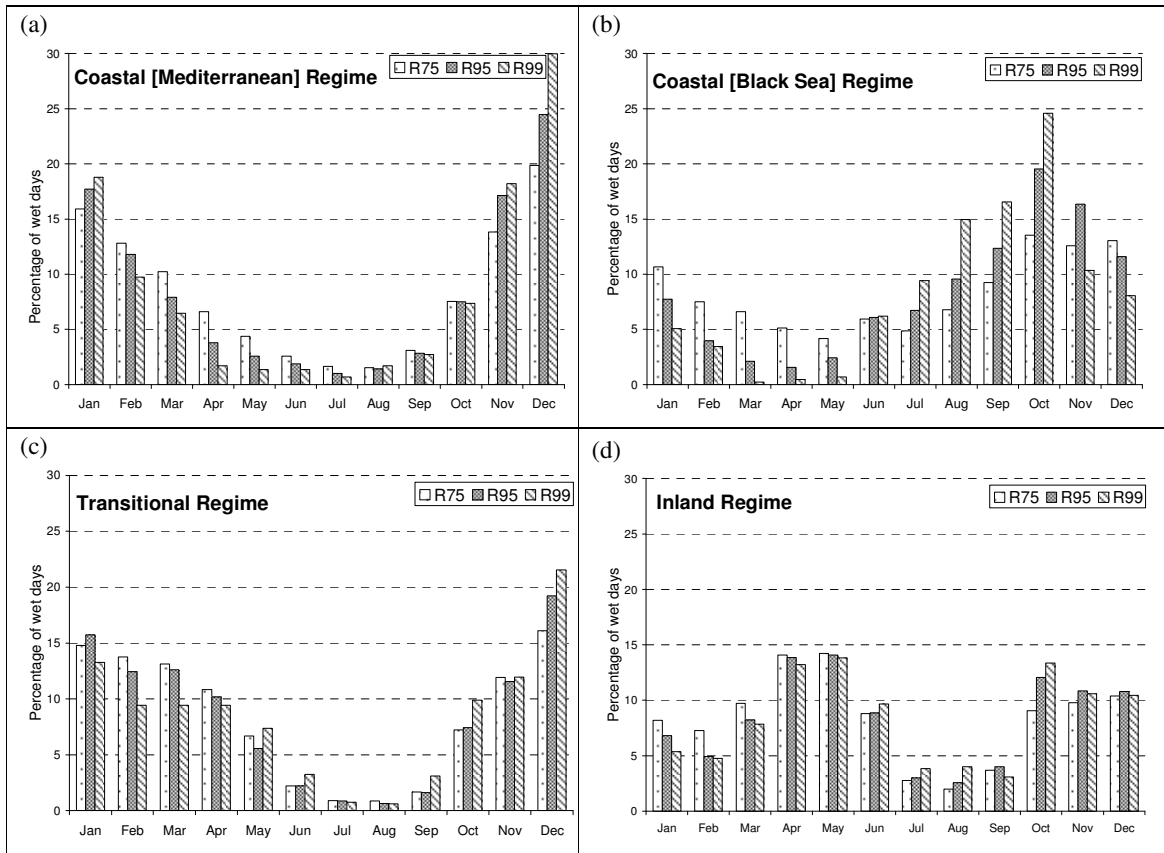


Figure 5.1 Intra-annual variability in percentage of moderate wet (R75), very wet (R95) and extremely wet days (R99) among the precipitation regime regions.

5.3 Patterns in precipitation extremes

The extreme precipitation climatology of Turkey is evaluated in this section by explaining the intra-annual variability patterns, magnitude of extreme events and regional differences.

5.3.1 Seasonality and magnitude characteristics of precipitation extremes

The number of days which are categorised as moderately wet days (R75), very wet days (95) and extremely wet days (R99) were evaluated to show the intra-annual variability for each regime region (Figure 5.1). The coastal regime region is represented by two sub-regions that discriminate the nature of seasonality within this regime region. The Mediterranean coastal region has a typical Mediterranean climate with enhanced seasonality and having higher number of wet extremes during winter months (Figure 5.1a). The highest percentage values

were detected (ranging between 15% and 30% days per month) in December and January, while the long period spanning from May to September can be defined with low percentage values below 8%. The Coastal Black Sea regime is delineated by high percentage in October consisting of 25% of the annual total (Figure 5.1b). Higher wet period was observed for September-December. The periods with least wet extreme episodes are spring. The percentage of wet days ranged between 8% and 2% for this period. The transitional regime has a long period with less than 5%, which is represents an extended summer (to September) (Figure 5.1c). The autumn, winter and spring period show similarity in terms of their contribution percentages to the annual total. However, December has a distinct character with the highest percentage (22%). The monthly proportion of wet days is less than 15% for the inland regime, which is fairly distributed throughout all seasons, although lower proportions occur during summer months (below 5%). April and May represents the peak period in terms of extreme event occurrence for the inland regime region (Figure 5.1d).

The average threshold values of stations for each regime region are used to display magnitude characteristics of extreme precipitation indices among the precipitation regime regions using Box and Whiskers plots (Figure 5.2). Box plots indicate that the highest values are observed for coastal regime region for all threshold levels. The transitional regime region is defined with high and/or moderate threshold values, while the inland regime is represented by low percentile values. The range for the 75 percentile threshold spans between 8- 23 mm for the coastal, 8-20 mm for the transitional and 7-10 mm for the inland regimes (Figure 5.2a; values are not given in the figures). For the coastal regime, the threshold amounts can reach up to 76 mm and 154 mm for at the 95% and 99% levels, respectively. However, the maximum threshold values are less than 85 mm and 40 mm for the transitional and inland regimes, respectively. Although it seems that the coastal and transitional regimes have similar

threshold values for R75, the precipitation amount is remarkably high for R95 and R99 for coastal regime compared with transitional and inland regime regions (Figures 5.2b and 5.2c).

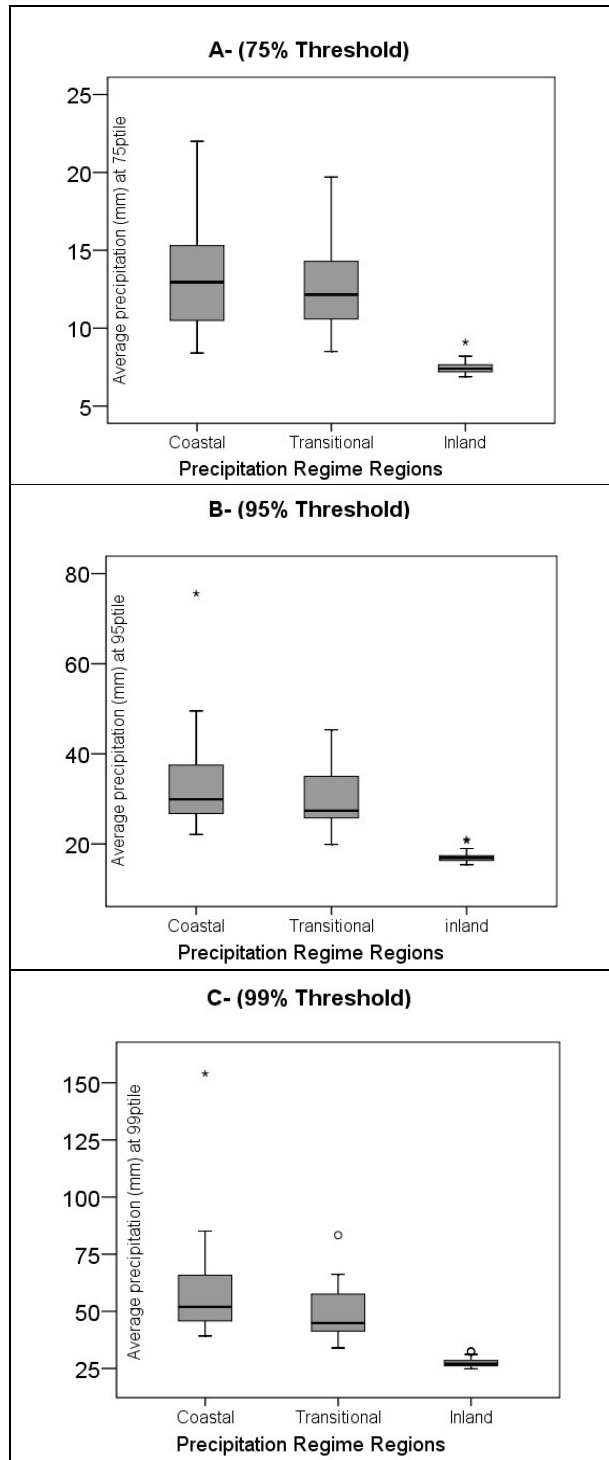


Figure 5.2 Box and Whiskers plots of precipitation regime regions for extreme precipitation threshold values.

5.3.2 Extremely heavy precipitation days

The number of days having more than 60 mm/day precipitation at a single station was calculated to detect the changes in frequency of days with extremely heavy precipitation events among the precipitation regime regions during the last four decades. Table 5.2 summarises the results for the calculation of the number of days with extremely heavy precipitation amounts. The number of events is 2069 for the period 1963-2002 across 107 stations. The number of events for sub-periods of 4 decades was calculated. When total events are allocated into sub periods, it is apparent that there is no clear decadal variability over the 40 year time span. The percentage of extreme precipitation events is quite high for the coastal regime regions and exceeds 75% for the entire period. The proportion for the transitional regime ranges from 15% to 19%, while the inland regime is only represented by less than 2% of the extreme precipitation events. It is interesting to note that during the last decade (1993-2002), the number of extreme precipitation events for the transitional regime has decreased notably, while those for the coastal regime have increased (Table 5.2). Figure 5.3 illustrates the percentage values for extremely heavy precipitation events per month for all detected (2069) events. For autumn and winter months 35% and 41% of the extreme precipitation events are recorded, respectively. December has the highest proportion with 20% of the total events.

Table 5.2 The percentage of events defined with extremely heavy precipitation amounts.

| Period (87 Stations) | Number of Events | Percentage by region (%) | | |
|----------------------------|------------------------|--------------------------|---------------------|---------------|
| | | <i>Coastal</i> | <i>Transitional</i> | <i>Inland</i> |
| 1963-2002 | 2069 | 81.39 | 17.21 | 1.40 |
| 1963-1972 | 534 | 80.34 | 18.35 | 1.31 |
| 1973-1982 | 496 | 79.84 | 18.95 | 1.21 |
| 1983-1992 | 471 | 81.10 | 17.41 | 1.49 |
| 1993-2002 | 568 | 83.98 | 14.44 | 1.58 |

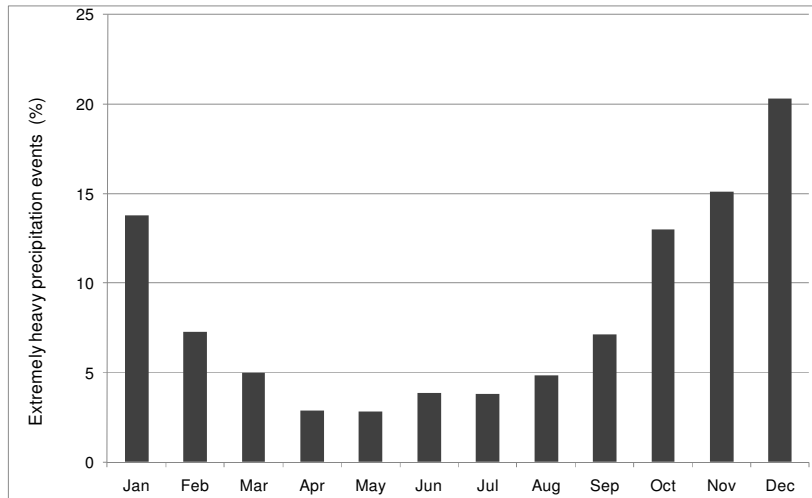


Figure 5.3 The intra-annual variability of the extremely heavy precipitation events.

5.3.3 Regional characteristics of precipitation extremes

The spatial distribution of magnitude regime characteristics for precipitation extremes are derived from classifying average annual precipitation values for the 107 stations at R75, R95 and R99 percentiles exceedance thresholds. Four classes successfully define the spatial variability for magnitude regimes of precipitation extremes (Table 5.3):

- Class 1. Low with the lowest values for three annual indices (37 stations).
- Class 2. Intermediate with second lowest values for all indices (44 stations).
- Class 3. Moderately-high with the second highest values for all indices (19 stations).
- Class 4. High with the highest values for all indices (7 stations).

Magnitude classes of precipitation extremes indicate the large gradient across Turkey. The annual averages of threshold values span from 7.5 mm to 96.5 mm.

Figure 5.4 illustrates the spatial distribution of magnitude classes. Regime 1 indicates the lowest percentile amount of precipitation extremes, and corresponds spatially to Central and Eastern Anatolia but also predominates in the more inland parts of the Black Sea region. Regime 2 is concentrated mainly on transitional areas between coastal and more inland regions and also includes northwest Turkey (Thrace). This regime demonstrates the

distribution of the intermediate percentile amounts of precipitation extremes, which is the most prominent magnitude class throughout the country. Regime 3 is located clearly in the Aegean region and Southeast Anatolia and also partly in the Black Sea coastal region. Regime 3 can be defined by the high percentile magnitudes which represents the second highest percentile amounts. Two stations located on the northeast coast of the Black Sea region correspond with the coastal stations along the south coast of the Mediterranean region are identified with Regime 4, which is characterised by the highest percentile amount of precipitation extreme events.

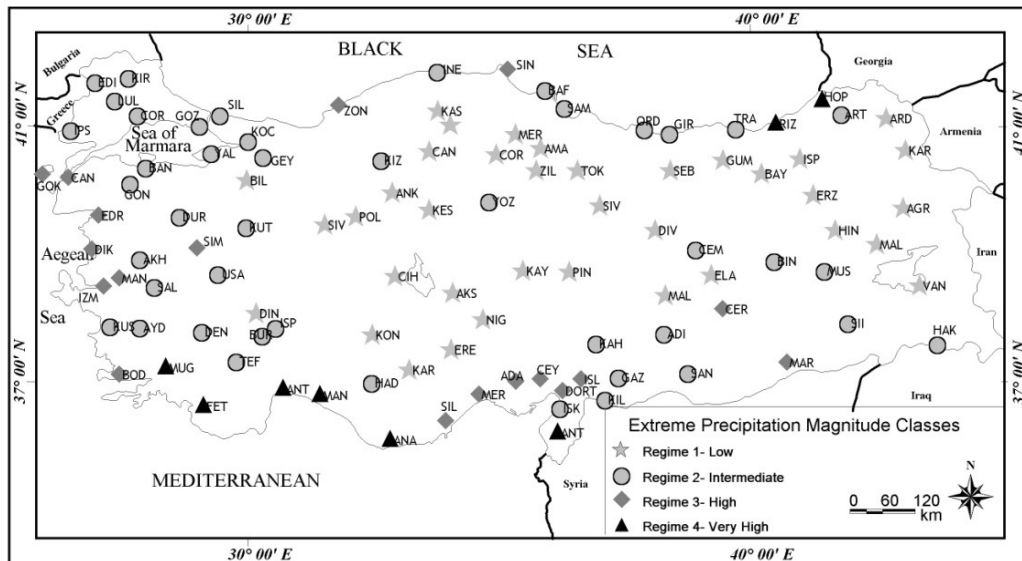


Figure 5.4 Spatial distribution of extreme precipitation magnitude regime classes across Turkey.

Table 5.3 Average precipitation amount (mm) of thresholds for extreme precipitation indices within the four regime magnitude classes (1: low; 2: intermediate; 3: high; 4: very high).

| Class Average | | | | | |
|-----------------|------|------|------|------|----------------|
| Thresholds | 1 | 2 | 3 | 4 | (All Stations) |
| R75 | 7.5 | 11.2 | 14.7 | 21.4 | 11.2 |
| R95 | 17.2 | 27.1 | 36.6 | 55.4 | 27.2 |
| R99 | 27.8 | 45.2 | 65.4 | 96.5 | 46.1 |
| No. of stations | 37 | 44 | 19 | 7 | 107 |

5.4 Trend analysis

Long-term trends in the annual series of the number of extreme precipitation events and precipitation percentile amounts of 107 stations in Turkey were also analysed by considering their spatial and temporal variability. Table 5.4 and Table 5.5 summarize the results of M-K test obtained for precipitation extreme events and precipitation percentile series, respectively.

5.4.1 Trends in precipitation extremes

Results of trend analysis indicate that the number of wet days have not statistically changed over the period 1963-2002. The rate for significant decreasing or increasing trends is quite low for all precipitation extreme indices for Turkey (Table 5.4). Figure 5.5 shows the geographical distribution of the long-term trends in extreme precipitation events. Although there is not any clear spatial coherence, there is a decreasing tendency that can be observed in the west, northwest, and southeast of the Turkey for moderately wet days (Figure 5.5a). These areas are mainly represented by coastal and transitional regimes that are characterised by a winter peak and a dry summer with moderate and high precipitation amounts. Continental Anatolia and the northeast Turkey regions show an increasing trend for all variables. Similar to the increasing tendency, the decreasing trends are not statistically significant and only detected for individual stations. The trend analysis results of precipitation extremes do not imply any substantial changing pattern for the number of moderately wet, very wet and extremely wet days (Figure 5.5a, 5.5b and 5.5c).

5.4.2 Trends in precipitation percentiles

A relatively strong and consistently increasing trend in the precipitation percentile series can be detected especially for P75 and P95 (Table 5.5). The rate of positive trends is more than 70% for Turkey as a whole for both high and very high precipitation series. The spatial

pattern of changing conditions is illustrated in Figure 5.6. Two regions can be distinguished by having geographically coherent results. In northwest Turkey, the stations around the Marmara Sea and the Aegean coast (western Turkey) are defined with strong increasing trends for both the P75 and P95 series (Figure 5.56a and 5.6b). This observed increasing trend in the amount of high and very high precipitation series might indicate important changing conditions in daily precipitation intensity. For extreme precipitation (P99) series, the test results are not significant (Figure 5.6c).

Table 5.4 Results of trend analysis for extreme precipitation indices among the precipitation regime regions.

| R(75)-Moderate Wet Days | | Decreasing | | Significant Decreasing | | Increasing | | Significant Increasing | |
|--------------------------|-------------------|-------------|----------|------------------------|----------|-------------|----------|------------------------|----------|
| Region | Number of Station | Num. of St. | Rate (%) | Num. of St. | Rate (%) | Num. of St. | Rate (%) | Num. of St. | Rate (%) |
| Coastal Regimes | 44 | 25 | 56.82 | 1 | 2.27 | 18 | 40.91 | 0 | 0.00 |
| Transitional Regimes | 24 | 16 | 66.67 | 3 | 12.50 | 5 | 20.83 | 0 | 0.00 |
| Inland Regimes | 39 | 20 | 51.28 | 0 | 0.00 | 17 | 43.59 | 2 | 5.13 |
| TURKEY | 107 | 61 | 57.01 | 4 | 3.74 | 40 | 37.38 | 2 | 1.87 |
| R(95)-Wet Days | | Decreasing | | Significant Decreasing | | Increasing | | Significant Increasing | |
| Region | Number of Station | Num. of St. | Rate (%) | Num. of St. | Rate (%) | Num. of St. | Rate (%) | Num. of St. | Rate (%) |
| Coastal Regimes | 44 | 14 | 31.82 | 2 | 4.55 | 28 | 63.64 | 0 | 0.00 |
| Transitional Regimes | 24 | 18 | 75.00 | 2 | 8.33 | 4 | 16.67 | 0 | 0.00 |
| Inland Regimes | 39 | 15 | 38.46 | 0 | 0.00 | 23 | 58.97 | 1 | 2.56 |
| TURKEY | 107 | 47 | 43.93 | 4 | 3.74 | 55 | 51.40 | 1 | 0.93 |
| R(99)-Extremely Wet Days | | Decreasing | | Significant Decreasing | | Increasing | | Significant Increasing | |
| Region | Number of Station | Num. of St. | Rate (%) | Num. of St. | Rate (%) | Num. of St. | Rate (%) | Num. of St. | Rate (%) |
| Coastal Regimes | 44 | 18 | 40.91 | 3 | 6.82 | 22 | 50.00 | 1 | 2.27 |
| Transitional Regimes | 24 | 13 | 54.17 | 0 | 0.00 | 11 | 45.83 | 0 | 0.00 |
| Inland Regimes | 39 | 16 | 41.03 | 1 | 2.56 | 20 | 51.28 | 2 | 5.13 |
| TURKEY | 107 | 47 | 43.93 | 4 | 3.74 | 53 | 49.53 | 3 | 2.80 |

Table 5.5 Results of trend analysis for precipitation percentile amounts among the precipitation regime regions.

| P(75)-High Precipitation | | Decreasing | | Significant Decreasing | | Increasing | | Significant Increasing | |
|-------------------------------|-------------------|-------------|----------|------------------------|----------|-------------|----------|------------------------|----------|
| Region | Number of Station | Num. of St. | Rate (%) | Num. of St. | Rate (%) | Num. of St. | Rate (%) | Num. of St. | Rate (%) |
| Coastal Regimes | 44 | 7 | 15.91 | 0 | 0.00 | 28 | 63.64 | 9 | 20.45 |
| Transitional Regimes | 24 | 8 | 33.33 | 1 | 4.17 | 13 | 54.17 | 2 | 8.33 |
| Inland Regimes | 39 | 11 | 28.21 | 1 | 2.56 | 19 | 48.72 | 8 | 20.51 |
| TURKEY | 107 | 26 | 24.30 | 2 | 1.87 | 60 | 56.07 | 19 | 17.76 |
| P(95)-Very High Precipitation | | Decreasing | | Significant Decreasing | | Increasing | | Significant Increasing | |
| Region | Number of Station | Num. of St. | Rate (%) | Num. of St. | Rate (%) | Num. of St. | Rate (%) | Num. of St. | Rate (%) |
| Coastal Regimes | 44 | 10 | 22.73 | 0 | 0.00 | 29 | 65.91 | 5 | 11.36 |
| Transitional Regimes | 24 | 10 | 41.67 | 1 | 4.17 | 13 | 54.17 | 0 | 0.00 |
| Inland Regimes | 39 | 7 | 17.95 | 0 | 0.00 | 25 | 64.10 | 7 | 17.95 |
| TURKEY | 107 | 27 | 25.23 | 1 | 0.93 | 67 | 62.62 | 12 | 11.21 |
| P(99)-Extreme Precipitation | | Decreasing | | Significant Decreasing | | Increasing | | Significant Increasing | |
| Region | Number of Station | Num. of St. | Rate (%) | Num. of St. | Rate (%) | Num. of St. | Rate (%) | Num. of St. | Rate (%) |
| Coastal Regimes | 44 | 19 | 43.18 | 2 | 4.55 | 23 | 52.27 | 0 | 0.00 |
| Transitional Regimes | 24 | 14 | 58.33 | 0 | 0.00 | 10 | 41.67 | 0 | 0.00 |
| Inland Regimes | 39 | 14 | 35.90 | 0 | 0.00 | 23 | 58.97 | 2 | 5.13 |
| TURKEY | 107 | 47 | 43.93 | 2 | 1.87 | 56 | 52.34 | 2 | 1.87 |

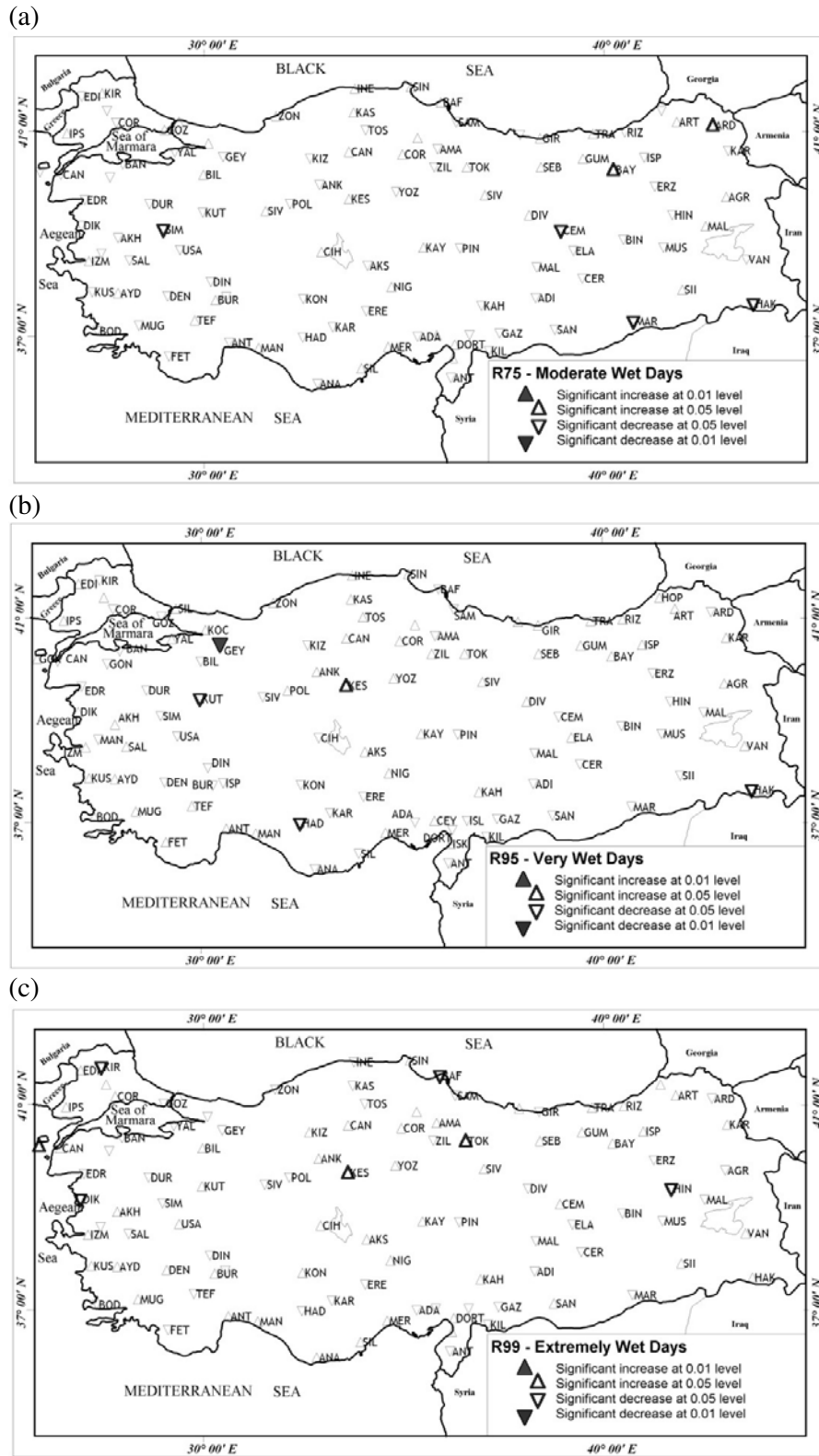


Figure 5.5 Spatial distribution of the long-term trends of annual precipitation extremes across the Turkey: (a) R75, (b) R95 and (c) R99.

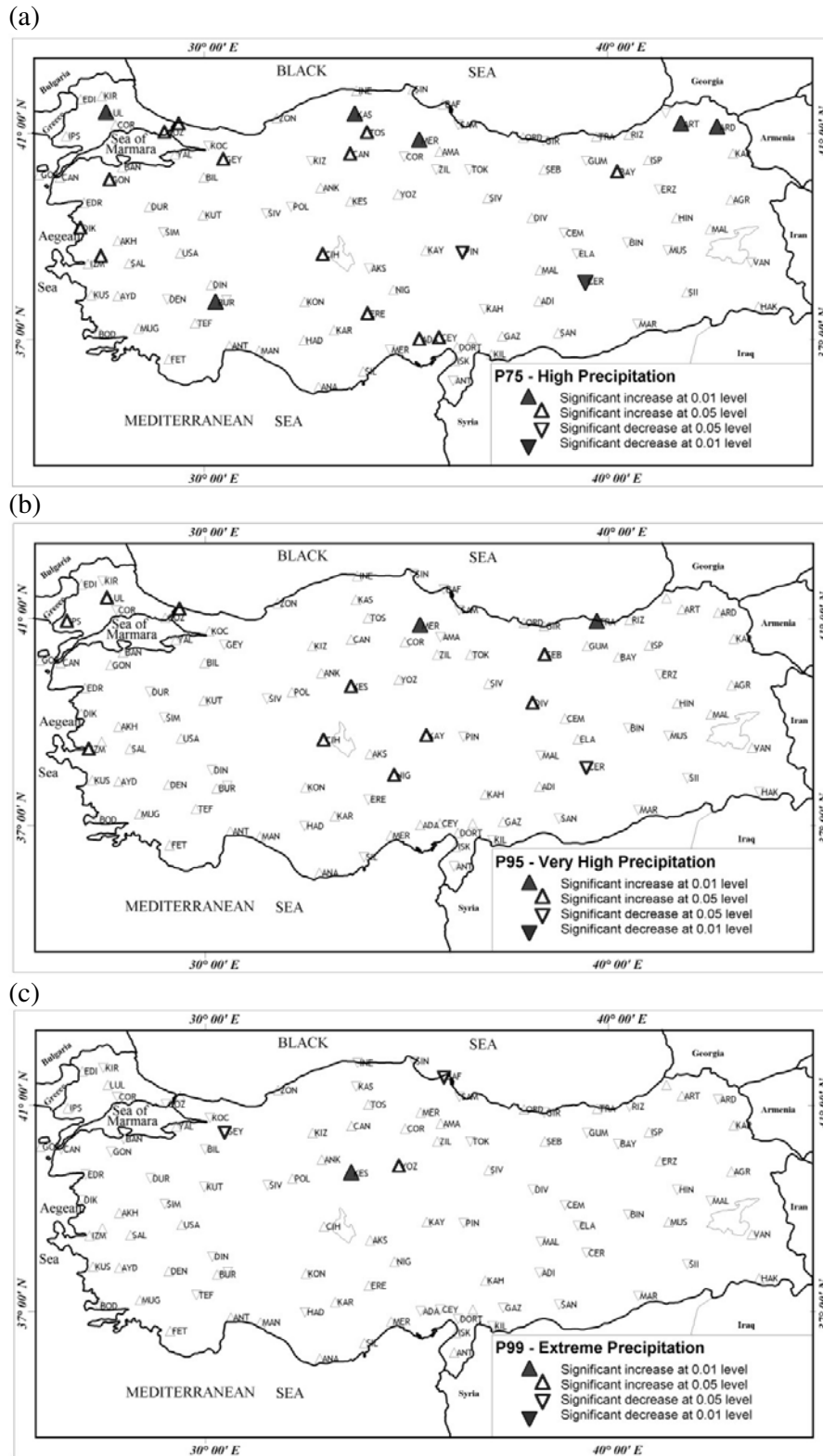


Figure 5.6 Spatial distribution of the long-term trends of annual precipitation percentiles across the Turkey: (a) P75, (b) P95 and (c) P99.

5.4.3 Inter-annual fluctuations and change points

Year-to-year variability and change points in P75 series can be shown by plotting graphics of annual series and long-term averages. Figure 5.7 shows the time-based changes for some stations that were designated as statistically significant. This approach improves understanding of temporal change in high precipitation amounts. A five-point Gaussian filter (as a low-pass filter) was selected to allow visual inspection of the long-term fluctuations in the series.

For Luleburgaz (LUL), an increasing trend can be discerned (Figure 5.7a). The amount of at P75 has a strong increasing episode which become clear for the period 1982-2001. Çermik (ÇER) illustrates negative trends for transitional regime (Figure 5.7b). The P75 series display important decreases, which are stronger for the last two decades of the observation period. This decreasing trend started in 1981 and persisted for a 20 years period. Burdur (BUR) demonstrates long-term increasing trend for transitional regime region (Figure 5.7c). This increasing tendency has showed a weak but consistent behaviour, with the trend strengthening after 1997. Merzifon (MER) shows long-term changes in extreme precipitation amount for inland regime regions (Figure 5.7d). The main trend was strong increasing, which has been prevailing for the last two decades of the study period.

All time series plots from sample stations indicated an evident change in high precipitation pattern for a particular time. This changing point was identified by early 1980s. Therefore, two equal 20 years period are designated as 1963-1981 and 1982-2002 and the means of time series for these periods were tested by using t-test to assess whether the means of two periods are statistically different from each other and the significance of the difference for the means

of two periods were found. Statistically significant difference was obtained for all sample stations which proved that the changing conditions has become more evident and persistent by early 1980's. This situation also implies a strong variability for the precipitation amounts across Turkey and a clear shift to the drier (wetter) conditions than normal, for selected stations having decreasing (increasing) trends.

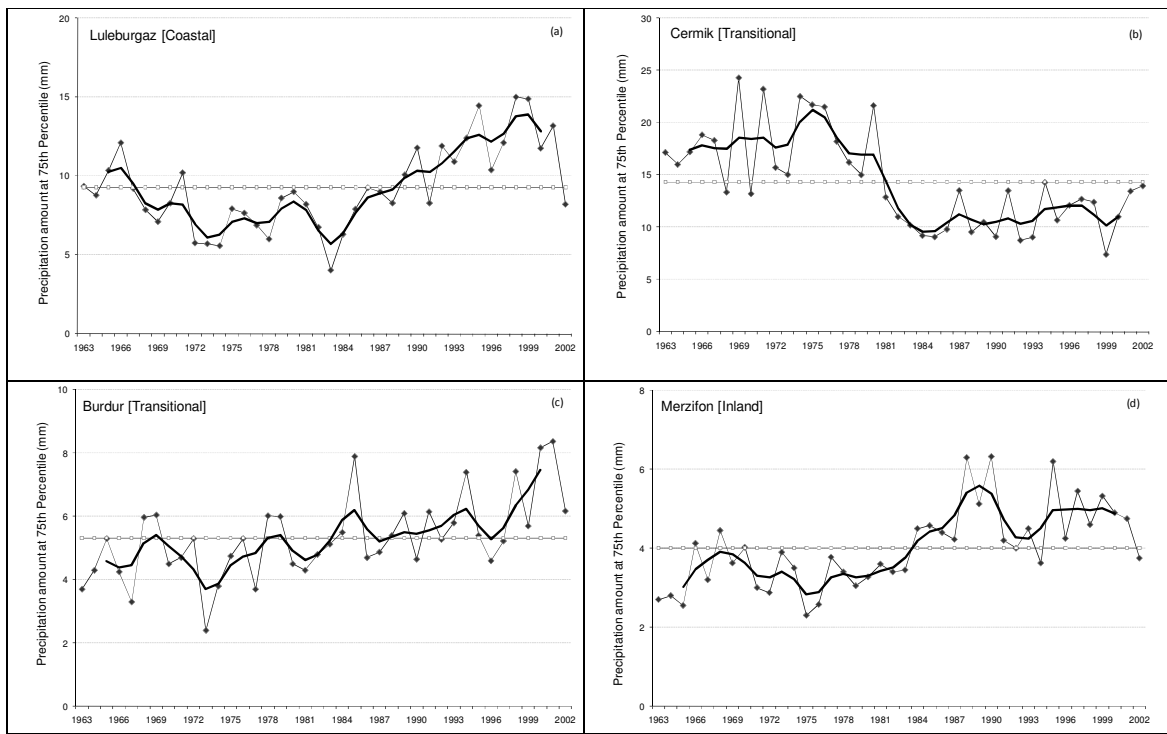


Figure 5.7 Year to year variations (—◆—) in annual precipitation for 75% percentile series at selected representative stations of precipitation regime regions [(—) and (—○—○—) displays the Gaussian Filter and the long-term average of the series, respectively].

5.5 Discussion and conclusion

This chapter aimed to define spatiotemporal variability in precipitation extremes by analysing extreme wet days and high precipitation totals for Turkey. The results reveal that the coastal regime regions have the highest proportion of precipitation extremes. All the approaches examined suggest that the maximum frequency of extreme precipitation events and the highest precipitation amount have been obtained for the Mediterranean and Black Sea coastal regimes. The peak time of extreme precipitation events is December in Mediterranean coastal

region and October in Black Sea coastal region. In transitional regime region, the number of wet extremes is quite similar with Mediterranean coastal regime; but the amount of precipitation is lower than Mediterranean region for the selected percentiles. For the inland regions, both the number of extreme precipitation events and the amount of precipitation for selected percentiles are relatively low. The magnitude regionalisation of average precipitation percentiles reveals that the coastal and transitional regions are important zones in terms of representing the high and very high precipitation extremes.

The seasonality of the number of wet days displays that October, December and January are the most significant months in terms of frequency of extreme precipitation events, which are observed mostly in coastal and transitional regime regions. The higher precipitation extremes periods of December-January and October can be explained by winter rainfall supplied from mid-latitude (northeast Atlantic) and Mediterranean depressions which are most active during winter and by the frequent northeastern Atlantic originating depressions in autumn (Karaca *et al.*, 2000; Trigo *et al.* 1999). The coastal regime regions represent almost half of the observed events. The obtained results imply that, the timing and the observed frequency of extreme precipitation events across Turkey is highly related with the winter conditions, which are characterised by large-scale circulation patterns originated from North Atlantic and Mediterranean Basin and influential on annual regimes of coastal and transitional regime regions of Turkey (Türkeş, 1998; Kostopoulou & Jones, 2007; Sariş *et al.*, 2010). Moreover, extreme events are also related with orographically enhanced frontal rainfall pattern for the coastal regions which high precipitation for these coastal locations is the combined result of frontal and orographic rains (Sariş *et al.*, 2010).

The long-term trends in precipitation extreme events were detected by analysing the year to

year changes in the time series of wet extreme events for different thresholds (R75, R95 and R99). The Mann-Kendall test results revealed a weak serial correlation for extreme days variability and very few statistically significant decreasing trends were detected in the time series. However, it does not identify any spatially coherent pattern. The amount of precipitation per year at the P75, P95 and P99 percentiles was tested in order to explain the changing conditions in daily precipitation intensity. The precipitation percentile amounts significantly increased during the observation period. An increasing trend is detected for all three exceedance thresholds; and this tendency is consistent for almost all of Turkey at P75. All significant results specify a strong increasing trend, except for two stations. The strongest trend was observed for high precipitation amounts (P75). Mediterranean and Aegean coastal zones and Thrace were characterised by positive trends in high and very high precipitation (P95) series. Continental Anatolia exhibited increasing trends for high and very high precipitation, with a very strong and spatially consistent trend in continental northeast Anatolia. The observed increasing tendency has been strengthened after 1980 and continued for the last 20 years of the observation period. Extreme precipitation series (P99) have not been identified by any considerable or comprehensive trends, unlike the high (P75) and very high precipitation (P95).

The observed trends in precipitation extremes have some commonality with other Mediterranean-based work (Brunetti, 2004; Zhang *et al.*, 2005; Norrant and Douguédroit, 2006; Nastos and Zerefos, 2007 and Bartholy and Pongrácz, 2007) that indicates a decreasing number of wet days but a notable increase in intensity of heavy rainfall. In contrast with the results of annual precipitation totals, Turkish precipitation extremes show an increasing trend, which is most marked in coastal regions. Importantly, the findings demonstrate an important differentiation for the variability patterns between mean precipitation and extreme

precipitation.

These results imply an enhanced heavy precipitation proportion and also a growing risk of hazardous events such as floods and landslides. Considering the increased frequency and intensity of hydro-meteorological hazards over Turkey (Ceylan and Kömüşçü, 2007a and 2007b), the results of precipitation analyses must be evaluated with high priority.

5.6 Chapter summary

This chapter has examined extreme precipitation characteristics of Turkey and found that the northeast and southwest coastal regions of Turkey are characterised by the highest frequency of extreme precipitation events. The hydroclimatological characteristics of northeast region of Turkey will be analysed in the next chapter to identify climate regime patterns of northeast Turkey and to examine long-term (inter-annual) trends in climatological variables.

6. DEFINING CLIMATIC REGIONS AND VARIABILITY IN NORTHEAST TURKEY (1981-2007)

6.1. Introduction

Mediterranean countries are located within the sub-tropical zone that is characterised by highly variable climatic regimes, including severe rainfall events as well as prolonged dry and warm periods (Bolle, 2002). Hence, Mediterranean countries (such as Turkey) are sensitive and highly vulnerable to future climatic shifts. Simulations for Turkey (e.g., Apak and Ubay, 2007) indicated that generally, temperatures are predicted to increase (annual mean temperature rise estimated to be around 2-3°C for the entire country) with winter time temperature increases projected to be higher in the eastern half of the country. Alongside increases in average annual temperatures, model results suggest significant changes in precipitation including a decrease in winter and spring precipitation along the Aegean and Mediterranean coastal regions while a substantially more precipitation is predicted for the Black Sea coastal region of Turkey (Apak and Ubay, 2007). Therefore, the modern analysis of spatiotemporal variability in climate regimes and extremes at long-term time scales is a significant contribution as underpinning of the mechanisms and processes driving the variability. Since the development of adaptation strategies to safeguard the sustainability of socio-economic and ecological systems is crucial; improvement of this knowledge can also help inform adaptation plans and management decisions (Climate Change, 2007).

Previous studies of the climatic variability of Turkey do not adequately explain intra-regional or local scale variability; and this is especially pertinent for the northeast part of the country which covers a relatively large area, has a with a distinct climate (Sariş *et al.*, 2010, Türkeş 1996, 1998, Ünal *et al.*, 2003) and variable physiographic characteristics (Figure 6.1; Akcar *et al.* 2007). Tatli *et al.* (2004) conclude that present climate models are not sufficiently resolved to capture completely and explain the controlling climatic factors for the northeast region of Turkey region due mainly to the complex topography of the region. To date, the northeast region of Turkey has been understudied; only in the northwest section of northern Turkey has detailed research been undertaken on streamflow and precipitation variability and the projected impacts of future climate change and climate variability (Akkemik *et al.*, 2007; Aksoy *et al.*, 2007; Alexandrow *et al.*, 2005). National scale studies are inherently useful in highlighting the broad principal variability aspects of climate but lack detail of sub-regional patterns. These national scale studies highlight the particular hydroclimatological features of the Black Sea region and how it substantially differs from other regions (e.g. Türkeş 1996, 1998, Türkeş *et al.*, 2009; Kadioglu 2000, Kadioglu *et al.*, 1999, Sen and Habib 2000). Nevertheless, the shortcomings of knowledge on the regional aspects of climatic regimes, extremes and influence on river flow variability motivate to undertake a regional-scale study.

Northeast Turkey includes the North Anatolian mountain range (local name is East Black Sea Mountains) with many peaks exceeding elevations of 3000 m and capped with extant glaciers. Precipitation totals and river flow discharge volumes for the region are relatively high which significantly increases the likelihood of major flood and landslide events as well as the potential to provide freshwater (Ergünay, 2007). Northeast Turkey is also an important part of the Caucasian Ecological Corridor; however, these special ecological and hydrological

systems are under excessive pressure of several ongoing and planned dam and hydroelectric power plant projects (Berkun, 2010; Uzlu, 2011). Regional to local scale studies focusing on spatiotemporal variability of sub-regional and catchment scale climatological characteristics have the potential to increase the scientific knowledge and understanding of climatic variability. For this reason, instrumental climatological data from surface meteorological stations in northeast Turkey requires systematic analysis using a range of modern hydroclimatic analytical methods at high time resolutions to (i) define and highlight regional climate regimes and fluctuations, (ii) to examine intra-regional variations and (iii) to relate emergent patterns to the physiographic characteristics and climatological processes.

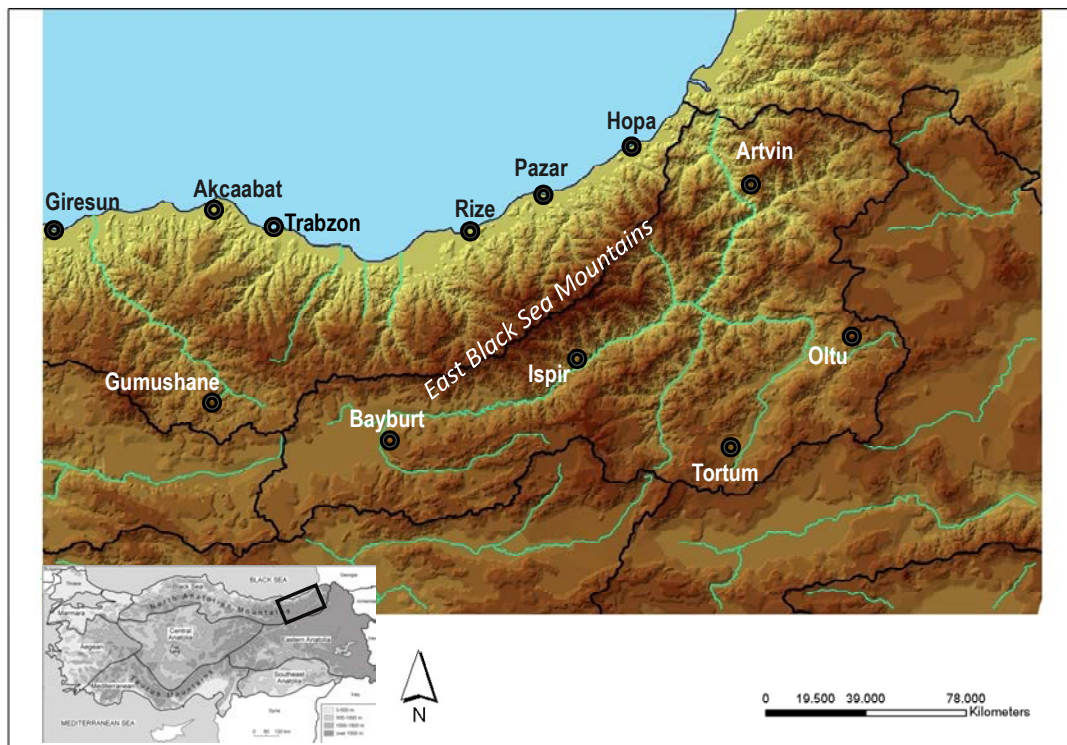


Figure 6.1 Basic characteristics of study area and locations of meteorological stations.

Given this context, the overall aim of this chapter is to define, for the first time, the climatic characteristics of northeast Turkey using a multivariate classification approach and to detect space-time changes in climate regimes over the last three decades. This will be achieved

through the analysis of: (i) the spatiotemporal variability of several meteorological variables (mean, maximum and minimum air temperature, precipitation, cloudiness and relative humidity) to establish climatic regimes of northeast Turkey and to highlight regions with similar seasonality and magnitude regimes; (ii) annual water budgets and their relationship with climate type; and (iii) year-to-year trends to highlight long-term patterns of variability over the last three decades.

6.1.1. Background on eastern Mediterranean and Turkish climate

Climate variability across Turkey is predominantly influenced by the coupled effects of large-scale atmospheric circulation, physical characteristics such as geomorphology, the marine effect and continentality. Climatic conditions in winter in the eastern Mediterranean are predominantly controlled by strong westerly/north westerly circulation originating from northern Europe, whereas in summer circulation is controlled by the Atlantic (Azores) anticyclone and the Asian Thermal Low (Kostopoulou and Jones 2007). In autumn, the region is characterised by a rapid transition from warm to cold seasons showing climatic features for both summer and winter seasons (Kostopoulou and Jones 2007) and Xoplaki *et al.* (2004) have shown that October to March precipitation variability of the Mediterranean basin is directly influenced by large-scale circulation patterns over North Atlantic. The controlling influence of these large scale seasonal shifts in the position of the dominant pressure systems, air masses and main cyclone trajectories over Turkey have been discussed in previous studies (Karaca, Deniz and Tayanç, 2000; Tatli, *et al.*, 2004)) and recently summarised by Sariş *et al.* (2010). The seasonal variation of the polar jet is also highly effective especially on climatic conditions for coastal regions of Turkey. The increasing effect of higher elevations and ‘topographic ruggedness’ towards the east of the country are an important determinant in the climatic variability of continental Anatolia (Tatli *et al.*, 2004).

Generally, Turkey is described as having a warm, moderate climate with the highest maximum summer temperature recorded in the southeast of the country. Temperatures decrease gradually towards the northwest and northeast. At lower elevations, coastal regions are warmer than the more inner or continental regions, which are generally separated from the coastal regions by high mountain ranges on north and south. On average, Mediterranean coastal regions record the highest temperatures, followed by the Aegean, then Marmara and then the western part of the Black Sea coastal region. In eastern Anatolia, owing to continental effects and higher elevations, there is a widespread temperature decrease with increasing distance from the coast (Tatli *et al.*, 2005). Regional climatic differences of Turkey have been mostly investigated through the analysis of precipitation regime classification (*cf.* Türkeş, 1996; 1998; Kadioglu *et al.* 1999; Kadioglu, 2000; Sen and Habib, 2000; Türkeş, Koc and Sariş, 2009; Sariş *et al.* 2010). For precipitation, Turkey has been identified by coastal regime characteristics over the Mediterranean coast with a winter rainfall peak. A marked autumn precipitation prevails along the Black Sea coast. Inland areas exhibit spring rainfall maxima; while the transitions areas on the west and the southeast Anatolia were defined with modified Mediterranean climate regime displaying both coastal and continental character. Northeast Turkey region is represented by both coastal and inland precipitation regimes and evaluated as a climatologically distinct region (Sariş *et al.*, 2010). Ünal *et al.* (2003) redefined the climate zones of Turkey using cluster analysis for regionalization. They identified seven different climate zones, as in conventional climate zones defined by Erinç (1984), but with considerable differences at the boundaries. According to this classification, the area representing northeast Turkey are characterised largely with Black Sea region and partly with Eastern Anatolia region. However, physical interpretation of annual climate characteristics of identified regions; apparently, these two regions display remarkable differences especially in

average precipitation and minimum temperatures values.

6.2. Study area and data

The study area, located in the northeastern part of Anatolia is 43949 km² in extent and has a coastal border with the Black Sea (Figure 6.1). The highest and most rugged part of the North Anatolian Mountains (e.g., Kaçkar Dağları, 3937m) is located in this region; the local name being the “East Black Sea Mountains” (Atalay and Mortan, 2003). This mountain range is one of the few regions of Turkey where there are extant glaciers (albeit shrinking over recent times) together with abundant geomorphological evidence of late Quaternary glacier-related landforms and deposits (e.g., cirque lakes, moraines) (Akcar *et al.* 2007). The region comprises two major river basins, namely the EBS and Çoruh River basins. The EBS basin is located on the northern side of the East Black Sea Mountains which form a divide with the ÇRB to the south (Figure 6.1).

There are several factors influencing climatic variability over this region which include elevation, continentality, marine effect and exposure to regional circulation. Two important air masses prevail in this region, which have a pronounced seasonal effect on meteorological conditions. During the winter season, the region is affected by the strong thermal Siberian High Pressure System. The positions of the jet streams and jet maxima are important in determining surface pressure and rainfall patterns but the relationships are extremely complex. Marine Polar air masses (mP) bring humid and cold air from the polar North Atlantic which are then further modified and collect more moisture as they advance over the Black Sea. Continental Polar air masses (cP) transport dry, cold air from Siberia and as they travel across the Black Sea, they take up moisture, which then precipitates onto the northern coasts of Turkey (Akcar *et al.*, 2007). The high mountainous terrain of northeastern Anatolia,

in particular, has an important physical influence on this regional atmospheric circulation in terms of orographic uplift, which results in extremely complex rain and snowfall patterns and a marked rain shadow effect to the south of the Black Sea Mountains.

The long-term average values for several meteorological parameters measured at the 12 stations present useful information on the distinct climatic character over the study area (Table 6.1). A large elevation range exists over the region varying between sea level to ~4,000 m. This elevational range also affects the elevations of the network of monitoring stations with these ranging from 6-1584 m; however, there is a noticeable absence of monitoring stations in the East Black Sea Mountains. Given this physiographic complexity, clear climatological trends can be discerned between northern and southern parts of the study area. For example, there are distinct annual mean temperature differences of 7° and 14°C for the coastal and continental stations, respectively. Similarly, annual precipitation totals are below 1000 mm for the majority of the stations in the southern parts of the region while the northern part of the region experiences a distinct rainy season with some stations recording some of the highest precipitation amounts for the entire country with in excess of 2000 mm being recorded for the coastal eastern part of the region. This region receives rainfall for over 100 days throughout the year (Çiçek *et al.*, 2006). Snow cover (daily average of existing snow) is observed at all stations with an average thickness of 6 cm for the most pronounced snow period (November to April; Table 6.1). Mean wind speed, cloudiness and relative humidity exhibit such a relatively uniform character for the entire region when compared to other climatic parameters, while the average days for thunderstorm events are markedly higher for stations located within inland parts of the study area. This latter parameter is considered to be particularly important given the intense nature of heavy rainfall over short durations with the propensity to cause flash flooding events (Ceylan *et al.*, 2007a).

Table 6.1 Long-term averages of meteorological variables for selected stations.

| Station Name | Elevation (m) | Temperature (C°) | | | Precipitation (mm) | Rainy Days | Wind Speed (m/sec) | Snow Cover (cm) | Snow Period | Thunderstorm Days | Cloudiness (s/10) | Relative Humidity (%) |
|--------------|---------------|------------------|-------|---------|--------------------|------------|--------------------|-----------------|-------------|-------------------|-------------------|-----------------------|
| | | Minimum | Mean | Maximum | | | | | | | | |
| Akçaabat | 6 | 11.20 | 14.19 | 17.85 | 733.30 | 139.13 | 1.65 | 5.32 | Dec-Apr | 12.82 | 6.27 | 74.01 |
| Artvin | 628 | 7.91 | 11.98 | 16.85 | 722.61 | 131.59 | 1.62 | 11.78 | Nov-Apr | 20.12 | 5.39 | 65.14 |
| Bayburt | 1584 | 0.95 | 6.98 | 13.26 | 443.01 | 100.84 | 1.96 | 7.05 | Oct-Apr | 16.88 | 4.20 | 61.43 |
| Giresun | 37 | 11.83 | 14.45 | 17.68 | 1246.23 | 158.41 | 1.18 | 4.38 | Nov-Apr | 21.73 | 5.96 | 73.95 |
| Gümüşhane | 1219 | 4.00 | 9.49 | 15.99 | 464.91 | 115.38 | 1.66 | 5.64 | Oct-Apr | 26.42 | 4.88 | 64.68 |
| Hopa | 33 | 10.47 | 14.29 | 18.68 | 2243.38 | 181.28 | 2.45 | 8.02 | Nov-Apr | 13.21 | 6.06 | 71.69 |
| Ispir | 1222 | 4.50 | 10.40 | 15.68 | 478.00 | 95.66 | 2.02 | 6.69 | Oct-Apr | 34.73 | 4.48 | 60.23 |
| Oltu | 1322 | 4.04 | 9.94 | 16.46 | 384.74 | 103.53 | 2.00 | 2.58 | Oct-Apr | 19.09 | 4.37 | 61.48 |
| Pazar | 79 | 10.16 | 13.30 | 17.33 | 2068.16 | 158.28 | 1.98 | 7.74 | Nov-Apr | 23.15 | 6.34 | 72.79 |
| Rize | 9 | 10.98 | 14.26 | 18.08 | 2241.41 | 169.19 | 1.41 | 4.63 | Nov-Apr | 13.97 | 5.93 | 75.81 |
| Tortum | 1572 | 1.85 | 8.27 | 15.17 | 470.69 | 116.16 | 1.14 | 5.25 | Oct-Apr | 20.85 | 4.42 | 61.24 |
| Trabzon | 30 | 11.52 | 14.64 | 18.15 | 831.51 | 139.81 | 2.20 | 4.20 | Nov-Apr | 18.55 | 5.75 | 71.62 |

6.2.1. Data

Meteorological data were obtained from the Turkish State Meteorological Service for 16 stations within the study area for the period 1975 to 2007. Twelve stations have the longest and continuous record for the particular meteorological parameters analysed in this study. Although some of the stations have temperature and precipitation records extending back to the 1930s, most of the records are incomplete for some meteorological parameters such as snow cover, wind speed, total evaporation and thunderstorm events during the observation period. Stations with complete records of variables including *monthly mean, minimum and maximum temperature, total precipitation, mean cloudiness and mean relative humidity* therefore are those evaluated as part of this study; the period 1981 to 2007 is the optimum long-term period with complete data for selected variables. Basic information about the stations together with long-term average values of measured variables are listed in Table 6.1, while Figure 6.1 shows the locations of the stations used in this study.

Several research studies have reported the analysis of Turkish precipitation (Türkeş 1996, 1998; Gokturk *et al.* 2008; Türkeş *et al.* 2009) and temperature data (Türkeş *et al.* 1996, Tayanç *et al.* 1998, Türkeş, Sumer and Demir 2002a). The most recent and comprehensive

study analysing Turkish meteorology data set were carried out by Sahin and Cigizoglu (2010). They performed (relative and absolute) homogeneity analyses to test the departures from the homogeneity on meteorological data from 232 stations for the period 1974-2002 including six variables (maximum, minimum and mean temperature, precipitation, relative humidity and local pressure). They also applied missing value interpolation method and used reference series to estimate the missing values of the time series in a given station. They achieved a comparison between absolute and relative homogeneity analysis, however all procedure and obtained results cannot be given here. 30 of the 232 stations were inhomogeneous for precipitation data, which is one of the most important finding obtained from this study. Some of these stations are located in northeast region of Turkey. These inhomogeneities are most likely related to long-period fluctuations and significant trends, because only a few of the stations display abrupt changes. Furthermore, they revealed that most of the inhomogeneities for the temperature data series were detected for stations located along the Mediterranean and Aegean coastal regions and suggested that these inhomogeneities were mostly caused by non-natural effects such as relocation of the meteorological station.

For northeast Turkey, 12 stations were selected by considering the length of the observation period and continuous record availability. The spatial representativeness of the monitoring stations is not good as desired; especially the stations located in EBS exclusively represent the coastal zone. Northeast Turkey does not have a spatially dense network of meteorology monitoring. 12 stations are largely used for climatology studies in Turkey, and most of them were defined as homogenous. In this study, a range of data quality procedures were applied to the monthly time series in order to detect inhomogeneities. Initially, the quality of data was controlled by examining the metadata files of the 12 stations within the study area. Only one station recorded its relocation for this region; the new location of the station has the same

environmental conditions as the previous location, so therefore, no abrupt changes could be detected in the metadata files following relocation.

Table 6.2 Percentages of significant results obtained from K-W (a), runs (b) and M-K (c) tests for monthly series of meteorological variables.

| (a) K-W Homogeneity Test | | | | | | | | | | | | |
|--------------------------------------|----------|----------|----------|----------|----------|----------|----------|----------|----------|----------|----------|----------|
| <i>Variables</i> | J | F | M | A | M | J | J | A | S | O | N | D |
| <i>Maximum</i> | 25.0 | 0.0 | 0.0 | 0.0 | 0.0 | 8.3 | 16.7 | 8.3 | 8.3 | 16.7 | 0.0 | 0.0 |
| <i>Mean</i> | 0.0 | 0.0 | 0.0 | 0.0 | 8.3 | 0.0 | 41.7 | 33.3 | 16.7 | 0.0 | 0.0 | 8.3 |
| <i>Minimum</i> | 0.0 | 0.0 | 0.0 | 0.0 | 8.3 | 8.3 | 25.0 | 16.7 | 16.7 | 16.7 | 0.0 | 8.3 |
| <i>Relative Hum.</i> | 41.7 | 16.7 | 50.0 | 33.3 | 33.3 | 33.3 | 50.0 | 41.7 | 41.7 | 41.7 | 25.0 | 33.3 |
| <i>Precipitation</i> | 0.0 | 0.0 | 16.7 | 0.0 | 0.0 | 0.0 | 0.0 | 0.0 | 0.0 | 0.0 | 0.0 | 0.0 |
| <i>Cloudiness</i> | 16.7 | 0.0 | 0.0 | 8.3 | 16.7 | 25.0 | 16.7 | 8.3 | 0.0 | 0.0 | 0.0 | 8.3 |
| (b) Runs Test | | | | | | | | | | | | |
| <i>Variables</i> | J | F | M | A | M | J | J | A | S | O | N | D |
| <i>Maximum</i> | 0.0 | 0.0 | 0.0 | 0.0 | 0.0 | 0.0 | 16.7 | 41.7 | 16.7 | 16.7 | 8.3 | 0.0 |
| <i>Mean</i> | 0.0 | 8.3 | 0.0 | 0.0 | 0.0 | 0.0 | 0.0 | 16.7 | 8.3 | 16.7 | 0.0 | 0.0 |
| <i>Minimum</i> | 0.0 | 0.0 | 0.0 | 8.3 | 16.7 | 0.0 | 25.0 | 33.3 | 25.0 | 0.0 | 0.0 | 0.0 |
| <i>Relative Hum.</i> | 50.0 | 33.3 | 0.0 | 8.3 | 25.0 | 33.3 | 66.7 | 66.7 | 66.7 | 50.0 | 50.0 | 66.7 |
| <i>Precipitation</i> | 0.0 | 0.0 | 0.0 | 0.0 | 0.0 | 0.0 | 0.0 | 0.0 | 0.0 | 0.0 | 0.0 | 0.0 |
| <i>Cloudiness</i> | 8.3 | 33.3 | 0.0 | 0.0 | 8.3 | 8.3 | 8.3 | 25.0 | 8.3 | 0.0 | 8.3 | 33.3 |
| (c) M-K Rank Correlation Test | | | | | | | | | | | | |
| <i>Max. Temperature</i> | J | F | M | A | M | J | J | A | S | O | N | D |
| Trend | 0.0 | 0.0 | 0.0 | 0.0 | 33.3 | 50.0 | 25.0 | 75.0 | 25.0 | 41.7 | 0.0 | 0.0 |
| Neg.Per | 0.0 | 0.0 | 0.0 | 0.0 | 0.0 | 0.0 | 0.0 | 0.0 | 0.0 | 0.0 | 0.0 | 0.0 |
| Pos.Per | 0.0 | 0.0 | 0.0 | 0.0 | 100 | 100 | 100 | 100 | 100 | 100 | 0.0 | 0.0 |
| <i>Mean Temperature</i> | J | F | M | A | M | J | J | A | S | O | N | D |
| Trend | 0.0 | 0.0 | 0.0 | 8.3 | 8.3 | 25.0 | 58.3 | 75.0 | 41.7 | 66.7 | 0.0 | 0.0 |
| Neg.Per | 0.0 | 0.0 | 0.0 | 100 | 0.0 | 0.0 | 0.0 | 0.0 | 0.0 | 0.0 | 0.0 | 0.0 |
| Pos.Per | 0.0 | 0.0 | 0.0 | 0.0 | 100 | 100 | 100 | 100 | 100 | 100 | 0.0 | 0.0 |
| <i>Min. Temperature</i> | J | F | M | A | M | J | J | A | S | O | N | D |
| Trend | 0.0 | 0.0 | 0.0 | 0.0 | 16.7 | 41.7 | 58.3 | 75.0 | 50.0 | 66.7 | 8.3 | 8.3 |
| Neg.Per | 0.0 | 0.0 | 0.0 | 0.0 | 0.0 | 0.0 | 0.0 | 0.0 | 0.0 | 0.0 | 100 | 100 |
| Pos.Per | 0.0 | 0.0 | 0.0 | 0.0 | 100 | 100 | 100 | 100 | 100 | 100 | 0.0 | 0.0 |
| <i>Rel. Humidity</i> | J | F | M | A | M | J | J | A | S | O | N | D |
| Trend | 50.0 | 58.3 | 41.7 | 33.3 | 33.3 | 50.0 | 75.0 | 75.0 | 58.3 | 50.0 | 50.0 | 66.7 |
| Neg.Per | 16.7 | 42.9 | 40.0 | 25.0 | 0.0 | 50.0 | 22.2 | 11.1 | 14.3 | 0.0 | 16.7 | 12.5 |
| Pos.Per | 83.3 | 57.1 | 60.0 | 75.0 | 100 | 50.0 | 77.8 | 88.9 | 85.7 | 100 | 83.3 | 87.5 |
| <i>Precipitation</i> | J | F | M | A | M | J | J | A | S | O | N | D |
| Trend | 0.0 | 8.3 | 33.3 | 0.0 | 0.0 | 0.0 | 0.0 | 16.7 | 16.7 | 8.3 | 8.3 | 8.3 |
| Neg.Per | 0.0 | 100 | 25.0 | 0.0 | 0.0 | 0.0 | 0.0 | 0.0 | 0.0 | 0.0 | 100 | 0.0 |
| Pos.Per | 0.0 | 0.0 | 75.0 | 0.0 | 0.0 | 0.0 | 0.0 | 100 | 100 | 100 | 0 | 100 |
| <i>Cloudiness</i> | J | F | M | A | M | J | J | A | S | O | N | D |
| Trend | 33.3 | 33.3 | 8.3 | 25.0 | 41.7 | 16.7 | 50.0 | 33.3 | 33.3 | 0.0 | 16.7 | 16.7 |
| Neg.Per | 100 | 100 | 100 | 100 | 100 | 100 | 100 | 75.0 | 100 | 0.0 | 100 | 50.0 |
| Pos.Per | 0.0 | 0.0 | 0.0 | 0.0 | 0.0 | 0.0 | 0.0 | 25.0 | 0.0 | 0.0 | 0.0 | 50.0 |

The homogeneity of the meteorological parameters was also tested using K-W test for the

period 1981-2007 which indicated significant inhomogeneities especially for the relative humidity series all year around (Table 6.2a). In addition to this, important inhomogeneities were also detected for cloudiness and temperature series during the summer and autumn seasons (from June to October). Inland stations produced more homogeneous series than coastal stations. Of these coastal stations, Hopa, Giresun and Rize exhibited significant inhomogeneities, mostly for relative humidity and temperature series (station based results not shown). The randomness in the time series was also analysed by using runs test (Table 6.2b) in order to define the serial correlation pattern. Most of the stations were found to be random against serial correlation.

The coastal stations of Hopa, Rize, Giresun and Trabzon exhibited significant persistency especially for relative humidity series for the same period as detected in K-W test. Inland stations (Artvin, Bayburt, Gümüşhane, Oltu and Tortum) displayed significant persistency for relative humidity series for summer and autumn months. Spatially and temporally coherent results were not obtained for the rest of the climatic variables. However, significant results were observed for the temperature series of Rize and Akçaabat during summer and autumn for minimum and maximum temperature series. These inhomogeneities might be related to significant trends; this argument is discussed and supported by the results of the trend test in section 4.3. The K-W and runs tests are concisely explained in the methodology section.

6.3. Methods

In this study, a range of statistical techniques are employed to analyse climatological time series from the 12 meteorological stations to highlight climate variability [and fluctuations] both in space and time for the period 1981-2007.

6.3.1. Climate regime classification

Climate regime classification was achieved by hierarchical, agglomerative cluster analysis using Ward's method. The "shape" and "magnitude" regimes (devised by Hannah *et al.*, 2000; adapted by Harris *et al.*, 2000; evaluated by Bower *et al.*, 2004; Kansakar *et al.*, 2004; Hannah *et al.*, 2005 and Sariş *et al.*, 2010) were separately identified to assess the timing and size of climate regimes. Shape classification identifies stations with a similar form of annual regime, regardless of the absolute magnitude. The 12 long-term mean monthly observations for each climatic parameter were standardised on a station-by-station basis using z -scores (mean = 0, standard deviation = 1) prior to clustering. The magnitude classification is based upon four indices (i.e. the mean, minimum, maximum and standard deviation of monthly values across the 27-year record) for each station, regardless of their timing. It was necessary to standardize between indices (to control for differences in their relative values) by expressing each index as z -scores. Six different climatic parameters were used to identify climatic regimes of the study area. These two different classification approaches help to classify stations into homogenous groups according to the timing and magnitude similarity of these different variables. This approach has the advantage that these two important regime attributes may be interpreted separately as well as jointly by simply combining shape and magnitude classes for each station to yield a "composite" classification. The structure of the cluster dendrogram and breaks of slope in the agglomeration schedule (scree) plot are used to determine the appropriate number of clusters (Griffith & Amrhein, 1997). Thus, the classification of the northeast stations was based on the shape and magnitude regimes, which also permitted a composite regime classification to be constructed.

The solutions obtained from the two-stage clustering procedure are tested by discriminant

function analysis (DFA) for assessing whether the percentage of the original grouped cases were correctly classified or not (Bower *et al.*, 2004). The adopted approach for the classification processes is schematised in Figure 6.2.

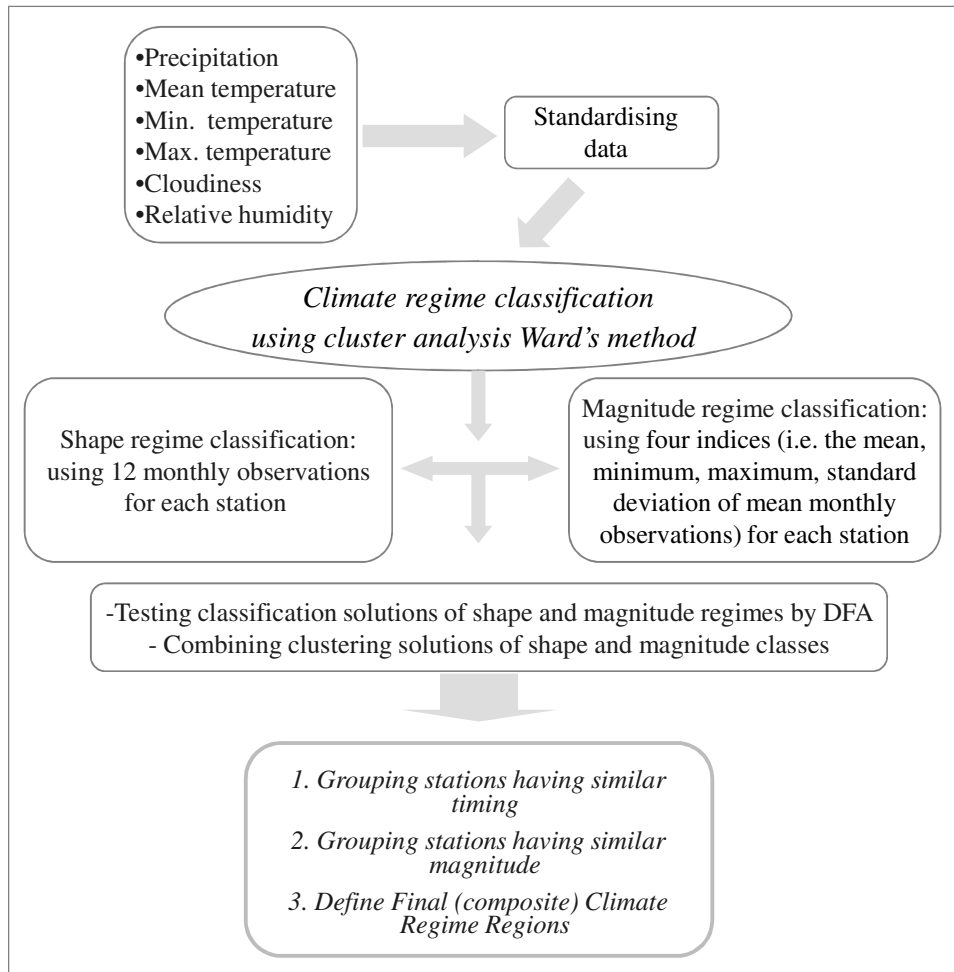


Figure 6.2 Flow chart illustrating the approach for regime classification procedure.

6.3.2. Water budget calculations

Annual water balance and climate type of *stations of northeast Turkey* were calculated by using Thornthwaite's water budget and moisture index calculations. Climatic water budget is calculated from air temperature and precipitation data. Unadjusted potential evapotranspiration (*UPE*), adjusted *PE* (*APE*), soil moisture storage (*ST*), actual evapotranspiration (*AE*), soil moisture deficit (*DEF*) and soil moisture surplus (*SURP*) in mms parameters were obtained. Climate types of northeast Turkey were determined that

negative values of the moisture index indicate dry climates, while positive values are found in moist climates.

The Thornthwaite method uses an accounting procedure to analyze the allocation of water among various components of the hydrological system for a specific location (Mather 1978 and 1979). Computations of monthly water budget components of the hydrological cycle can be evaluated as both research and assessment tools since it produces outputs include monthly potential and actual evapotranspiration, soil moisture storage, snow storage, surplus, and runoff.

6.3.3. Time series analysis

Non-parametric Kruskal-Wallis (K-W), runs and Mann-Kendall (M-K) rank correlation tests were used to discern the deterministic components in the time series such as homogeneity, persistence and trend for detecting non-random changing process. The calculation and assessment procedures of employed test were explained in Section 3.3. The homogeneity test of K-W was applied to determine the homogeneity or in homogeneity of the time-series. The persistency of the time series was checked by non-parametric runs tests in order to evaluate the results of K-W. Long-term trends in climate series were detected using the well-known M-K rank correlation test. Trend in temperature percentiles were also evaluated. The monthly x -percentile, P_x , of temperature was obtained for each year (i). Trend tests were employed to the time series of $P_x(i)$, where $i = 1, \dots, t$ years (Dixon *et al.*, 2006; Osborn *et al.*, 2000).

Table 6.3 Shape, magnitude and composite climate regime classification results.

| <i>Stations</i> | <i>Shape Regimes</i> | <i>Magnitude Regimes</i> | <i>Composite Regimes</i> |
|-----------------|----------------------|--------------------------|--------------------------|
| Akcaabat | B | 2 | 2B |
| Artvin | B | 1 | 1B |
| Bayburt | A | 1 | 1A |
| Giresun | B | 2 | 2B |
| Gumushane | A | 1 | 1A |
| Hopa | C | 3 | 3C |
| Ispir | A | 1 | 1A |
| Oltu | A | 1 | 1A |
| Pazar | C | 3 | 3C |
| Rize | C | 3 | 3C |
| Tortum | A | 1 | 1A |
| Trabzon | B | 2 | 2B |

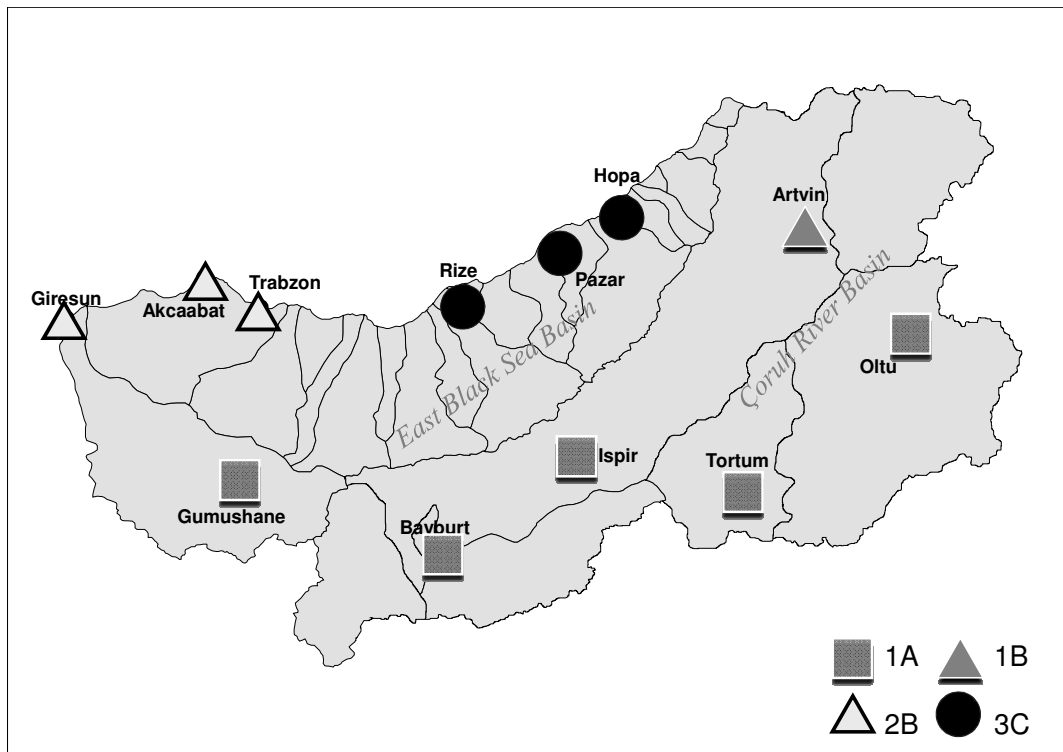


Figure 6.3 Annual climate regime classification map.

6.4. Results

6.4.1. Climate regime regions of northeast Turkey

Three climate regime shape and magnitude classes were identified (Table 6.3). The original grouped solutions were reassessed by DFA to examine robustness of the classification. DFA results indicate that the hierarchical CA classification is successful at 91.7% accuracy. A composite climate regime classification was constructed by combining shape and magnitude classes, which permits standardised seasonal responses to be scaled by magnitude of climatic elements. Of the 9 possible combinations, 4 composite regimes were produced for the region (Figure 6.3). The analyses produced regimes with distinct climate characteristics as follows:

- Regime 1A (inland regime): cool with the lowest mean, minimum and maximum temperatures, wet spring with May rainfall peak, relatively dry summer, secondary autumn (October) peak and dry winter with the lowest values for precipitation as well as for relative humidity and cloudiness (P, RH & C). Includes Bayburt, Gümüşhane, Ispir, Oltu and Tortum stations.
- Regime 1B (transition regime): warm with intermediate temperatures, December rainfall peak with gradual onset of wet winter and gradual cessation into dry summer and moderately-high magnitude regime with third highest values for P, RH & C. Includes Artvin station.
- Regime 2B (western coastal regime): warm with high temperatures, October rainfall peak with rapid onset, and wet autumn-winter, and high magnitude regime with the second highest values for P, RH & C. Includes Giresun, Akçaabat and Trabzon stations.

- Regime 3C (eastern coastal regime): warm with highest temperatures, October rainfall peak with very rapid onset, and very wet autumn-winter and with the highest values for P, RH & C. Includes Rize, Pazar and Hopa stations.

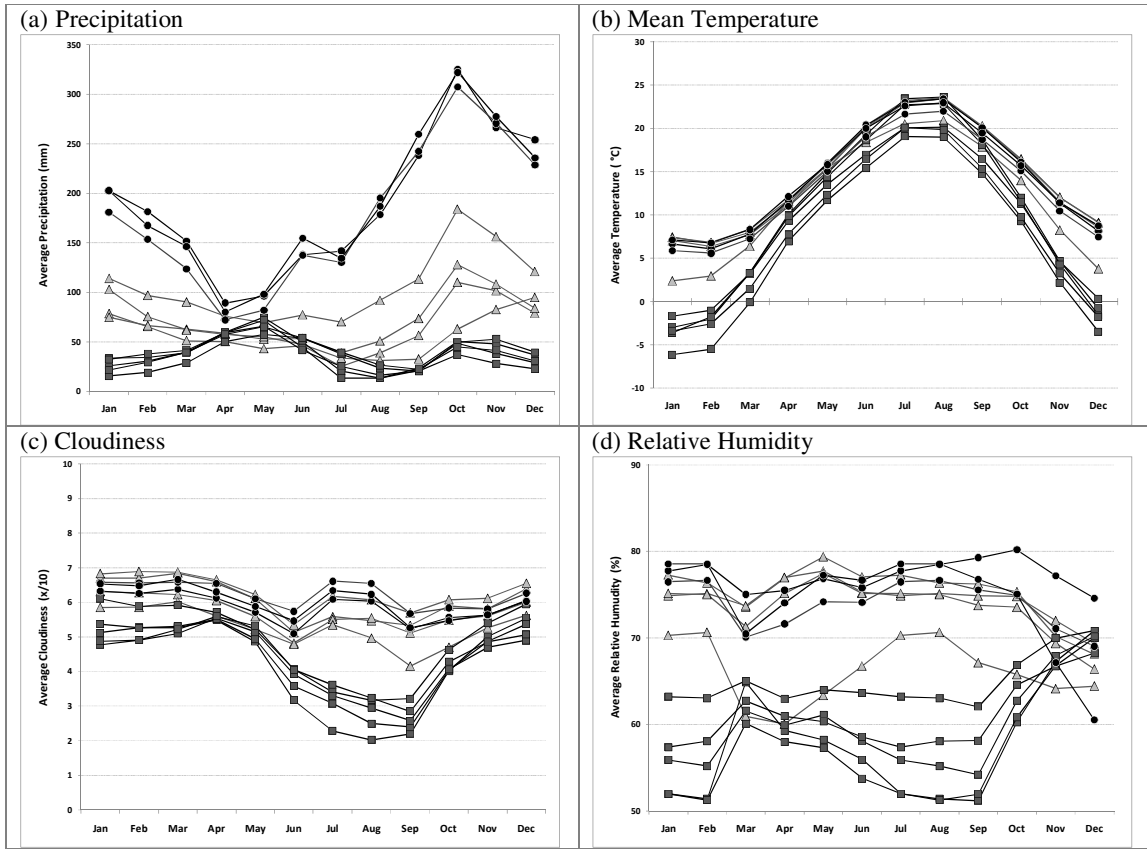
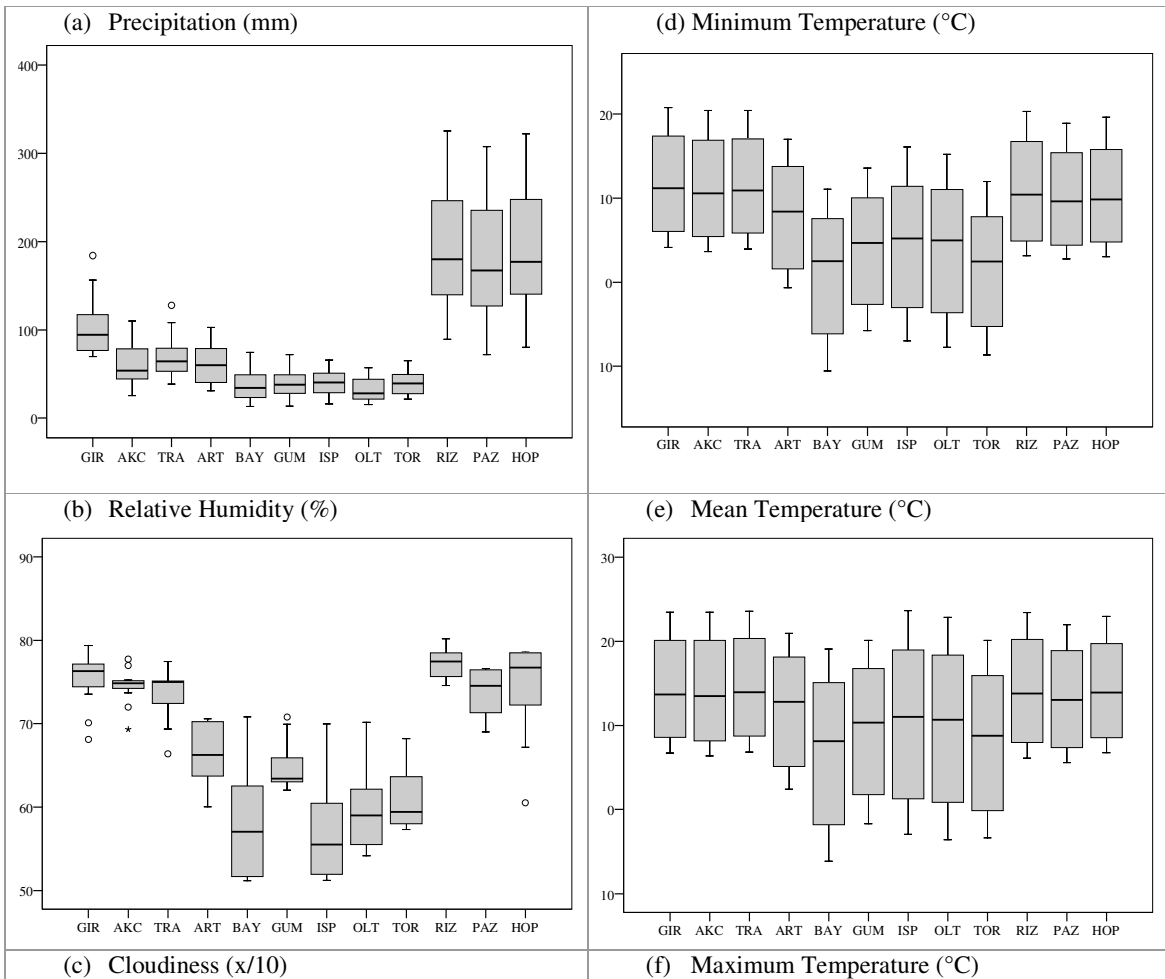


Figure 6.4 Line plots illustrating seasonality of climate variables (Lines are defined as; (A:-■-) Bayburt, Gümüşhane, Ispir, Oltu and Tortum; (B:-▲-) Giresun, Akçaabat; Trabzon and Artvin; (C:-●-) Rize, Hopa and Pazar).

Figure 6.4 shows the intra-annual variability of precipitation, temperature, cloudiness and relative humidity time series for each of the 12 stations. The stations were grouped according to results of climate shape regimes classification: ((A) Bayburt, Gümüşhane, Ispir, Oltu and Tortum; (B) Giresun, Akçaabat; Trabzon and Artvin; (C) Rize, Pazar and Hopa) and interpreted on the basis of climatological seasons.

Since the seasonality of minimum, mean and maximum temperatures are quite similar, only the mean temperature graph is presented (Figure 6.4B). Intra-annual variability of temperature

indicates markedly seasonal regime for all stations. The temperature regime of northeast Turkey can be characterised by high summer and low winter averages and the magnitude of temperature only slightly differs among the regime regions. A cooler temperature regime can be observed during December and January; temperature then increases gradually in spring with the highest temperatures being recorded during the summer with July and August the warmest months.



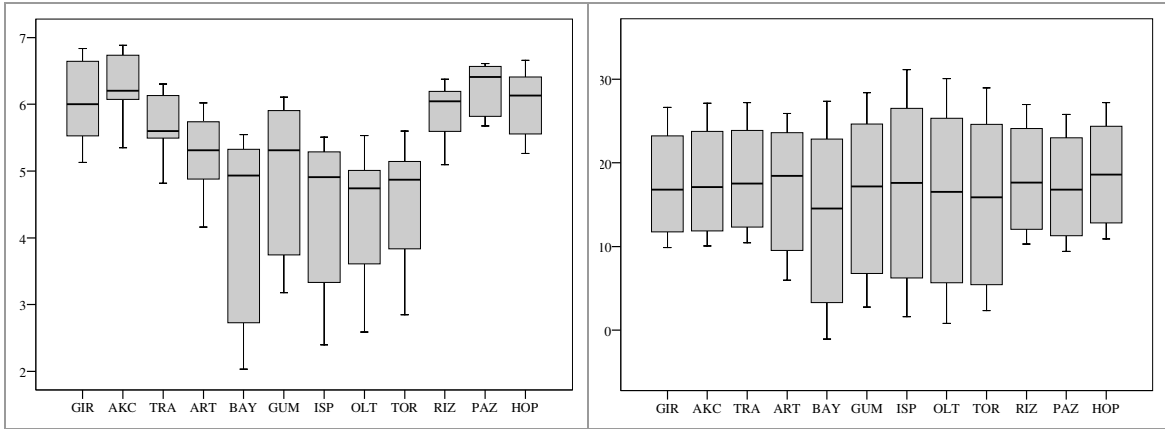


Figure 6.5 Box plots illustrating variability in magnitude of climate variables.

Box plots for each climate variable display the magnitude differences for each station (Figure 6.5). Stations are ordered by climate magnitude classes: (1) Bayburt, Gümüşhane, Ispir, Oltu and Tortum, Artvin; (2) Giresun, Akçaabat and Trabzon; (3) Rize, Pazar and Hopa. Box plots show that precipitation is the most distinctive variable and indicative component for classifying regime characteristics. The eastern coastal regime stations have the highest precipitation amounts (Figure 6.3 and 6.5A), while inland basin is characterised by lower precipitation amounts. Inland stations are characterised by very low annual precipitation amounts. Coastal and inland discrimination for relative humidity and cloudiness (Figure 6.5C, 6.5E) is evident for the entire region. Annual averages of relative humidity and cloudiness are lower for inland stations, and higher values for coastal stations. Once again, Artvin can be highlighted as a transition station between coastal and inland regimes having an intermediate regime.

All plots for minimum, mean and maximum temperature exhibit similar spatial variability (Figure 6.5B, 6.5D, 6.5F), although a coastal–inland distinction is evident. While coastal stations have similar regime characteristics with equitable temperatures, these being neither very high nor ever falling below 0°C during the observation period, inland stations are distinctive in having very low temperatures, particularly Bayburt which has the lowest temperature values for all series. Once again, Artvin’s transitional character is highlighted with temperatures lower than coastal stations, but not as low as inland stations (Figure 6.5B, 6.5D, 6.5F).

The foregoing multivariable climate regime classification of northeast Turkey emphasises the considerable differences between the East Black Sea and the Çoruh River basins (coastal – inland) both in seasonality and magnitude regime classes. Precipitation in particular is a

variable that is capable of delimiting the spatial differences across the region, while the magnitude characteristics of the climate variables appears to be very effective in distinguishing coastal stations across an west-east transect .

Table 6.4 Climate type classification of northeast Turkey stations according to Thornthwaite method based on moisture index.

| Stations | Moisture index | Climatic type |
|------------------|----------------|--------------------------|
| Rize | 167.81 | A Perhumid |
| Pazar | 163.31 | A Perhumid |
| Hopa | 171.05 | A Perhumid |
| Giresun | 51.76 | B2 Humid |
| Artvin | 8.14 | C2 Moist Subhumid |
| Trabzon | 6.71 | C2 Moist Subhumid |
| Akçaabat | -0.57 | C1 dry subhumid |
| Bayburt | -1.80 | C1 dry subhumid |
| Tortum | -7.81 | C1 dry subhumid |
| Gümüşhane | -12.16 | C1 dry subhumid |
| Ispir | -14.62 | C1 dry subhumid |
| Oltu | -25.21 | D Semiarid |

6.4.2. Annual water balance and climate types

The spatial variability of annual water balance was analysed by using long-term averages of monthly temperature and precipitation data on the basis of the Thornthwaite (1948) method (most recently applied by Türkeş and Akgündüz, 2011). The calculated annual water balance outputs highlight the interaction between precipitation, temperature and evapotranspiration at a station. Climatic types of northeast Turkey stations were also determined using Thornthwaite’s climate classification based on moisture index. According to this classification, northeast Turkey can be characterised by 5 climatic types which vary from semiarid to perhumid (Table 6.4). The coastal stations of Rize, Pazar and Hopa are defined as *Perhumid* (A) climatic type, while Giresun is defined as *Humid* climatic type (B2). ‘A’ and

'B2' climatic types are identified as moist climates where precipitation amounts significantly decrease during the summer months, where evapotranspiration rates are relatively high, but the water is excessive throughout the year due to the precipitation occurs during most of the year. Trabzon and Artvin stations are characterised as *Moist Subhumid* type (C2) with having little or no water deficiency. Akçaabat and the inland stations of Bayburt, Gümüşhane and Tortum are characterised as *Dry Subhumid* climate type (C1) with little or no water surplus throughout the year. Finally, Oltu is defined as *Semiarid* (D), the driest climatic type with a moderate winter water surplus.

Figure 6.6 shows the annual water budget of Giresun (B2), Rize (A), Artvin (C2), Gümüşhane (C1) and Oltu (D) stations which are selected to display the variability of water over the year for each climatic type. In each graph, the left y-axis represents actual evapotranspiration (AET), and potential evapotranspiration (PET) in mm, while right y-axis represents precipitation (mm), while the x-axis is the calendar year evaluated for December to November to detect seasonal variability. Rize (A, perhumid) is characterised by excessive precipitation for most of the year with a relatively high water surplus for the period October to March; the driest period occurring during the summer. Giresun (B2, humid) is quite similar to Rize although the actual amount of precipitation is significantly lower than Rize, but summer water minimum values are identical. Artvin (C2, moist subhumid) is characterised by having a water surplus between October and April with excessive water during winter (DJF). Water deficiency is observed for Artvin for the summer months. The dry period starts during May, and a distinct precipitation deficient period can be discerned for July to September as. Gümüşhane (C1, dry subhumid) is characterised with a little water surplus throughout the year, although this is concentrated during the winter months and a notable summer water deficit. Oltu (D, semiarid) is drier than Gümüşhane, but the seasonality of the water regime is

quite similar; winter water surplus is more important and intense at Oltu. The inferential indicators of water balance for northeast Turkey demonstrate the physically and climatologically distinct character of the region which yields a complicated climate types within a relatively small area of Turkey.

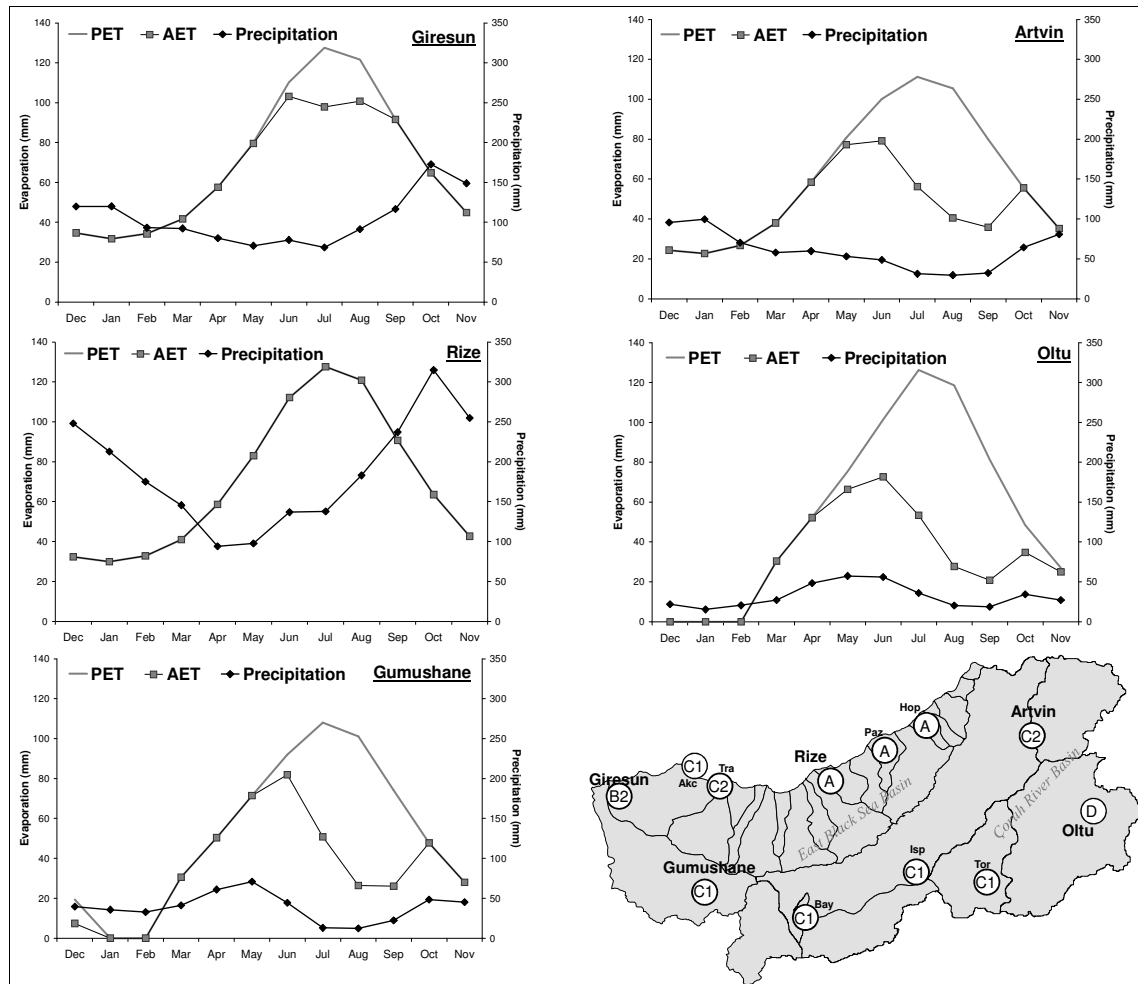


Figure 6.6 Graphs illustrating annual water balance in selected stations.

Perhumid (A) and dry subhumid climate types of Thornthwaite’s climate type classification are equal to 3C and 1A regime classes of hierarchical CA, respectively. The rest of the stations, which are represented by moist subhumid and humid climate types, correspond 2B and 1B regimes. Although the Oltu was grouped together with 1A in CA solutions, it defined as semiarid (driest) climate type in Thornthwaite’s classification.

6.4.3. Temporal variability of climate series

Significant trends can be detected for most variables including relative humidity, cloudiness and temperature (Table 6.2c). M-K test results highlight that May and October has a considerable temporal variability for the temperature series. The increasing trend in mean, maximum and minimum temperature is most significant for the Rize, Hopa and Trabzon (coastal) stations (Figure 6.7). This significant increasing trend in temperature series for Rize was also documented by Tecer and Cerit (2009) for the period 1975-2007. For monthly maximum temperature series, significant increasing trends were also detected specifically for the period July to October for all coastal stations, while all stations (apart from Giresun, Gümüşhane and Oltu) tended to experience warmer conditions for August. Similarly, mean temperature series show an increasing tendency for the period July to October for the coastal stations and also for Artvin with August being the most pronounced month in terms of demonstrating the same strong positive trend over the region. Minimum temperature series tended to increase between the same period of July to October for most of the coastal stations and also for Artvin and Oltu stations of the interior region (Figure 6.7). This positive variability pattern in temperature series for northeastern Turkey is the most important and dominant character of temporal change identified for the June-October period. Coastal stations, in particular, exhibit a consistency in having strong positive and statistically significant results which indicate a clear tendency to a warmer temperature regime. Significant positive changes in average relative humidity and cloudiness series can also be identified from the datasets.

For relative humidity, a marked change was observed for most of the stations within the study area. For Artvin, Bayburt and Giresun, negative trends can be interpreted from the time series, while predominantly positive trends can be identified for Gümüşhane and Rize. The

decreasing tendency in Tortum and Trabzon stations is also significant, but it is not quite strong. In addition to this, important decreasing trends are also demonstrated for the cloudiness series for all months (except October and March) for Artvin, Rize, Pazar and Ispir stations. The results for precipitation series do not demonstrate any prominent trends. Although statistically the overall rate of change is not high, some significant increasing trends for March and August were detected, while a few decreasing trend was observed for February and March for inland stations. To conclude, the significant results of the trend analyses can help to provide explanations for the reason of detected results from homogeneity test. Inhomogeneities in time series are highly possible to be related with the trends.

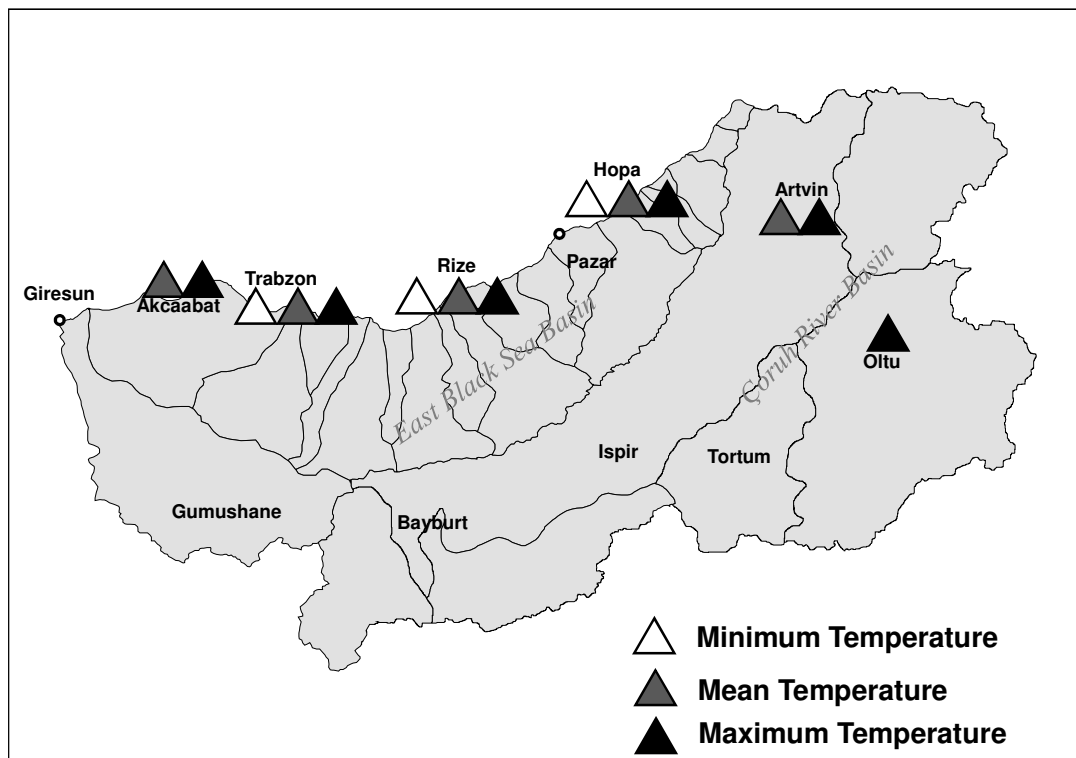


Figure 6.7 Spatial variability of the significant increasing trends for temperature series observed the period between July and October.

The significant increasing tendency in temperature series of northeast Turkey over the last three decades is the main indicator of climatic variability in this region. Therefore, daily records were analysed to calculate time series of temperature percentiles at monthly. Trends

in temperature percentiles provides the daily temperature distribution (spanning from coldest to warmest) and enables to evaluate the extent of temperature change. Four temperature percentiles (5th, 25th, 75th and 95th) were subsequently evaluated. These percentiles represent (1) very low temperature, (2) low temperature, (3) high temperature and (4) very high temperature, respectively. The test results also demonstrate the dominant positive trend for the temperature percentiles.

Table 6.5 Percentages of significant results showing the increasing trends for monthly temperature percentile series.

| Percentile | JAN | FEB | MAR | APR | MAY | JUN | JUL | AUG | SEP | OCT | NOV | DEC |
|------------|-----|-------|-----|-----|-------|-------|-------|--------------|-------|-----------|-----|-------|
| T95 | | | | | 8.333 | 16.67 | 33.33 | 66.67 | 8.333 | 16.67 | | |
| T75 | | 8.333 | | | 16.67 | 8.333 | 41.67 | 83.33 | | 50 | | |
| T25 | | | | | | 8.333 | 33.33 | 83.33 | 8.333 | | | 8.333 |
| T5 | | | 25 | | | 8.333 | 33.33 | 75 | | | | |

| Percentile | AKC | ART | BAY | GIR | GUM | HOP | ISP | OLT | PAZ | RIZ | TOR | TRA |
|------------|-------|-------|-------|-------|-------|-------|-------|-------|-------|-------|-------|-------|
| T95 | 16.67 | 16.67 | 16.67 | 8.333 | | 33.33 | | 16.67 | | 16.67 | | 25 |
| T75 | 33.33 | 16.67 | 16.67 | 16.67 | 8.333 | 25 | 16.67 | 16.67 | 8.333 | 25 | | 25 |
| T25 | 33.33 | 8.333 | 8.333 | 8.333 | 8.333 | 25 | | | 8.333 | 16.67 | 8.333 | 16.67 |
| T5 | 16.67 | 16.67 | 16.67 | 8.333 | | 33.33 | | 16.67 | | 16.67 | | 25 |

Table 6.5 summarises the percentage values of the significant positive trends detected in the trend analysis and shows the results for the months and stations, respectively. The most notable increasing trends were detected for the summer months, especially for the 25th and 75th percentile series. For August, a strong increasing tendency can be observed for nearly all stations. Overall, the most significant trends were obtained for mostly the coastal stations, namely Trabzon, Rize and Hopa. Figure 6.8 illustrates the deviations from the August average temperature for the 75th percentile series, and thus shows the year by year variability for these coastal stations and the strong positive tendency in deviations has become stronger since 1998, this date may be referred as a change point for positive temperature trend. These data suggest that the last decade has been one that has experienced important deviations from average temperature with a clear significant trend of increasing temperatures.

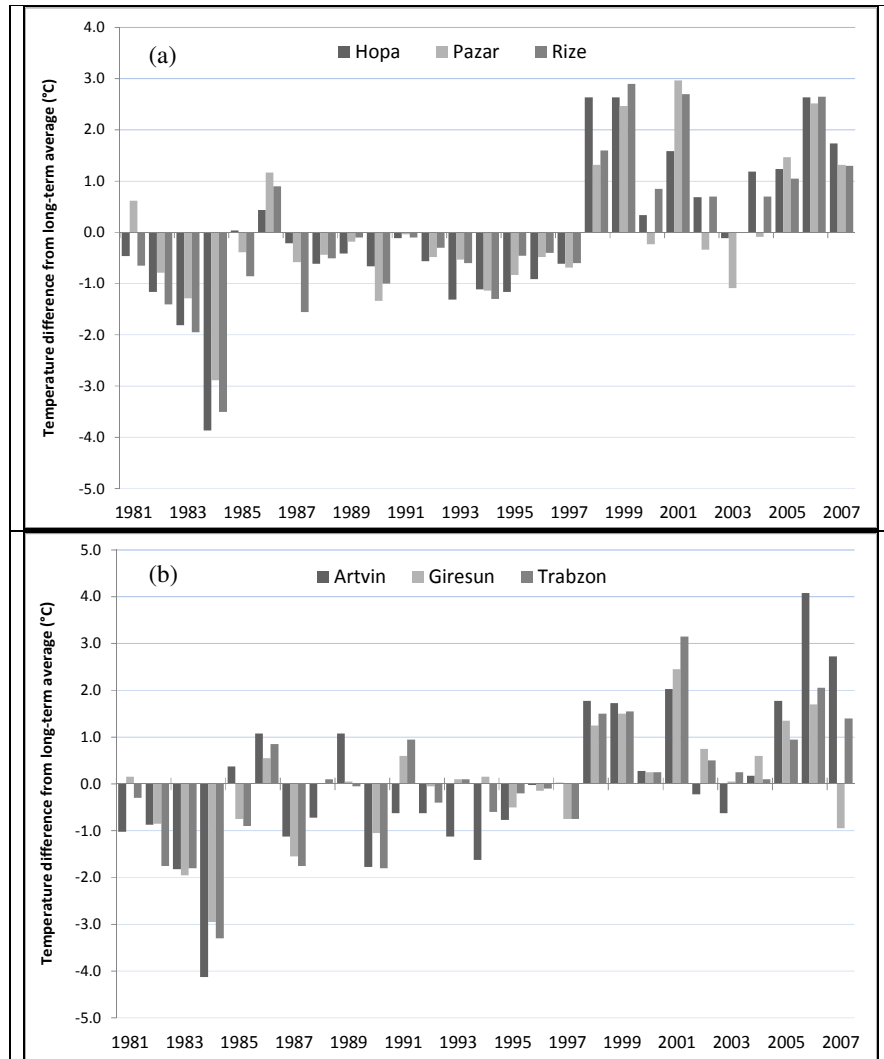


Figure 6.8 Year by year deviations from average temperature series at 75th percentile for August series of coastal stations.

6.5. Discussion and conclusion

This chapter was aimed to analyse the climatological characteristics of northeast Turkey and to evaluate regions and longer term patterns in climate time series (including trends) for the last three decades.

Climate regime analyses identified four climatic regimes for the northeast Turkey: (i) inland regime; (ii) transition regime; (iii) western coastal regime (WCR) and (iv) eastern coastal

regime (ECR). The western and eastern coastal regimes belong to East Black Sea Basin area and are characterised by October rainfall peaks with very wet and extremely wet precipitation regimes, respectively, and the warmest temperature regime with high annual averages. A transition regime was demonstrated by Artvin, which is characterised by a wet precipitation regime with a December rainfall peak and a moderately warm temperature regime. The inland regime includes the Çoruh River Basin, which is characterised by a moderately wet precipitation regime with a May rainfall peak and the coolest temperature regime for the northeast region. These data demonstrate the considerable differences that exist between the East Black Sea and Çoruh River basins both in terms of seasonality and magnitude of climate regimes. Artvin is highlighted distinctly as being located in a transition zone between these two basins. Precipitation is a particularly suitable parameter to designate the spatial variation over northeast Turkey, because only one temperature seasonality regime was identified for the entire region. The magnitude characteristics of the climate variables are highly important and effective in distinguishing the east-west oriented coastal stations. The eastern section of coastal (EBS) basin has a wetter climate regime than western section, which has more Mediterranean type regime characteristics. The eastern section, which is represented by Rize, Pazar and Hopa stations, has a milder winter and precipitation occurrence over a more extended period of the year.

According to Thornthwaite-based water balance calculations and climate type classification, northeast Turkey can be characterised by 5 climatic types varying from semiarid to perhumid. The eastern coastal regime is defined with Perhumid (A) climatic type. Giresun from western coastal regime is defined by Humid type (B2), while Trabzon (WCR) and Artvin (transition regime) are characterised by Moist Subhumid type (C2). Akçaabat (WCR) and the inland regime stations [except Oltu] are characterised by Dry Subhumid climatic type (C1). Finally,

Oltu is defined with the driest climatic type of Semiarid (D). For the areas defined with semiarid and dry subhumid (and even in moist subhumid) have a notable water deficient through the year, which makes these environments vulnerable to the aridity conditions. In this case, anthropogenic factors are of greater importance in terms of increasing the land degradation and eventuating in desertification as a combined effect of excessive human activities and climatic variations (Türkeş & Akgündüz, 2011).

Significant rising trends can be detected for monthly temperature series, particularly for Rize, Hopa and Trabzon stations (located in EBS). Significant increasing trends in temperature are observed for July-October period, and coastal stations display a consistency in having this significant positive trend for all minimum, mean and maximum temperature series. Statistically significant trends were also detected for average relative humidity and cloudiness series, but results for precipitation series did not display any significant pattern. For relative humidity, Rize, Trabzon, Gümüşhane and Tortum have positive trends while negative trends were observed for Artvin, Bayburt and Giresun. Important decreasing trends were obtained in cloudiness series throughout the year (except October and March) for Artvin, Rize, Pazar and Ispir. To provide a much more detailed and comprehensive analysis of the predominant positive tendency observed in temperature series of northeast Turkey, [daily] temperature percentiles were calculated and evaluated at monthly resolutions. These percentiles represent (5th) very low temperature, (25th) low temperature, (75th) high temperature and (95th) very high temperature events, respectively. These analyses confirm a significant positive trend for the 25th and 75th temperature percentiles for the summer months. In particular, the 75th percentile for August temperature series show important deviations from the average temperature with a significant warming trend since 1998. This rising temperature tendency will have profound impact on water resources, by accelerating permanent snowmelt.

This research has proved the spatial discrepancies across northeast Turkey by identifying climate regimes which yields a detailed understanding on the present-day climatology of northeast Turkey. The spatiotemporal variability patterns defined for this region provides a framework for further understanding of spatiotemporal variability of climatological conditions of Turkey at the regional scale. The only limitation of the present study is the spatially limited network of the surface monitoring stations, particularly low elevations of the stations, in the East Black Sea Basin. The temporal variability pattern of the several climatic parameters may prove the climate change impact showing itself as a shift towards a warmer temperature regime. This strong increasing trend must be taken into account which is highly possible to accelerate both glacier and snow melt and directly affect the river flow variability and regimes.

6.6. Chapter summary

This chapter provides the first systematic analysis of climatic variability focused on northeast Turkey using seven different climatic parameters at monthly resolutions. Stations were grouped into homogenous regions based on the similarity between their seasonality and magnitude. In Chapter 7, river flow regimes are regionalised across northeast Turkey and links are quantified between seasonal river flows and various climatic components presented in this chapter.

7. RIVER FLOW REGIMES OF NORTHEAST TURKEY: SPACE-TIME VARIABILITY AND LINKS WITH LOCAL CLIMATE

7.1. Introduction

River flow variability over time and space is driven by both regional climate and large-scale atmospheric variations and modified by basin properties (Laize & Hannah, 2010). Identification of the physical (climate soil, topography, geology, vegetation etc.) factors controlling the nature and magnitude of variability in river flows is required to discriminate their relative importance and to allow comparisons of the long-term behaviour of (physically different) hydrological catchments. The potential impacts of climate change on hydrology may include changes in the amount and timing of precipitation, evaporation, snowmelt and river flow characteristics of a basin (Climate Change, 2007).

Northeast Turkey has a distinct physical geography which is characterised by remnant mountain glaciers, seasonal snow accumulation and ablation, relatively high annual precipitation amounts and a dense river drainage networks (Atalay and Mortan, 2003). These physical characteristics result in a complexity of hydroclimatological processes driving river flow dynamics. Climate models for Turkey have not been able to sufficiently capture climate patterns for northeast Turkey due mainly to its varied topography (Tatli, *et. al.*, 2004). Previous research on the climatology and hydrology in Turkey have yielded important data and increased the knowledge and understanding of hydroclimatological processes at national

scales; however, these studies are relatively coarse and do not resolve hydroclimatological variability (reviewed below) at the sub-regional and catchment scale.

Previous hydroclimatological research studies in Turkey have focussed at the national scale and mainly on the detection of trends in flow series and regionalisation of river flows. Topaloğlu (2006a) investigated the regional significance of trends for annual and monthly river flows for 75 sites in Turkey and found significant decreasing trends for only the Marmara, Aegean, Mediterranean and Central Anatolia regions for the period 1968-1997. Topaloğlu (2006b) analysed monthly, mean, minimum and maximum river flow records for 84 gauging stations for 26 basins of Turkey and found significant decreasing and spatially coherent trends were evident for the western basins of Turkey. An important result of Topaloğlu (2006a, b) is the detection of an increasing trend in maximum flows for the East Black Sea and Çoruh River basins. Ödemiş and Evrendilek (2007) analysed hydrological data for 38 rivers in Turkey and found that, for the relatively short analytical period of 1995 to 2002, catchments in Turkey showed considerable spatial variation with a general decreasing trend of 16% in flow rates attributing to the increased evapotranspiration, decreased precipitation, or a combination of both parameters. Ödemiş and Evrendilek (2007) suggest these results may be the first signal of the impacts of global climate change on hydrological systems.

Using Principal Component Analysis (PCA) with a varimax orthogonal function, Kahya *et al.*, (2008a) evaluated monthly river flow data from 78 gauging stations for the period 1964–1994 to identify homogenous river flow regions for Turkey. They identified that the 7 river flow regions correlated well with the climate zones for Turkey as defined by Ünal *et al.* (2003). Kahya *et al.* (2008a) also applied annual cycle analysis using Harmonic vectors to

identify seasonal variation of river flow in Turkey. Seven annual cycle types were identified. Spatial variability in annual cycle of river flow showed that for the mountainous areas of northeast Turkey in particular, the timing of peak flows was designated as May (reflecting a December-February dry period for this region). Kahya *et al.* (2008b) undertook another river flow regionalisation study by applying hierarchical cluster analysis from 80 river flow stations across Turkey. Similar to the previous study of Kahya *et al.*, (2008a), river flow pattern zones correlate well with the redefined climate regimes of Ünal *et al.* (2003). Hierarchical cluster and rotated principal component analysis identified similar river flow variability patterns for Turkey. For northeast Turkey, Kahya *et al.* (2008b) showed that the East Black Sea Basin can be divided into two sub-regions based upon the analysis of river flow patterns for January, April, May, June and July.

Isik and Singh (2008) combined three regionalization techniques to obtain homogeneous regions and compute river flow at selected ungauged sites for 26 river basins in Turkey having 1,410 river gauging stations. Their approach included (i) an agglomerative hierarchical clustering algorithm, (ii) a *k*-means partitioning method to define homogenous regions and (iii) a flow duration curve method to estimate river flow discharge at ungauged sites within homogeneous regions. Their results suggest that Turkey can be grouped into six homogeneous regions. Aksoy *et al.* (2006) analysed instantaneous maximum flows for eleven hydrometric stations in the Eastern Black Sea region to detect randomness, jump, trend, and probability distribution function. The maximum instantaneous river flow time series of the region was considered to be natural after the random structure of the time series was determined. Only two stations were found with a trend while no trends were detected for the majority of stations. No jumps were identified across all stations.

One of the major shortcomings of hydroclimatological research in Turkey is the lack of detailed regional-scale dynamical studies, especially for relatively geographically complex regions such as northeast Turkey. To increase the knowledge and understanding of the patterns and processes that climate variability has on river flow increases in Turkey, there is a pressing need to more fully understand hydroclimatic variability on a regional basis, particularly in challenging regions with complex physical geographies. Northeastern Turkey has several specific characteristics in terms of its ecological, geomorphological and hydrological properties (Figure 7.1a and 7.1b) that require special consideration. The altitude and continentality of the mountains, topography, geology (mainly granite formations), glacial landforms, high precipitation, expansive forest cover and intensive drainage system are all factors that have a specific and variable influence on hydroclimatological characteristics of region. Many of these factors may affect the hydroclimatological processes in this region and have operated at different intensities both spatially and temporally. Therefore this chapter aims to undertake the first detailed analysis of the interaction between climate and hydrology for northeast Turkey to understand how space-time variability in river flow is influenced by climate and other drivers. To meet this aim, a classification of river flows into homogeneous regimes to identify inter-annual regime stability is undertaken followed by the detection of long-term trends to characterise the temporal variability of river flows between and within regions. The influence of local climatic conditions (precipitation, temperature and evaporation) on river flow variability is analysed to determine controls on river flow variability.

This research will advance understanding of hydroclimatological processes in northeast Turkey by identifying key factors, highlighting intra-regional discrepancies, and providing

information to underpin to sustainable management of freshwaters in the context of climate variability and change.

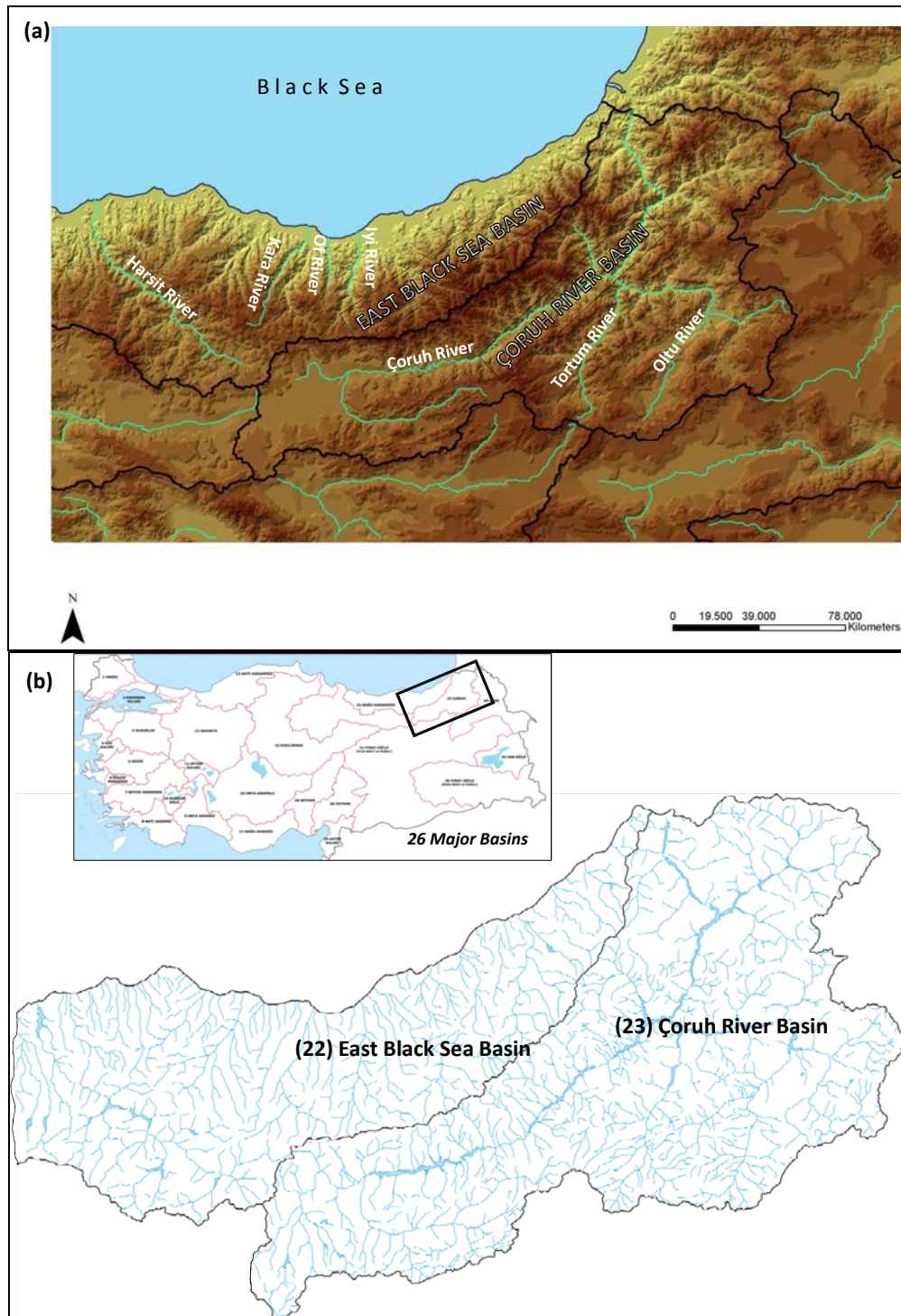


Figure 7.1 Physiographic (a) and river network (b) maps of study area

7.2. Study area and data

7.2.1. Study area

The study area is located in the northeastern part of Turkey and is nearly 44000 km² in extent. Northeast Turkey has a coastal border with the Black Sea, and the highest and most rugged part of the North Anatolian Mountains (Kaçkar, 3937m) is located within this region (Figure 7.1a). The “East Black Sea Mountains” (the local name for these mountains; Atalay and Mortan, 2003) are one of the major regions of Turkey where there are extant glaciers together with abundant geomorphological evidence of late Quaternary glacier-related landforms and deposits (e.g., cirque lakes, moraines) (Akcar *et al.* 2007) Two major river basins are located within the region; the EBS basin is situated on the northern side of the mountains whereas the ÇRB is on the southern part (Figure 7.1b).

7.2.1.1. East Black Sea Basin

This basin is surrounded by the Eastern Black Sea Mountains to the south and the Black Sea to the north. The basin’s boundary extends to the Terme River on the west and to the Georgia boundary on the east. The total basin area is 24,077 km² and the mean annual flow is 14.9 km³. The mean annual average river flow yield of EBS is 19.5 lt/sn/km² and this basin provides 8% of Turkey’s total surface flow (Uzlu *et al.*, 2008). In this study, the rivers located on the western section of the basin (for this study East Black Sea Basin is restricted by Harşit River Basin located to the east of Giresun) are not evaluated in EBS, to achieve a physically interpretable comparison with ÇRB. Average annual rainfall for Turkey is 643 mm, the East Black Sea Basin receives 1198.2 mm rain in an average year (See Chapter 6). The rivers, which rise on the northern part of the mountain range, are relatively short in length and drain into the Black Sea with a parallel drainage network. The geology of the region is generally

impermeable or semi permeable volcanic rocks, which prevents the percolation of much of the rainfall and forces the water to flow as runoff (Figure 7.2). The rivers that rise in the northern part of the East Black Sea Mountain range (nearer the Georgian border) are relatively shorter, generally flow north and drain into the Black Sea with a parallel drainage network and river basins have high slope characteristics, more specifically on the eastern section of EBS which the EBS Mountains are located (Figure 7.3). These include the Harşit, Karadere, Solaklı, Yanbolu, Değirmendere, Iyidere and Firtına (Figures 7.1 and 7.2). The EBS Basin has excellent potential in terms of hydropower due to the annual average precipitation value (the highest in Turkey) and the basin geomorphology which includes sharp valleys, many rivers with steep gradients which all produce rivers with a considerable amount of flow rate and head (Uzlu *et al.*, 2008). The EBS Basin contains *Alluvial, Grey-Brown Podzolic, Brown, Brown Forest, Non Calcic Brown Forest, Colluvial, Yellow-Red Podzolic and High Mountain Pasture soils. Grey Brown Podzolic, Yellow Red Podzolic and High Mountain Pasture soils* occupy 80.3% of the basin (Aydinalp & FitzPatrick, 2004).

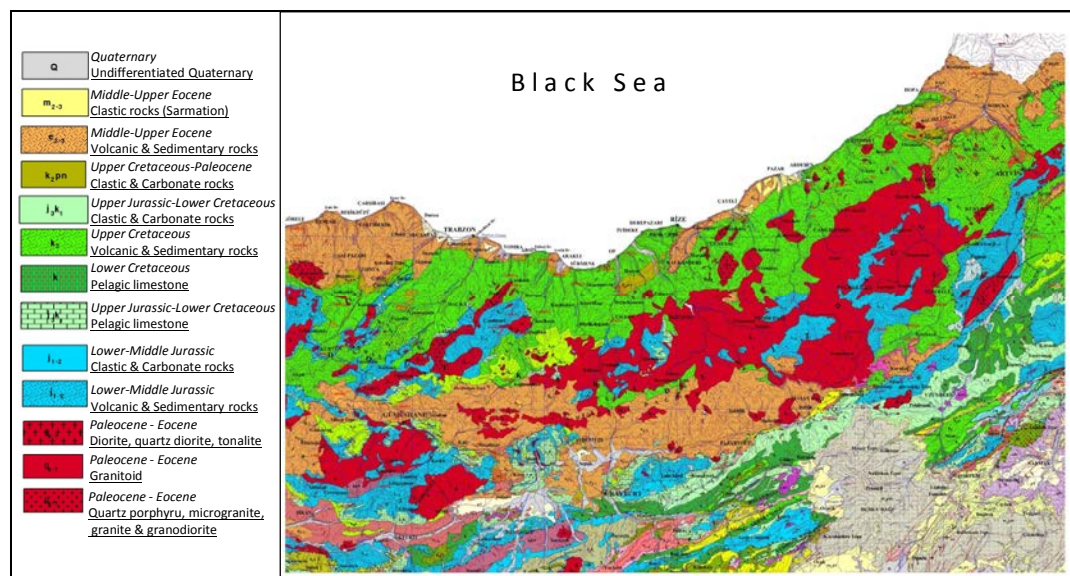


Figure 7.2 Geological characteristics of the northeast Turkey.

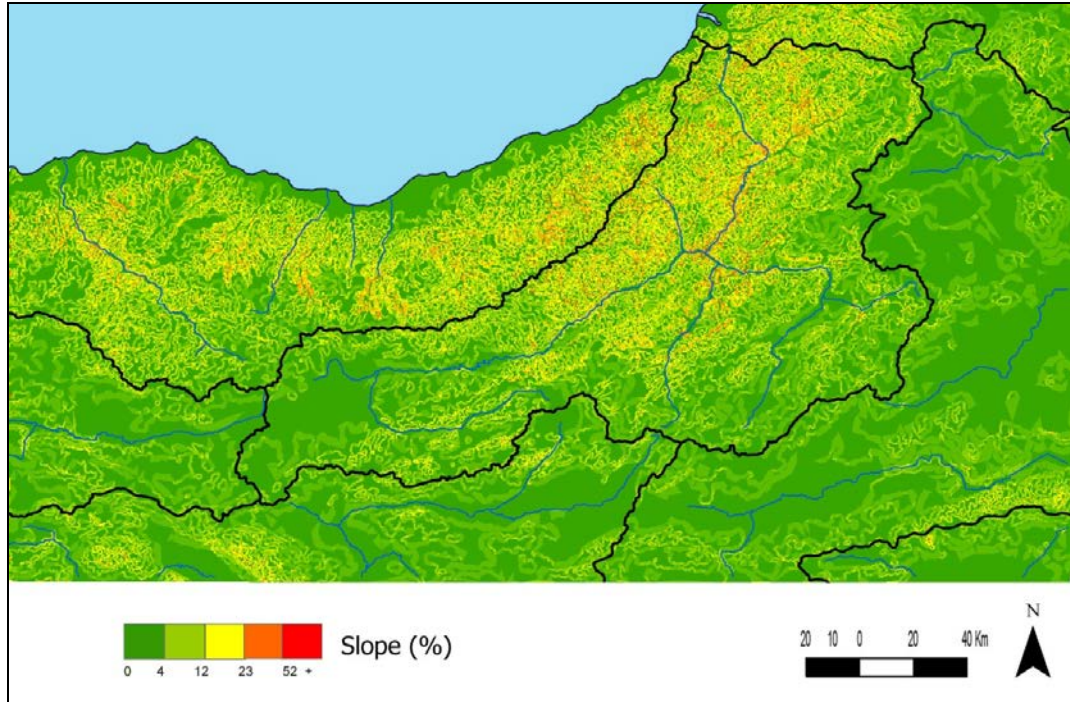


Figure 7.3 Slope characteristics of the northeast Turkey.

7.2.1.2. Çoruh River Basin

The Çoruh River originates in the western part of the Mescit mountains at an elevation of over 3000 m and is generally located to the north-west of the Erzurum-Kars Plateau. From these mountains the Çoruh first flows west, then turns east with a sharp bend at the Bayburt Plain; thereafter it follows a tectonic depression which separates the East Black Sea coastal mountain range from the inner mountain range (Figures 7.1 and 7.2). The Çoruh valley located in the eastern part of Ispir, is one of the deepest valleys in Turkey. Having flowed past the town of Yusufeli and the confluence with the Oltu River, the Çoruh then flows north and has shaped a mountain landscape with deep canyons. After having flowed through the cities of Artvin and Borçka, it then leaves Turkish territory near the city of Muratlı. Approximately 91% of the Çoruh Basin's drainage area (21,100km²) is located within Turkey. The Çoruh river is 427 km long (400 km of which lies within Turkey) and its principal tributaries are the Tortum and Oltu rivers (Akpınar *et al.*, 2009 and 2011). The Çoruh River, which is the fastest flowing river in Turkey with high water potential, is also one of the basins that is being

exposed to the most erosion due to the combined effect of high slope (Figure 7.3), soil (permeability) and geological (Figure 7.2) properties. The basin generally has a transitional climate between the Black Sea Basin's mild and wet weather and the generally cold and drier East Anatolia's climate. The Çoruh Basin receives 475 mm average annual rainfall; however, this comprises mainly of snowmelt (Akpınar *et al.*, 2011). The mean annual flow is 6.3 km³ and the mean annual river flow yield is 10.1 lt/sn/km² and the basin provides 3.31% of Turkey's total surface flow (Akpınar *et al.* 2009). The river carries high levels of sediment and deposits (estimated at 5 mcm/yr) which stem from erosion in the Turkish mountain regions. This basin contains *Yellow-Red Podzolic*, *Brown Forest*, *Non Calcic Brown Forest* soil groups (TGM, 1984).

7.2.1.3. Climate and vegetation

Two important air masses prevail in this region, both of which have pronounced seasonal effects on meteorological conditions. During winter, the region is affected by the strong thermal Siberian High Pressure System. The positions of the jetstreams and jet maxima are important in determining surface pressure and rainfall patterns but the relationships are extremely complex. Marine Polar air masses (mP) bring cold, humid air from the polar North Atlantic and have a more pronounced influence when they advance over the Mediterranean Sea. Continental Polar air masses (cP) transport cold, dry air from Siberia. As they travel over the Black Sea, they take up moisture, and then precipitate onto the northern coasts of Turkey. The high mountainous terrain of eastern Anatolia, in particular, has an important physical influence on the atmospheric circulation in this region. Because the positions of the Black Sea Mountains form an obstacle, as well as a corridor, pronounced precipitation maxima occur due to the orographic effects of these mountains (Akcar *et al.* 2007). The temperature regime is characterised generally by high summer and low winter averages while the temperature range differs depending upon the catchments; the ÇRB records more severe cold winters,

while a cool temperature regime is characteristic for December and January. Temperature gradually increases during spring to a summer maximum with July and August being the warmest months with annual average temperature of 11°C.

The East Black Sea region has abundant vegetation cover. In the northeastern part of the mountain ranges, broad leaf flora (*Quercus*, *Acer*, *Alnus*, *Ulmus*, *Castanea*, *Carpinus* and *Fagus orientalis*) are found up to about 1000 m elevation. Coniferous forests comprising *Picea orientalis* becomes widespread from 1000 to 2000 m elevation range. Above 2500 m elevation subalpine vegetation unit is found. However, in the more southerly parts of the region the climate is less moist (due to the marked rain shadow effect) and vegetation is more open and comprises steppic formations. Broad leaf flora is only able to spread in this region in areas with increased moisture for example in sheltered river valleys. Coniferous formations are also different in the southern part of the East Black Sea Mountains OR in the southern mountain ranges south of the Çoruh (in the drier, colder interior) comprising mainly *Pinus nigra*, *P. sylvestris*, *Juniperus* and *Abies nordmanniana*. Phytogeographically, Northeast Turkey region is also an important part of the Caucasus Ecoregion (Atalay and Mortan, 2003).

7.2.1.4. Land use properties and changes

Figure 7.4 shows land cover characteristics of northeast Turkey for 2006. In ÇRB the grassland and pastures comprise the significant amount of land cover, which intensify on the southwest (headwater) part of the basin. In this area, the proportion of complex cultivation class is also substantial. Towards to northeast (lower basin) the forest cover becomes an important land cover class, especially on the area Around Artvin, Borçka and Savaşat which is also characterised by a transition climate between inland and coastal climate regimes. The bare rock areas expand on the eastern part of the basin around Tortum and Hopa. In this area,

important proportion of grassland and pasture cover is found. Lands for “Agricultural with natural vegetation” class are found in south-southeast part of the basin, but do not have a considerable amount. The urban fabric settlement areas are concentrated on the city centres and the rural settlements around them. These land use classes are represented by very small percentage within land cover classification.

Previous studies have investigated land use changes for some of the forest units in provinces in northeast Turkey (Sancar, Turan and Kadiogullari 2009, Sivrikaya *et al.* 2007, Kadiogullari *et al.* 2008, Reis 2008, Kadiogullari and Baskent 2008, Keles *et al.* 2008). Some outstanding changes were detected for northeast Turkey. Keles *et al.* (2008) found a ~10% reduction in the total forested area of Artvin for the thirty year period between 1972 and 2002. Since 2000, the region has also seen the construction of many dams along the Çoruh River. One of these, the Deriner Dam near the Artvin Forest Planning Unit has seen the water area in planning unit decreased by 67 ha while the dam area has increased to 108 ha. Furthermore, in terms of spatial configuration and as a result of unplanned exploitation, settlement, dam and road construction, insect and pathogen outbreaks on spruce stands, conversion and over utilization, many natural forest ecosystems have been fragmented into smaller parcels in the AFPU and the total number of forest fragments has rapidly increased from 108 to 202. For Gümüşhane and Rize, decreasing in percentage of forest cover areas is too small. No significant changes in the percentage of water bodies for the Rize, Torul (in Gümüşhane) and Camili (In Artvin on Georgian border) and Gümüşhane Forest Enterprise Units is recorded (Reis 2008, Sivrikaya *et al.* 2007, Kadiogullari *et al.* 2008, Kadiogullari and Baskent 2008). Sancar *et al.* (2009) investigated the effects of urbanization on ecosystem structure (landscape) and to quantify urban growth of the city of Trabzon. An important change has been detected on the water bodies. For the period 1987 to 2008, the area of water bodies decreased to approximate

160 ha, being replaced by new settlements and vegetation uses.

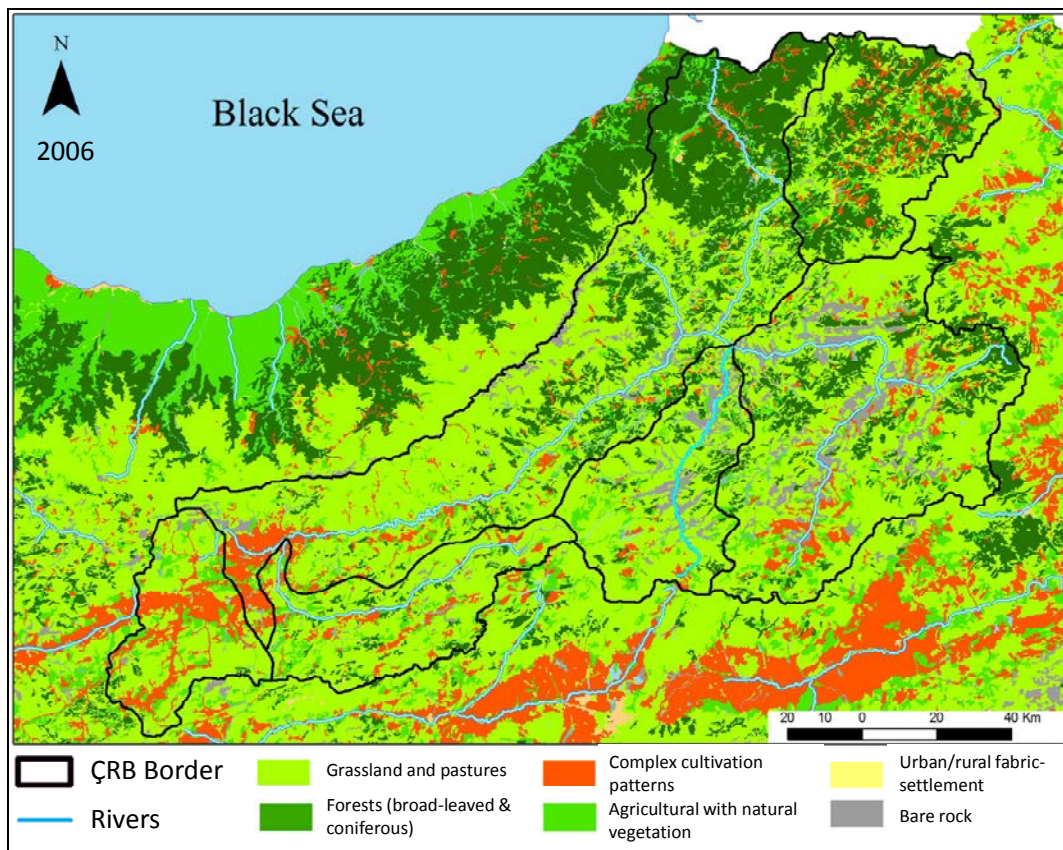


Figure 7.4 Land cover map of northeast Turkey for 2006.

A list of factors that might affect river flow (Raghunath, 2006) is provided below. In this research, meteorological factors are widely described.

- Storm characteristics
 - Type or nature of storm and season
 - Intensity
 - Duration
 - Areal extent (distribution)
 - Frequency
 - Antecedent precipitation
 - Direction of storm movement
- Meteorological characteristics
 - Temperature
 - Humidity
 - Wind velocity,
 - Pressure variation
- Storage characteristics
 - Depressions
 - Pools and ponds / lakes
 - Stream
- Channels
- Check dams (in gullies)
- Upstream reservoir /or tanks
- Flood plains, swamps
- Ground water storage in pervious deposits (aquifers)
- Basin characteristics
 - Size
 - Shape
 - Slope
 - Altitude (elevation)
 - Topography
 - Geology (type of soil)
 - Land use /vegetation
 - Orientation
 - Type of drainage net
 - Proximity to ocean and mountain ranges

7.2.2. Data

Daily mean river flow data were obtained from the Electrical Power Resources Survey and Development Administration (Turkish Abbreviation EIEI) and State Hydraulics Work (Turkish Abbreviation DSI) of Turkey. The EIEI has a well-distributed river gauging network in the ÇRB, while the DSI has a larger number of gauging stations as part of their network in the EBS Basin. After all records were examined, the resultant number of gauging stations with long-term data was rather limited (Figure 3.3 summarizes the changes in a number of open and closed stations for the two basins in northeast Turkey). There are only 12 gauging stations in total (7 in the EBS basin and 5 in the ÇRB) that have continuous records for the period 1982 to 2005, which is the longest period with the highest number of station. The aim was to select stations on the length of the observation period, the location of the station within the basin and the distance to other stations. A further aim was to assign each station as representative of an individual sub-basin. However, the spatial representativeness of the monitoring network was partly restricted due to the lack of long-term observations for many river gauging stations. Therefore, three different data sets were prepared in order to overcome problems associated with spatial representativeness and a sufficient number of stations for statistical analysis of the data:

- (i) Monthly minimum, mean and maximum river flow data of 12 stations for the period 1982 to 2005 [24 years] for regime classification and trend analysis;
- (ii) Monthly mean river flow data of 22 stations for the period 1992 to 2001 [10 years] in order to achieve a more precise regime classification;
- (iii) Seasonal river flow data of 9 river gauging stations and 10 meteorology stations for the period 1979 to 2005 [27 years] for regression analysis.

Table 7.1a and 7.1b shows key information for the long-period and short-period data sets used in this study. Daily flow charts were examined and inspected for any abrupt change in river flow data.

DSI stations, do not have detailed information on metadata of stations and station history. However, some information derived through the interviews with DSI local staff during the fieldwork. Most of the stations have very short monitoring period, and/or lots of missing data during their observation period. This situation resulted from three possible reasons: (i) discontinued monitoring at the station, (ii) damaged gauging station after a catastrophic flood or landslide, and (iii) suspension of measurement due to the lack of staff. On the contrary, EIE stations have more regular, continuous and long-period record and metadata information which is provided by data. For EIE stations, some equipment maintenance, replacement, and improvement records were found. There is only one station relocation (2232), which was carried from 237 m to 500 m in 1992. No abrupt change was observed for that period related to this altitudinal change.

Kruskal-Wallis homogeneity tests and runs test were employed to check the inhomogeneity and randomness in the monthly data series, respectively. Instrumental meteorological data for 10 stations including seasonal average temperature, total precipitation and evaporation were also analysed. The data quality controlling procedure for the meteorological time series is discussed elsewhere (Chapter 6) while Table 7.1c provides basic information on the meteorological stations. Figure 7.5a shows the delineation of the sub-basins of the region and Figure 7.5b shows the location of each meteorological and river gauging station in the study area based on sub-basin delineation map. For the river gauging stations in particular, underlined stations are those comprising shorter periods of data.

Table 7.1 Main hydrological characteristics of river gauging stations (A, B) and basic climatic information of meteorological stations (C) evaluated in this chapter.

| A-Long-Period: Station Name | River | Catchment Area (km²) | Run off (mm) | Discharge (m³s⁻¹) | Mean/Median Ratio | Elevation (m) |
|---|--------------|--|-------------------------------|--|------------------------------|--------------------------|
| 2202 Ağnas | Kara | 635.7 | 545.7 | 11.0 | 1.8 | 78 |
| 2218 Şimşirli | İyidere | 834.9 | 1053.8 | 27.9 | 1.6 | 338 |
| 2232 Topluca | Fırtına | 763.2 | 1219.0 | 29.5 | 1.5 | 237 |
| 2233 Tozköy | Tozköy | 223.1 | 947.1 | 6.7 | 2.4 | 1296 |
| 2240 Eymur | Harşit | 3132.8 | 402.7 | 40.0 | 1.9 | 120 |
| 2272 Arılı | Arılı | 92.2 | 2156.0 | 6.3 | 1.4 | 175 |
| 2304 Bayburt | Çoruh | 1734.0 | 280.1 | 15.4 | 2.1 | 1545 |
| 2305 Peterek | Çoruh | 7272.0 | 304.0 | 69.9 | 2.3 | 654 |
| 2316 Ispir | Çoruh | 5505.2 | 220.5 | 38.5 | 2.5 | 1170 |
| 2321 Dutedere | Parhal | 586.0 | 753.4 | 14.0 | 2.0 | 705 |
| 2328 Ferhatlı | Ardanuç | 546.8 | 346.0 | 6.0 | 2.6 | 365 |
| 2330 Çamlıkaya | Çamlıkaya | 113.6 | 805.1 | 2.9 | 2.0 | 995 |
| | | | | | | |
| B-Short-Period: Station Name | River | Catchment Area (km²) | Run off (mm) | Discharge (m³s⁻¹) | Mean/Median Ratio | Elevation (m) |
| 2215 Dereköy | Çamlıdere | 945.2 | 37.0 | 13.5 | 1.9 | 942 |
| 2258 Cücen | Görece | 162.7 | 89.2 | 5.6 | 1.2 | 300 |
| 2259 Çiftdere | Kalyon | 121.5 | 53.3 | 2.5 | 1.5 | 250 |
| 2262 Konaklar | Hemşin | 496.7 | 90.3 | 17.3 | 1.5 | 300 |
| 2282Kömürcüler | Salarha | 83.3 | 186.7 | 6.0 | 1.3 | 250 |
| 2285 Kaptanpaşa | Şenöz | 231.2 | 107.6 | 9.6 | 1.2 | 400 |
| 2301 Berta | Berta Suyu | 1680.0 | 41.3 | 26.8 | 2.2 | 310 |
| 2315 Karşıköy | Çoruh Nehri | 19654.4 | 27.3 | 207.0 | 1.7 | 57 |
| 2323 Işhan Köprü | Oltu Suyu | 6854.0 | 12.9 | 34.0 | 1.8 | 572 |
| 2325 Asağı Kumlu | Oltu Suyu | 1762.0 | 10.4 | 7.1 | 1.8 | 1129 |
| | | | | | | |
| C-Meteorology Stations: | Basin | Ave. Temp (°C) | Precipitation (mm) | Rainy Days | Snow Period | Elevation (m) |
| Artvin | ÇORUH | 11.98 | 722.61 | 131.59 | Nov-Apr | 628 |
| Bayburt | ÇORUH | 6.98 | 443.01 | 100.84 | Oct-Apr | 1584 |
| Giresun | EBS | 14.45 | 1246.23 | 158.41 | Dec-Mar | 37 |
| Gümüşhane | EBS | 9.49 | 464.91 | 115.38 | Nov-Apr | 1219 |
| Hopa | EBS | 14.29 | 2243.38 | 181.28 | Dec-Mar | 33 |
| Ispir | ÇORUH | 10.40 | 478.00 | 95.66 | Nov-Apr | 1222 |
| Pazar | EBS | 13.30 | 2068.16 | 158.28 | Dec-Mar | 79 |
| Rize | EBS | 14.26 | 2241.41 | 169.19 | Dec-Mar | 9 |
| Tortum | ÇORUH | 8.27 | 470.69 | 116.16 | Oct-Apr | 1572 |
| Trabzon | EBS | 14.64 | 831.51 | 139.81 | Dec-Mar | 30 |

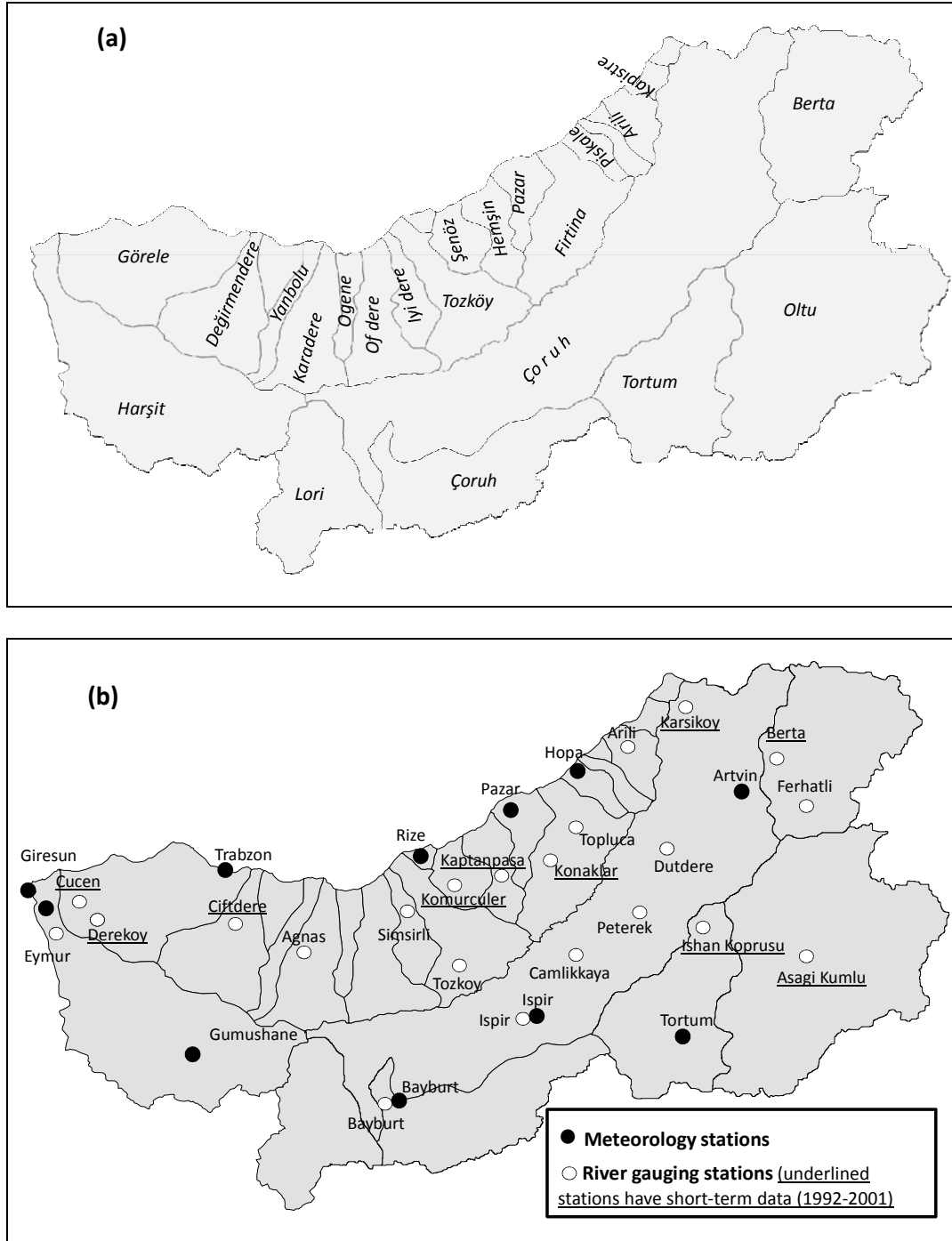


Figure 7.5 Basin delineation map of the study area (a) and location of the stations (b).

Fieldwork was undertaken during summer of 2008, in order to visit, appraise and evaluate each gauging station and the physical environment within the study area. Twenty-eight river gauging stations were evaluated and appraised as part of the summer 2008 fieldwork programme: 16 in the EBS Basin and 12 in the ÇRB (See Appendix III and IV for fieldwork

photographs. Coordination and technical information for each gauging station including construction, monitoring equipment (e.g., stage board, cable way, electronic monitoring etc.) as well as condition maintenance was also noted. Channel cross-sections, and river channel planform observations were also undertaken. Field observations of the physical factors such as channel width, depth, slope and blockage, inchannel vegetation forms, riparian land-use and vegetation were also noted together with evidence of channel change and/or anthropogenic impact within the immediate vicinity of the gauging station was also noted via detailed field logs and photographs. The local offices of the DSI and EIEI were each visited in order to discuss with local officials and technical engineers issues relating to the reliability of the datasets (e.g., type and nature of the river gauging stations, data collection techniques etc.). The local offices of DSI and EIEI were visited in Gümüşhane, Trabzon, Rize, Artvin and Erzincan provinces. Detailed information on the network of gauging stations, catchment areas, measurement techniques and field observations were acquired. Useful materials such as photographs, maps, database lists, rating curve samples and some reports for small-scale extreme events were received from these local offices. 18 of 22 stations used in this study were visited.

In general, all gauging stations visited during the summer 2008 fieldwork programme appeared to be well-maintained and complied with international standards. Channel planform of rivers at gauging sites look straight. Planforms for Aşağıkumlu and Çamlıkaya (Çoruh) rivers suggested that these rivers had been subjected to some change. One of the most important characteristics for the accuracy of measurements at river gauging sites is the quality of the cross-sections. Most of the stations have ideal cross-sections apart from Eymür (EBS), Ishan Kopru, Asagi Kumlu and Çamlıkaya (Çoruh) stations. For these gauging sites the location of the cross-section is not ideal and might affect high flow measurements. Channel

characteristics (width, depth, and slope) were also observed which differentiate depends on river morphology. In summary, channel form is deep, steep and narrow for most of those in the EBS Basin gauging stations, while channel form is relatively wider, less steep and shallower for those rivers in the Çoruh River gauging sites. In-channel vegetation was only observed for one station, Şimşirli station of EBS. Apart from a few stations that are located within settlement areas (e.g., Eymür, Cücen and Bayburt (Çoruh)), the vegetation within the vicinity of the gauging sites comprised broad leaf formations including hazelnut orchards. Although for most of the stations channels were observed as not being 'directly blocked', channels at many stations comprised of fallen rock debris, and/or inchannel sedimentation, upstream and/or downstream of the observation point. Ishan Kopru (Çoruh), Tozköy and Eymür (EBS) stations were noted as having significant quantities of inchannel material which presumably would cause significant channel blockage. Any evidence of channel change or anthropogenic impact around gauging station affecting river flow measurement was also observed. Evidence of anthropogenic manipulation of the channel was evident at Şimşirli station which included reinforcement of the channel and a slight change in channel geomorphology was evident at Çamlıkaya station. However, some stations in the EBS Basin (e.g., Eymür and Cücen), hazelnut plantations may be considered to be an anthropogenic impact. Only a few stations were noted as having a significant problem which may impact upon accurate flow measurements. At Eymür, for example, bedrock juts out into the channel adjacent to the gauging station which would presumably obstruct the river flow at a variety of levels. This channel obstruction may confound accurate downstream current velocities due to it pushing the main body of water to the opposite bank away from the gauging station.

7.3. Methods

7.3.1. Cluster analysis

The timing and magnitude of river flows over an annual cycle are assessed by adopting a multivariate technique to separately classify river flow regimes according to their shape and magnitude. The classification procedure is similar to that devised by (Hannah *et al.* 2000) and adapted by (Harris *et al.* 2000) and applied by (Bower and Hannah 2002, Bower, Hannah and McGregor 2004), (Hannah *et al.* 2005a, Hannah, Kansakar and Gerrard 2005b) and (Sarıç, Hannah and Eastwood 2010). The shape classification identifies stations (for regionalization) or station-years (to assess inter-annual regime variability) with similar regime forms, regardless of magnitude; whereas the magnitude classification is based upon four indices (i.e. the mean, minimum, maximum and standard deviation) derived from long-term mean monthly values or monthly mean values for each station or station-year, respectively, regardless of timing. Bower *et al.* (2004) suggested that this approach gives two separate sets of regime classification results: (i) regionalization stations based upon long-term average values to examine spatial patterns; (ii) annual regimes for each station-year (based upon monthly mean values) are grouped to identify temporal (between-year) variability.

The aim of this chapter is to identify river flow regimes in northeast Turkey to highlight inter-annual regime variability. For regionalization purposes, mean monthly river flow values across all years were used to estimate the long-term regime for a single station. To classify regime shape independently of magnitude, the 12 monthly observations for each station are standardised separately using z -scores (mean=0, standard deviation=1). The four magnitude indices are derived for the long-term regime for each station; however, it is necessary to standardize (z -score) between indices to control for differences in their relative values. Both

shape and magnitude classification is achieved using Ward's hierarchical, agglomerative cluster analysis method (Yarnal, 1992; Griffith and Amrhein, 1997). Ward's method produces the most robust clusters with fairly equal membership (Bower *et al.*, 2004; (Sariş *et al.* 2010). The 12 stations are subsequently grouped by regime shape and magnitude; the spatial distribution of classes allows identification of regime regions.

Regimes for individual station-years were classified using monthly mean values in order to identify inter-annual regime classes. To standardize for absolute magnitude differences between stations, the 12 monthly observations for each station-year are z -scored before shape classification. To classify the magnitude indices for all stations jointly, it is necessary to control for between-station differences in the indices (Bower *et al.*, 2002, 2004). This is achieved by expressing each index as z -scores over the 24-year record for individual stations prior to amalgamating the z -scores for all stations into the four indices. Regime shape and magnitude classes are identified for the 288 station-years using the same statistical procedures as for regionalization. Bower *et al.* (2004) note that: (i) regime classes are not interchangeable between long-term and station-year regime classifications, as analyses are performed upon different input data matrices; and (ii) magnitude classes for regionalization identify *absolute* differences between stations whereas magnitude classes for regime stability identify *relative* inter-annual variations at a station. Together, these classifications characterize spatial and temporal regime dynamics (Bower *et al.* 2004).

7.3.2. Homogeneity and trend tests

Non-parametric K-W, runs and M-K tests were used to discern the deterministic components in the time series such as homogeneity, persistence and trend for understanding non-random changing process. The homogeneity test of K-W was applied to determine whether the time-

series are homogeneous or not. K-W is a non-parametric, distribution-free test and is based on the comparison means or variances of time series within sub-periods for detecting any abrupt changes. The persistency of the time series was checked by non-parametric runs test in order to support the results of K-W. The randomness of monthly river flow time series is rejected for the high values of Z at one-sided distribution. Test statistics which are above the 5% and 1% significance levels ($\alpha \leq 0.05$ and 0.01 ; two-tailed test) can be accepted as significant.

Long-term trends in river flow series were detected by using the well-known Mann-Kendall rank correlation test. The explanation of M-K was made methods section of previous chapters (See sections 3.3, 5.2.2.3 and 6.3.3.). The ability of the M-K trend test is also affected by temporal autocorrelation within a time series and cross-correlation between sites (von Storch and Navarr, 1995; (Burn and Elnur 2002) (Yue and Pilon 2004, Yue *et al.* 2002). The presence of serial correlation can complicate the identification of trends insofar as a positive serial correlation can increase the expected number of false positive outcomes for the Mann-Kendall test. Pre-whitening method has been increasingly applied to flow series data prior to trend analysis to remove serial correlation. For this study, a slightly different approach was adopted and this is based on the autocorrelation and partial correlation function calculation for seasonal river flow time series. Thus, stations with high autocorrelation, which may be the result of significant change, can be detected.

7.3.3. Multiple linear regression

Regression analyses refer to a complete process of studying the causal relationship between one dependent variable and a set of independent, explanatory variables (Rogerson, 2001). Regional climate and flow relationships for northeast Turkey were investigated through multiple linear regression analyses by using a stepwise procedure. All analyses were carried

out for the seasonal river flow, precipitation and temperature and evaporation data for the period 1979-2005. Evaporation data are available for only 4 stations while temperature and precipitation data are available for 10 stations, while river flow data are available for 9 stations. Results from the multivariate linear regressions (R^2) are presented only if they are significant at the 5% level (i.e. T test, p value ≤ 0.05).

7.4. Results and discussion

7.4.1. River flow regimes

River flow regime analyses were carried out for two different data sets consisting of (i) 12 stations for the period 1982-2005 (24 years) and (ii) 22 stations for the period 1992-2001 (10 years) to maximise use of available data. The second data set was developed to increase the spatial coverage of river flow regime classification.

7.4.1.1. Flow regime shape

Two flow regime shape classes were identified for the longer period data set (1982-2005) (Figure 7.6a, and 7.6b). The flow regime shape classes grouped stations according to similarity in seasonality of flows as follows:

L–Class A. April–May peak (6 stations);

L–Class B. May–June peak (6 stations).

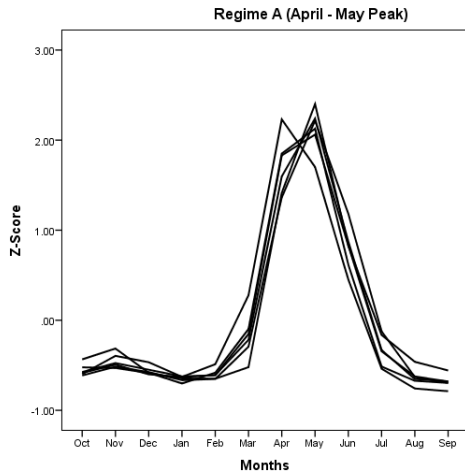
Three flow regime shape classes were identified for the shorter period data set (1992-2001) (Figure 7.6c, 7.6d and 7.6e):

S–Class A. April–May peak (11 stations);

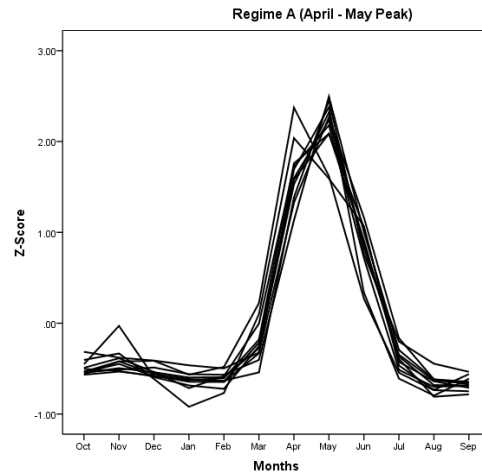
S–Class B. May–June peak (9 stations);

S–Class C. Marked April peak (2 stations).

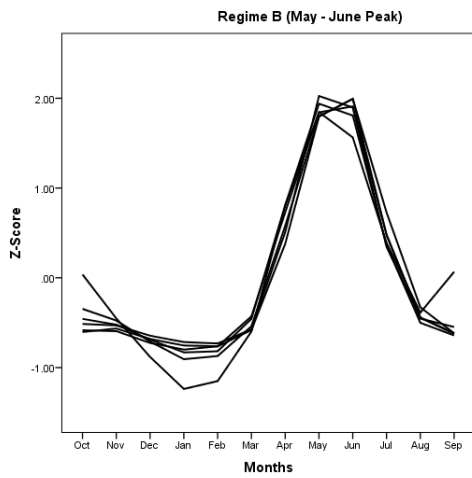
LA: Long Period –Regime A



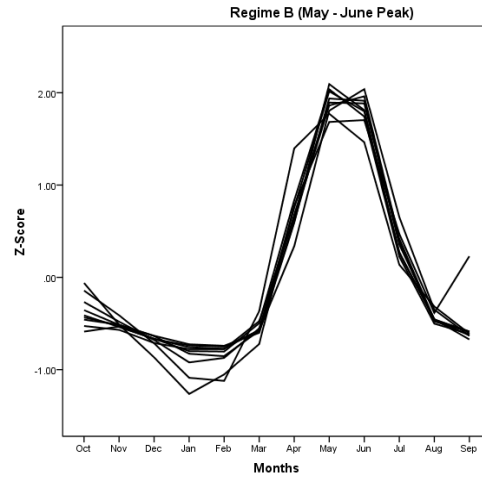
SA-Short Period –Regime A



LB-Long Period –Regime B



SB-Short period – Regime B



SC-Short period – Regime C

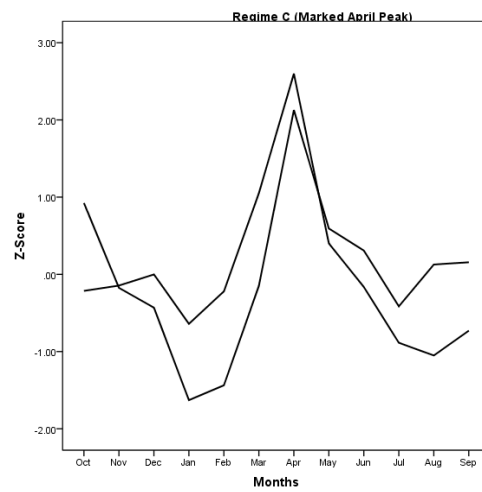


Figure 7.6 Standardised long-term regimes for all stations within each of the river flow shape class

Figure 7.6 show the intra-annual patterns in mean monthly river flows for all stations grouped by shape classes for the long (a, b) and short (c, d and e) period data sets. The regime classification results for the long period data indicates two different flow regime peaks. In L-Class A (Figure 7.6a), a steep rise is observed in April; peak river flow occurs during April and May and a sharp cessation to the dry summer period can be observed. The time period for peak high flow is relatively short and produces a regime that is markedly seasonal. In L-Class B (Figure 7.6b), a slight delay can be observed in the timing of peak flow in comparison to Class A; peak flow occurs during May to June and has a less steeper onset and sharp cessation and is also characterised by a dry summer and autumn. The peak flow period for L-Class B is relatively longer than Class L-A. January and February are characterised as the driest season for both regime shape classes. The flow regime shape classification for the shorter period data (1992-2001) included a higher number of stations (22) and produced three flow regime shape classes, two of which are similar as the flow shape classes for the longer period data set. S-Class A and S-Class B have similar characteristics with the April-May and May-June regime shape classes for the longer period classification (Figure 7.6c and 7.6d), although a marked April peak regime (S-Class C) can also be observed for the shorter period data classification (Figure 7.6e). For S-Class C, this peak flow period spans March through to May, while January-February is characterised as a low flow period and autumn represents a secondary wet period with August being the third driest month.

Melt water contribution and direct measurements of precipitation data at river gauging sites are not available; therefore explanations are based on the precipitation data of the nearest meteorological station. Seasonality of river flow regimes across northeast Turkey suggests that high (maximum) river flows are confined to a very short time period: namely April, May

and June. The inland (continental) climatic regime produces cooler/warmer climatic conditions than coastal climate regimes during winter/summer (Chapter 6.4.1). Different temperature regimes may cause a delay on the timing of maximum temperature and have a concomitant effect on the timing of rapid snowmelt. The Regime A (April-May peak flow) is governing for the majority of the ÇRB stations which are defined by an inland regime character (Chapter 6). Together with rapid snowmelt period in spring, the spring rainfall maxima may jointly determine the river flow regime for the ÇRB.

EBS Basin is characterised by a wet coastal regime character (Section 6.4.1 and Figure 6.3). Autumn is the wettest period for the EBS Basin. For Regime B (dominating the EBS Basin), the May-June period is defined as peak flow period. Snowmelt seems to be the governing processes for peak river flow occurrence as evidenced by rising temperature (Akpınar *et al.*, 2011; Chapter 6). As mentioned above, the delay of the high temperature period may cause a lag in river flow peak, namely from April-May to May-June for this regime. Although river flow has a markedly seasonal character in this region, these data suggest clearly that Regime B (Both L-Class B and S-Class B) does not exhibit a prolonged low flow period when compared with Regime A (Both L-Class A and S-Class A) and this is most likely related to the longer rainy period, less evaporation and higher humidity conditions for the coastal basin. These data also suggest a secondary river flow peak period for autumn by reason that this period is characterised as rainfall peak for the EBS (Section 6.4.1). In summary, the actual timing of peak flows for the EBS and ÇRB indicates that snowmelt is by far the most important contributor of river flow maxima, rather than direct rainfall.

L-Class C with a clear April peak is represented by two physically distant stations over EBS. The seasonality of this flow regime class has similarities with Regime A in terms of peak

time, but it also has a relatively higher river flow episode during autumn similar to Regime B. This character of the seasonality regime (especially for the station located within the Regime B dominated area) can be explained by an earlier increase in temperature. The period of lowest flow regimes is January and February as a consequence of a cool temperature regime and winter snowfall.

7.4.1.2. Flow regime magnitude

Three magnitude classes can be defined as follows for the longer period data set (1982-2005) (Figure 7.7):

L–Class 1. Low with the lowest values for all indices (9 stations);

L–Class 2. Intermediate with values between Classes 1 and 3 for all indices (2 stations);

L–Class 3. High with the highest values for all indices (1 station).

And three magnitude classes are also defined for short period data set (1992-2001) (Figure 7.7):

S–Class 1. Low with the lowest values for all indices (16 stations);

S–Class 2. Intermediate with values between Classes 1 and 3 for all indices (5 stations);

S–Class 3. High with the highest values for all indices (1 station).

Table 7.2a and 7.2b presents the average values for the river flow indices for the flow regime magnitude classes for the longer period and shorter period data sets, respectively. Magnitude regime characteristics of the study area and the spatial pattern of regime variability are interpreted depending on the short period grouping results. As mentioned in earlier section explanations are based on the precipitation data of the nearest meteorological station. Sixteen,

five and one river gauging stations were detected for low (1), intermediate (2) and high (3) river flow magnitude classes, respectively. A marked precipitation maximum is clearly detected for the EBS Basin, especially for the eastern section. However, all stations of the EBS Basin are grouped in the low magnitude class apart from Eymür (Harşit River), which is located on the western border of the basin. Low flow characteristics for the EBS Basin can be explained by geological characteristics because of the permeable, sedimentary lithology of the region (Figure 7.2).

Intermediate and high flow magnitude classes were obtained for the ÇRB, where the elevational range is markedly larger than the EBS Basin. The denser drainage network, less permeable geology and soil, and less well vegetated, steeper slope properties of the ÇRB basin may be significant in generating higher magnitude regimes on top of climatic differences with the EBS basins.

Table 7.2 Average values for the runoff indices for all basins within the flow regime magnitude classes.

| Long-Period: Flow index | Class average (mm monthK1) | | | All stations (mm monthK1) |
|--------------------------------|-----------------------------------|----------|----------|----------------------------------|
| | 1 | 2 | 3 | |
| <i>Mean</i> | 13.3 | 39.2 | 69.9 | 22.3 |
| <i>Standard deviation</i> | 12.3 | 44.8 | 76.3 | 23.1 |
| <i>Minimum</i> | 3.0 | 5.6 | 13.6 | 4.4 |
| <i>Maximum</i> | 66.2 | 263.9 | 362.0 | 123.8 |
| <i>No. Stations</i> | 9 | 2 | 1 | 12 |

| Short-Period: Flow index | Class average (mm monthK1) | | | All stations (mm monthK1) |
|---------------------------------|-----------------------------------|----------|----------|----------------------------------|
| | 1 | 2 | 3 | |
| <i>Mean</i> | 11.4 | 50.8 | 232.9 | 30.4 |
| <i>Standard deviation</i> | 9.5 | 54.5 | 229.1 | 29.7 |
| <i>Minimum</i> | 2.5 | 7.6 | 49.0 | 5.8 |
| <i>Maximum</i> | 44.6 | 261.4 | 1206.0 | 146.7 |
| <i>No. Stations</i> | 16 | 5 | 1 | 22 |

Figure 7.7 shows box plots of mean and maximum magnitude indices for each class for both long (a,b) and short (c,d) period data sets. These two analysis periods show consistent patterns of classification across the 3 magnitude classes for those stations present in both datasets, except for the Eymür (EBS) that shifts from high to intermediate between the longer and shorter term classification. For the shorter term classification, the high magnitude regime is represented only by Karşıköy station (s2315) on Çoruh River, which has extremely high river flows (Figure 7.7c).

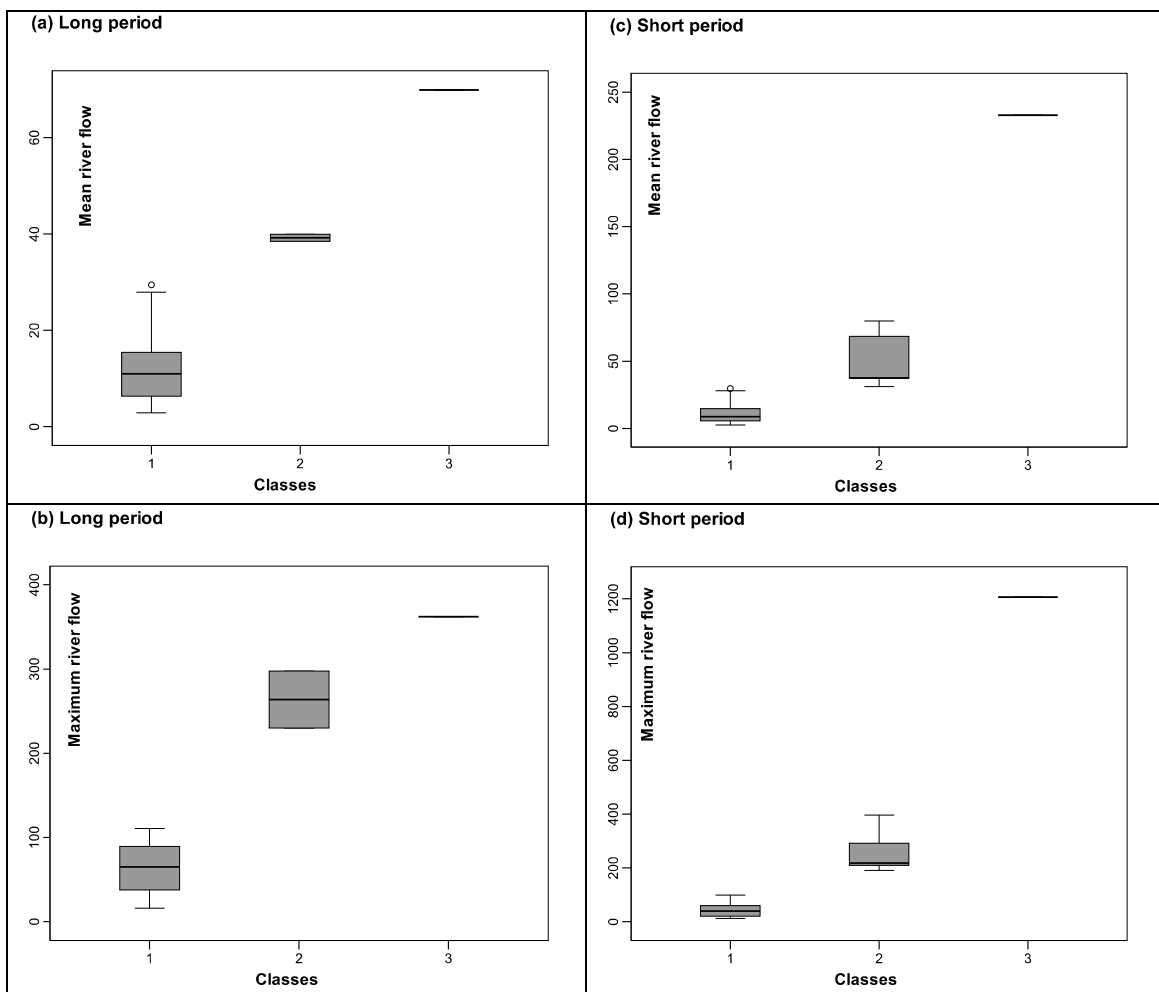


Figure 7.7 Box and Whiskers plots of station mean and maximum river flow for magnitude classes of long (a,b) and short (c,d) period classifications.

A composite river flow regime classification may be achieved by combining shape and

magnitude classes which permits the standardised seasonal responses to be scaled by river flow amount. Of the 6(9) possible, 4(5) composite classes can be produced for the study area for the longer (shorter) period data sets. Figure 7.8 illustrates the spatial distribution of these composite regimes for the longer period (a) and the shorter period (b) data sets.

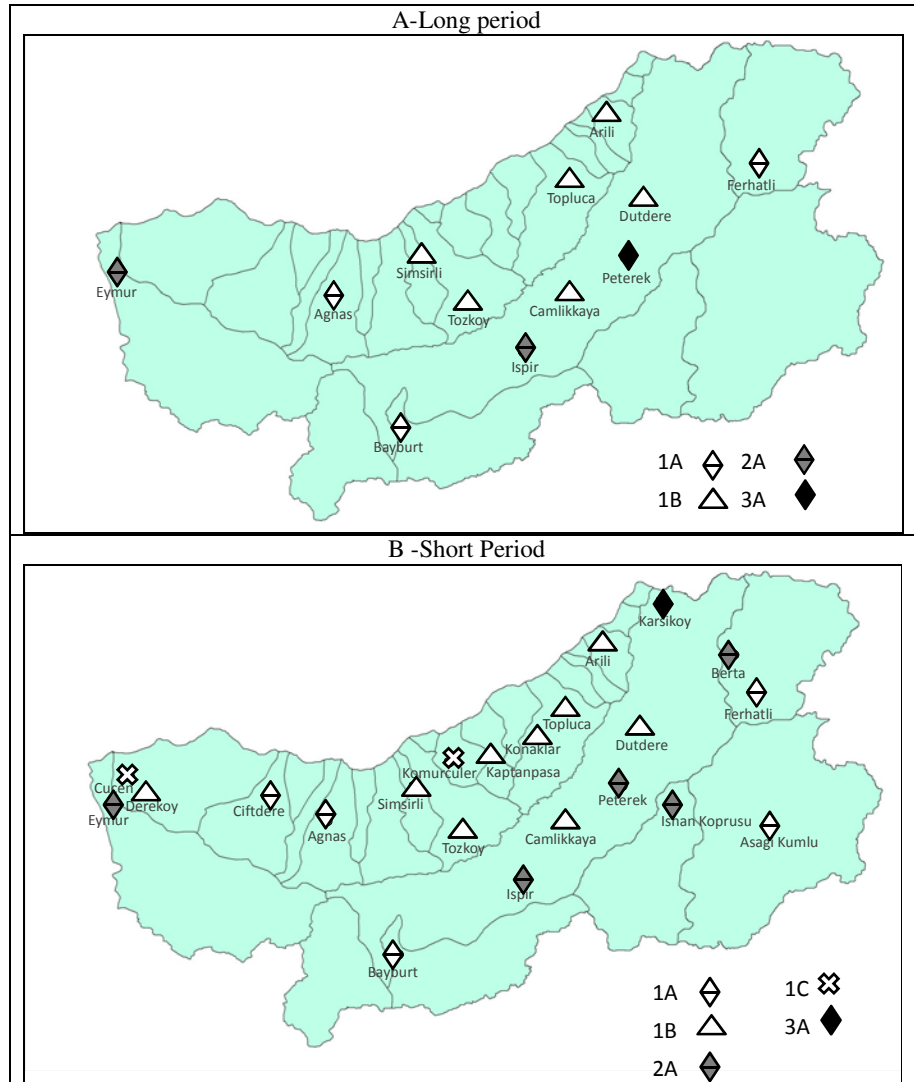


Figure 7.8 Spatial distribution of stations within river flow regime shape classes.

The spatial variability of river flow regimes for northeast Turkey produces mainly two flow regime regions: the mountainous area of north-northeast (East Black Sea Mountain range) and the rest of the study area, which comprises the majority of the ÇRB stations (Figure 7.8a and

7.8b). Stations representing May-June peak flow regime (class) are located around the Kaçkar Mountains, while the April-May peak flow regime (class) are located in the western part of the EBS Basin (Harşit River), within the main basin of the Çoruh River and also the sub-basins (tributaries) of Oltu (Oltu River) and Berta (Berta and Ardanuç rivers). Again, topography, continentality/maritime-influence and precipitation regimes appear to be the major drivers of river flow variability for northeast Turkey.

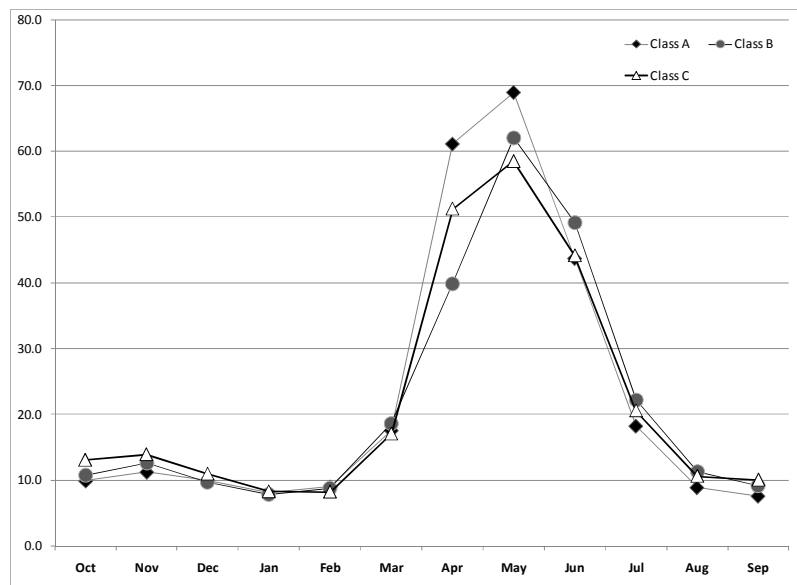


Figure 7.9 Inter-annual regime variability: standardised average regimes of all station-years within each shape class for annual river flow.

7.4.1.3. Regime stability (year-to-year regime dynamics)

Stability of regime shape and magnitude are classified using monthly mean flow for each year for the 12 stations in northeast Turkey (i.e. individual station-years) to provide the basis for quantification of inter-annual regime stability. A total of 288 station years were evaluated for the period 1982-2005. Table 7.3 shows the inter-annual regime magnitude and shape variability for river flow for northeast Turkey stations.

Shape. Three shape classes are produced (Figure 7.9) with differences in flow seasonality:

Class A. April-May Peak (123 station-years);

Class B. May-June Peak (110 station years);

Class C. May with extended spring and secondary autumn peak (55 station years).

Magnitude. Three magnitude classes (that characterises relative differences between sites) are produced, which can be described by using the following indices definitions (which is in agreement with regionalisation solutions):

Class 1. Low with the lowest values for all indices (124 station-years);

Class 2. Intermediate with values of all indices, between Classes 1 and 3 (111 station-years);

Class 3. High with the highest values for all indices (53 station-years).

Table 7.3 Inter-annual regime (a) magnitude and (b) shape variability for river flow (A/1 [*]; B/2[+]; C/3[#]).

| | | | | | | | | | | | | | | | | | | | | | | | | | |
|------------------------------|-------|-------|-------|-------|-------|-------|-------|-------|-------|-------|-------|--------------------------|-------|-------|-------|-------|-------|-------|-------|-------|-------|-------|-------|-------|------|
| * | * | + | # | # | * | # | # | # | + | * | + | 2005 | * | * | * | * | * | + | * | # | * | * | * | * | 2005 |
| * | * | + | # | # | * | * | # | # | + | + | # | 2004 | + | + | + | + | + | # | + | + | + | + | + | + | 2004 |
| * | + | * | * | # | * | + | + | * | * | # | + | 2003 | * | * | # | * | * | # | * | # | * | * | * | # | 2003 |
| + | # | # | # | * | + | + | + | + | + | + | + | 2002 | + | # | + | # | * | * | + | + | + | + | # | * | 2002 |
| + | + | * | * | * | * | + | + | + | * | # | + | 2001 | + | + | + | * | + | # | * | * | + | + | + | + | 2001 |
| + | + | * | * | * | * | + | + | + | + | + | + | 2000 | * | * | * | * | * | * | # | # | # | * | * | * | 2000 |
| * | + | + | + | * | * | + | * | * | + | + | + | 1999 | + | + | # | + | * | + | * | * | * | # | # | * | 1999 |
| * | * | + | # | # | * | # | # | # | + | + | + | 1998 | + | * | * | * | * | # | * | # | * | * | * | * | 1998 |
| * | * | + | # | # | + | # | * | * | + | * | + | 1997 | * | + | # | + | * | # | + | * | + | # | * | * | 1997 |
| * | + | * | * | * | * | * | * | * | * | # | + | 1996 | # | + | # | + | + | # | + | * | + | # | + | # | 1996 |
| + | + | * | + | * | * | * | * | * | + | # | * | 1995 | + | + | # | + | + | + | + | * | + | # | + | * | 1995 |
| + | + | * | * | * | * | + | + | + | * | + | + | 1994 | * | * | * | * | * | * | * | # | * | * | * | * | 1994 |
| # | * | + | # | + | + | # | # | # | # | * | # | 1993 | + | + | + | # | * | + | * | * | * | + | * | + | 1993 |
| * | # | + | # | * | # | + | * | * | * | * | # | 1992 | + | # | + | # | * | + | + | + | + | + | # | + | 1992 |
| + | + | + | + | * | * | + | * | * | * | + | * | 1991 | * | + | + | * | * | + | * | # | * | + | * | * | 1991 |
| # | # | + | + | # | + | * | * | * | + | + | + | 1990 | * | + | # | + | + | + | * | * | * | * | + | * | 1990 |
| + | # | + | # | * | + | + | * | * | # | + | + | 1989 | * | * | * | * | # | # | # | # | # | * | * | # | 1989 |
| * | + | + | # | + | + | # | # | # | # | + | # | 1988 | + | # | + | # | * | + | + | * | * | + | # | + | 1988 |
| * | + | * | * | + | * | * | # | # | + | + | # | 1987 | + | + | # | + | + | + | + | * | + | # | # | * | 1987 |
| + | + | * | + | * | * | + | * | * | + | + | # | 1986 | + | # | + | # | + | # | * | + | + | + | * | + | 1986 |
| * | + | * | * | * | * | + | + | * | * | + | + | 1985 | + | * | * | + | * | # | * | # | * | * | * | * | 1985 |
| * | + | + | * | * | * | * | * | * | * | * | * | 1984 | # | # | + | # | + | + | + | + | + | + | + | * | 1984 |
| * | + | * | + | * | * | + | + | + | * | + | * | 1983 | + | + | + | + | + | + | + | * | + | * | * | * | 1983 |
| * | * | * | * | * | * | * | * | * | * | * | * | 1982 | * | * | * | * | * | * | * | * | * | * | * | * | 1982 |
| s2202 | s2218 | s2232 | s2233 | s2240 | s2272 | s2304 | s2305 | s2316 | s2321 | s2328 | s2330 | Cl.3 | s2202 | s2218 | s2232 | s2233 | s2240 | s2272 | s2304 | s2305 | s2316 | s2321 | s2328 | s2330 | Cl.3 |
| Magnitude Stability Clusters | | | | | | | | | | | | Shape Stability Clusters | | | | | | | | | | | | | |

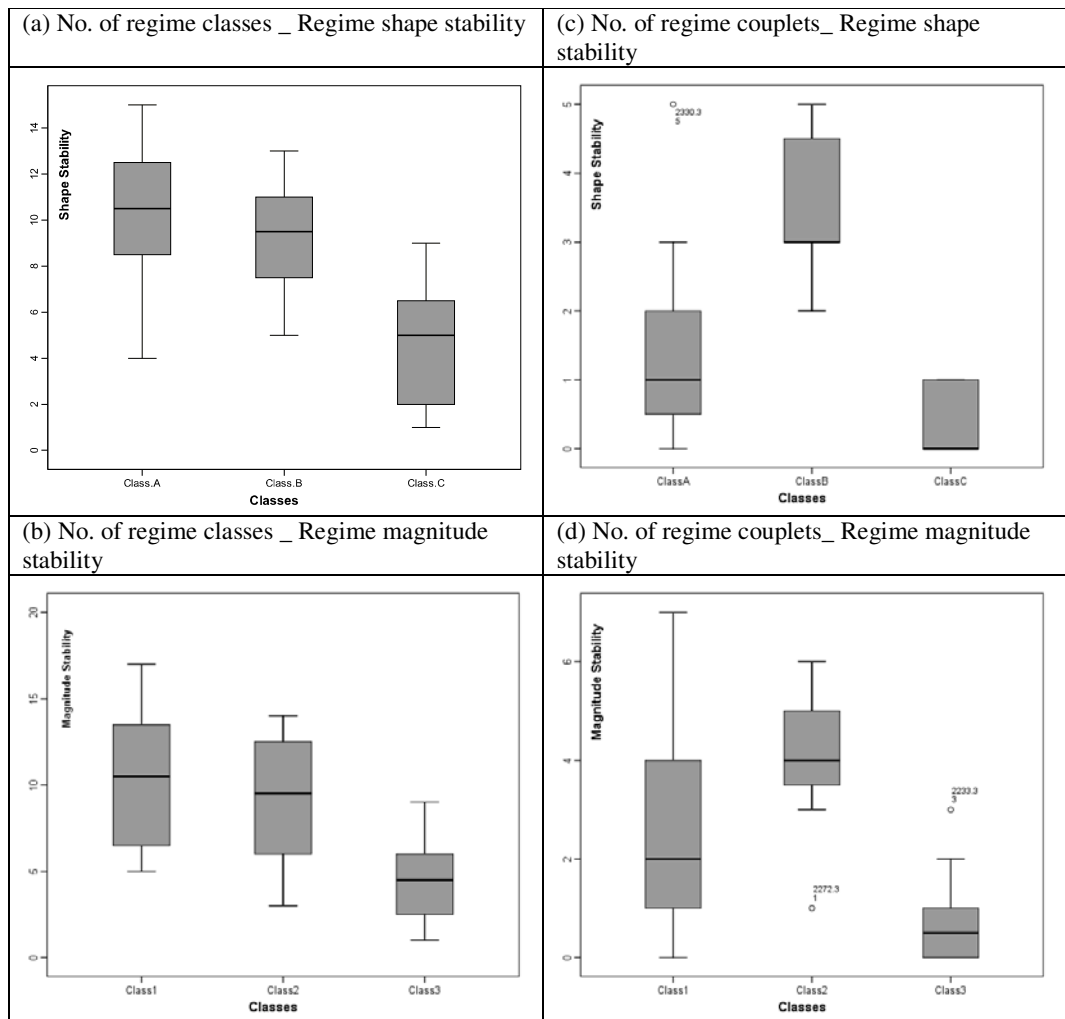


Figure 7.10 Box-plots showing the stability of regime shape and regime sequencing at stations (a and b) number of regime classes, (c and d) number of regime couplets.

Regime frequency variability over the whole period is assessed to consider switching of classes between-years. The number of regime classes and regime frequency of 2-year sequences (couplets) is illustrated with box plots (Figure 7.10). The number of years per station are categorised into three different classes is plotted for regime shape and magnitude stability (Figure 7.10a and 7.10b). Class A and Class 1 have the largest number of years, followed by Class B and Class 2 and Class C and Class 3. The proportion of Class A and Class 1 is very important as this class represents almost 50% of the total station years. The box

plots of regime couplets identifies that Class B and Class 2 have the highest number of sequencing years, which means these classes represent the most persistent regime pattern (Figure 7.10c and 7.10d). Similar to the frequency of classes-between years, the regime couplets are represented by small numbers for Class C and Class 3.

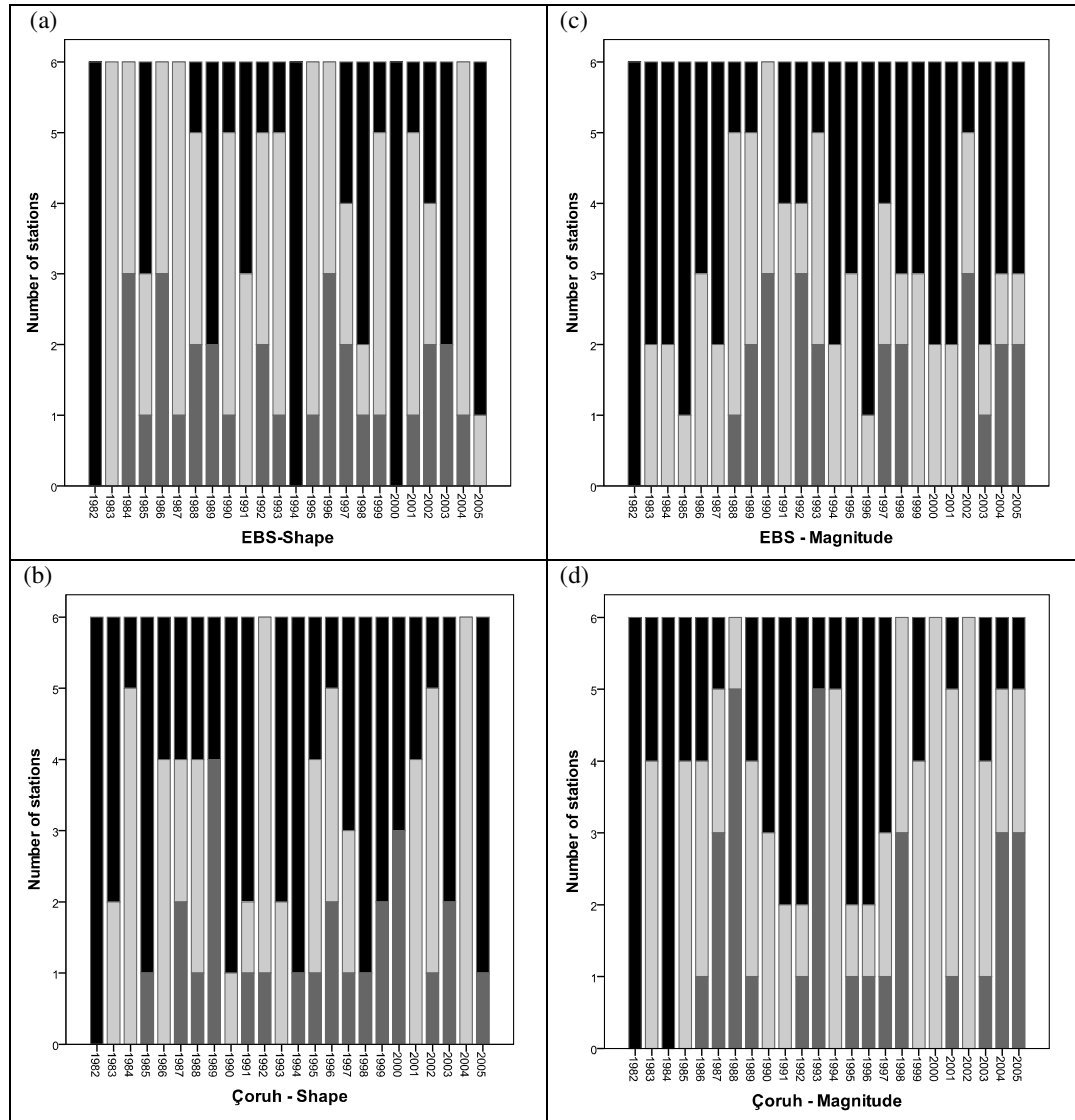


Figure 7.11 Basin frequencies of flow regime shape and magnitude (■:A/1, ■:B/2, ■:C/3).

Figure 7.11 illustrates the annual frequency of regimes by basin and identifies periods when particular shape and magnitude classes dominate across the EBS and Çoruh River basins. The dominant shape class is represented by Class B (May-June peak) for the EBS Basin, while the

Çoruh is characterised by mostly Class A (April-May peak). Widespread low flows occurred in the periods 1982-1987, 1994-2001 and 2003-2005 station years in the EBS Basin, while the Çoruh Basin does not appear to have experienced any long and severe low flow periods. However, the EBS Basin experienced low flow conditions for the periods 1982-1987, 1989-1992 and 1994-1997.

7.4.2. Temporal variability of river flows

Results of monthly trend analysis for mean, minimum and maximum river flow data are summarised in Table 7.4a. The number of detected significant trends is low. However, all significant decreasing trends were found in ÇRB, while statistically significant increasing trends were detected in the EBS basin. The 75% of the significant results were detected in Tozköy (EBS) and Çamlıkaya (ÇRB) (Table 7.4b). According to the table, the period December through February can be defined as most important period in terms of river flow trends. In addition to that period, May is also characterised by significant trends observed in river flows. January and May minimum and maximum river flows of Çamlıkaya have statistically significant decreasing trends. For Tozköy station, significant increasing trends observed in mean flow (D-J-F and May), minimum and maximum flows (January and December) are most notable results of monthly trend analysis.

Significant trends observed for the seasonal time series are presented in Table 7.4c. Significant results have been obtained for some of the individual stations especially for the winter and autumn periods of the EBS Basin Rivers.

Table 7.4 Results of trend test: summarizing table for monthly flows (a), test statistics of selected stations (b) and seasonal river flow series (c) (The number in brackets indicates the total number of statistically significant trends and shaded cells indicate significant test statistics.).

| (a) | Mean | Minimum | Maximum |
|-----------------|------------|------------|------------|
| Decreasing (7) | 67 | 69 | 69 |
| Increasing (10) | 77 | 75 | 75 |
| CRB | [1] | [3] | [3] |
| Decreasing (7) | 36 | 39 | 39 |
| Increasing | 36 | 33 | 33 |
| EBSB | [4] | [3] | [3] |
| Decreasing | 31 | 30 | 30 |
| Increasing (10) | 41 | 42 | 42 |

| (b) | Mean Flow | | Minimum Flow | | Maximum Flow | |
|-----|-----------|-------|--------------|-------|--------------|-------|
| | Tozkoy | Ckaya | Tozkoy | Ckaya | Tozkoy | Ckaya |
| Oct | 0.16 | 0.00 | -0.01 | 0.02 | -0.01 | 0.02 |
| Nov | 0.07 | -0.12 | 0.05 | -0.26 | 0.05 | -0.26 |
| Dec | 0.31 | -0.29 | 0.22 | -0.27 | 0.22 | -0.27 |
| Jan | 0.36 | -0.12 | 0.40 | -0.30 | 0.40 | -0.30 |
| Feb | 0.35 | -0.10 | 0.33 | -0.12 | 0.33 | -0.12 |
| Mar | 0.16 | 0.04 | 0.10 | -0.06 | 0.10 | -0.06 |
| Apr | 0.25 | 0.01 | 0.27 | 0.05 | 0.27 | 0.05 |
| May | 0.34 | -0.11 | 0.18 | -0.30 | 0.18 | -0.30 |
| Jun | 0.09 | -0.26 | 0.11 | -0.27 | 0.11 | -0.27 |
| Jul | -0.07 | -0.17 | 0.02 | -0.13 | 0.02 | -0.13 |
| Aug | -0.02 | -0.17 | 0.11 | -0.01 | 0.11 | -0.01 |
| Sep | 0.04 | -0.15 | 0.08 | -0.09 | 0.08 | -0.09 |

| (c) | DJF | MAM | JJA | SON |
|------|-------------|-------------|-------|-------|
| 2202 | 0.08 | -0.06 | -0.14 | -0.15 |
| 2218 | 0.01 | -0.03 | -0.06 | -0.01 |
| 2232 | 0.28 | 0.13 | -0.05 | 0.22 |
| 2233 | 0.38 | 0.38 | -0.01 | 0.17 |
| 2240 | -0.30 | -0.14 | -0.27 | -0.30 |
| 2272 | 0.01 | 0.30 | 0.03 | 0.30 |
| 2304 | -0.14 | 0.06 | 0.06 | -0.04 |
| 2305 | -0.09 | 0.06 | -0.02 | 0.00 |
| 2316 | -0.17 | 0.09 | -0.13 | -0.15 |
| 2321 | 0.12 | 0.14 | -0.01 | 0.30 |
| 2328 | 0.12 | -0.12 | -0.07 | 0.11 |
| 2330 | -0.26 | -0.30 | -0.30 | -0.08 |

Seasonal river flow series provides similar trend patterns, especially for Tozköy, Eymür and Arili stations in the EBS Basin which have significant trends. Eymür (s2240) displays decreasing trends which is contrary to the general increasing trend that can be observed for the EBS Basin. Significant results for the ÇRB stations are only few in number and do not display any systematic pattern of change. Seasonal results of runs test do not suggest any significant and consistent non-random pattern for stations. The spring series of minimum river flow for Eymür, the autumn series of maximum flows for Arili and Peterek, the winter series of maximum flows for Ağnas and finally the spring series of maximum flows for Topluca stations all appear to have significant persistency.

Autocorrelation function in the seasonal river flow series was analysed to assess hydrological persistence. Results suggest that three river gauging stations in the ÇRB (Çoruh, Peterek and Ispir) have serially correlated (significant at 0.05 and lag-4) time series.

7.4.3. Relationship between seasonal river flow and regional climate

Climatic parameters such as precipitation, temperature, evaporation, snowmelt along with the physical properties of the hydrological basin must be taken into account to explain river flow regime variability. The rest of this section discusses the climatological processes responsible for seasonal flow regime characteristics. MLR was used to model the seasonal flows for each station as a function of precipitation, temperature and evaporation to detect the sensitivity of the river flows to regional climatic drivers (Table 7.5). The results indicate significant ($p \leq 0.05$) model fits and; therefore, identifying the nature and strength of relationships for the three climate predictors. Both concurrent and preceding season datasets of the climatic drivers were evaluated to assess river flow variability links to regional climate.

Table 7.5 Significant results of MLR analysis.

| Season | Stations EBS | Preceding Season | | | Concurrent Season | | | |
|--------|-----------------|------------------|---------------|------|------------------------------|------------------------------|-------------|------|
| | | Precipitation | Temperature | Fit | Precipitation | Temperature | Evaporation | Fit |
| Winter | 2202 | Tortum | | 0.18 | Gumushane | | | 0.23 |
| | 2218 | Hopa | Rize | 0.56 | | | | |
| | 2232 | Hopa / Ispir | | 0.34 | Trabzon | | | 0.3 |
| | 2233 | Rize | | 0.45 | | | | |
| | 2240 | | | | Gumushane | | | 0.21 |
| Spring | 2202 | Gumushane | | 0.36 | Gum./Rize | Gumushane | | 0.17 |
| | 2218 | Artvin | Hopa | 0.49 | | | | |
| | 2232 | Artvin | | 0.42 | | | Gumushane | 0.16 |
| | 2233 | Artvin | | 0.18 | | | Trabzon | 0.36 |
| | 2240 | | | | | Hopa | | 0.23 |
| Summer | 2202 | Artvin | Art./Tortum | 0.5 | Gir./Gum./Hop ./Paz./Riz. | | Trabzon | 0.26 |
| | 2218 | Artvin | Tor./Isp./Gir | 0.69 | Giresun | | Gumushane | 0.28 |
| | 2232 | Artvin | Tortum | 0.36 | Gir./ Paz. | | Gumushane | 0.34 |
| | 2233 | Artvin | Tortum | 0.42 | Gir./Paz. | | Gumushane | 0.27 |
| | 2240 | | | | Gir./Gum./Hop ./Tra. | Gum./Tra | Gum./Tra. | 0.39 |
| Autumn | 2202 | Gumushane | | 0.55 | Gumushane | Gir./Gum. | | 0.47 |
| | 2218 | Gumushane | | 0.22 | Gum./Hop./Riz | Gir./Gum./Paz | | 0.36 |
| | 2232 | Pazar | | 0.18 | Gum./Hop./Pa z./Riz./Tra. | Gumushane | | 0.25 |
| | 2233 | Gumushane | | 0.24 | Gum./Hop. | Gumushane | | 0.49 |
| | 2240 | | | | Gumushane | Gir./Gum./Paz ./Riz./Tra. | Gumushane | 0.55 |

| Season | Stations Çoruh | Preceding Season | | | Concurrent Season | | | |
|--------|-------------------|------------------|-------------|------|-------------------|---------------|-------------|------|
| | | Precipitation | Temperature | Fit | Precipitation | Temperature | Evaporation | Fit |
| Winter | 2304 | Ispir | | 0.17 | | | | |
| | 2305 | Ispir | | 0.47 | | | | |
| | 2316 | Gum./Trabzon | | 0.57 | Artvin | | | 0.16 |
| | 2321 | Hopa | | 0.29 | | | | |
| Spring | 2304 | Ispir | | 0.27 | | | | |
| | 2305 | Ispir | | 0.4 | | | | |
| | 2316 | Ispir | | 0.49 | | | | |
| | 2321 | Artvin | | 0.39 | | | | |
| Summer | 2304 | | Tortum | 0.28 | Ispir | Bay./Isp./Tor | | 0.32 |
| | 2305 | Artvin | Tortum | 0.42 | Ispir | Isp./Tor. | | 0.27 |
| | 2316 | Artvin | Tortum | 0.42 | Bay./Isp. | Isp./Tor. | | 0.25 |
| | 2321 | Art./Gum. | Tortum | 0.41 | Ispir | Isp./Tor. | | 0.24 |
| Autumn | 2304 | Hopa | | 0.35 | Bay./Isp. | Ispir | | 0.41 |
| | 2305 | Hop./Gum./Tra | | 0.61 | Bay./Isp./Tor. | Ispir | | 0.53 |
| | 2316 | Hop./Gum./Tra | | 0.6 | Bay./Isp | Ispir | | 0.44 |
| | 2321 | Gumushane | | 0.17 | Art./Bay./Isp. | Artvin | | 0.51 |

For evaporation data, only four stations have complete data for the analysis period (Gümüşhane-Trabzon and Bayburt-Ispir represented EBS and Çoruh River basins, respectively). As expected given simple proximity, the EBS climate stations are good predictors for EBS Basin Rivers, while inland stations are good predictors for Çoruh River

and its tributaries. For winter and spring river flows, precipitation appears to be the main predictor, while for summer and autumn flows, temperature has as much stronger association. The contribution of evaporation to the model fit is generally poor, except the summer period for the EBS Basin river flows (e.g. 2218, 2232 and 2233 were correlated with evaporation in Gümüşhane).

For the preceding season analysis, EBS winter flows are affected from autumn precipitation conditions of the coastal stations of the EBS Basin (Hopa and Rize). For the other seasons, the inland stations of Artvin and Gümüşhane have a significant influence on the conditions of seasonal river flow of the EBS Basin Rivers. Spring temperature conditions at Tortum appear to be a good predictor for summer river flows for the EBS Basin. Some more complex relationships have been revealed for the preceding season analysis. Summer precipitation conditions for the coastal stations of Hopa and Trabzon are correlated with autumn river flow of the Çoruh River Basin.

Concurrent analyses of the EBS Basin river flows provide more physically interpretable predictors which are represented by Gümüşhane (inland) and Trabzon, Hopa and Pazar (coastal) stations of the EBS Basin. Also in the concurrent analyses, autumn and summer are jointly important as being good mostly double predictors specifically for the Harşit River station. Gümüşhane evaporation was also one of the important contributors for summer river flows of the EBS Basin Rivers (Table 7.5).

In the ÇRB, autumn and winter precipitation of Ispir station was detected as the main predictor for most of the stations for winter and spring river flow. Conversely, no significant results were obtained from concurrent data analysis for these periods. In summer, spring conditions of Artvin precipitation and Tortum temperature are important predictors. For

concurrent analyses, Ispir precipitation and Ispir-Tortum temperature for the summer period appears to be a good predictor for river flow fluctuations for ÇRB stations.

Interestingly, summer precipitation for Hopa and Trabzon on the Black Sea coast was detected as a predictor of autumn river flow for the ÇRB stations together with Gümüşhane (an inland station of EBS Basin). For the concurrent analyses, the inland stations of Bayburt and Ispir precipitation are good predictors of autumn river flow change for ÇRB, while Ispir temperature (and Artvin has an impact on river flow of 2321 Dutdere station) fit the model for most of the river flow stations, alone (Table 7.5).

Sample time series indicating a significant climate (independent) and river flow (dependent) relationship were plotted in order to interpret the relationship between river flow and regional climate predictors (Figure 7.12). In the graphs the average z-scores for each basin during each season were used to illustrate the nature of the relationship between river flow and the climatic drivers. These data suggest that the wet precipitation period correlates with high river flow. High temperature episodes commonly result in low river flow periods. However, precipitation is the most important and strong predictor on river flow. These links between regional climate and river flow variability tend to be more stable in the ÇRB; the EBS Basin can be interpreted by more complex relationships. This disagreement is highly related with the continental characteristic of Çoruh River Basin. In summary, the MLR results demonstrates the climate and river flow links over northeast Turkey by providing initial results on joint analysis of temperature, precipitation, evaporation and river flow.

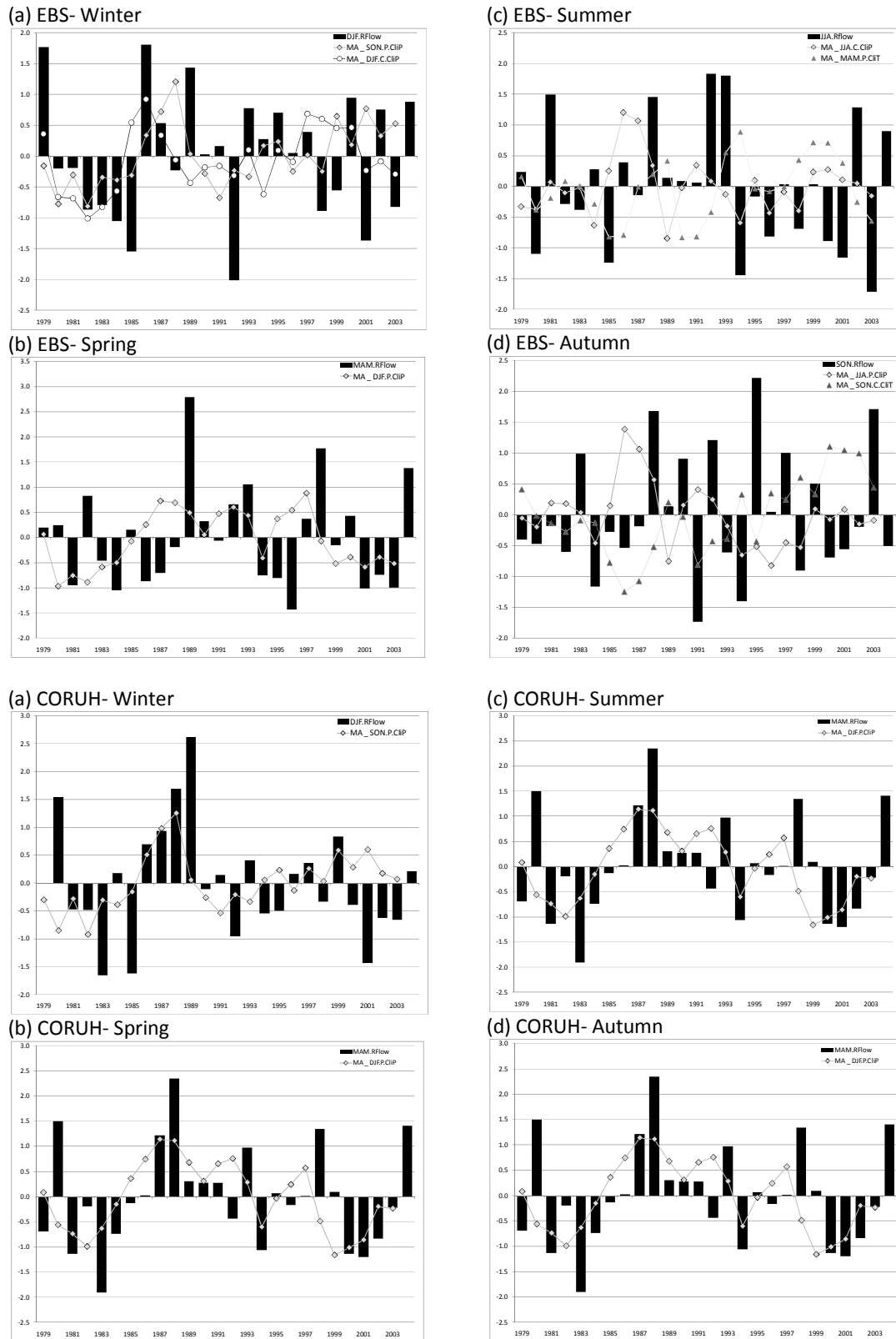


Figure 7.12 Seasonal composite river flow, precipitation and temperature (z-scores displaying negative and positive values).

7.5. Conclusions

This study has provided first comprehensive and detailed information on river flow regimes, river flow variability and explanations regarding the controlling factors on river flow variability together with the physical processes (on the interpretation on northeast Turkey).

Bower *et al.* (2004) state that the classification of regime shape and magnitude which was adapted and used as part of this study considers the whole annual cycle rather than isolating a single month or season for analysis. Regime classification analysis has achieved the first, most extensive and robust definition of river flow regimes for rivers in northeast Turkey. Regime classifications for both longer and shorter period data sets and their between-year stability (longer period data) were produced for the EBS and Çoruh River basins of northeast Turkey. These results suggest that rivers in northeast Turkey are characterised by markedly seasonal flows with an April-May-June maximum flow period. The spatial variability of the flow regime seasonality is largely dependent on the topography of the study area. The EBS Basin, where the North Anatolian Mountains cover the majority of the total area of the eastern part of it, is characterised by a May-June peak, while the ÇRB is defined by having April-May peak. The timing of river flows indicates that snowmelt is an important process and contributor of river flow maxima for both basins. The inland (continental) regime has a cooler character than the coastal climate regime and warming (so snowmelt) period begins earlier than the EBS Basin. However, the maritime effects on the coast (e.g., orography, cyclonic activity etc.) construct more complex processes which increase the humidity causing a delay in the timing of temperature maxima, thereby affecting the timing of snowmelt. Low and intermediate (EBS and ÇRB) prevail across the region. The driest period of flow regimes is January and February.

Three (low, intermediate, high) river flow regime magnitude classes were identified. Intermediate and low regime magnitude classes are concentrated over the study area and detected for both the Çoruh River and EBS basins respectively. Based on the combination results derived from composite regime classification, northeast Turkey can be characterised by two flow regime types and regions, namely: the mountainous area of north-northeast EBS (East Black Sea Mountain range) and the rest of the study area, which comprises the majority of the ÇRB. The mountainous area of the EBS Basin is characterised by a low river flow regime magnitude and a May-June peak regime shape composite class, while the ÇRB together with the western part of the EBS Basin can be defined as having an intermediate flow magnitude and an April-May peak regime.

Regime stability analysis for the 288-stations depicts important differences between the two major basins. May peak intermediate flow regime is the most common class. Widespread low flows occurred in 1982-1987, 1994-2001 and 2003-2005 station years in the EBS Basin, while the Çoruh Basin has not been experienced any long and severe low flow periods like those that have affected the EBS Basin. However, the ÇRB experienced low flows for the periods 1982-1987, 1989-1992 and 1994-1997. A novel river flow classification was made for northeast Turkey which provides a large-scale perspective on hydroclimatology knowledge of the region.

Results of monthly trend analysis for mean, minimum and maximum river flow data did not refer any significant change with a spatially coherent pattern. A general decreasing and increasing tendency were observed in Çoruh River and EBS basins. Similar to this, very few significant decreasing and increasing trends (approximately 4% of 432 time series) were

found in ÇRB and EBS Basin, only. The period December through February can be defined as most important period in terms of river flow trends. Weak seasonal trends were detected for mean river flows. Trends results do not suggest any significant long-term change for northeast Turkey river flows. Previous studies investigation river flow trends for Turkish rivers documented similar results; however, a much higher number of stations were evaluated in this study, which strengthens the spatial representativeness findings.

MLR analyses indicate that precipitation is the primary predictor for river flow variability. Results suggest that climatic conditions that generate precipitation are the main driver on river flow uniquely for winter and spring seasons. For summer and autumn, precipitation and temperature appear to be good double predictors. There are three stations in ÇRB that seem to be representative for regional climatic conditions over the year which shape river flow variability. This implication is not valid for the EBS Basin because of two reasons: (i) the spatial representativeness of stations (elevation and location status) and (ii) the dynamic conditions of the regional climate (being affected by both the diverse physiographic conditions and also cyclonic activity) during the year.

Intra-annual variability in the timing of river flow (i.e. regime shape) over northeast Turkey is controlled mainly by the regional climatic variability. Spring rainfall maxima associated with snowmelt contribution generates high river flow amounts for the ÇRB. The May-June river flow peak in the EBS Basin appears to be linked to late snowmelt. The hydrogeological character of the EBS Basin appears to exert a more important role on river flow seasonality. Monthly and seasonal time series do not exhibit any spatially coherent significant changes.

7.6. Chapter summary

River flow regimes were identified by classifying stations to examine spatial variability and also by grouping annual regimes for each station-year to identify temporal (between-year) variability. Trends in monthly and seasonal (minimum, mean and maximum) river flow series of northeast Turkey and the regional climate controls on seasonal river flows were investigated. This chapter highlights the regime characteristics and driving climate and river basin factors. In the next chapter, further analysis of river flows is undertaken, focussing on spatiotemporal variability in river flow quartiles and extreme calculations.

8. DETECTING CHANGING FREQUENCY AND LONG-TERM TRENDS IN PRECIPITATION, TEMPERATURE AND RIVER FLOW EXTREMES FOR NORTHEAST TURKEY

8.1. Introduction

Heavy rainfall events have become more frequent and significant increases have been observed in the number of extreme precipitation events (Frich *et al.* 2002, Alexander *et al.* 2006). These global, widespread and significant increases in precipitation extremes imply a tendency toward wetter conditions throughout the 21st century for Northern Hemisphere midlatitudes (Alexander *et al.* 2006). Groisman *et al.* (2005) found that both the empirical evidence from instrumental meteorological data and model projections of a greenhouse-enriched atmosphere indicate an increasing probability of intense precipitation events for many regions around the globe including for many extratropical regions including the United States. Multiproxy reconstructions of monthly and seasonal surface temperatures for Europe back to 1500 AD indicate that the late 20th- and early 21st century European climate is very likely warmer than that of any time during the past 500 years. The coldest European winter was 1708/1709 and 2003 was by far the hottest recorded summer (Luterbacher *et al.* 2004, Xoplaki *et al.* 2005). A significant warming trend has been observed for all temperature indices in Europe (Moberg *et al.* 2006). Winter precipitation totals have increased significantly by 12% per 100 years (Moberg *et al.* 2006). Luterbacher *et al.*, (2007) discuss the reverse impacts of the high warming trend in Europe and highlight some species of

flowering plants were found to have a distinctly earlier flowering which commenced occurring after the winter 2007 (Luterbacher *et al.* 2007).

Long-term changes in the frequency and intensity of extreme events have been documented for many regions across Europe and the Mediterranean countries (Brunetti *et al.* 2004, Brunetti *et al.*, 2001, Kutiel *et al.*, 1996, Klein-Tank and Konnen 2003, Toreti *et al.* 2010, Zhang *et al.* 2005, Founda and van Loon 2008, Oikonomou *et al.* 2008, Costa and Soares 2009, Hertig *et al.*, 2010, Kioutsioukis *et al.*, 2010). For example, Klein-Tank and Können (2003) studied trends in indices of climate extremes based on daily series of temperature and precipitation data for Europe for the period 1946-99. In particular, for the subperiod 1946-75 a slight cooling trend was detected and the annual number of warm extremes decreased. However, this situation changed significantly after 1975 and for the 1976-99 subperiod because a period of pronounced warming was detected with the annual number of warm extremes increasing two times faster than the corresponding decrease in the number of cold extremes. Upon examination of precipitation data, Klein-Tank and Können (2003) detected that the all Europe-average indices of wet extremes increased during the 1946-99 period, although the spatial consistency of the trends is low. For Mediterranean countries and the Middle East, the regional patterns of extreme climatic events are highly complex and generally results do not have spatial coherence especially for rainfall intensity trends (Zhang *et al.*, 2005; Kioutsioukis *et al.*, 2010). However, a general drying tendency over many areas of the Mediterranean have been reported (Founda and Van Loon, 2008; Costa and Soares, 2009 and Oikonomou *et al.*, 2008). Studies of the teleconnection patterns appear to suggest that atmospheric conditions centred over the Northern Atlantic and northern Europe appear to affect the duration of the longest dry spells over the Eastern Mediterranean (Oikonomou *et al.*, 2010). In addition to this, surface synoptic scale systems in northern Africa have a

substantial role on dry conditions (Oikonomou *et al.*, 2010). Toreti *et al.*, (2010) analysed the behaviour of precipitation extremes and estimated return periods for heavy precipitation at 20 stations around Mediterranean basin during October-March period. Precipitation extremes have an important contribution to make seasonal totals (approximately 60%). Toreti *et al.*, (2010) also investigated the relationship between extreme precipitation events and the large scale atmospheric circulation at the upper, mid and low troposphere by using NCEP/NCAR reanalysis data. For the eastern Mediterranean, the identified anomaly patterns for extreme precipitation events suggest warm air advection connected with anomalous ascent motions and an increase of the low- to mid-tropospheric moisture (Toreti *et al.*, 2010). Furthermore, the Jet Stream position supports the eastern Mediterranean basin being in a divergence area, where ascent motions are favoured (Toreti *et al.*, 2010). Hertig *et al.* (2010) detected that increases in Mediterranean extreme temperatures were observed for only the western Mediterranean region; and an opposing trend was detected for the eastern Mediterranean region, suggesting that changes in temperature extremes do not follow a simple shift to higher values of the whole temperature series.

Coastal regions of Turkey are characterised by the highest frequency of extreme precipitation events (number of rainy days with high rainfall) and also the highest precipitation records of daily precipitation totals (Chapter 5). Southwest and northeast Turkey are characterised by the highest number of extreme precipitation events. The number of wet days does not exhibit very strong trends in any direction across Turkey (Chapter 5). On the contrary, the results of the precipitation percentile series demonstrate a consistently increasing trend that is evident for all P75, P95 and P99 series (Chapter 5). The most significant trends were observed for the 'high' precipitation (P75) series.

Sensoy *et al.* (2008) detected spatially coherent warming trend affecting both maximum and minimum temperatures. In particular, their results show that the number of summer days and ‘tropical nights’ (i. e. number of days per year above 20°C) have been increasing across all over Turkey while the number of ice days and frost days have been decreasing. For precipitation, there results suggest complex changing patterns with major differences between regions. The number of heavy precipitation days (heavy precipitation/rainfall has an exact threshold value rather than a percentile threshold value but in the Ceylan *et. al.*, (2007a) the threshold value has not been given) has been increasing especially for the Black Sea and Mediterranean regions, which have been responsible for an increase in the number of extreme flood events (Ceylan *et. al.*, 2007a) while annual precipitation totals have declined for the Aegean and continental Anatolia regions. They also report a significant rising trend for consecutive dry and wet days in the Marmara, Aegean and Black Sea regions. However, comprehensive regional analyses on the changes of hydroclimatic extremes are unavailable.

Given the above content, there is an urgent need to establish the climatic processes driving these phenomena to deal effectively with future events under climatic change. Northeast region of Turkey is a region that has witnessed an increase in the number of heavy precipitation and extreme events which have caused flash floods and severe landslide events that have been responsible for serious loss of life and economical cost (Ergünay, 2007). Therefore, there is a pressing need to identify the frequency of extreme events for precipitation, temperature and river flow series in this region of Turkey not only for understanding the variability in the pattern of extreme events in the past, but also to increase the knowledge and understanding of associated contemporary climatic processes that will contribute to mitigation and adaptation strategies. Thus, this chapter aims to identify extreme

events through the analysis of temperature, precipitation and river flow series, to detect spatiotemporal variability and trends in the calculated extreme series and ultimately to quantify the driving climatic factors behind extreme river flows for northeast Turkey. To meet this aim, the objectives of this chapter are: (1) to calculate precipitation and temperature extremes based on selected climatic indices referred by the CLIVAR programme; (2) to detect low/high river flow extremes based on quartile calculations which is also adapted from the climate extreme indices; (3) to analyse long-term trends in the detected extreme precipitation, temperature and river flow series and (4) to explain climatic drivers which are influencing the extreme river flow variability.

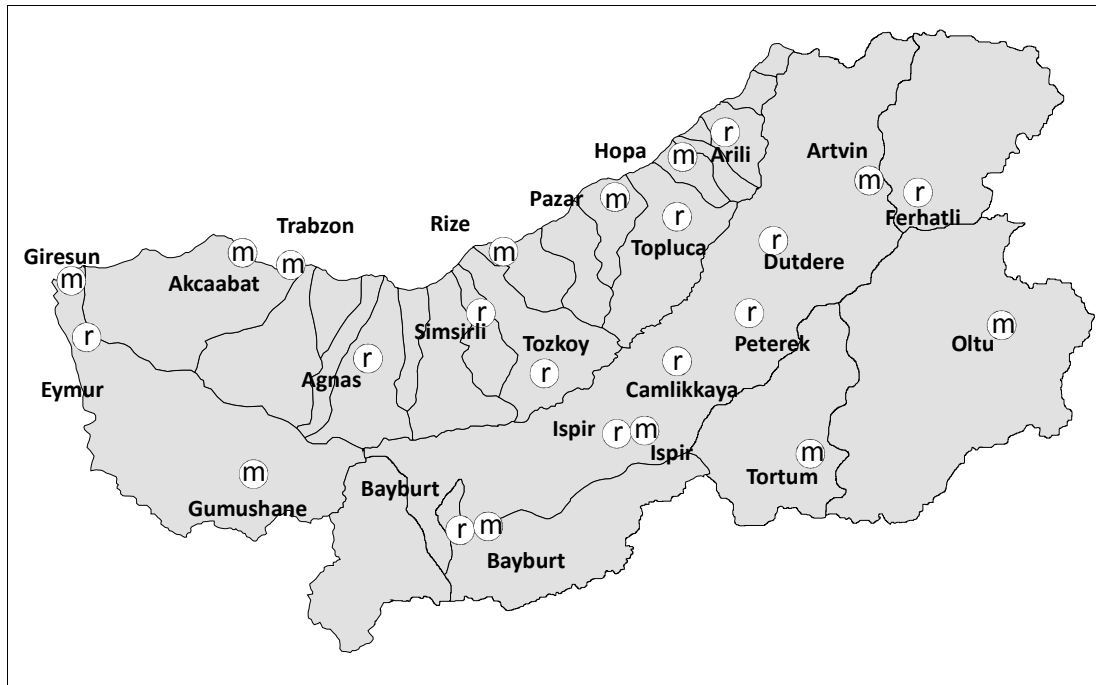


Figure 8.1 Location of stations evaluated for extreme analyses [m and r indicate meteorology and river gauging stations, respectively].

Table 8.1. Main properties of climate and river gauging stations selected for analysis.*(a) Climate Stations*

| Station Name | BASIN | Temperature (°C) | Precipitation (mm) | Rainy Days | Elevation (m) |
|--------------|-------|------------------|--------------------|------------|---------------|
| Akçaabat | EBS | 14.2 | 733.3 | 139.1 | 6 |
| Artvin | ÇORUH | 12.0 | 722.6 | 131.6 | 628 |
| Bayburt | ÇORUH | 7.0 | 443.0 | 100.8 | 1584 |
| Giresun | EBS | 14.5 | 1246.2 | 158.4 | 37 |
| Gümüşhane | EBS | 9.5 | 464.9 | 115.4 | 1219 |
| Hopa | EBS | 14.3 | 2243.4 | 181.3 | 33 |
| Ispir | ÇORUH | 10.4 | 478.0 | 95.7 | 1222 |
| Oltu | ÇORUH | 9.9 | 384.7 | 103.5 | 1322 |
| Pazar | EBS | 13.3 | 2068.2 | 158.3 | 79 |
| Rize | EBS | 14.3 | 2241.4 | 169.19 | 9 |
| Tortum | ÇORUH | 8.3 | 470.7 | 116.2 | 1572 |
| Trabzon | EBS | 14.6 | 831.5 | 139.8 | 30 |

(b) River Gauging Stations

| Station Name | River | Catchment Area (km ²) | Elevation (m) | Run off (mm) | Discharge (m ³ s ⁻¹) |
|----------------|-----------|-----------------------------------|---------------|--------------|---|
| 2202 Ağnas | Kara | 635.7 | 78 | 545.7 | 11.0 |
| 2218 Şimşirli | İyidere | 834.9 | 338 | 1053.8 | 27.9 |
| 2232 Topluca | Fırtına | 763.2 | 237 | 1219.0 | 29.5 |
| 2233 Tozköy | Tozköy | 223.1 | 1296 | 947.1 | 6.7 |
| 2240 Eymur | Harsit | 3132.8 | 120 | 402.7 | 40.0 |
| 2272 Arili | Arili | 92.2 | 175 | 2156.0 | 6.3 |
| 2304 Bayburt | Çoruh | 1734.0 | 1545 | 280.1 | 15.4 |
| 2305 Peterek | Çoruh | 7272.0 | 654 | 304.0 | 69.9 |
| 2316 Ispir | Çoruh | 5505.2 | 1170 | 220.5 | 38.5 |
| 2321 Dutdere | Parhal | 586.0 | 705 | 753.4 | 14.0 |
| 2328 Ferhatlı | Ardanuc | 546.8 | 365 | 346.0 | 6.0 |
| 2330 Çamlıkaya | Çamlıkaya | 113.6 | 995 | 805.1 | 2.9 |

8.2. Data and study area**8.2.1. Data sets**

Daily precipitation and temperature data from 12 climate stations within the study area were obtained from the State Meteorological Service (DMI) of Turkey for the period 1976-2007 (Figure 8.1). Daily mean river flow data were obtained from the Electrical Power Resources Survey and Development Administration (EIEI) and the State Hydraulics Work (DSI) of

Turkey. The number of river gauging stations with the same length of record as those from the climate stations is, unfortunately, quite limited (8 stations). Therefore, in order to achieve good representation of the spatial pattern, 12 river gauging stations were selected for a shorter period of study (i.e., 24 years; 1982-2005). The aim is to minimise data gaps by selecting the most continuous and longest records for all the data sets. The data quality controlling procedure was outlined in Chapter 2, Section 2.2., while Table 8.1 lists the main properties of selected stations.

8.2.2. Study area

Northeast Turkey is characterised by two major river basins: the East Black Sea Basin (EBS- on the northern side of the East Black Sea Mountains) and the Çoruh River Basin (ÇRB - on the southern side of the mountains) (Figure 8.1). Distinct geographic features of northeast Turkey such as the Black Sea to the north, high elevation mountain ranges between the coast and the inland part together with steep elevations and gradients over very short distances all exert an important role on local climatic conditions (See Sariş *et al.* (2010) for details).

North-south directed oscillations of the polar front systems have a significant effect on meteorological conditions during winter as well as the influence of Siberian high pressure centre which tends to bring cold air and which tends to produce heavy snowfalls on the mountains after having passed over a relatively moist Black Sea. The region also has rains associated with depressions that pass over the Black Sea in summer. Since the continental polar air mass (Siberian originated) does not have any effect in summer, the number of rainy days and rainfall intensity tends to increase in Northeast Anatolia. These local thermal conditions in inland regions serve to accelerate convective activity, which also determines the precipitation character of the Çoruh Basin, the more inland of the two river basins.

The climate of the Black sea coast is wet and humid (summer 23°C, winter 7°C), while the inland Çoruh Basin is characterised by lower annual mean temperatures (summer 17°C, winter -13°C). A cool temperature regime is observed during autumn which gets more severe in winter, especially for December and January. The winter period is much longer for the inland basin and snow remains on the ground from November until the end of April. Temperatures gradually increase in spring and achieve maximum levels in summer; July and August are the warmest months.

Northeast Turkey is characterised by mainly coastal and inland precipitation regimes. The western part of the Black Sea coast is characterised by high precipitation in October and partly in December (with annual average of 840 mm). However, the eastern part of the Black Sea coast is characterised by very high rainfall totals (2180 mm) for all seasons (apart from spring), with a clear October peak (Sariş *et al.*, 2010). The more inland regions which include the ÇRB, are characterised by a wet spring (May peak) generally lower precipitation totals (450 mm). River flow regimes for the EBS and Çoruh River basins exhibit similarity in the timing of discharge with a spring flow maxima and a summer low flow season (See Chapter 6, Section 4.1. for further details). However, the ÇRB is characterised by an early peak with a rapid onset in April-May, but the EBS Basin has a delayed but extended May-July maximum flow period, due to climatological differences. In terms of monthly flow magnitudes the river flows are markedly higher for the ÇRB.

Due to its distinct geographical (also climatological and geomorphological) character, northeast Turkey experiences several hydrometeorological-induced hazards throughout which include floods, droughts, landslides and avalanches. The provinces of Trabzon, Rize and

Artvin are three of the worst affected provinces in Turkey for having the highest recorded number of hazardous events. Flooding and landslides occur very frequently in Rize and Trabzon and are responsible for much loss of life and infrastructure damage (Ergünay, 2001).

8.3. Methods

8.3.1. Extreme indices calculations

The indices of the WMO–CCL and CLIVAR were referred to for identifying extreme events (Klein-Tank and Können, 2003). The set of 5 (Highest 1-day, highest consecutive 5-days, P75, P90 and P95) precipitation and 4 temperature (FD, SD, TG10p and TG90p) indices of climate extremes were selected for analysis for this study. For precipitation extremes, additional indices (e.g., P5, P10 and P25 percentiles) were also calculated in order to detect low precipitation extremes. Index definition for river flow extremes were adopted from precipitation index.

Table 8.2 shows the definitions of the criteria for the selected extreme indices. A ‘Wet day’ is defined and denoted as $P > 1$ mm in this study. Annual and seasonal data sets have also been developed. Annual and monthly results were used to present extreme characteristic and trends, while seasonal analysis were undertaken in order to identify seasonal trends as well as the linkages between regional climate and river flow extremes.

8.3.2. Trend test

The long-term trends in annual and seasonal extreme percentile series were detected by using the non-parametric Mann-Kendall rank correlation test (See Section 3.3). Test statistics which are above the 5% and 1% significance levels ($\alpha \leq 0.05$ and 0.01 of two-tailed test) were accepted as significant.

Table 8.2 Definitions of selected extreme indices.

| Indices of precipitation extremes | | |
|--|---|---|
| PX1 day | Highest 1-day precipitation amount (absolute extreme) | Maximum precipitation sums for 1-day interval. |
| PX5 day | Highest 5-day precipitation amount (absolute extreme) | Maximum precipitation sums for the consecutive 5-day interval. |
| P5% | Extremely dry days (percentage threshold) | Number of days per year with precipitation amount below a specific threshold value for extremely dry days. |
| P10% | Dry days (percentage threshold) | Number of days per year with precipitation amount below a specific threshold value for dry days. |
| P25% | Moderately dry days (percentage threshold) | Number of days per year with precipitation amount below a specific threshold value for moderately dry days. |
| P75% | Moderately wet days (percentage threshold) | Number of days per year with precipitation amount above a specific threshold value for moderately wet days. |
| P90% | Wet days (percentage threshold) | Number of days per year with precipitation amount above a specific threshold value for wet days. |
| P95% | Extremely wet days (percentage threshold) | Number of days per year with precipitation amount above a specific threshold value for extremely wet days. |
| Indices of temperature extremes | | |
| FD | Frost days | Number of days per year with temperature below 0°C (Day count; fixed threshold) |
| SU | Summer days | Number of days per year with temperature above 25°C (Day count; fixed threshold) |
| TG10p | Cold days (TG < 10ptile) | Number of days per year with temperature below a specific threshold value for cold days. |
| TG90p | Warm days (TG < 90ptile) | Number of days per year with temperature above a specific threshold value for warm days. |
| Indices of river flow extremes | | |
| QX1 day | Highest 1-day average river flow (absolute extreme) | Maximum river flow average for 1-day interval. |
| QX5 day | Highest 5-day average river flow (absolute extreme) | Maximum river flow average for the consecutive 5-day interval. |
| Q95% | Very low flows | Number of days per year with river flow amount below a specific threshold value for 95%. |
| Q90% | Low flows | Number of days per year with river flow amount below a specific threshold value for 90%. |
| Q75% | Moderately low flows | Number of days per year with river flow amount below a specific threshold value for 75%. |
| Q25% | Moderately high flows | Number of days per year with river flow amount above a specific threshold value for 25%. |
| Q10% | High flows | Number of days per year with river flow amount above a specific threshold value for 10%. |
| Q5% | Very high flows | Number of days per year with river flow amount above a specific threshold value for 5%. |

8.3.3. Multiple linear regression

Regression analyses refer to a complete process of studying the causal relationship between one dependent variable and a set of independent, explanatory variables (Rogerson, 2001). The influence of climatic drivers on extreme event variability was investigated through MLR analysis. Results from multivariate linear regressions (R^2) are presented only if they are significant at the 5% level (i.e. T test, p value ≤ 0.05).

Table 8.3 Annual extreme threshold values of stations.

| A- Threshold values for daily precipitation (long-term average) | | | | | | | Temperature | |
|---|------------|------------|------------|-------------|-------------|-------------|-------------|------------|
| Precipitation | <i>P5</i> | <i>P10</i> | <i>P25</i> | <i>P75</i> | <i>P90</i> | <i>P95</i> | <i>T10</i> | <i>T90</i> |
| Akcaabat | 0.1 | 0.1 | 0.5 | 5.9 | 13.1 | 19.9 | 5.5 | 22.9 |
| Giresun | 0.2 | 0.3 | 0.8 | 9.7 | 20.3 | 29.1 | 5.6 | 23.1 |
| Hopa | 0.1 | 0.2 | 1.1 | 16.7 | 32.8 | 47.8 | 4.8 | 22.8 |
| Pazar | 0.1 | 0.2 | 1.0 | 14.9 | 32.5 | 46.0 | 4.4 | 21.9 |
| Rize | 0.2 | 0.3 | 1.2 | 16.8 | 34.1 | 47.2 | 5.3 | 23.1 |
| Trabzon | 0.0 | 0.1 | 0.3 | 5.9 | 13.1 | 19.8 | 5.6 | 23.3 |
| Gumushane | 0.0 | 0.0 | 0.3 | 4.5 | 9.3 | 13.3 | -2.3 | 20.3 |
| Artvin | 0.1 | 0.2 | 0.8 | 6.3 | 12.7 | 19.5 | 1.5 | 21.2 |
| Bayburt | 0.1 | 0.2 | 0.5 | 5.2 | 10.1 | 13.5 | -6.8 | 19.1 |
| Ispir | 0.0 | 0.1 | 0.5 | 5.0 | 10.0 | 14.2 | -3.1 | 23.5 |
| Oltu | 0.1 | 0.2 | 0.6 | 4.8 | 9.1 | 12.7 | -3.6 | 22.9 |
| Tortum | 0.1 | 0.1 | 0.5 | 4.9 | 10.3 | 14.6 | -4.1 | 20.0 |

| B -Threshold values for daily river flow (long-term average) | | | | | | |
|--|-----------|------------|------------|------------|------------|------------|
| River Flow | <i>Q5</i> | <i>Q10</i> | <i>Q25</i> | <i>Q75</i> | <i>Q90</i> | <i>Q95</i> |
| Ağnas | 2.2 | 2.6 | 3.9 | 13.0 | 26.8 | 36.5 |
| Şimşirli | 9.2 | 10.2 | 12.3 | 36.5 | 63.8 | 75.8 |
| Topluca | 8.4 | 9.7 | 12.5 | 38.5 | 66.5 | 81.9 |
| Tozköy | 1.4 | 1.5 | 1.9 | 8.2 | 19.3 | 25.3 |
| Eymur | 5.0 | 6.5 | 10.0 | 50.0 | 105.0 | 136.5 |
| Arili | 1.8 | 2.1 | 2.8 | 7.9 | 12.5 | 16.1 |
| Bayburt | 4.3 | 4.8 | 5.7 | 15.1 | 41.5 | 56.8 |
| Peterek | 14.3 | 16.8 | 21.3 | 89.0 | 197.0 | 248.0 |
| Ispir | 8.3 | 9.5 | 11.8 | 42.8 | 113.0 | 146.0 |
| Dutdere | 2.6 | 3.2 | 4.3 | 20.1 | 37.1 | 44.7 |
| Ferhatli | 0.9 | 1.1 | 1.4 | 6.9 | 18.5 | 24.0 |
| Çamlıkaya | 0.6 | 0.7 | 0.9 | 3.6 | 7.6 | 9.7 |

8.4. Results and discussion

8.4.1. Spatial patterns in river flow, precipitation and temperature extremes

The magnitude characteristics of extreme indices were evaluated based on results of annual calculations. Table 8.3 shows the long-term average of the threshold values for selected indices of precipitation, temperature and river flow (shaded rows represent stations located in the EBS Basin). The daily threshold values were calculated for each station spanning the whole period of 1976-2007 (meteorological data) and 1981-2005 (hydrological data) and then the number of days that exceed this threshold were counted. The variability in the range of the long-term threshold value for the stations was assessed and then the variability in the number of days that exceed the long-term threshold value were analysed.

For precipitation, threshold values of high precipitation extremes (P75, P90 and P95) clearly fluctuate between stations. Similar to the precipitation regime classification (Section 6.4.1), Hopa, Pazar and Rize stations (shaded and bold) are defined with the highest threshold values of precipitation. These data also show an evident inland-coastal discrimination (Table 8.3).

T10 and T90 (Cold and warm days) threshold values are presented for temperature indices. As expected, the threshold values for cold day extremes display a distinct spatial division. Continentality together with marine factors are the primary driving mechanisms governing temperature distribution over northeast Turkey (Section 6.4.1). However, threshold values defining warm days do not significantly differ across the region; the lowest value for warm days was detected in Bayburt (Table 8.3). The threshold values of river flow extreme quartiles are significantly different than the river flow magnitude regime values classification which was derived from mean monthly river flows (See Chapter 7).

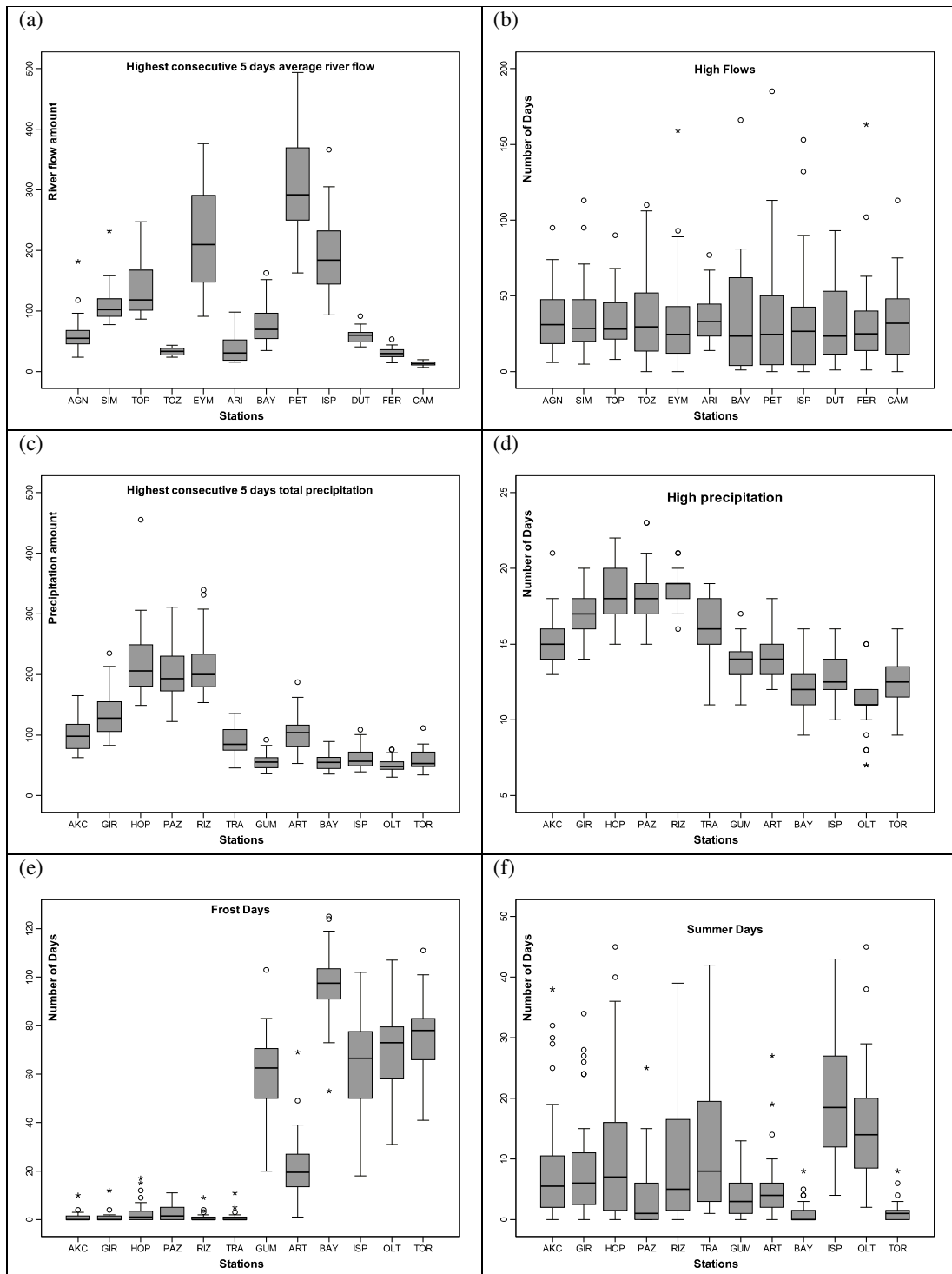


Figure 8.2 Sample magnitude characteristics of selected annual extremes.

Peterek (highest), Eymür and Ispir represent the stations having the highest extreme river flow

threshold values of the region, similar to flow regime magnitude classification. In particular, Dutedere, Şimşirli and Topluca stations are defined as having moderately high extreme threshold values. The rest of the stations are characterised by having low (lowest group) extreme river flow threshold values of the region.

Figure 8.2 shows box plots for selected indices, which indicate the range of inter-annual variability of calculated extremes for each station. Figure 8.2a illustrates the variability among the stations for the highest consecutive 5 days average river flow, which has been calculated for each observation year (the box plots represent the magnitude range throughout the observation period of 24 years). Again, Peterek, Ispir and Eymür have the highest river flows, While Topluca, Şimşirli and Bayburt are characterised with relatively (moderately) high river flows compared to the other stations. The QX5 day (high river flow quartile) pattern differentiates river flow regime magnitude, which is based on long-term monthly averages. This implies a different pattern in daily river flow distribution, which might be highly variable and sensitive to short duration weather events. The number of high flow days is presented in Figure 8.2b. The regional average amount of highest consecutive 5 days river flow and number of high flow days are 108.2 ms^{-1} and 35 days, respectively.

The magnitudes of precipitation and temperature extremes for selected indices are in agreement with regime magnitude characteristics (Chapter 6) with a coastal-inland discrimination evident. Hopa, Pazar and Rize have the highest magnitudes for the highest consecutive 5 days total precipitation (PX5) (Figure 8.2c). The inland stations of Bayburt, Gümüşhane and Oltu are characterised by having the lowest amount of precipitation for this extreme precipitation category. Annual extreme values of high precipitation (wet) days have a quite similar spatial pattern with the PX5 indice. However, the difference in magnitude range

between other coastal stations and inland stations is not marked (excluding Rize, Hopa and Pazar stations) (Figure 8.2d). The mean value of the number of moderately wet days is 25 for northeast Turkey, while the highest consecutive 5 days total precipitation amount is 112 mm for the entire region.

The number of frost and summer days (below 0°C and above 25 °C thresholds respectively) for each year has been evaluated for each station (32 year period). The inter-annual range of these temperature indices are displayed on Figure 8.2e and 8.2f to show the spatial differences and overall average for the region. As mentioned above, coastal-inland distinction are apparent, which represent cool and warm temperature regimes. The inland stations have the highest number of frost days with an average of 64 days, while the coastal stations record very few frost days (1.5 days) for the period 1976-2007 (Figure 8.2e). The number of days categorised as summer days is high especially for Hopa, Ispir, Oltu, Rize and Trabzon (Figure 8.2f) while an inland-coastal pattern cannot be detected for summer days. The overall (regional) average numbers of frost and summer days are 33 and 104 days, respectively, which suggest that summer days are notably higher than frost days.

Table 8.4 Proportion of significant trends detected in annual extremes.

| Annual | River Flow | | | | | | | |
|--------------------|-----------------------------|-------------|------|-------------|-------------|------|--------|-------------|
| <i>Significant</i> | Q ₅ ⁹ | Q90 | Q75 | Q25 | Q10 | Q5 | QX5DAY | QX1DAY |
| Decreasing | 0 | 0 | 8.3 | 8.3 | 8.3 | 8.3 | 0 | 16.7 |
| Increasing | 8.3 | 8.3 | 8.3 | 0 | 0 | 0 | 0 | 8.3 |
| Annual | Precipitation | | | | | | | |
| <i>Significant</i> | P5 | P10 | P25 | P75 | P90 | P95 | PX5DAY | PX1DAY |
| Decreasing | 8.3 | 8.3 | 16.7 | 0 | 16.7 | 8.3 | 0 | 0 |
| Increasing | 25 | 8.3 | 8.3 | 33.3 | 25 | 16.7 | 8.3 | 0 |
| Annual | Temperature | | | | | | | |
| <i>Significant</i> | FD | SD | TG10 | TG90 | | | | |
| Decreasing | 0 | 0 | 0 | 0 | | | | |
| Increasing | 0 | 58.3 | 0 | 91.7 | | | | |

8.4.2. Long-term trends in precipitation, temperature and river flow extreme events

Table 8.4 shows the proportion of significant trends obtained in annual precipitation,

temperature and river flow extreme series. Trends in annual river flow extremes are weak. QX1 day river flows display the most significant results and highlight 16.7% decreasing and 8.3% increasing trends for stations (three out of twelve). Trends in annual precipitation extremes are clearer than river flows with the P5 and P25 percentiles of dry extremes and, P75 and P90 percentiles of wet extremes detecting significant trend (Table 8.4). In particular, the increasing trends in very low, moderately high and high precipitation extremes are evident. For the air temperature series, a warming trend is detected, which is supported by significant increasing trends in summer (58.3%) and warm days (91.7%) extreme temperature series.

For seasonal trend analysis, river flow, precipitation and temperature series were evaluated based on a standard index to achieve a comparative approach among different parameters. The scale (including six extreme percentiles span the range from *very low* to *very high*) was adopted to quantify extreme events. The percentile threshold values for each parameter and each station were calculated and then the number of days exceeding the long-term threshold values was ascertained. Next, the seasonal pattern in the number of days was examined by trend analysis. This comparative approach provides a long-term evaluation of the trends while also allowing the opportunity to examine the intra-annual and spatial differences.

Table 8.5 shows the proportion of significant the positive and negative test statistics for the seasonal trend analyses. For winter, some remarkable results have been detected showing high and very high river flows and very low and low precipitation extremes. Temperature extremes do not exhibit any significant or spatially coherent trends (Table 8.5a). For spring, very low river flow extremes tend to increase, with a parallel trend, dry precipitation extreme were also increasing. Spring precipitation extremes display a significant and strongly increasing trend, for both low and very low indices. This spring trend is also positively associated with an

increase in river flow, but clearly the correlation is not very strong (Table 8.5b). High and very high temperature extremes with a significant increasing trend (41%) were detected. River flow percentiles do not exhibit any significant trend for the summer months. However, very low and low precipitation (equal increasing and decreasing precipitation trend) as well as all temperature percentiles were characterised by significant and strong trends.

The increasing tendency in temperature is in agreement with all the trend analyses derived for the temperature series (annual, seasonal, monthly and annual extremes), which highlights clearly an important warming trend for northeast Turkey (Table 8.5c). For autumn, a significantly increasing trend for river flow series for high flow percentiles only was also detected alongside significant trends for precipitation percentiles for autumn. Very low and low precipitation percentiles were detected with important increasing trends (25%) together with a 16.7% decreasing trend, respectively; whereas wet precipitation extremes were exhibited with increasing trends only. For temperature, similar to spring, warm temperature extremes have substantial results indicating rising temperature trends in autumn transition season as well (Table 8.5d).

Table 8.5 Proportion of significant trends detected in seasonal extremes.

A- Winter

| River Flow | WIN_95 | WIN_90 | WIN_75 | WIN_25 | WIN_10 | WIN_5 |
|----------------------|-------------|-------------|--------|--------|-------------|-------------|
| % Sig. Result | 16.7 | 8.3 | 16.7 | 8.3 | 33.3 | 25.0 |
| % Sig. Inc. | 8.3 | 8.3 | 8.3 | 8.3 | 25.0 | 16.7 |
| % Sig. Dec. | 8.3 | 0.0 | 8.3 | 0.0 | 8.3 | 8.3 |
| Precipitation | WIN_5 | WIN_10 | WIN_25 | WIN_75 | WIN_90 | WIN_95 |
| % Sig. Result | 50.0 | 41.7 | 16.7 | 0.0 | 0.0 | 0.0 |
| % Sig. Inc. | 33.3 | 25.0 | 8.3 | 0.0 | 0.0 | 0.0 |
| % Sig. Dec. | 16.7 | 16.7 | 8.3 | 0.0 | 0.0 | 0.0 |
| Temperature | WIN_5 | WIN_10 | WIN_25 | WIN_75 | WIN_90 | WIN_95 |
| % Sig. Result | 8.3 | 8.3 | 8.3 | 8.3 | 8.3 | 0.0 |
| % Sig. Inc. | 0.0 | 0.0 | 0.0 | 0.0 | 0.0 | 0.0 |
| % Sig. Dec. | 8.3 | 8.3 | 8.3 | 8.3 | 8.3 | 0.0 |

B- Spring

| River Flow | SPR_95 | SPR_90 | SPR_75 | SPR_25 | SPR_10 | SPR_5 |
|----------------------|-------------|-------------|-------------|--------|-------------|-------------|
| % Sig. Result | 25.0 | 8.3 | 0.0 | 16.7 | 8.3 | 8.3 |
| % Sig. Inc. | 25.0 | 8.3 | 0.0 | 8.3 | 8.3 | 8.3 |
| % Sig. Dec. | 0.0 | 0.0 | 0.0 | 8.3 | 0 | 0 |
| Precipitation | SPR_5 | SPR_10 | SPR_25 | SPR_75 | SPR_90 | SPR_95 |
| % Sig. Result | 41.7 | 50.0 | 25.0 | 0.0 | 0.0 | 0.0 |
| % Sig. Inc. | 25.0 | 33.3 | 25.0 | 0.0 | 0.0 | 0.0 |
| % Sig. Dec. | 16.7 | 16.7 | 0.0 | 0.0 | 0 | 0 |
| Temperature | SPR_5 | SPR_10 | SPR_25 | SPR_75 | SPR_90 | SPR_95 |
| % Sig. Result | 0.0 | 0.0 | 8.3 | 0.0 | 41.7 | 41.7 |
| % Sig. Inc. | 0.0 | 0.0 | 0.0 | 0.0 | 41.7 | 41.7 |
| % Sig. Dec. | 0.0 | 0.0 | 8.3 | 0.0 | 0.0 | 0.0 |

C- Summer

| River Flow | SUM_95 | SUM_90 | SUM_75 | SUM_25 | SUM_10 | SUM_5 |
|----------------------|-------------|-------------|-------------|-------------|-------------|-------------|
| % Sig. Result | 16.7 | 8.3 | 8.3 | 0.0 | 0.0 | 0.0 |
| % Sig. Inc. | 0.0 | 0.0 | 0.0 | 0.0 | 0.0 | 0.0 |
| % Sig. Dec. | 16.7 | 8.3 | 8.3 | 0 | 0 | 0 |
| Precipitation | SUM_5 | SUM_10 | SUM_25 | SUM_75 | SUM_90 | SUM_95 |
| % Sig. Result | 50.0 | 50.0 | 16.7 | 8.3 | 0.0 | 0.0 |
| % Sig. Inc. | 25.0 | 25.0 | 8.3 | 8.3 | 0.0 | 0.0 |
| % Sig. Dec. | 25.0 | 25.0 | 8.3 | 0 | 0 | 0 |
| Temperature | SUM_5 | SUM_10 | SUM_25 | SUM_75 | SUM_90 | SUM_95 |
| % Sig. Result | 41.7 | 58.3 | 91.7 | 58.3 | 50.0 | 50.0 |
| % Sig. Inc. | 41.7 | 58.3 | 91.7 | 58.3 | 50.0 | 50.0 |
| % Sig. Dec. | 0.0 | 0.0 | 0.0 | 0.0 | 0.0 | 0.0 |

D- Autumn

| River Flow | AUT_95 | AUT_90 | AUT_75 | AUT_25 | AUT_10 | AUT_5 |
|----------------------|-------------|-------------|--------|-------------|-------------|-------------|
| % Sig. Result | 0.0 | 0.0 | 0.0 | 0.0 | 16.7 | 33.3 |
| % Sig. Inc. | 0.0 | 0.0 | 0.0 | 0.0 | 16.7 | 25.0 |
| % Sig. Dec. | 0.0 | 0.0 | 0 | 0 | 0 | 8.3 |
| Precipitation | AUT_5 | AUT_10 | AUT_25 | AUT_75 | AUT_90 | AUT_95 |
| % Sig. Result | 41.7 | 41.7 | 16.7 | 25.0 | 25.0 | 25.0 |
| % Sig. Inc. | 25.0 | 25.0 | 16.7 | 25.0 | 25.0 | 25.0 |
| % Sig. Dec. | 16.7 | 16.7 | 0 | 0 | 0 | 0.0 |
| Temperature | AUT_5 | AUT_10 | AUT_25 | AUT_75 | AUT_90 | AUT_95 |
| % Sig. Result | 0.0 | 0.0 | 8.3 | 41.7 | 25.0 | 41.7 |
| % Sig. Inc. | 0.0 | 0.0 | 8.3 | 41.7 | 25.0 | 41.7 |
| % Sig. Dec. | 0.0 | 0.0 | 0.0 | 0.0 | 0.0 | 0.0 |

Spatial variability of detected trends in river flow, precipitation and temperature percentile series are presented to assess regional similarities and spatial consistency of trends (Figures 8.3, 8.4 and 8.5). The plotted maps for significant river flow series indicates an overall increasing trend for high-very high flow (winter), very low flow (spring) and very high flow (autumn) quartiles. Although the number of statistically significant results are not high, it is clear that the river gauging stations are characterised by wetter than normal conditions for the last 24 years apart from Çamlıkaya in the ÇRB. This station is identified with a strongly decreasing trend in winter and autumn with very high and high river flow extremes (Figures 8.3a, 8.3c and 8.3d). Statistically significant positive trends can also be detected for Tozköy and Topluca (EBS Basin) and Bayburt and Ispir (ÇRB). Arılı also showed a strongly positive trend particularly for winter and autumn high and very high flows. However, these detected increasing trends in high river flow extremes do not actually imply a major shift in the annual regimes, rather they can be considered as indicators of the increased frequency of short-term events.

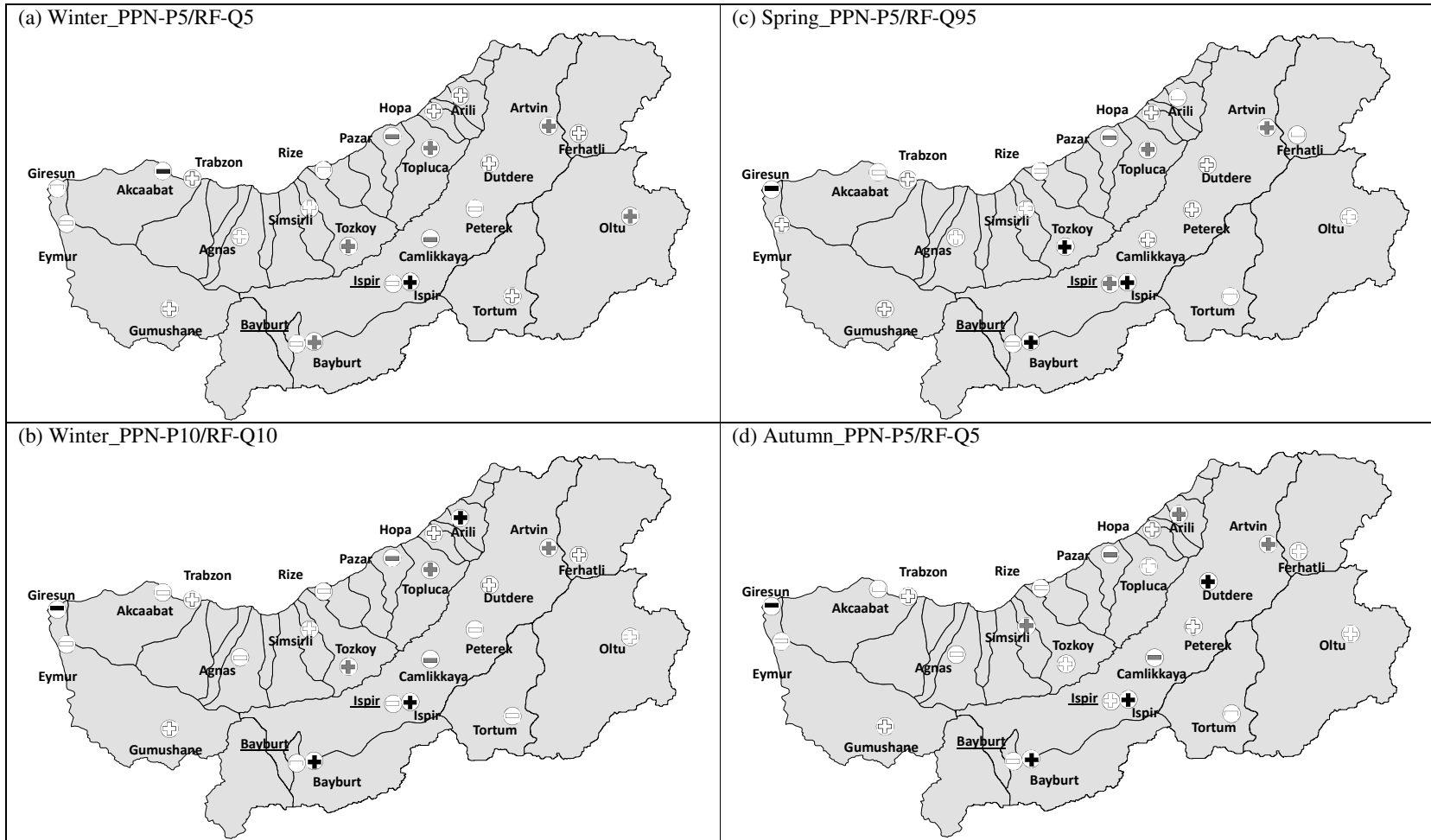


Figure 8.3 Results of M-K test for seasonal river flow and precipitation percentile [(\oplus/\ominus) insignificant increasing/decreasing trend; (\oplus/\ominus) significant increasing/decreasing trend at 0.05; (\oplus/\ominus) significant increasing/decreasing trend at 0.01].

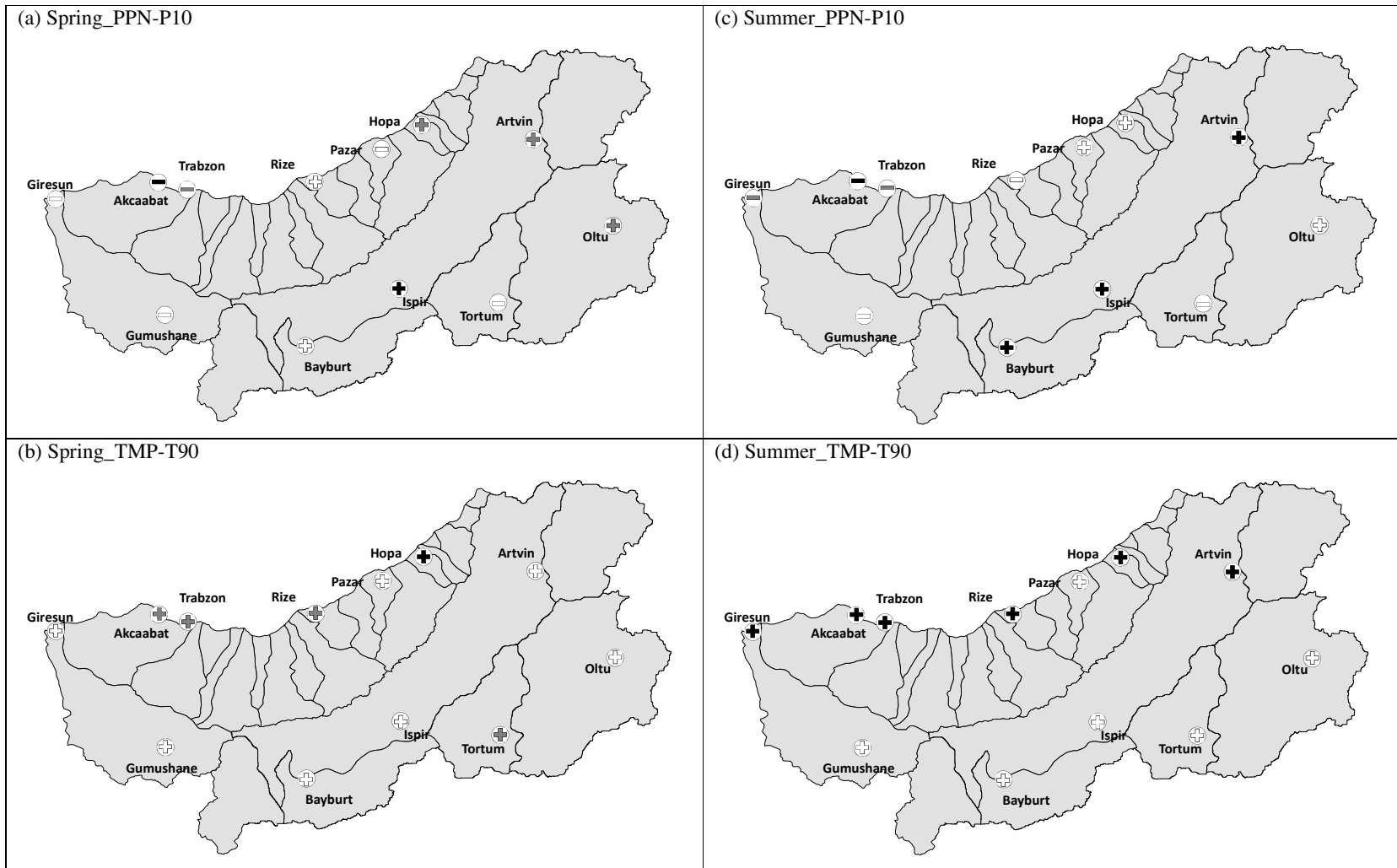


Figure 8.4 Results of M-K test for spring-summer precipitation and temperature percentiles.

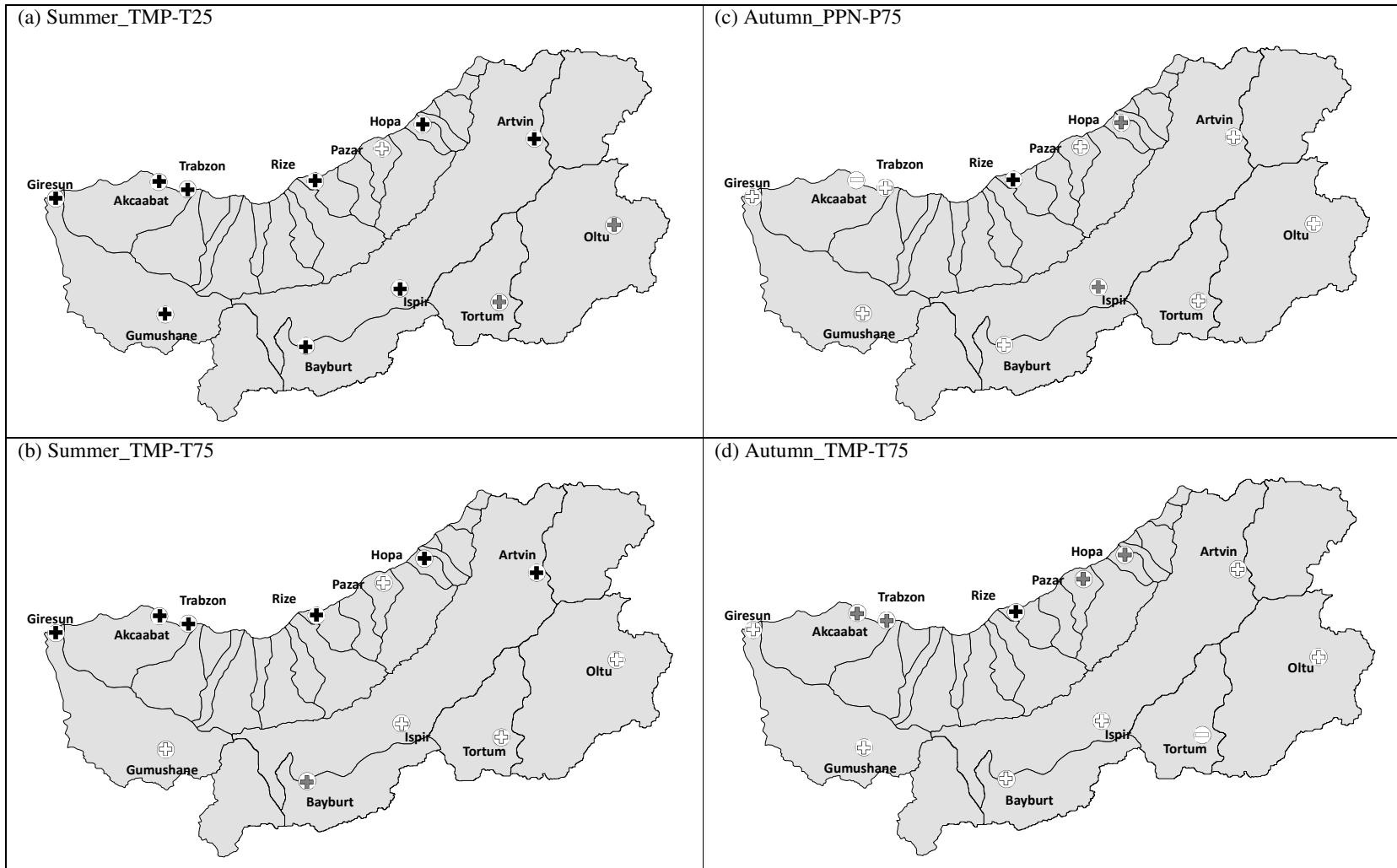


Figure 8.5 Results of M-K test for summer-autumn precipitation and temperature percentiles.

Figure 8.3 shows some of the significant trends in precipitation percentiles together with selected river flow quartiles. A broad dissimilarity between stations located in the East Black Sea and Çoruh River basins is evident for river flows. For precipitation, significant decreasing trends in amount of low (dry) precipitation percentiles for winter, spring and autumn were detected for EBS Basin stations (e.g., Giresun, Pazar and Akçaabat), and Artvin (ÇRB) (Figure 8.3). These data suggest that the proportion of low precipitation percentile significantly decrease (or remain stable) for the coastal stations. The proportion of drier climatic conditions is becoming more frequent for Artvin (transitional regime).

Figure 8.4 shows the trends observed for low and high percentile categories of precipitation and temperature series for spring and summer. In spring and summer, low precipitation percentiles have similar patterns with very low winter and spring percentiles series which suggests a negative [positive] trend for coastal [inland] stations negative trend for coastal stations and an opposite trend for inland stations (Figure 8.4a and 8.4c). The proportion of significant results is higher than very low precipitation percentile series and the discrimination between basins (regime regions) is clearer. For temperature series, both spring and summer high temperature extremes display spatially consistent and significant rising temperature trends, especially for coastal stations (Figures 8.4b and 8.4d). Figure 8.5 illustrates the spatial distribution of trends in temperature and precipitation extremes for summer and autumn which demonstrates the strong and more coherent positive trends for northeast Turkey. A statistically significantly increasing trend for moderately low temperatures was detected for all stations except Pazar (Figure 8.5a). Moderately high temperatures for summer and autumn depicted a similar pattern of an increasing temperature trend, which is largely significant for stations in the EBS Basin and implies a warming tendency that has persisted for the last three decades (Figures 8.5c and 8.5d). Moderately high precipitation for autumn displays an

increasing tendency which is statistically significant in Rize, Hopa and Ispir (Figures 8.5b).

Table 8.6 Results of regression analysis for ÇRB.

| DJF | Autumn | | | | MAM | Winter | | | | Spring | | | | |
|-----|----------|-------|---------------|-------------|------|--------|----------|-------|---------------|-------------|---------|---------------|--------------|---------|
| | Stations | Coruh | Precipitation | Temperature | | Fit | Stations | Coruh | Precipitation | Temperature | Fit | Precipitation | Temperature | Fit |
| Q95 | 2304 | | | Artvin | 0.22 | Q95 | 2304 | | | | Trabzon | | 0.2 | |
| | 2305 | | Ispir | | 0.36 | | 2305 | | | | | | | |
| | 2316 | | Gum., Olt. | | 0.52 | | 2316 | | | | | | | |
| | 2321 | | Artvin | | 0.29 | | 2321 | | | | | | Ispir | 0.28 |
| | 2328 | | Akc., Olt. | | 0.41 | | 2328 | | | | | | | |
| | 2330 | | Oltu | | 0.29 | | 2330 | | Gumushane | | | 0.21 | | |
| Q90 | 2304 | | | Artvin | 0.22 | Q90 | 2304 | | | | | | | |
| | 2305 | | Ispir | | 0.25 | | 2305 | | | | | | | |
| | 2316 | | Gumushane | | 0.38 | | 2316 | | | | | | | |
| | 2321 | | Hopa | Oltu | 0.48 | | 2321 | | | | | | | |
| | 2328 | | Olt., Akc. | | 0.45 | | 2328 | | | | | | Ispir | 0.18 |
| | 2330 | | Oltu | | 0.29 | | 2330 | | | | | | | |
| Q75 | 2304 | | | Isp., Hop. | 0.38 | Q75 | 2304 | | | | Rize | | 0.25 | |
| | 2305 | | Ispir | | 0.33 | | 2305 | | | | | Rize | 0.21 | |
| | 2316 | | Gumushane | | 0.36 | | 2316 | | | | | | Akc., Hopa | 0.54 |
| | 2321 | | Hopa | | 0.31 | | 2321 | | | | | | Akc., Hopa | 0.53 |
| | 2328 | | Olt., Akc. | | 0.41 | | 2328 | | Giresun | | | 0.17 | | |
| | 2330 | | Oltu | | 0.22 | | 2330 | | | | | | | |
| Q25 | 2304 | | Ispir | Isp., Gum. | 0.74 | Q25 | 2304 | | Tortum | 0.31 | Pazar | | Hopa | 0.24 |
| | 2305 | | Ispir | | 0.46 | | 2305 | | Gumushane | 0.42 | | | Hopa | 0.42 |
| | 2316 | | Gumushane | | 0.45 | | 2316 | | Gumushane | 0.37 | | | Hopa | 0.44 |
| | 2321 | | Artvin | | 0.41 | | 2321 | | Akcaabat | 0.35 | | | | |
| | 2328 | | Artvin | | 0.42 | | 2328 | | Artvin | 0.35 | | | | |
| | 2330 | | | Giresun | 0.36 | | 2330 | | | | | | Rize, Ispir. | 0.38 |
| Q10 | 2304 | | Ispir | Ispir | 0.37 | Q10 | 2304 | | Tortum | 0.25 | Hopa | | 0.25 | |
| | 2305 | | Gumushane | | 0.48 | | 2305 | | Gumushane | 0.32 | | | Hopa | 0.24 |
| | 2316 | | Gumushane | | 0.52 | | 2316 | | Tortum | 0.24 | | | Hopa | 0.23 |
| | 2321 | | Hopa | | 0.32 | | 2321 | | Artvin | 0.28 | | | | |
| | 2328 | | Artvin | | 0.33 | | 2328 | | Artvin | 0.23 | | | | |
| | 2330 | | Ispir | Giresun | 0.55 | | 2330 | | Giresun | 0.21 | | | Hopa., Gum. | 0.44 |
| Q5 | 2304 | | Ispir | | 0.19 | Q5 | 2304 | | Tortum | 0.26 | Pazar | | Hopa | 0.22 |
| | 2305 | | Gumushane | | 0.45 | | 2305 | | Gumushane | 0.33 | | | Hopa | 0.22 |
| | 2316 | | Gumushane | | 0.51 | | 2316 | | Tortum | 0.22 | | | Hopa | 0.34 |
| | 2321 | | Hopa | | 0.26 | | 2321 | | Artvin | 0.31 | | | | |
| | 2328 | | Trabzon | | 0.27 | | 2328 | | Artvin | 0.34 | | | Tor., Pazar | 0.36 |
| | 2330 | | Ispir | Giresun | 0.57 | | 2330 | | Giresun | 0.24 | | | Paz., Ispir | Giresun |

8.4.3. Assessing the influence of climatic variability on frequency of extreme events

Multiple linear regression was used to model the winter and spring river flow quartiles for each station as a function of precipitation and temperature to detect the sensitivity of river flow extremes to the regional climatic drivers (Tables 8.6 and 8.7). Presented results indicate a significant ($p \leq 0.05$) model fit that designates the potential utility of climate predictors of river flow variability. Preceding season datasets of climatic drivers were evaluated to assess winter and spring river flow variability links to regional climate. Concurrent season analysis for spring (i.e. peak river flow period) was also undertaken.

Table 8.6 presents result for the ÇRB. Precipitation is designated as the primary predictor for all quartiles, while temperature is a major predictor for river flow extreme variability for Bayburt (2304) and Çamlıkaya (2330) stations for winter river flows extremes. Autumn precipitation series of inland region (including Ispir, Artvin and Gümüşhane) are the primary predictors for river flow extremes for autumn (especially in Ispir [2316], Peterek [2305] and Bayburt gauging stations). However, low river flow percentiles appear to have a more complex relationship with the climate predictors. For example, Oltu autumn precipitation appears to have an impact on winter low flows.

High flow extremes for spring are highly correlated with climate predictors, which are most probably related to the river flow maxima during spring over the ÇRB. Winter precipitation conditions in Gümüşhane, Tortum and Artvin stations of inland region affects the variability of high river flow. Spring precipitation (Pazar) and temperature (Hopa) displays an unexpected relationship with high river flow extremes for the ÇRB for spring. However, the R square values for the model are not high (R square value for model fit is given for each significant parameter in tables 8.6 and 8.7), even though they have significant regression. Strong model fits are obtained for preceding precipitation and temperature predictors and autumn and winter river flow extremes, which demonstrate that river flow extremes are dependent partly on the regional climate regime of the preceding season.

Table 8.7 illustrates the results for regression analysis for river flow extremes for the stations in the EBS Basin. Contrary to the ÇRB, the relationships between river flow extremes and regional climate are more significant but also more complicated. R-square values are considerably higher especially for the models of high river flow extreme variability; however,

this resulted from a high number of predictors for a single station.

Table 8.7 Results of regression analysis for EBS Basin.

| DJF | Autumn | | | | MAM | Winter | | | | Spring | | | |
|-----|-----------------|-----------------|-------------|------|-----|-----------------|---------------|----------------|------|---------------|-------------|------|------|
| | Stations EBS | Precipitation | Temperature | Fit | | Stations EBS | Precipitation | Temperature | Fit | Precipitation | Temperature | Fit | |
| Q95 | 2202 | Hopa | | 0.24 | Q95 | 2202 | | | | Hopa | | 0.19 | |
| | 2218 | Hopa | Oltu | 0.4 | | 2218 | Art., Hopa | | 0.62 | Gumushane | | 0.37 | |
| | 2232 | | | | | 2232 | | | | Tortum | | 0.37 | |
| | 2233 | Rize | | 0.42 | | 2233 | | | | Riz., Paz., | | 0.69 | |
| | 2240 | Rize | | 0.18 | | 2240 | Gumushane | | 0.26 | Artvin | | 0.26 | |
| | 2272 | | | | | 2272 | | | | Gum., Art. | | 0.48 | |
| Q90 | 2202 | Hopa | | 0.2 | Q90 | 2202 | | | | Hopa | | 0.21 | |
| | 2218 | | Oltu | 0.26 | | 2218 | Art., Hopa | | 0.64 | Gumushane | | 0.35 | |
| | 2232 | | | | | 2232 | | | | Ispir | | 0.31 | |
| | 2233 | Rize | | 0.42 | | 2233 | | | | Riz., Paz., | | 0.7 | |
| | 2240 | Rize | | 0.2 | | 2240 | Gumushane | | 0.24 | Artvin | | 0.29 | |
| | 2272 | | | | | 2272 | | | | Gum., Art. | | 0.48 | |
| Q75 | 2202 | Hopa | | 0.23 | Q75 | 2202 | | Hopa | 0.17 | | | | |
| | 2218 | Hopa | Oltu, Bay. | 0.66 | | 2218 | Art., Hopa | Hopa | 0.57 | | Akc., Hopa | | 0.5 |
| | 2232 | | | | | 2232 | Art., Hopa | Hopa | 0.51 | | Akc., Hopa | | 0.41 |
| | 2233 | Rize | | 0.44 | | 2233 | | | | | Akc., Hopa | | 0.55 |
| | 2240 | Rize | | 0.22 | | 2240 | | Tortum | 0.18 | Artvin | | 0.39 | |
| | 2272 | | | | | 2272 | Artvin | Art., Oltu | 0.61 | | | | |
| Q25 | 2202 | Artvin | | 0.27 | Q25 | 2202 | Gumushane | | 0.47 | Artvin | Ispir | 0.47 | |
| | 2218 | Artvin | Rize | 0.58 | | 2218 | Artvin | Hopa | 0.55 | | | | |
| | 2232 | Paz., Isp., Olt | | 0.63 | | 2232 | Artvin | | 0.42 | | | | |
| | 2233 | Artvin | | 0.46 | | 2233 | Pazar | | 0.24 | | | | |
| | 2240 | Rize | | 0.25 | | 2240 | Gumushane | Tortum | 0.45 | Hopa | | 0.26 | |
| | 2272 | | | | | 2272 | Artvin | Art., Tor., | 0.8 | Tortum | | 0.19 | |
| Q10 | 2202 | Tortum | | 0.33 | Q10 | 2202 | Oltu | Isp., Bay. | 0.58 | Akcaabat | Oltu | 0.52 | |
| | 2218 | Hopa | Rize | 0.56 | | 2218 | Artvin | | 0.29 | | | | |
| | 2232 | Paz., Isp. | | 0.54 | | 2232 | Artvin | | 0.38 | | | | |
| | 2233 | Art., Gum. | | 0.57 | | 2233 | | | | | | | |
| | 2240 | Gumushane | | 0.18 | | 2240 | Akcaabat | | 0.18 | Giresun | Ispir | | |
| | 2272 | Paz., Oltu | | 0.36 | | 2272 | Akcaabat | Ar., Ol., Is., | 0.86 | Tortum | | 0.27 | |
| Q5 | 2202 | Oltu | | 0.29 | Q5 | 2202 | Oltu | | 0.31 | Akcaabat | Artvin | 0.54 | |
| | 2218 | Hopa | Rize | 0.55 | | 2218 | Artvin | Hopa | 0.41 | | | | |
| | 2232 | Paz., Isp. | | 0.55 | | 2232 | Artvin | | 0.37 | | | | |
| | 2233 | Rize, Gum. | | 0.44 | | 2233 | | | | | | | |
| | 2240 | Gumushane | Rize | 0.35 | | 2240 | Akcaabat | | 0.19 | | | 0.37 | |
| | 2272 | Artvin | Oltu | 0.34 | | 2272 | Akc., Tor. | Ar., Ol., Is., | 0.84 | Tortum | | 0.22 | |

As with the ÇRB, precipitation is the main predictor for EBS river flows. Winter low flow extremes are dependent upon autumn precipitation of Rize and Hopa stations in the EBS Basin, which represents the rainfall maxima for the entire region. Autumn temperature for Oltu (Rize) appears to have a significant relationship with low (high) river flow extremes for Şimşirli (2218) station. Several climatic predictors (also including ÇRB stations) have influence on EBS high flow extremes. Nevertheless, the most robust model fit was established between the precipitation series of meteorological stations located in EBS Basin (namely: Hopa, Rize and Pazar).

In spring, high river flow quartiles are significantly correlated with the regional climate conditions in winter. Both temperature and precipitation determines the regional dynamics of extreme river flow. Winter temperatures for Artvin, Tortum and Oltu stations located within the inland regime appear to have significant relationship with spring high flow extremes for Eymür (2240) and Arili (2272) station affect spring high flow extremes of Arili station. Spring river flows of these stations were also related with winter precipitation of Artvin and Gümüşhane stations of inland basin. However, winter temperature series for Hopa have a notable influence on moderately low flows for spring in Ağnas (2202), Şimşirli and Topluca (2232). Spring temperature series for some of the inland and coastal stations (for very low and low river flow quartiles) are good predictors. For example, Akçaabat and Hopa temperature appear to be good predictors for moderately low river flow extremes for spring at Şimşirli, Topluca and Tozköy (2233). The regression model for high river flow extremes for spring is relatively weak, except when using climate predictors for Ağnas.

The most important climate (independent) variable and river flow (dependent) variable were plotted to detect the relationship between river flow and regional climate predictors (Figures 8.6 and 8.7). Figure 8.6 shows the average z-scores for each station located in ÇRB for each related season to illustrate the nature of the relationship between river flow and climatic drivers. These data suggest that the wet precipitation period equals high river flow for ÇRB stations and *vice versa*. Periods of high temperatures result in low (dry) river flow periods for Çamlıkaya station (Figure 8.6c). The relationship between EBS flow quartiles and regional precipitation indicates a similar pattern which is detected by high (low) precipitation episodes corresponding high (low) river flow extremes for selected stations (Figure 8.7(1) and (2)).

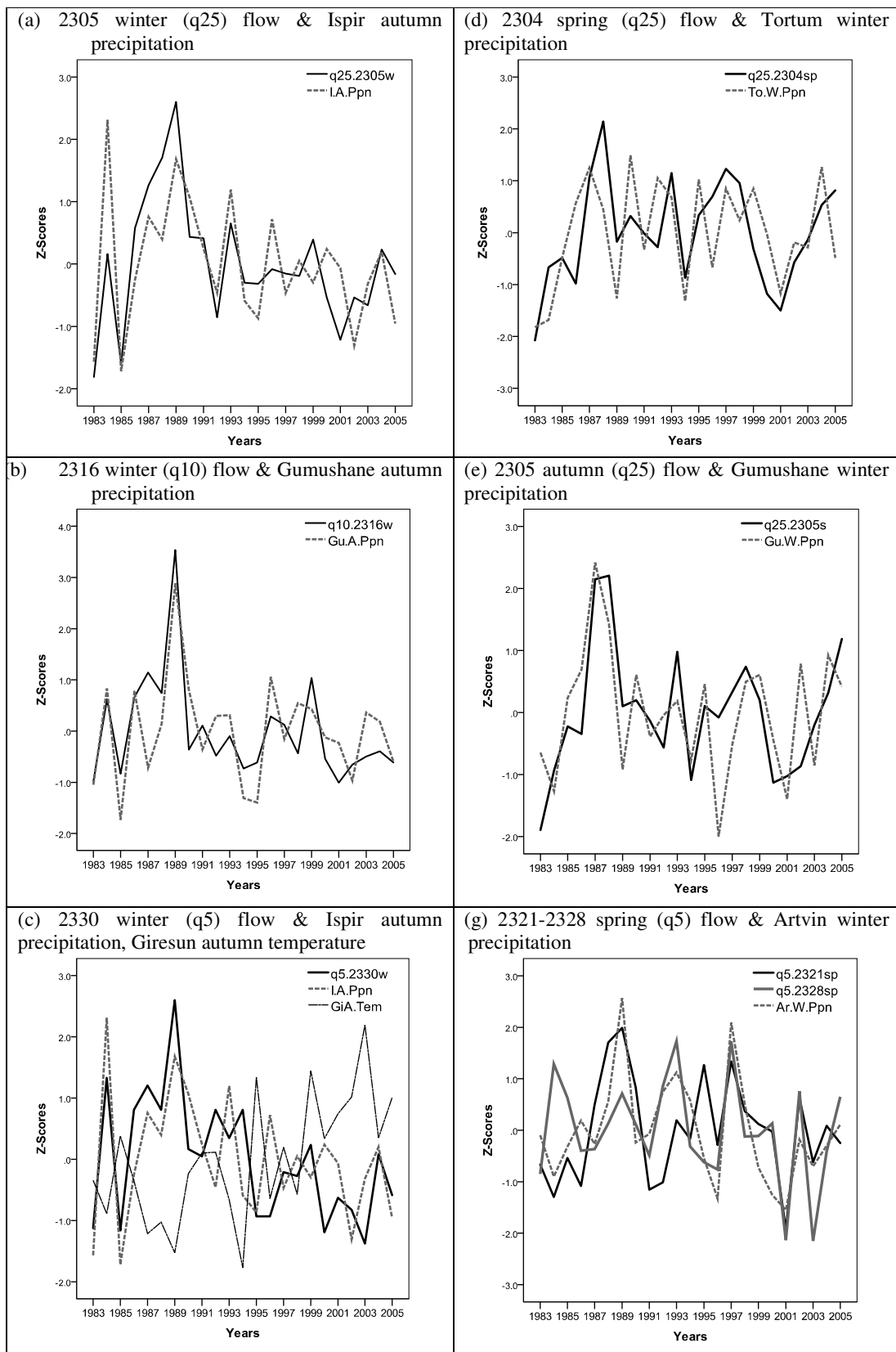


Figure 8.6 Seasonal composite river flow, precipitation and temperature percentile series (z-

scores displaying negative and positive values) for selected stations of the ÇRB.

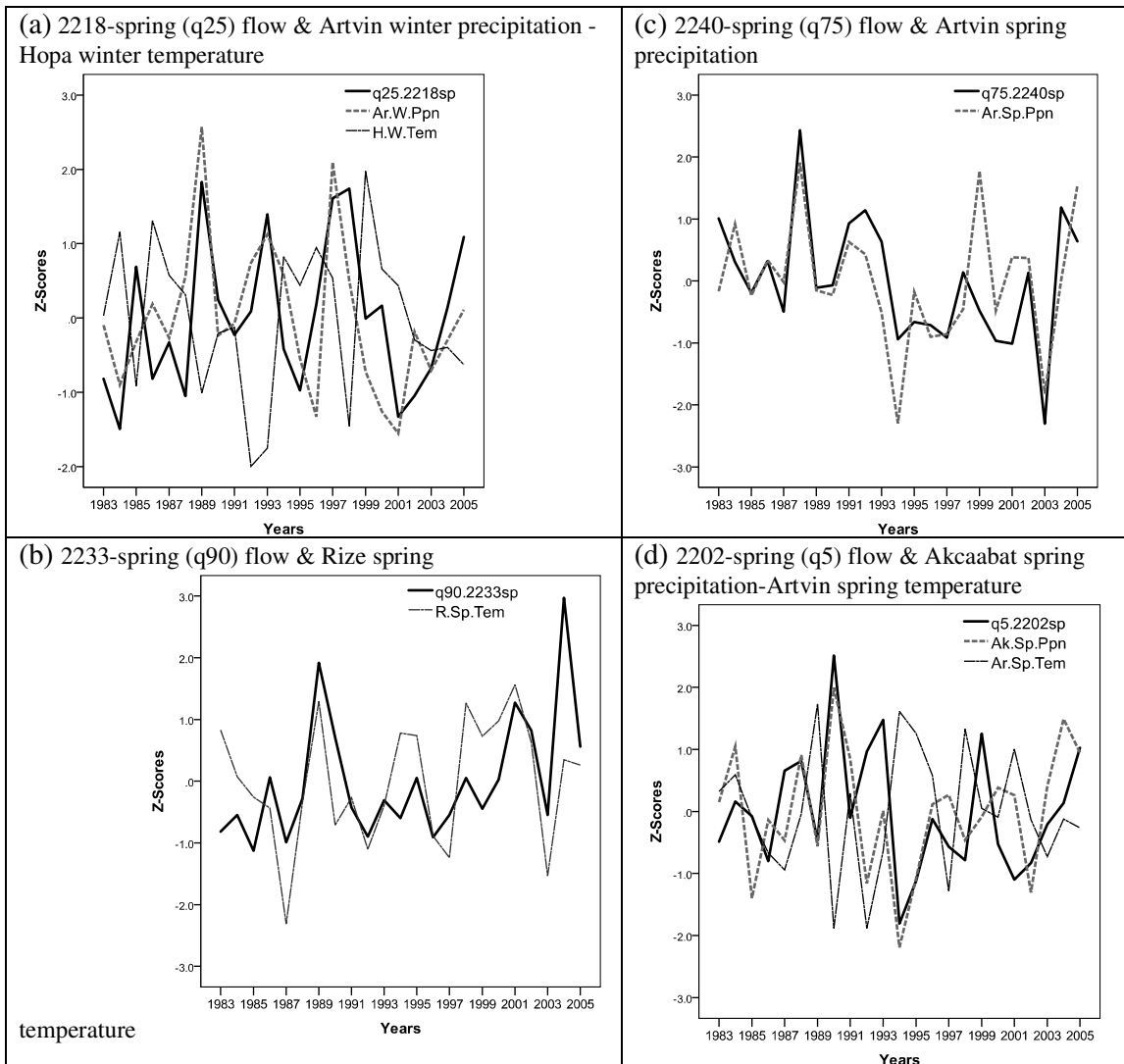


Figure 8.7(1) Seasonal composite river flow, precipitation and temperature percentile series (z-scores displaying negative and positive values) for selected stations for the EBS Basin.

Temperature appears to have a more complex influence on river flow extremes. High temperature episodes strongly influence low (dry) river flow periods (Figure 8.7). Figure 8.7(2), suggests a strong influence of high spring temperature on river flow extremes, probably due to accelerated snowmelt in these high mountain basins.

In summary, precipitation is the strongest predictor on river flow. The link between regional

climate and river flow variability appears to be more stable for the ÇRB, while the EBS Basin exhibit complex relationships. This condition of ÇRB is highly related with the continental characteristic of the basin.

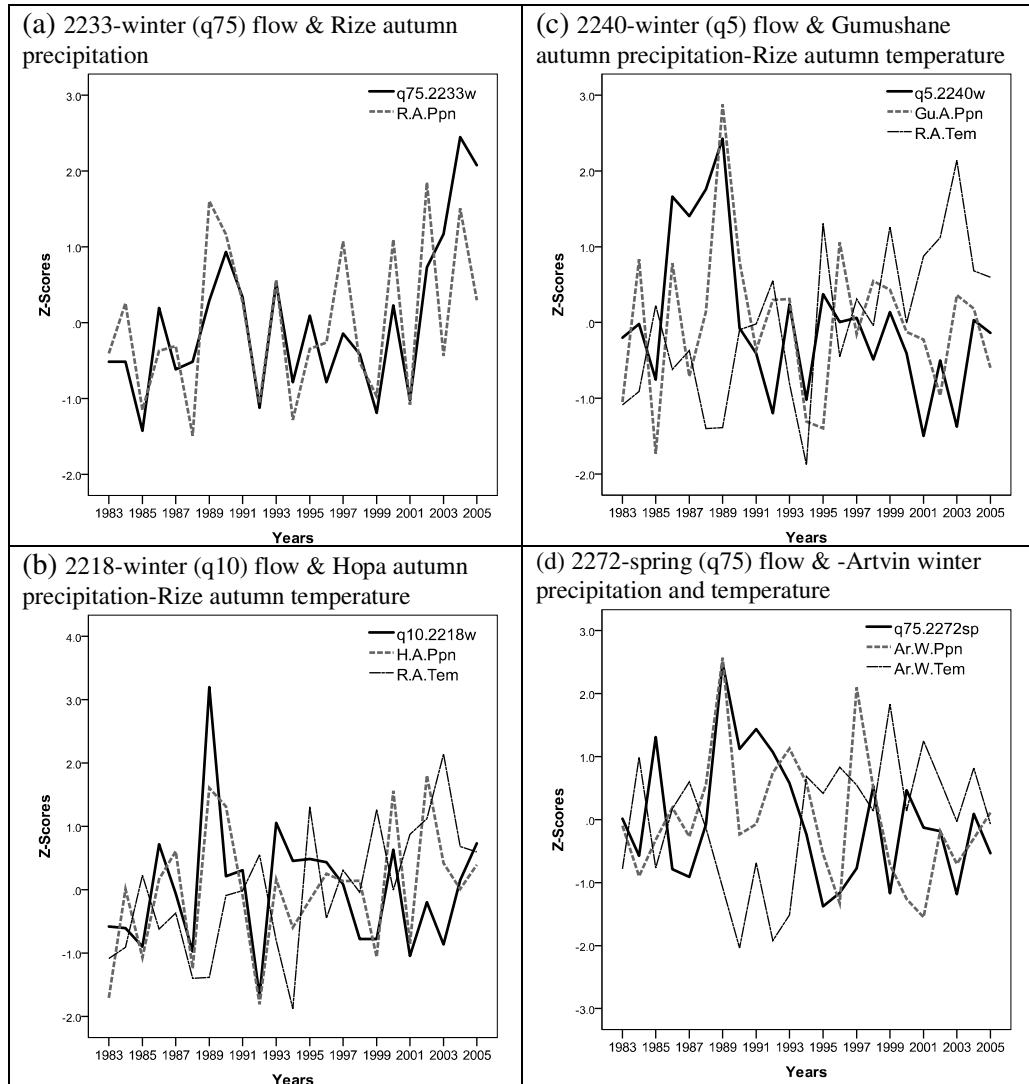


Figure 8.7(2) Seasonal composite river flow, precipitation and temperature percentile series (z-scores displaying negative and positive values) for selected stations of the EBS Basin.

8.5. Conclusions

This chapter has examined and analysed long-term data of 12 meteorology and 12 river gauging stations to assess for the first time space-time patterns in hydroclimatological extremes for northeast Turkey. A clear inland-coastal discrimination is apparent. Important

trends were detected for summer and autumn series of precipitation and temperature data. Most importantly, significant trends were detected in low and high precipitation and river flow percentiles, contrary to the results obtained from mean monthly and/or seasonal trend analysis (Chapter 7). High-very high flows and very low-low precipitation extremes were identified with an increasing trend in winter. For temperature series, spring, summer and autumn high temperature extremes display spatially consistent and significant rising temperature trends, especially for the coastal stations. Together with the changes in temperature indices (especially warm and summer days), the changing pattern in river flow extremes suggest an increasing shift towards more variable climatic and hydrological conditions.

MLR analyses suggest that regional climate is a driving mechanism behind the extreme river flow variability, although patterns are complex and strength of association varies. Precipitation was designated as the primary predictor for almost each seasonal time series. Climate data sourced from the coastal EBS Basin [inland ÇRB] are influential on the extreme river flow variability of river gauging stations located on EBS [Çoruh]. Interestingly, winter climatic conditions for the inland stations are also affected on spring river flows of EBS, which can be explained by the enhanced impact of vast high pressure cells during winter season. To conclude, wet precipitation period equates to high river flow, while high temperature episodes cause to low flow periods. Other factors, namely the degree to which the physical geography exerts a controlling influence on river flows in the region along with the relatively poor representativeness of observation network are other important factors.

This is the first comprehensive research jointly analysing seasonal precipitation, temperature and river flow extremes of northeast Turkey. Previous knowledge on hydroclimatic variability

of Turkey has not concluded important results for this region, in particular for extreme events variability. Therefore, this research provides valuable information on hydroclimatic extremes for northeast Turkey. This research demonstrates that examining long-term averages for mean values of parameters tended to hide the distribution characteristics of time-based changes. However, these first-time results from analysis of extremes suggest that significant changes have occurred in the EBS and Çoruh River basins. This knowledge is essential for northeast Turkey since it has a unique character of having highest precipitation records, flood and landslide events (Ergünay, 2007).

These thresholds values may give an idea for preliminary studies of an early warning system over the study area. Given the catastrophic impact of heavy rainfall (which triggers the flood and landslide events) it is very important to consider variability of the threshold values all over the region. This calculated threshold analysis can be improved by interpolation of patterns over the study area by using hydrological and spatial analysis of GIS (also considering other factors affecting river flow etc.) and detect critical spots having high risk in terms of hydro-meteorological hazards and any special coherence within sub-basins.

8.6. Chapter summary

In this chapter, the overall characteristics of extreme temperature, precipitation and river flow events over northeast Turkey have been explored. The long-term trends in extreme series were quantified and changes driving climatic factors behind river flow extremes of northeast Turkey were explained. In addition to the analyses of regional river flow-climate regimes, and extremes (presented in this chapter), there is a research need to identify the influence of large-scale atmospheric patterns on hydroclimatic variability in northeast Turkey. Thus, the connections between Northern Hemisphere atmospheric patterns and surface hydroclimatic

components (monthly and seasonal temperature, precipitation and river flow series) are the main focus of the next chapter.

9. TELECONNECTION AND SURFACE HYDROCLIMATOLOGY OF NORTHEAST TURKEY

9.1. Introduction

Teleconnection patterns (i.e. recurring and persistent large-scale atmospheric pressure and circulation phenomena) have prominent effects on the spatial and temporal variability of hydroclimatic conditions (Hurrell & Van Loon, 1997). In order to evaluate the sensitivity of hydrological systems to climatic fluctuations, improved understanding is needed of the process cascade linking large-scale climate to regional river flow (Kingston *et al.* 2009). In the eastern Mediterranean region where Turkey is located, the most dominant large scale circulation mode is the North Atlantic Oscillation (NAO) (Dunkeloh and Jacobeit 2003). However, other teleconnection patterns may also have an important influence on the hydroclimatology of Turkey, potentially the North Sea-Caspian Pattern (NCP) (Kutiel *et al.* 2002) and the East Atlantic/Western Russia Pattern (EA/WR) (Krichak and Alpert 2005).

The NAO has been identified as a major atmospheric circulation governing seasonal to interdecadal variability in the circum North Atlantic region (Hurrell, 1995). The NAO is a large-scale atmospheric pressure fluctuation that exists in the regions between the subtropical Azores high pressure system (anticyclone) and the subpolar low pressure near Iceland and represents one of the most important teleconnection or anomaly patterns of the North Atlantic-European area, where it is most pronounced in winter (Hurrell and VanLoon 1997; Wanner *et al.* 2001). However, it has also been shown that the NAO has a noticeable

influence on Mediterranean circulation patterns, where Xoplaki *et al.*, (2006) and Krichak and Alpert (2005) outline that the NAO plays an important role in inter-annual to centennial low frequency variability of wet season precipitation over the Mediterranean basin.

The zonally oriented East Atlantic/Western Russia (EA/WR) pattern has two main anomaly centres located over the Caspian Sea and western Europe in winter. During negative (positive) EA/WR phases, wetter (drier) than normal weather conditions are observed over a large part of the Mediterranean region (Barnston and Livezey, 1987). Positive phases of the pattern are characterised by negative pressure anomalies throughout western and southwestern Russia and positive pressure anomalies over northwestern Europe. Over the eastern Mediterranean (EM) region, positive EA/WR winter periods are associated with more intense northerly air flows; whereas, negative EA/WR phases are associated with positive pressure anomalies over the Caspian Sea and western Russia and negative pressure anomalies over northwestern Europe. A positive EA/WR lasted for several decades of the previous century (Krichak and Alpert 2005; Krichak *et al.*, 2002). Physical mechanisms responsible for the EA/WR trend are not fully understood (Paeth *et al.*, 1999). The trend could be caused by the positive trend of the NAO, as a consequence of the intensification of the southern NAO centre of action (Paeth *et al.*, 1999). Other explanations of the phenomena have been also suggested. The NAO and EA/WR trends could be a representation of more complex non-linear interactions (Feldstein, 2000). An eastward shift of the southern NAO positive centre (Ulbrich and Christoph, 1999) could be playing a role in the process. The trend could also be affected by a decline in intensity and eastward shift of the Siberian anticyclone (Panagiotopoulos *et al.*, 2005). Independent of the physical nature of its origin, the EA/WR trend has played a role in the recent past European climate.

Other large-scale modes of atmospheric circulation [namely the Eastern Atlantic (EA) and the Scandinavia (SCAND) patterns] also appear to have important influences on precipitation patterns over Europe (Garcia-Herrera *et al.* 2007, Fagherazzi *et al.* 2005, Hirschi and Seneviratne 2010, Zveryaev 2009). Recent research (Nesterov 2009) suggests that the East Atlantic (EA) is most prominent in winter with negligible effects during the summer months; the EA pattern consists of a north-south circulation dipole that spans the entire Atlantic Ocean with its main centre further southeast than the NAO centre. The EA pattern was found to be significantly correlated with spatial and temporal variability in annual precipitation on the Iberian Peninsula (Rodrigue-Puebla *et al.*, 1998) and winter rainfall in the British Isles (Murphy and Washington, 2001). The Eastern Mediterranean Pattern (EMP) is a dipole teleconnection pattern located in northeastern Europe and the eastern Mediterranean and has been identified as influencing winter upper troposphere weather. More specifically, positive phases of the EMP appear to be associated with decreases in temperature and increases in precipitation, while the opposite appears to operate for negative phases of the EMP (Hatzaki *et al.* 2009). The EMP appears to have some influence on weather patterns in the western part of Turkey (Hatzaki *et al.* 2009).

Krichak *et al.*, (2005) suggested that the NAO trend is not the only climatically important feature of Europe that could contribute to weather variations. The positive trend of another prominent European teleconnection pattern, the EA/WR (Krichak *et al.*, 2002), could play a significant role. Rogers (1997) found that the cyclone trajectories (storm tracks) in the North Atlantic are determined to a large extent by pressure anomalies in the northeastern North Atlantic, while the NAO is associated with the latitudinal change in storm tracks in the central North Atlantic (see also in Franzke and Feldstein, 2005). A similar result was obtained by

Mailier *et al.*, (2006); they indicated that the NAO index does not describe the variability of the number and tracks of cyclones in the storm track southeastern part. They also stress the important role of EA, EA/WR, SCA, and POL in the variability of characteristics of Atlantic-European cyclones. These studies indicate that the NAO index alone is not sufficient to describe the variability of the Atlantic-European circulation.

Recent hydroclimatological research of these various atmospheric oscillations and anomalies on Turkey shows that the NAO, ENSO (El-Nino and Southern Oscillation), La-Nina, NCP (North Sea-Caspian Pattern) and Arctic Oscillation (AO) patterns have effects on the year-to-year variability of seasonal and regional temperature, precipitation and river flows as well as extreme phases which suggests the presence of relationships (Kahya and Karabork 2001; Kutiel *et al.* 2002; Karabork and Kahya 2003, 2009; Karabork *et al.*, 2005, Kutiel and Türkeş 2005; Karabork *et al.*, 2007; Tatli 2007; Türkeş and Erlat 2009, 2003, 2005, 2006, 2008; Cullen and deMenocal 2000; Cullen *et al.*, 2002; Kalayci and Kahya 2006). Of these various pressure oscillations and anomalies, recent research by Türkeş and Erlat (2003, 2005, 2006) suggests that the NAO has the most significant influence on temperature, precipitation and river flow variability over Turkey and found that anomaly patterns of the NAO and Turkish precipitation are negatively correlated. This association being most evident for western regions is close association indicates that the severity of wetter (drier) conditions are largely controlled by more negative (positive) NAOI phases and these appear to affect both annual weather patterns and also winter and autumn seasons. Cullen and deMenocal (2000) developed composite indices of Turkish winter temperature and precipitation to examine inter-annual-decadal climate variability for the Tigris-Euphrates headwater region and found that these indices are significantly correlated with the NAO, with 27% of the variance in precipitation accounted for by the NAOI. They explained that the NAO influence on

Euphrates river flow is even more profound when extreme NAO years are considered, as evidenced by widespread drought events in 1984, 1989 and 1990. The annual streamflow time series, measured from September–August, exhibits many of the same interdecadal trends evident in the NAO (SLP) index, with low flow values during the 1950s and high flow values during the early 1940s and the late 1960s. The calculated average river runoff at Keban for the three highest (1945, 1949 and 1961; mean=447 m³s⁻¹) and the three lowest (1940, 1963 and 1969; mean=983 m³s⁻¹) NAO years demonstrates that the Euphrates streamflow exhibits ~40% of the variability about the 35-year mean value (663 m³s⁻¹) linked to the NAO extreme. Kalayci and Kahya (2006) and Karabork *et al.* (2005) found a significant relationship between the Turkish hydroclimatology (i.e. temperature, precipitation and river flow) and the NAO. During positive phases of the North Atlantic Oscillation indices (NAOIs), northeasterly circulation increased, and more spatially coherent and significantly colder weather signals dominate over much of Turkey. However, during negative phases of the NAOI with, prevailing westerly winds that originate from the subtropical northeast Atlantic increase, more spatially coherent and significantly warmer weather signals prevail over the Anatolian peninsula (Türkeş and Erlat, 2009).

Although previous research has provided a national picture of the links between surface hydroclimatology of Turkey and some teleconnection patterns, there is a crucial need to focus on regional or local (River Basin) scale connections. This is especially so for geographically diverse regions such as northeast Turkey where two closely located but distinct major river basins (i.e. the East Black Sea coastal littoral Basin and the Çoruh River Basin) are located. The teleconnections of regional climate-river flow variability need to be elucidated for this region because water issues are of pressing concern in present day of Turkey (Sümer, 2011). It is important to establish the regional and/or basin scale hydroclimatic response to

atmospheric oscillations. More importantly, whereas the impact of NAO and ENSO on hydrological systems in Turkey has been widely studied, there is a dearth of research on the influence of Eurasian and East Atlantic teleconnection patterns on Turkey's hydroclimatology (as reviewed above). The magnitude and nature of any associations between various atmospheric circulation patterns and surface hydroclimatology needs to be analysed at more local scales to elucidate strength of relationships. Such research will positively contribute to increase the knowledge and understanding on the role of atmospheric dynamics on regional climate and river flow, and, thus, guide other scientific efforts regarding future predictions of hydroclimatic variability.

This chapter aims (1) to investigate the role of *North Atlantic Oscillation* (NAO), *East Atlantic Pattern* (EA), *Scandinavia Pattern* (SCAND), *East Atlantic/Western Russia Pattern* (EA/WR) and *Polar/Eurasia Pattern* (POL) on surface hydroclimatology variability in northeast Turkey and (2) to highlight associations between anomaly indices and temperature, precipitation and river flow series at seasonal and monthly resolutions.

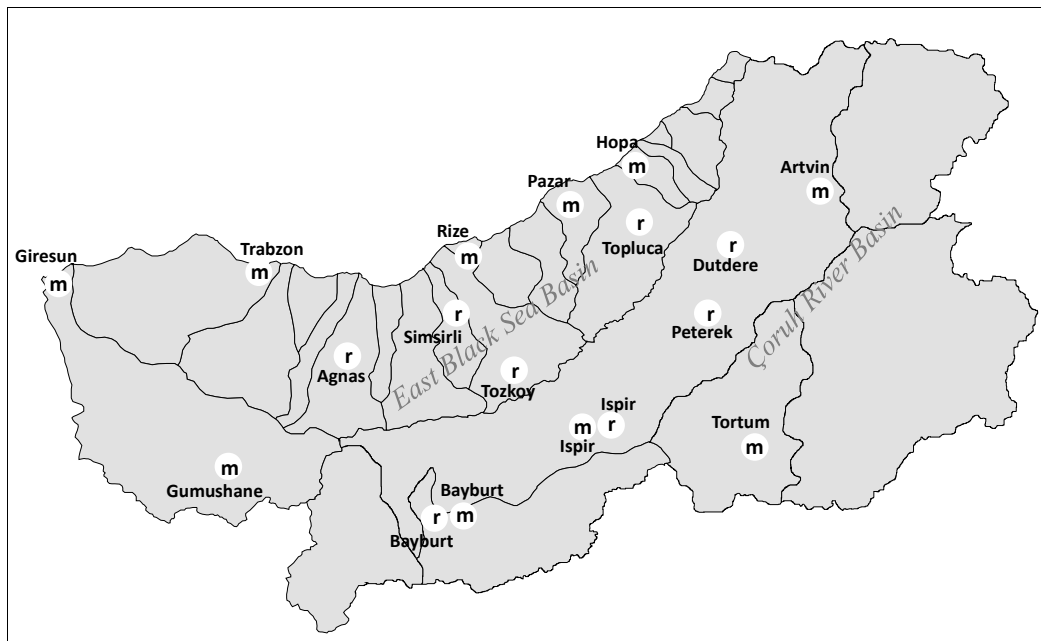


Figure 9.1 Location of stations evaluated for teleconnection analyses [m and r indicate meteorology and river gauging stations respectively].

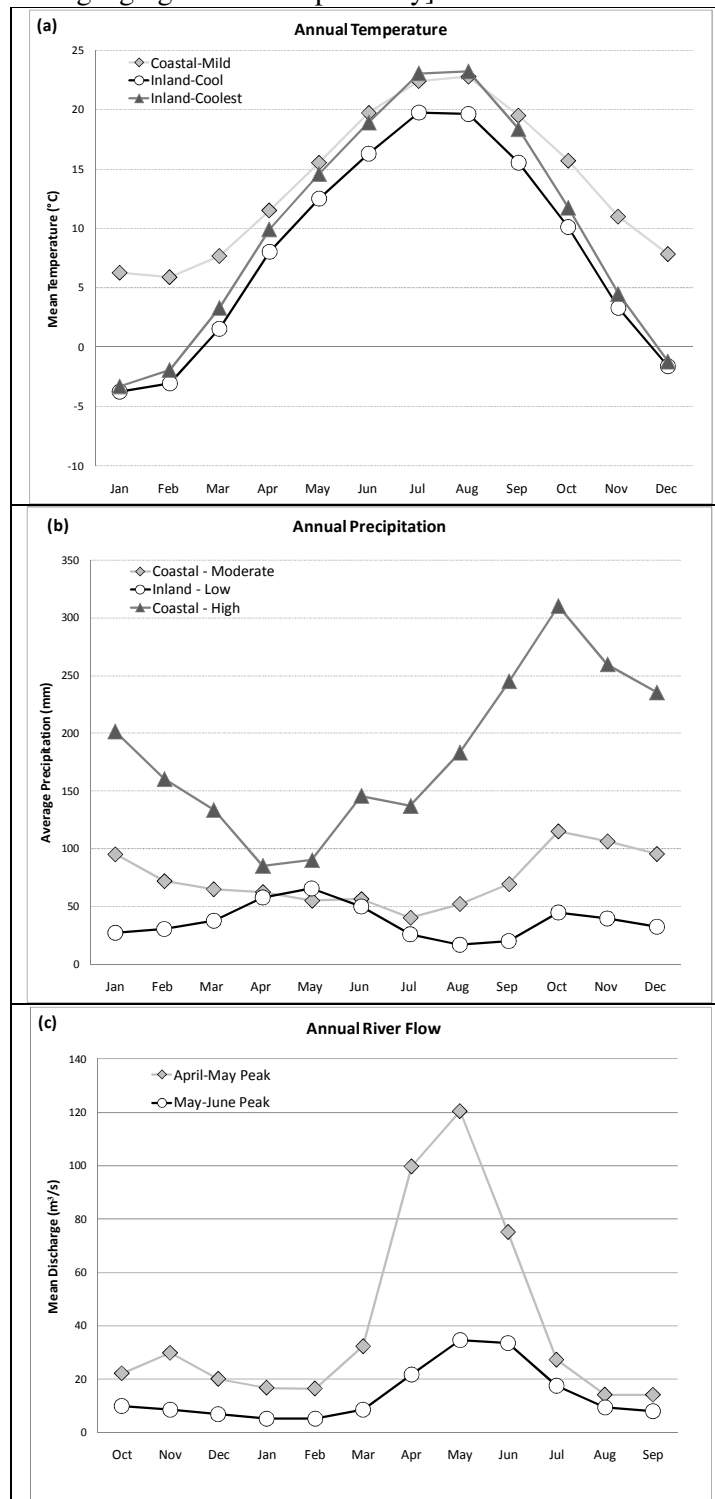


Figure 9.2 Annual temperature, precipitation and river flow regime characteristics.

9.2. Study area

9.2.1. Temperature, precipitation and river flow characteristics of the study basins

Intra-annual variability of temperature indicates a markedly seasonal regime for northeast Turkey (Figure 9.2a) characterised by high summer and low winter average temperatures. The magnitude of temperature differs for inland and coastal basins; the inland ÇRB is characterised by more severe cold winters, while a cool temperature regime is characteristic for December and January. Temperatures then increase gradually in spring and achieve maximum values in summer with July and August being the warmest months.

Three major precipitation regime regions can be identified for the region: (i) high and moderate rainfall amounts with clear October peak (also high for the [DJF] winter period) located mainly in the west-northwestern part of the coastal zone; (ii) wet spring (May peak) season with low and very low precipitation totals reflecting a predominantly continental regime character and includes those stations located in the interior part of the region and in the ÇRB in particular and (iii) very high rainfall totals distributed throughout the year apart from spring, but with a noticeable October peak, which prevails along the east-northeastern part of the Black Sea coast (Figure 9.2b).

Spring river flows make up the majority of annual flow, this being followed by a relatively drier summer period (for both basins). In Figure 9.2c, the line for April-May peak represents the ÇRB, while the May-June peak line signifies the EBS basin. However, two distinct differences exist in the flow characteristics for both basins in terms of the magnitudes and monthly mean flow. The flow totals of the ÇRB are markedly higher (Figure 9.2c); the peak time of flow magnitude being May for both basins. The three month period of April, May and

June is the period of highest flow for the ÇRB, whereas the period of highest flows for the EBS Basin also includes July (Figure 9.2c) due mainly to climatological differences between basins.

Table 9.1 Basic information about data source used in correlation analysis.

(a) Climate Stations

| Station Name | Elevation (m) | Temperature (C°) | Precipitation (mm) | Rainy Days |
|--------------|---------------|------------------|--------------------|------------|
| Artvin | 628 | 12.0 | 722.6 | 131.6 |
| Bayburt | 1584 | 7.0 | 443.0 | 100.8 |
| Giresun | 37 | 14.5 | 1246.2 | 158.4 |
| Gümüşhane | 1219 | 9.5 | 464.9 | 115.4 |
| Hopa | 33 | 14.3 | 2243.4 | 181.3 |
| Ispir | 1222 | 10.4 | 478.0 | 95.7 |
| Pazar | 79 | 13.3 | 2068.2 | 158.3 |
| Rize | 9 | 14.3 | 2241.4 | 169.19 |
| Tortum | 1572 | 8.3 | 470.7 | 116.2 |
| Trabzon | 30 | 14.6 | 831.5 | 139.8 |

(b) River Gauging Stations

| Station Name | River | Elevation (m) | Run off (mm) | Discharge (m ³ s ⁻¹) |
|---------------|---------|---------------|--------------|---|
| 2202 Ağnas | Kara | 78 | 545.7 | 11.0 |
| 2218 Şimşirli | İyidere | 338 | 1053.8 | 27.9 |
| 2232 Topluca | Fırtına | 237 | 1219.0 | 29.5 |
| 2233 Tozköy | Tozköy | 1296 | 947.1 | 6.7 |
| 2304 Bayburt | Çoruh | 1545 | 280.1 | 15.4 |
| 2305 Peterek | Çoruh | 654 | 304.0 | 69.9 |
| 2316 Ispir | Çoruh | 1170 | 220.5 | 38.5 |
| 2321 Dutdere | Parhal | 705 | 753.4 | 14.0 |

9.3. Data

Monthly mean temperature and total precipitation data for 10 meteorological stations (from DMI) and mean river flow data for 8 river gauging stations (from EIE) were obtained. Unfortunately, the number of stations with long-term data was quite limited, so selection of the stations had to be made on the basis of the continuity of the observation period, their location within the basins (Table 9.1). In order to increase reliability of statistic tests of time series, a 30 year period (1976 to 2005) was chosen which comprises the optimum length that

is also acceptable to analyse climatology and hydrology time series (Figure 9.1). Data quality assessment analyses were also undertaken and these verified the homogeneity of the data against any non-climatic changes (See Chapters 6 and 7). For the seasonal analysis, monthly time series were arranged as climatological seasons: winter comprising December, January and February (DJF); March, April and May (MAM) as spring; June, July and August (JJA) as summer and September, October and November (SON) as autumn. Time series were also standardised to reduce the likely effects of high year-to-year variability in seasons.

Table 9.2 List and definitions of evaluated atmospheric patterns.

| Pattern | Positive | Negative |
|--------------|--|---|
| NAO | The positive phase of the NAO reflects below-normal pressure around Iceland and above-normal pressure around the Azores. (Strong low and high) | The negative phase of the NAO reflects above-normal pressure around Iceland and below-normal pressure around the Azores. (Strong low and high) |
| EA | It is characterized by a dipole structure with a center of negative anomaly in the Icelandic low and the center of positive anomaly in the Azores high fostering the zonal transport like NAO. Both cases are characterized by a positive 70 monthly mean anomaly in Europe with maximums of more than 3°C in European Russia. However, this area is shifted eastward during EA > 0. | Characteristic dipole <i>P0</i> structure has the positive anomaly center between Iceland and Great Britain and the negative anomaly center in the eastern tropical Atlantic. The main difference from NAO with similar dipole structure is that the northern center is shifted southeastward, and the southern one to the south, and both centers are less intense than during negative NAO. |
| EA/WR | Negative pressure/height anomalies throughout western and southwestern Russia and positive pressure/height anomalies over northwestern Europe. | Positive pressure/ height anomalies over the Caspian Sea and western Russia and negative pressure/ height anomalies over northwestern Europe. |
| SCAND | Positive height anomalies, sometimes reflecting major blocking anticyclones, over Scandinavia and western Russia. | Negative height anomalies over Scandinavia and western Russia. |
| POL | Below-normal heights throughout the polar region and an enhanced circumpolar vortex, in combination with above-normal heights over much of Europe and eastern Asia. | Above-normal heights throughout the polar region and a weaker than normal polar vortex, in combination with below-normal heights over much of Europe and eastern Asia. |

Table 9.2 provides basic information about the selected teleconnection patterns and Figure 9.3 displays time series for the annual value of the NAO, EA, EA/WR, POL and SCAND indices.

The monthly standardised Northern Hemisphere teleconnection indices were obtained from the Climate Prediction Center (CPC) of the National Oceanic and Atmospheric Administration (NOAA). Three monthly average indices of the teleconnection patterns were derived from standardised monthly anomalies. The NAO is one of the most prominent teleconnection patterns in all seasons which consists of a north-south dipole of anomalies, with one centre located over Greenland and the other centre of opposite sign spanning the central latitudes of the North Atlantic between 35°N and 40°N (in the region of the Azores). The EA pattern is the second prominent mode of low-frequency variability over the North Atlantic, and appears as a leading mode in all months. The EA pattern is structurally similar to the NAO, and consists of a north-south dipole of anomaly centres spanning the North Atlantic from east to west. The anomaly centers of the EA pattern are displaced southeastward to an approximate location of the nodal lines of the NAO pattern. For this reason, the EA pattern is often interpreted as a “southward shifted” NAO pattern. The EA/WR pattern is one of three prominent teleconnection patterns that affect Eurasia throughout year and consists of four main anomaly centres. Positive phases are associated with positive height anomalies located over Europe and northern China, while negative phases are associated with negative height anomalies located over the central North Atlantic and north of the Caspian Sea. The Scandinavia pattern (SCAND) consists of a primary circulation centre over Scandinavia, with weaker centres of opposite sign over western Europe and eastern Russia/Western Mongolia. Positive phases of this pattern are associated with positive height anomalies, sometimes acting as major blocking anticyclones over Scandinavia and western Russia, while negative phases are associated with negative height anomalies in these regions. The Polar/Eurasia pattern appears in all seasons. Positive phases of this pattern consist of negative height anomalies over the polar region and positive anomalies over northern China and Mongolia. This pattern is mainly associated with above-average temperatures in eastern Siberia and below-average

temperatures in eastern China. It is also associated with above-average precipitation in the polar region north of Scandinavia (Barnston and Livezey 1987).

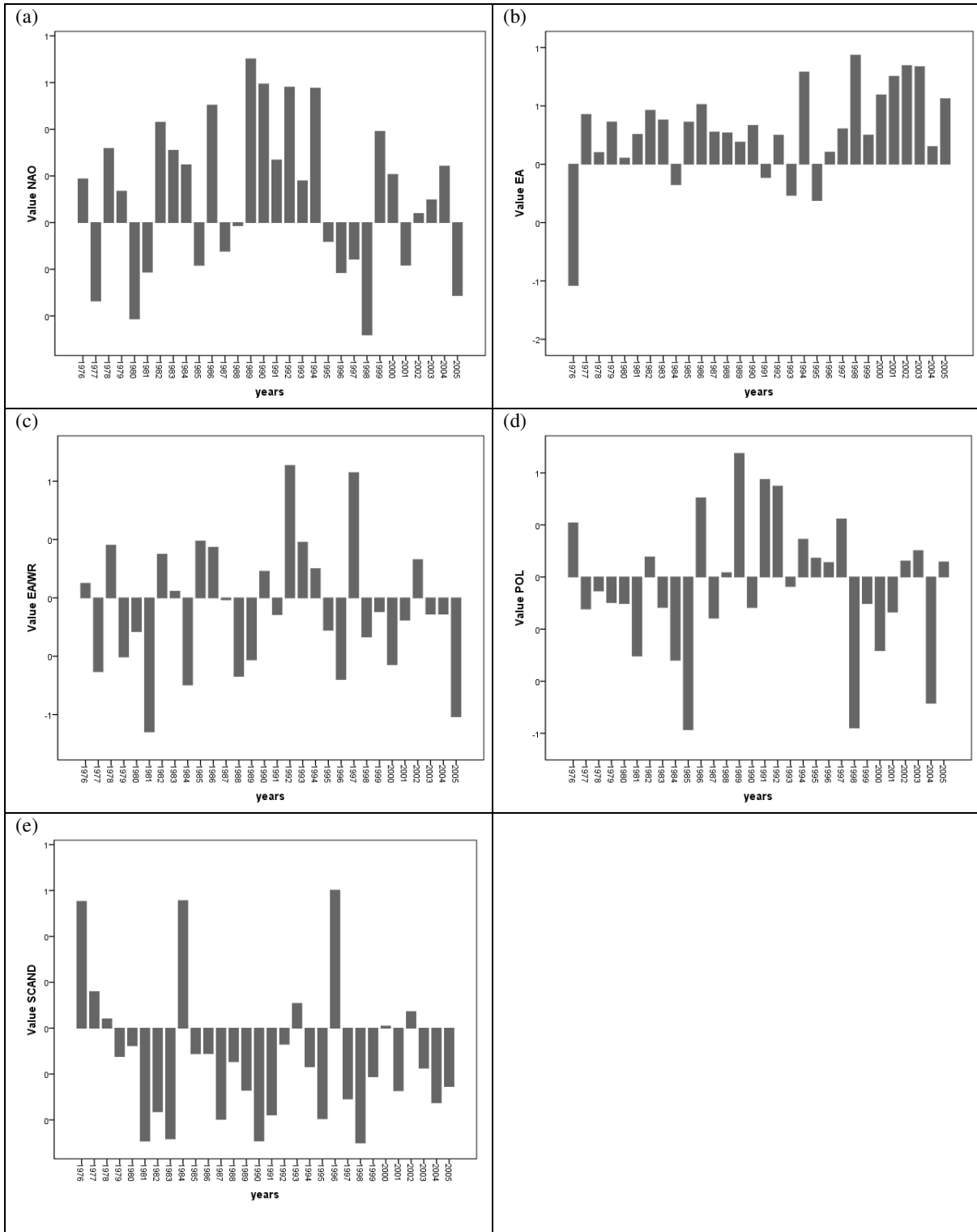


Figure 9.3 Comparison of time series for the annual value of the (a) NAO, (b) EA, (c) EA/WR, (d) POL and (e) SCAND indices.

As mentioned in the ‘study area’ sections of earlier chapters, northeast Turkey is characterised by the EBS and Çoruh River basins (Figure 9.1). The high mountainous terrain exerts a strong physical influence on the atmospheric circulation for this region. Two important air masses (mP and CP) have a pronounced seasonal effect on meteorological conditions. During winter, the region is affected by the strong thermal Siberian High Pressure System. The positions of the jet streams and jet maxima are important in determining surface pressure and rainfall patterns but the relationships are extremely complex. The frequency of the cyclonic systems appears to be highly influential on the fluctuation of the intra-annual precipitation and control the seasonality. The Black Sea together with the mountain ranges that run parallel to the coast have a positive contribute to precipitation amounts for coastal stations and serve to accelerate convective activity which further determines the precipitation character for interior stations.

9.4. Method

9.4.1. Pearson’s correlation

Pearson’s correlation coefficient was applied to detect the linear relationship between teleconnection indices and monthly and seasonal temperature, precipitation and river flow series. The Pearson’s correlation coefficient is a common measure of the degree of linear correlation between two variables. In the results, the correlation value ρ_{xy} ranges from -1 to $+1$. A correlation of 1 (-1) means that there is a perfect (negative) positive relationship between X and Y (Helsel and Hirsch, 2002). Using a two-tailed test, the correlation is attributed as significant for the large values of coefficient at 0.05 and 0.01 levels.

Table 9.3 Percentage of significant correlation results detected for monthly relationships (shaded cells highlights significant proportions equal and over 25%).

| January | NAO | EA | EA.WR | SCA | POL |
|--------------------|------|------|-------|------|------|
| % in Total | 7.1 | 3.6 | 53.6 | 3.6 | 3.6 |
| % in River Flow | 12.5 | 0.0 | 0.0 | 0.0 | 12.5 |
| % in Temperature | 0.0 | 0.0 | 100.0 | 0.0 | 0.0 |
| % in Precipitation | 10.0 | 10.0 | 50.0 | 10.0 | 0.0 |

| February | NAO | EA | EA/WR | SCA | POL |
|--------------------|------|------|-------|-----|-----|
| % in Total | 46.4 | 3.6 | 64.3 | 0.0 | 0.0 |
| % in River Flow | 37.5 | 12.5 | 0.0 | 0.0 | 0.0 |
| % in Temperature | 90.0 | 0.0 | 100.0 | 0.0 | 0.0 |
| % in Precipitation | 10.0 | 0.0 | 80.0 | 0.0 | 0.0 |

| March | NAO | EA | EA/WR | SCA | POL |
|--------------------|------|------|-------|------|------|
| % in Total | 17.9 | 3.6 | 0.0 | 3.6 | 10.7 |
| % in River Flow | 0.0 | 0.0 | 0.0 | 0.0 | 0.0 |
| % in Temperature | 0.0 | 0.0 | 0.0 | 0.0 | 0.0 |
| % in Precipitation | 50.0 | 10.0 | 0.0 | 10.0 | 30.0 |

| April | NAO | EA | EA/WR | SCA | POL |
|--------------------|------|------|-------|-----|-----|
| % in Total | 3.6 | 42.9 | 53.6 | 0.0 | 0.0 |
| % in River Flow | 0.0 | 37.5 | 12.5 | 0.0 | 0.0 |
| % in Temperature | 10.0 | 90.0 | 100.0 | 0.0 | 0.0 |
| % in Precipitation | 0.0 | 0.0 | 40.0 | 0.0 | 0.0 |

| May | NAO | EA | EA/WR | SCA | POL |
|--------------------|------|-----|-------|------|-----|
| % in Total | 35.7 | 0.0 | 14.3 | 3.6 | 0.0 |
| % in River Flow | 12.5 | 0.0 | 0.0 | 12.5 | 0.0 |
| % in Temperature | 90.0 | 0.0 | 30.0 | 0.0 | 0.0 |
| % in Precipitation | 0.0 | 0.0 | 10.0 | 0.0 | 0.0 |

| June | NAO | EA | EA/WR | SCA | POL |
|--------------------|------|-----|-------|------|------|
| % in Total | 14.3 | 0.0 | 0.0 | 10.7 | 14.3 |
| % in River Flow | 0.0 | 0.0 | 0.0 | 25.0 | 0.0 |
| % in Temperature | 30.0 | 0.0 | 0.0 | 0.0 | 40.0 |
| % in Precipitation | 10.0 | 0.0 | 0.0 | 10.0 | 0.0 |

| July | NAO | EA | EA/WR | SCA | POL |
|--------------------|------|------|-------|-----|------|
| % in Total | 7.1 | 28.6 | 14.3 | 0.0 | 14.3 |
| % in River Flow | 25.0 | 0.0 | 0.0 | 0.0 | 0.0 |
| % in Temperature | 0.0 | 80.0 | 40.0 | 0.0 | 30.0 |
| % in Precipitation | 0.0 | 0.0 | 0.0 | 0.0 | 10.0 |

| August | NAO | EA | EA/WR | SCA | POL |
|--------------------|------|------|-------|------|-----|
| % in Total | 3.6 | 25.0 | 0.0 | 3.6 | 0.0 |
| % in River Flow | 0.0 | 0.0 | 0.0 | 0.0 | 0.0 |
| % in Temperature | 10.0 | 70.0 | 0.0 | 10.0 | 0.0 |
| % in Precipitation | 0.0 | 0.0 | 0.0 | 0.0 | 0.0 |

| September | NAO | EA | EA/WR | SCA | POL |
|--------------------|------|------|-------|-----|-----|
| % in Total | 3.6 | 3.6 | 0.0 | 0.0 | 0.0 |
| % in River Flow | 0.0 | 0.0 | 0.0 | 0.0 | 0.0 |
| % in Temperature | 0.0 | 10.0 | 0.0 | 0.0 | 0.0 |
| % in Precipitation | 10.0 | 0.0 | 0.0 | 0.0 | 0.0 |

| October | NAO | EA | EA/WR | SCA | POL |
|--------------------|------|------|-------|------|-----|
| % in Total | 28.6 | 35.7 | 0.0 | 32.1 | 0.0 |
| % in River Flow | 0.0 | 0.0 | 0.0 | 0.0 | 0.0 |
| % in Temperature | 80.0 | 90.0 | 0.0 | 90.0 | 0.0 |
| % in Precipitation | 0.0 | 10.0 | 0.0 | 0.0 | 0.0 |

| November | NAO | EA | EA/WR | SCA | POL |
|--------------------|-------|------|-------|------|------|
| % in Total | 35.7 | 21.4 | 0.0 | 21.4 | 3.6 |
| % in River Flow | 0.0 | 0.0 | 0.0 | 0.0 | 0.0 |
| % in Temperature | 100.0 | 0.0 | 0.0 | 0.0 | 0.0 |
| % in Precipitation | 0.0 | 60.0 | 0.0 | 60.0 | 10.0 |

| December | NAO | EA | EA/WR | SCA | POL |
|--------------------|-----|-----|-------|------|-----|
| % in Total | 0.0 | 0.0 | 50.0 | 3.6 | 0.0 |
| % in River Flow | 0.0 | 0.0 | 0.0 | 12.5 | 0.0 |
| % in Temperature | 0.0 | 0.0 | 100.0 | 0.0 | 0.0 |
| % in Precipitation | 0.0 | 0.0 | 40.0 | 0.0 | 0.0 |

9.5. Results and discussion

Monthly and seasonal data of temperature, precipitation and river flow time series were analysed for the period 1976-2005 to assess, their responses to teleconnection patterns. Results show that the EA, EA/WR and NAO atmospheric anomaly patterns are the most persistent leading large-scale mechanisms influencing regional climate over northeast Turkey. The proportion of significant results for these three atmospheric patterns (Tables 9.3 and 9.4) is considerably higher for both monthly and seasonal data. Furthermore, the proportion of significant results for precipitation and temperature are stronger for the river flow. River flow have noticeably weaker correlation proportion (*shaded cells highlight significant correlation proportion over 25%*). These data suggest that these atmospheric anomaly patterns are highly

effective in influencing the variability of precipitation and temperature, whereas only weak associations exist for river flows. However, important patterns appear to exist on a seasonal basis; the atmospheric anomaly patterns appear to have a significant impact during (and also for the preceding) winter and spring for temperature and precipitation. EA/WR has the highest number of significant correlations for summer for temperature (Table 9.4). The nature and strength of the relationship between prominent (atmospheric phenomena) teleconnection patterns and surface hydroclimatic parameters (temperature, precipitation and river flow) of northeast Turkey are explained in the following sections. Seasonal teleconnections (both preceding and concurrent), their year-to-year variability, spatial character and influences are evaluated.

9.5.1. Relationship between the teleconnection indices and temperature

Seasonal temperature series of northeast Turkey have a strong, negative correlation with EA pattern, especially during winter and spring (Table 9.4a). For the DJFM extended winter period, the NAO and EA anomaly patterns are particularly effective on winter temperatures. Both preceding and concurrent EA anomalies appear to have a dominant impact on winter temperature. Winter (includes DJF, JFM and FMA three month periods) conditions of EA are negatively correlated with spring temperature, whereas the anomaly pattern of EA for MAM has relatively weak association. In summer, the EA and EA/WR anomaly patterns appear to have a significant influence on temperature with both negative and positive correlation values, respectively. These data suggest that the EA/WR anomaly pattern governs as the primary mode for summer (JJA) temperature variability throughout northeast Turkey. The NAO anomaly pattern for MJJ and the EA/WR for OND periods have a significant positive influence on spring-summer and autumn temperature regimes respectively, while EA anomaly pattern is negatively correlated for the SON period.

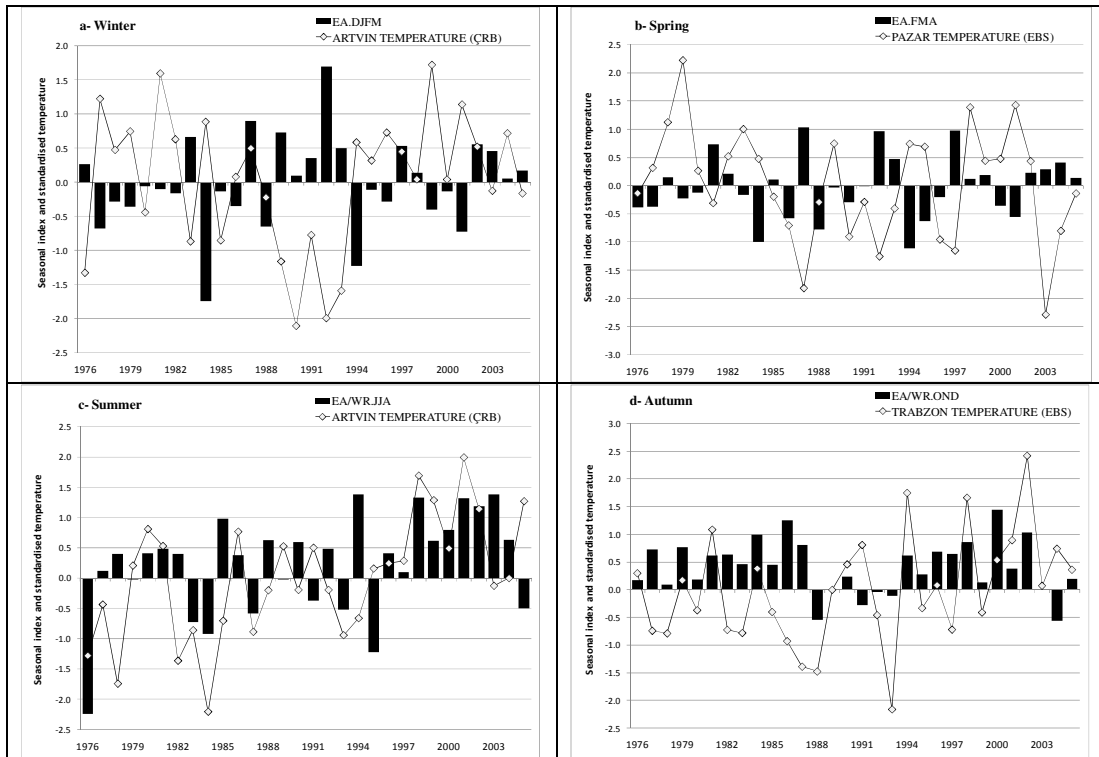


Figure 9.4 Year by year departures in standardised index values and temperature series for selected stations showing the correlation between seasonal temperature and the EA and EA/WR patterns.

Figure 9.4 shows the inter-annual variations in standardised atmospheric indices and temperature series for selected stations in the EBS and ÇRB for the EA and EA/WR anomaly patterns. In winter (DJFM), temperature for the Artvin station shows an opposite relationship with the EA anomaly pattern which has cooler (warmer) than normal temperatures during the positive (negative) phase for the EA anomaly pattern (Figure 9.4a). A negative correlation can also be detected for the spring temperature series for Pazar for the EA for the EA anomaly pattern for FMA (Figure 9.4b). Similar to winter, positive (negative) EA episodes mean cooler (warmer) temperatures for the Pazar station for spring. These data indicate that winter can be characterised by the sequencing of negative-warm, positive-cold, negative-warm periods (which implies decadal variation), while spring displays a more variable (short term persistent) pattern. For summer and autumn, a positive correlation is detected for the EA/WR anomaly pattern for the temperature time series for Artvin (Figure 9.4c) and Trabzon (Figure

9.4d) stations, respectively. For summer (JJA) a positive (negative) [or high (low)] phase is associated with warmer (cooler) than normal temperatures (Figure 9.4c). In particular, the EA/WR anomaly pattern indicates an intensified positive phase for the last decade of the observation period (i.e., from 1996) with temperatures significantly higher than the seasonal averages. In autumn, the relationship between EA/WR anomaly pattern and the temperature series for Trabzon for OND also shows a positive correlation pattern for the last decade, albeit not as strong as that for Artvin in summer. The positive relationship between these anomalies has been more persistent pattern after 1994 (Figure 9.4d).

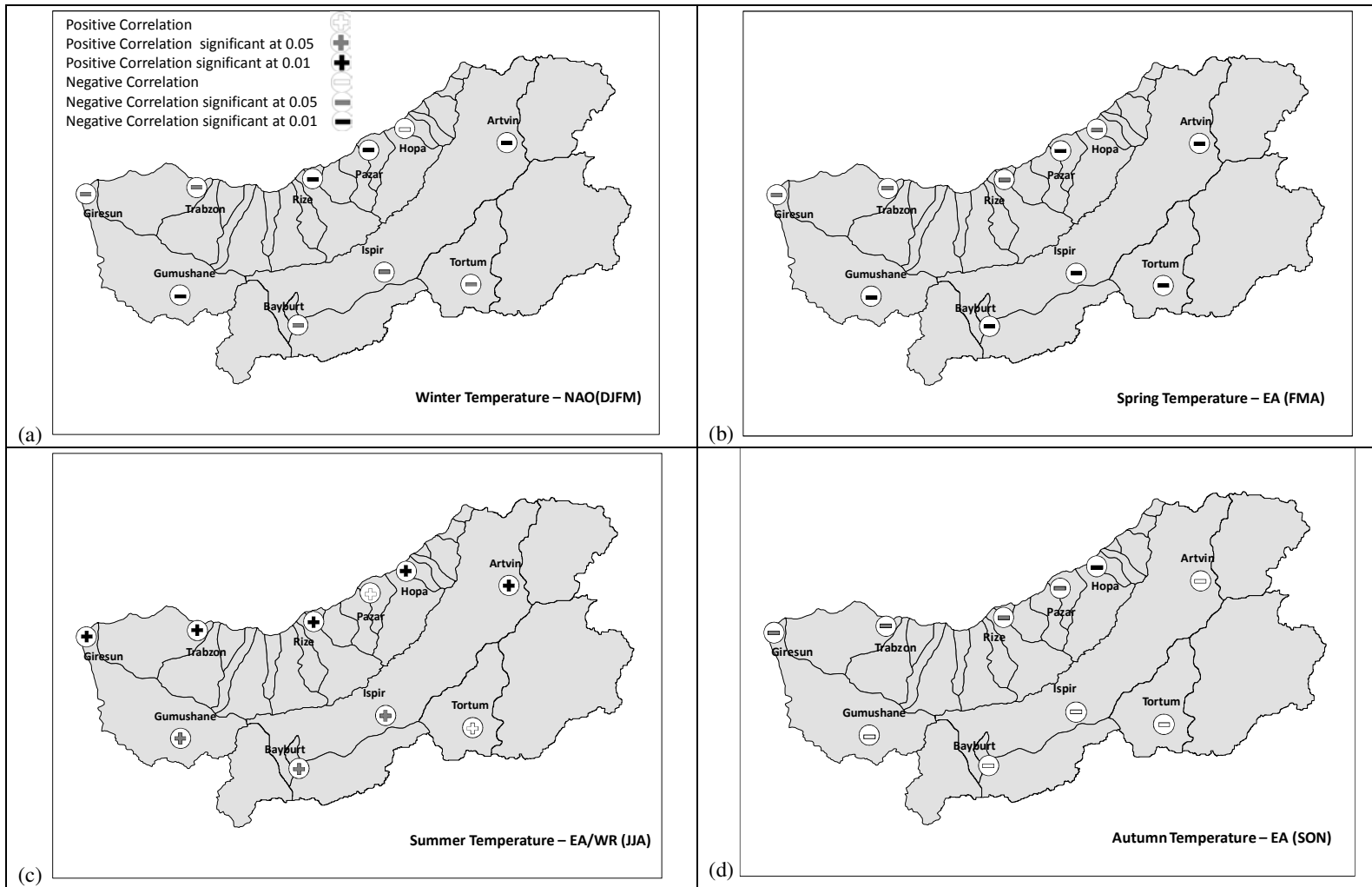


Figure 9.5 Associations between seasonal temperature and various large-scale atmospheric patterns.

Table 9.4 Percentage of significant correlation results detected for monthly relationships (shaded cells highlights significant proportions equal and over 25%, blue cells signifies significant positive correlation proportions).

| (a) Temperature | | DJF | JFM | FMA | MAM | AMJ | MJJ | JJA | JAS | ASO | SON | OND | NDJ | DJFM |
|-------------------|--------|------|------|------|------|------|------|------|------|------|------|------|------|------|
| EA | Winter | 100 | 0 | 0 | 0 | 0 | 0 | 0 | 0 | 20 | 80 | 0 | 0 | 100 |
| | Spring | 60 | 40 | 100 | 40 | 50 | 30 | 0 | 0 | 0 | 0 | 0 | 0 | 70 |
| | Summer | 0 | 0 | 0 | 0 | 0 | 0 | 70 | 10 | 0 | 70 | 0 | 0 | 0 |
| | Autumn | 0 | 0 | 10 | 0 | 0 | 0 | 0 | 0 | 10 | 50 | 0 | 0 | 0 |
| EA/WR | Winter | 0 | 0 | 30 | 0 | 0 | 30 | 40 | 0 | 0 | 0 | 10 | 0 | 0 |
| | Spring | 10 | 0 | 0 | 0 | 0 | 0 | 0 | 0 | 0 | 0 | 0 | 0 | 10 |
| | Summer | 0 | 30 | 0 | 30 | 10 | 40 | 80 | 80 | 90 | 0 | 0 | 0 | 0 |
| | Autumn | 0 | 0 | 0 | 0 | 0 | 30 | 0 | 0 | 0 | 30 | 60 | 0 | 0 |
| NAO | Winter | 0 | 20 | 60 | 0 | 0 | 0 | 0 | 0 | 0 | 0 | 0 | 0 | 90 |
| | Spring | 0 | 0 | 0 | 0 | 0 | 0 | 0 | 0 | 10 | 0 | 0 | 0 | 0 |
| | Summer | 0 | 0 | 0 | 0 | 0 | 0 | 0 | 0 | 0 | 0 | 0 | 0 | 0 |
| | Autumn | 0 | 0 | 0 | 0 | 80 | 100 | 0 | 0 | 0 | 0 | 0 | 0 | 0 |
| POL | Winter | 0 | 0 | 0 | 0 | 0 | 0 | 0 | 10 | 20 | 0 | 0 | 0 | 0 |
| | Spring | 0 | 0 | 0 | 0 | 0 | 0 | 0 | 0 | 0 | 0 | 0 | 0 | 0 |
| | Summer | 0 | 0 | 0 | 0 | 0 | 0 | 0 | 10 | 0 | 0 | 0 | 10 | 10 |
| | Autumn | 30 | 10 | 0 | 10 | 0 | 0 | 0 | 0 | 0 | 0 | 10 | 0 | 60 |
| SCAND | Winter | 0 | 0 | 0 | 0 | 0 | 30 | 0 | 0 | 0 | 0 | 0 | 0 | 0 |
| | Spring | 0 | 0 | 0 | 0 | 0 | 10 | 0 | 0 | 0 | 0 | 0 | 0 | 0 |
| | Summer | 0 | 0 | 0 | 0 | 0 | 20 | 20 | 0 | 0 | 0 | 0 | 0 | 0 |
| | Autumn | 0 | 0 | 0 | 0 | 40 | 0 | 0 | 0 | 0 | 10 | 0 | 0 | 0 |
| (b) Precipitation | | DJF | JFM | FMA | MAM | AMJ | MJJ | JJA | JAS | ASO | SON | OND | NDJ | DJFM |
| EA | Winter | 40 | 0 | 10 | 0 | 20 | 20 | 10 | 0 | 0 | 10 | 0 | 0 | 40 |
| | Spring | 30 | 0 | 0 | 0 | 10 | 0 | 10 | 10 | 20 | 20 | 0 | 0 | 20 |
| | Summer | 0 | 10 | 0 | 10 | 20 | 0 | 0 | 0 | 0 | 0 | 0 | 0 | 0 |
| | Autumn | 20 | 0 | 0 | 0 | 0 | 0 | 10 | 50 | 10 | 10 | 0 | 0 | 0 |
| EA/WR | Winter | 0 | 60 | 0 | 60 | 10 | 30 | 40 | 60 | 40 | 0 | 30 | 0 | 0 |
| | Spring | 0 | 0 | 0 | 0 | 0 | 0 | 0 | 20 | 20 | 0 | 0 | 30 | 0 |
| | Summer | 0 | 0 | 10 | 0 | 0 | 0 | 0 | 0 | 0 | 0 | 10 | 0 | 0 |
| | Autumn | 0 | 0 | 0 | 0 | 0 | 0 | 0 | 10 | 10 | 20 | 0 | 0 | 0 |
| NAO | Winter | 10 | 10 | 20 | 10 | 0 | 0 | 10 | 20 | 40 | 0 | 0 | 10 | 10 |
| | Spring | 0 | 0 | 60 | 40 | 0 | 0 | 0 | 10 | 0 | 0 | 0 | 0 | 10 |
| | Summer | 0 | 0 | 0 | 10 | 10 | 10 | 20 | 0 | 10 | 20 | 10 | 0 | 0 |
| | Autumn | 0 | 0 | 0 | 0 | 0 | 0 | 20 | 40 | 0 | 20 | 10 | 0 | 0 |
| POL | Winter | 0 | 0 | 0 | 0 | 0 | 10 | 10 | 20 | 10 | 0 | 0 | 0 | 0 |
| | Spring | 30 | 0 | 0 | 0 | 0 | 10 | 0 | 0 | 0 | 0 | 0 | 0 | 40 |
| | Summer | 0 | 10 | 0 | 10 | 20 | 10 | 0 | 0 | 0 | 0 | 0 | 0 | 0 |
| | Autumn | 0 | 20 | 0 | 20 | 10 | 0 | 0 | 0 | 0 | 10 | 10 | 0 | 0 |
| SCAND | Winter | 0 | 0 | 0 | 0 | 0 | 0 | 0 | 0 | 0 | 10 | 20 | 20 | 0 |
| | Spring | 0 | 10 | 0 | 10 | 40 | 0 | 0 | 0 | 0 | 20 | 0 | 0 | 0 |
| | Summer | 0 | 0 | 10 | 0 | 0 | 0 | 10 | 0 | 0 | 0 | 0 | 10 | 0 |
| | Autumn | 0 | 0 | 0 | 0 | 0 | 0 | 0 | 10 | 10 | 0 | 0 | 0 | 10 |
| (c) River Flow | | DJF | JFM | FMA | MAM | AMJ | MJJ | JJA | JAS | ASO | SON | OND | NDJ | DJFM |
| EA | Winter | 0 | 0 | 0 | 0 | 12.5 | 50 | 50 | 0 | 0 | 0 | 0 | 0 | 0 |
| | Spring | 25 | 0 | 0 | 0 | 12.5 | 12.5 | 12.5 | 12.5 | 0 | 0 | 0 | 0 | 12.5 |
| | Summer | 0 | 0 | 0 | 0 | 0 | 0 | 0 | 0 | 0 | 0 | 0 | 0 | 0 |
| | Autumn | 0 | 0 | 0 | 0 | 12.5 | 100 | 87.5 | 0 | 0 | 0 | 0 | 0 | 0 |
| EA/WR | Winter | 0 | 0 | 0 | 0 | 12.5 | 12.5 | 0 | 0 | 0 | 0 | 0 | 0 | 0 |
| | Spring | 0 | 0 | 0 | 0 | 12.5 | 0 | 0 | 12.5 | 0 | 0 | 50 | 50 | 0 |
| | Summer | 0 | 0 | 0 | 0 | 12.5 | 0 | 0 | 0 | 12.5 | 37.5 | 12.5 | 0 | 0 |
| | Autumn | 0 | 0 | 0 | 0 | 0 | 0 | 0 | 0 | 0 | 0 | 0 | 0 | 0 |
| NAO | Winter | 0 | 0 | 0 | 0 | 0 | 0 | 0 | 0 | 0 | 0 | 0 | 0 | 0 |
| | Spring | 0 | 0 | 25 | 0 | 0 | 12.5 | 0 | 0 | 0 | 0 | 0 | 25 | 25 |
| | Summer | 0 | 0 | 0 | 0 | 0 | 0 | 0 | 0 | 0 | 0 | 0 | 0 | 0 |
| | Autumn | 0 | 0 | 0 | 0 | 0 | 0 | 0 | 0 | 0 | 0 | 0 | 0 | 0 |
| POL | Winter | 0 | 0 | 12.5 | 0 | 0 | 0 | 12.5 | 0 | 0 | 0 | 0 | 0 | 0 |
| | Spring | 0 | 0 | 0 | 0 | 37.5 | 12.5 | 0 | 0 | 12.5 | 12.5 | 0 | 37.5 | 0 |
| | Summer | 0 | 0 | 0 | 0 | 12.5 | 0 | 0 | 0 | 0 | 0 | 0 | 0 | 0 |
| | Autumn | 0 | 12.5 | 0 | 12.5 | 0 | 0 | 0 | 0 | 0 | 25 | 0 | 0 | 0 |
| SCAND | Winter | 0 | 0 | 12.5 | 0 | 0 | 0 | 0 | 0 | 0 | 0 | 0 | 0 | 0 |
| | Spring | 37.5 | 0 | 0 | 0 | 0 | 0 | 0 | 0 | 0 | 0 | 0 | 0 | 37.5 |
| | Summer | 37.5 | 0 | 0 | 0 | 0 | 0 | 0 | 0 | 0 | 0 | 0 | 0 | 0 |
| | Autumn | 0 | 0 | 0 | 0 | 0 | 12.5 | 0 | 0 | 0 | 0 | 0 | 12.5 | 0 |

Maps for winter (9.5a), spring (9.5b), summer (9.5c) and autumn (9.5d) illustrate the negative connection of the teleconnection indices with seasonal temperature series for stations in northeast Turkey. For winter and spring, a spatially coherent pattern can be discerned for all stations with a significant negative relationship to the NAO (DJFM) and EA (FMA), respectively. In summer (JJA), a significant positive relationship with the EA/WR atmospheric anomaly pattern exist and temperature increases during positive phases of EA/WR for almost the entire region apart from Pazar and Tortum stations. Autumn (SON) temperatures for the EBS (ÇRB) stations have a statistically insignificant relationship with the EA atmospheric anomaly pattern.

Temperature variability over northeast Turkey is largely linked to oscillations in Northern Hemisphere indices. These large-scale dynamics have a significant impact on temperature, almost all year around, with a strong winter-spring dominated teleconnection. These results show that EA is a dominant atmospheric anomaly pattern on temperature regime. The negative correlation between EA indices and temperature series may indicate that during the positive phases of the EA northeasterly circulation increases, thus significantly colder signals dominate over the northeast Turkey. In contrary, during the negative phases of the EA, southwesterly circulation prevails and warmer signals over the region appear. Thus it seems that the EA can be assessed as good indicators of temperature variability for this region.

9.5.2. Relationship between the teleconnection indices and precipitation

Seasonal precipitation series for northeast Turkey have positive correlations with the EA and EA/WR atmospheric anomaly patterns during winter (Table 9.5b), while the spring precipitation series produce a negative correlation with NAO indices. No evident and/or

strong relationship can be detected for summer and autumn; however, NAO (EA) for JAS appears to have a positive (negative) influence on autumn precipitation for northeast Turkey. The DJF and DJFM periods for the EA atmospheric anomaly patterns appear to influence winter precipitation (40%), but the influence of the EA/WR atmospheric anomaly pattern for JFM and MAM for winter precipitation are much higher (60%). In contrast to the temperature datasets, the East Atlantic-derived atmospheric anomaly patterns do not appear to have a dominant impact on spring precipitation. Spring precipitation is negatively correlated with NAO (for FMA and MAM) and POL (DJFM) anomalies. Autumn (JAS) temperature series are positively (negatively) correlated with NAO (EA) patterns. Overall, the precipitation regime for northeast Turkey does not appear to be well-correlated with large-scale atmospheric indices; and detected links are relatively weak compared to associations between temperature and atmospheric anomaly patterns.

The inter-annual variability of winter and spring standardised precipitation (Figure 9.5) and their relationship with the EA/WR and POL atmospheric anomaly patterns are illustrated by Rize station located in the EBS Basin (summer and autumn series are not presented due the lack of coherent link to the atmospheric indices). Figure 9.6a shows for Rize a positive relationship between winter (JFM) precipitation and the EA/WR atmospheric anomaly pattern. The strong (weak) years of EA/WR anomalies is associated with high (low) [wet (dry)] winter precipitation totals for Rize (Figure 9.6a). However, the correlation is characterised by marked fluctuations for the observation period and, in particular, over the last 5 years. Spring precipitation for Rize exhibits a negative correlation for an extended winter period (DJFM) for the POL atmospheric anomaly pattern. High (low) POL phases are associated with normal than drier (wetter) conditions for this station. Two important negative POL anomaly episodes can be identified: 1980-1988 and 1997-2002; these periods are

characterised by high precipitation totals in spring (Figure 9.5b).

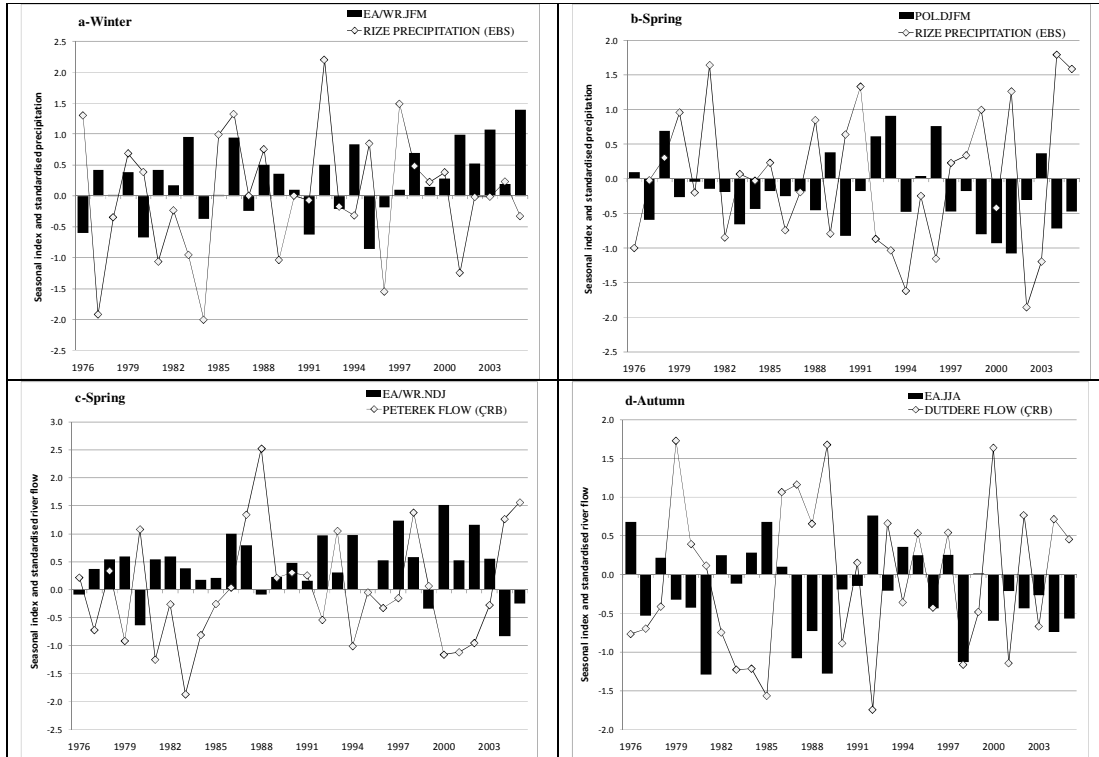


Figure 9.6 Year by year departures in standardised index values and river flow series at selected stations showing the correlation between seasonal precipitation-river flow and EA/WR, EA and POL patterns.

The spatial variability of positive correlation between the EA/WR atmospheric anomaly pattern and winter (JFM) precipitation series for northeast Turkey, show a spatially coherent (60% significant) pattern, represented mainly by coastal stations of the EBS Basin (Figure 9.7a). In comparison, the spring precipitation series have a general negative significant association with the NAO (FMA; Figure 9.6b) and POL (DJFM; Figure 9.7c) indices are also mostly significant for the coastal stations of the EBS Basin. Similar to the dominant correlation pattern for spring, autumn precipitation series of the EBS Basin, have significant negative link to EA (JAS) pattern. More continental stations of the ÇRB, only Tortum shows a strong response to large-scale variations (Figure 9.7a, 9.7b and 9.7d).

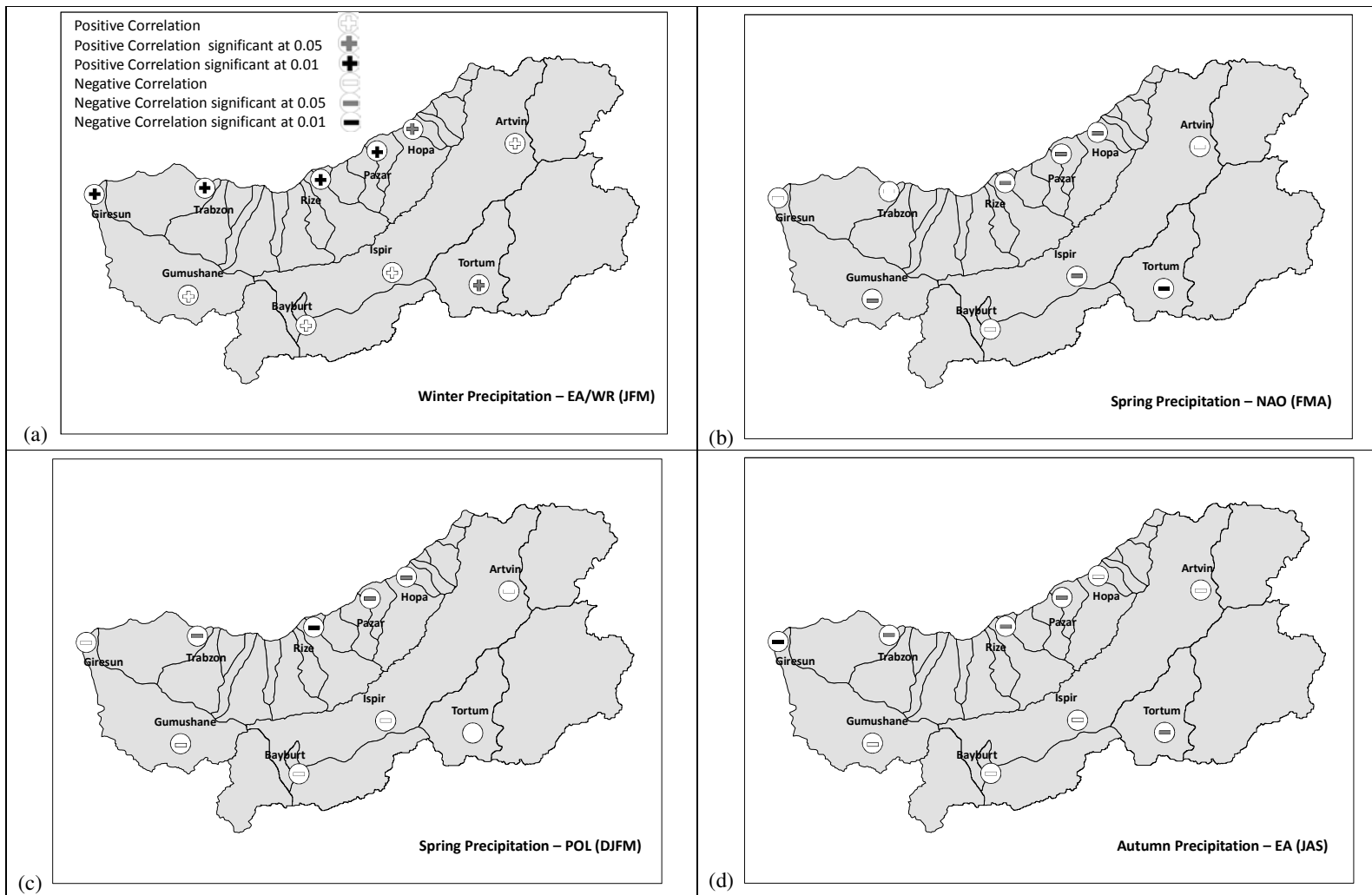


Figure 9.7 Associations between seasonal precipitation and various large-scale atmospheric patterns.

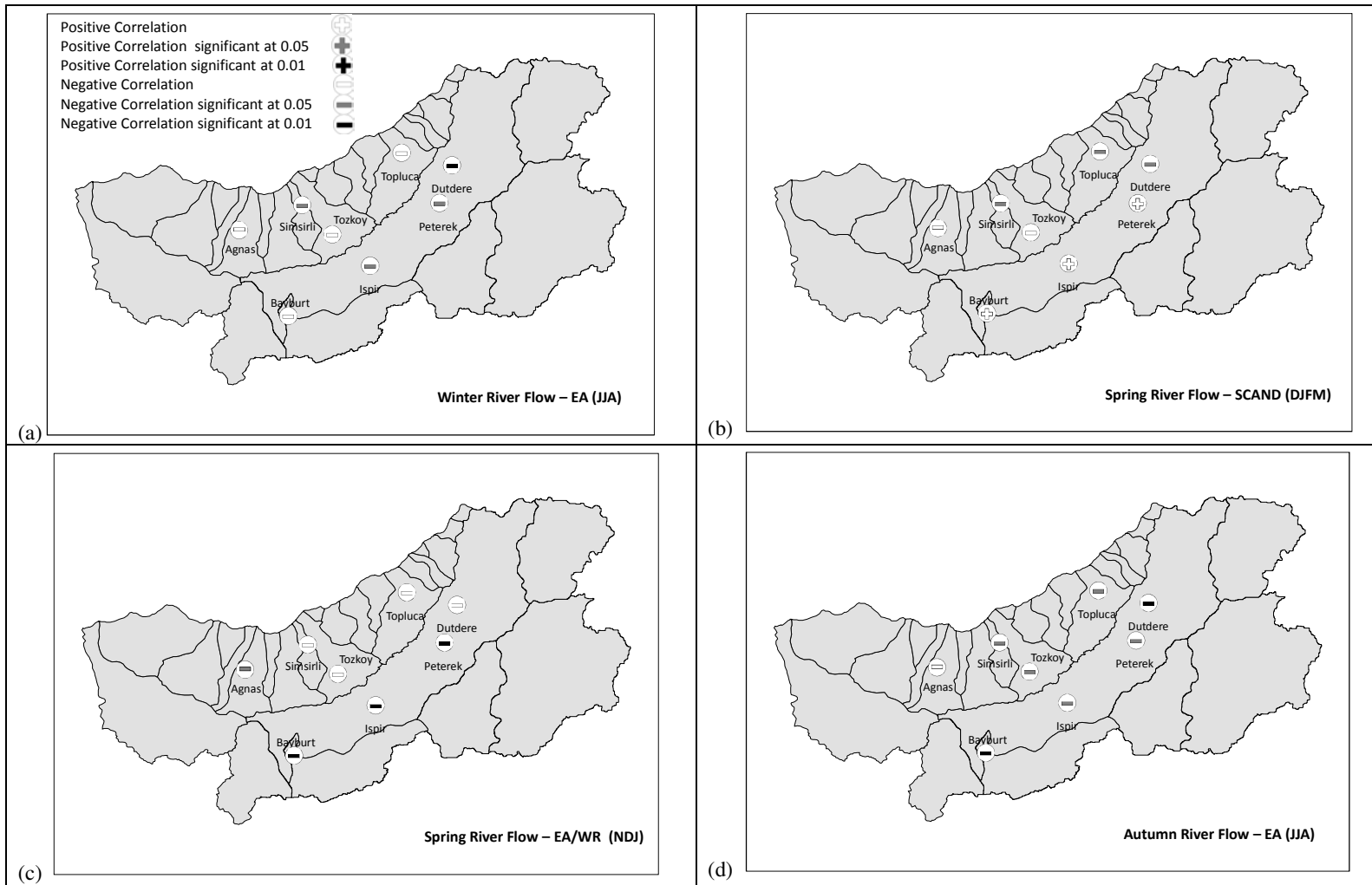


Figure 9.8 Associations between seasonal river flow and various large-scale atmospheric patterns.

It is clear that the Çoruh Basin is not as well connected to large-scale (teleconnection) atmospheric anomaly patterns as the EBS Basin, probably due mainly to its more interior geographical location that yields a stable (continental) local climate regime. Conversely, the precipitation regime for the EBS Basin is influenced by these teleconnection patterns, especially during winter and spring. The east-west trending Black Sea mountain range produces orographic uplift and serves intensify the influence of large-scale driving mechanisms.

9.5.3. Relationship between teleconnection indices and river flow

River flow variability in northeast Turkey does not appear to have any major associations with atmospheric teleconnections (Table 9.c). EA, EA/WR and SCAND atmospheric anomaly indices appear to have some significant negative influence on winter, spring and autumn river flow conditions. Spring river flow (which also represents the maximum period for river flow for northeast Turkey) is the most affected season by atmospheric teleconnection patterns. The EA/WR (for OND and NDJ) has a negative association with spring river flow (Table 9.4c). Spring river flow is also associated with the changes in EA (DJF) and SCAND (DFJ and DJFM) anomalies with 25% and 38% significance. Winter river flow also has a negative relationship (50% significance) with EA for MJJ and JJA seasons. Autumn river flow is also strongly negatively associated with EA (MJJ and JJA) patterns, which has the highest proportion of significant results among all the important teleconnection indices.

Spring and autumn, year-to-year river flow variability for Peterek and Dutdere (located in the ÇRB) are illustrated on Figure 9.6c and 9.6d, respectively. A negative correlation to EA/WR (NDJ) and EA (JJA) is evident for both spring and autumn river flow. A robust relationship can be detected insofar as lower (higher) than normal river flow amounts are related with

positive (negative) phases of the EA and EA/WR atmospheric anomaly patterns. For spring, the EA/WR (NDJ) pattern influences the spring river flow variability of Peterek station (Figure 9.6c). The indices belong to November -January period of EA/WR and NAO indices have more influence on seasonal river flow patterns. The negative relationship between river flow series and NDJ anomalies imply that, in the case of strong (weak) NDJ episodes, spring river flow decreases (increases) (Figure 9.6c). The same observation also applies for autumn river flows for Dutedere. For JJA, a positive (negative) pattern for the EA is linked with minimum (maximum) river flow records over the observational period (Figure 9.6d).

Of particular note, significant correlations are mostly found for river flows for the ÇRB. Figure 9.8 shows the spatial variability for winter (8a), spring (8b and 8c) and autumn (8d) river flow with various Northern Hemisphere teleconnection indices. A spatially significant correlation pattern can be observed for winter river flows for inland stations (and also for Şimşirli in the EBS Basin), where a negative association with EA for JJA is evident (Figure 9.8a). An extended winter anomaly pattern for the SCAND atmospheric anomaly pattern is also evident for spring river flow, especially for the EBS Basin (Figure 9.8b). The spring river flow series of the EBS Basin stations together with Dutedere (in the ÇRB) exhibit a significant negative correlation to the SCAND (DJFM) pattern (Figure 9.8b). In addition to this, the EA/WR atmospheric anomaly pattern for NDJ appears to have a spatially consistent negative impact on spring river flow; this association is highly significant for inland stations (and also for Ağnas station in the EBS Basin) (Figure 9.8c). The connection between autumn river flow and the EA atmospheric anomaly pattern for JJA represents the most important and widespread significant negative correlation obtained for river flow analysis, where a strong negative correlation pattern can be detected over the entire region except for Ağnas station (Figure 9.8d). The weather conditions (more specifically temperature and evaporation) caused

by the EA anomaly pattern during summer, may produce some kind of effect on autumn river flow; however, it appears a complicated relationship to explain based only correlation analysis results.

The detected links between river flows and teleconnection indices demonstrate that the role of large-scale atmospheric patterns is not as evident nor as strong as for temperature and precipitation, and links only prevails for specific seasons. Instead, local factors (topography, climate, marine effect and etc.) seem to be more influential for river flow.

9.6. Conclusions

This chapter highlights the influence that large-scale atmospheric drivers have on surface hydroclimatological processes in northeast Turkey by examining the year-to-year variability and spatial patterning. Results suggest that the EA, EA/WR and NAO are the most persistent large-scale atmospheric anomaly patterns that influence regional climate in northeast Turkey.

The strong negative correlation between seasonal temperature series for northeast Turkey and the EA atmospheric anomaly pattern especially during winter was revealed. Temperature series, particularly in winter, were detected being cooler (warmer) than normal temperatures during the positive (negative) phase for the EA anomaly pattern. For EA/WR pattern, anomalies for JJA appear to govern as a primary mode for summer temperature variability throughout the region whereby positive (negative) phases are associated with warmer (cooler) than normal summer temperatures. Spatiotemporal variability of temperature over northeast Turkey is largely linked with the oscillations in Northern Hemisphere indices.

Winter precipitation is positively associated with the EA (DJF and DJFM) and the EA/WR (JFM and MAM) atmospheric anomaly patterns, while spring precipitation is negatively correlated with the NAO (FMA and MAM) and POL (DJFM) atmospheric anomaly patterns anomalies. The strong (weak) years of the EA/WR and EA anomalies contributes to high (low) winter precipitation totals of coastal stations. High (low) phases of POL (DJFM) and NAO (FMA) determine normal than drier (wetter) conditions spring precipitation of EBS stations.

River flow variability in northeast Turkey does not produce any important associations with atmospheric anomaly patterns EA/WR and SCAND patterns have important negative impacts on spring river flow. Winter river flow has a negative relationship (50% significance) with EA (MJJ and JJA) patterns, while autumn river flow is also negatively associated with these patterns and has the highest proportion of significance for river flow analysis. A negative relationship can also be detected whereby lower (higher) than normal river flow amounts are related with strong (weak) phases of defined atmospheric patterns. River flow variability is controlled by temperature, precipitation (rainfall and snowfall) and evaporation patterns for a basin, which have their own physical characteristics. These complex hydrological interactions may explain why connections are weaker than for station climate data.

Results of correlation tests clearly reveal that temperature variability across northeast Turkey is closely linked to the large-scale climatic drivers and the significant results exhibit a spatially coherent pattern. Seasonal precipitation and river flow patterns appear to show some relationships with the teleconnection patterns, especially for winter and spring, but the relationship is not spatially consistent unlike the temperature series. Nevertheless, this study has evaluated the hydroclimatic links to teleconnection patterns of northern hemisphere and

results suggest that the NAO atmospheric anomaly pattern is not the dominant large-scale driver that influences the hydroclimatology of this region, contrary to the situation in the west and southern regions of Turkey. As mentioned in Introduction of this chapter, the influence of Northern Hemisphere indices (except the NAO) have not been studied; therefore, this research provides the first analysis of these hydroclimatological links for this region. However, results of analyses for both preceding and concurrent analysis of seasonal EA and EA/WR atmospheric anomaly patterns have showed conclusively that a significant influence on temperature for most months of the year. The influence of the EA and EA/WR atmospheric anomaly patterns on precipitation and river flow variability is most evident at more seasonal scales. The complexity and inconsistency in the hydroclimatic variability seen for the two river basins in northeast Turkey is mainly related to the highly distinctive physiographic characteristics of the region. This physical backdrop makes it difficult to fully identify the role of large-scale circulation on the precipitation and river flow processes, which are highly dependent on regional climate than large-scale atmospheric dynamics.

9.7. Chapter summary

In this chapter, the relationship between teleconnection patterns from the Atlantic-Eurasian region and surface hydroclimatic components (i.e. monthly and seasonal temperature, precipitation and river flow series) over northeast Turkey were quantified and the regional and/or basin scale behaviour to atmospheric oscillations were established. This chapter completes this thesis's multi-scale analysis of hydroclimatological process over northeast Turkey: large-scale atmospheric circulation to regional climate to local factors. The final chapter (Chapter 10) concludes this thesis by drawing together the key findings and proposing areas for further research.

10. SYNTHESIS AND FURTHER RESEARCH

This concluding chapter summarises the major findings of the research undertaken and links these to the original research objectives (Section 1.2 and Figure 3.1) and assesses how the objectives were achieved. The implication of the research for water resources is also evaluated; and recommendations for further research are advanced.

10.1. Key conclusions

The major findings of this research are:

- 1- **Precipitation regimes of Turkey:** Turkish annual precipitation regimes were analysed in Chapter 4 to provide a large-scale (national) perspective and to redefine precipitation regions. A composite (shape and magnitude) regime classification reveals the dominant controls on the spatial variability of precipitation. The classification methodology used was shown to be a powerful tool that identifies the physically-interpretable precipitation regions: (i) coastal regimes for Marmara, coastal Aegean, Mediterranean and Black Sea; (ii) transitional regimes in continental Aegean and Southeast Anatolia; and (iii) inland regimes across central and Eastern Anatolia. This is a significant advance which refines and extends the existing classifications of Turkish precipitation climatology. The emergent regime classes yield the most detailed and systematic joint analyses of spatial variation in magnitude and timing of precipitation across Turkey to date. This chapter has been published in Hydrological Sciences Journal (Appendix I).
- 2- **Precipitation extremes of Turkey:** Extreme precipitation characteristics of

Turkey were investigated in Chapter 5 and found that the coastal regions of Turkey are characterised by having the highest frequency of extreme precipitation events and also the highest precipitation amount(s) of daily precipitation records. Southwest and northeast Turkey, in particular, were found to be the two regions that are detected as having the highest extreme precipitation occurrence. Significant increasing trends were observed for the high precipitation (P75) series for northwest Turkey and central Anatolia. Crucially, these important results demonstrate differential patterns of variability between mean precipitation and extreme precipitation.

3- Climate regimes of northeast Turkey: Climate regime analyses (Chapter 6) identified four climatic regime types for northeast Turkey region: (i) inland regime (May rainfall peak, cool temperature regime); (ii) transition regime (December rainfall peak, moderately warm temperature regime); (iii) western coastal regime (WCR) and (iv) eastern coastal regime (ECR). The western and eastern coastal regimes belong to the East Black Sea Basin area and are characterised by October rainfall peaks with very wet and extremely wet precipitation regimes respectively, and the warmest temperature regime with high annual averages. The data also highlighted a shift towards a warmer temperature regime.

4- Flow regimes of northeast Turkey: Chapter 7 provided the first basin-scale research on river flow regimes of northeast Turkey by classifying stations (based upon long-term average values) to examine annual regimes and spatial patterns and to identify regime stability (between-year) for detecting temporal variability of regimes. Two major flow regime regions were defined (Chapter 7): namely the mountainous area of the north-northeast EBS Basin (May-June Peak) and the rest of the study area, which comprises the majority of the Çoruh River basin (April-May). MLR analyses indicate that precipitation is the most pronounced climatic driver affecting river flow variability. Intra-annual

variability in the timing of river flow (i.e. regime shape) over northeast Turkey is controlled mainly by the regional climatic variability. A spring rainfall maximum together with the contribution of snowmelt generates high river flow amounts for the Çoruh River basin. The May-June river flow peak in the EBS basin appears to be linked to delayed snowmelt.

5- Hydroclimatic extremes of northeast Turkey: A clear inland-coastal distinction is apparent for hydroclimatic extremes (Chapter 8). Significant trends have been detected in low and high precipitation and river flow percentiles. Together with the changes in temperature indices (especially warm and summer days), the changing pattern in river flow extremes suggest an increasing probability of severe climatic and hydrological conditions for northeast Turkey. Regional precipitation and temperatures for the period spanning September to May (autumn, winter and spring) have an important influence on river flow extremes. High precipitation equates with high river flow, while high temperature episodes cause to low flow periods.

6- Teleconnections and hydroclimatology of northeast Turkey: Temperature variability across northeast Turkey is closely linked to seasonal indices of EA, EA/WR and NAO teleconnection patterns, especially during winter (Chapter 9) and the significant results demonstrate a spatially coherent pattern across the region. However, seasonal precipitation and river flow patterns do not exhibit persistent relationships with these teleconnection patterns and the relationship is not spatially consistent as for temperature. Preliminary result of this chapter has subsequently been published in IAHS Red Book (Appendix II).

Systematic analysis of precipitation, temperature and river flow interactions for two major basins in the under-researched Northeast Turkey (East Black Sea and Çoruh River basins) was

the main aim of this study. This thesis has met this aim and, thus, provided comprehensive outcomes and improved understanding of the hydroclimatological process and dynamics of northeast Turkey.

10.2. Implications

This study has produced results that are of practical important on national as well as more regional and local scales. It has refined and increased the knowledge and understanding on the spatial structure of precipitation regimes and extreme variability over Turkey. These results have important societal and environmental applications for the assessment and prediction of water resources, particularly given the growing population and economic development of Turkey. The observed trends in precipitation extremes demonstrate an increasing in the number of heavy precipitation events and, thus, higher probability for intense events and a lower value of average precipitation, which were obtained from climate projections for the Mediterranean Basin (Giorgi and Lionello, 2008). The results of precipitation analyses presented in this thesis provide evidence to support an increased frequency and intensity of hydro-meteorological hazards in Turkey (Ceylan and Kömüştü, 2007).

The climate regime analysis has allowed more detailed understanding of the present-day climatology of northeast Turkey and constitutes a basis for the interpretation of results of river flow studies. River flow analyses have improved the understanding of the hydroclimatological processes operating over northeast Turkey as well as the water resources base. Moreover, given present concerns about future climatic variability, the long-period (average) and year-to-year variability in river flows (together with regional climate) provides crucial data for the assessment of future water resource stress. However, the links between regional hydroclimatology and large-scale dynamics do not display a consistent relationship as a result

of the extreme physical conditions that act to modify atmospheric drivers. Crucially, this study has demonstrated the strong increasing trend in temperatures across the region which undoubtedly will accelerate both glacier and snow melt, which will in turn have concomitant effects on river flow regimes and their variability.

10.3. Recommendations for further research

For northeast Turkey in particular, the physical geography produces microclimates which makes it especially difficult to identify fully the role of the regional climate on the hydroclimatic processes. The surface measurements for highlands of EBS and Çoruh River basins are not adequate such a large region like northeast Turkey.

Crucially, to gain a clear understanding on the altitudinal changes of climatic and hydrologic variables then there is a pressing need to expand the [spatial distribution] of monitoring stations within northeast Turkey, to improve data generation for ungauged rivers and/or basins. Furthermore, there is also a pressing need for an increase in the spatial distribution of meteorological weather stations at a range of elevations so that synoptic weather conditions over northeast Turkey can be established in greater detail.

This region has been affected from both a range of natural and anthropogenic changes as a result of different factors and mechanisms acting at various intensities through time. This mountainous region with extant glaciers is required systematic observations on meteorological and glacial conditions for detecting rate and/or speed of change and influences on river ecosystems.

For Turkey, explaining the links between extreme precipitation events and weather types may

help to explain the atmospheric reason behind the extreme events. Enhancing the knowledge about the extreme precipitation events will contribute to a better prediction of the possible consequences of future climate change.

The present use and future planning of water resources is vital for securing the sustainability of ecological, hydrological and social systems and must be based on scientific research rather than short term economic goals. More detailed basin-scale research must be undertaken to observe response of river ecosystems to the hydroclimatic variability. It is critical to establish the links between climate, hydrology and ecology in this diverse region. Ignoring the highly dynamic character of this region and continuing the largely unregulated use of natural resources will inevitably cause several environmental problems and severe hazards with irreversible consequences.

Findings can be utilized as a significant regional knowledge by local authorities, associations and Departments for Agriculture, National Parks, DSI, EIE and Disaster and Emergency Management. Detected large-scale (atmospheric) and regional-scale (climatic) links to the hydroclimatic variability pattern may contribute to the decision-making studies of these institutions. River flow regime information (timing, magnitude, peak time and duration of river flows) may contribute to the managing potable water resources and some economic sectors such as agriculture, fresh water fishing, tourism (recreation) and energy (*cf.* Poff *et al.*, (1997); Middelkoop *et al.*, (2001); Nilsson & Malm Renöfält (2008)). The calculated threshold values can be evaluated in hazard management and control studies.

APPENDIX I

Spatial variability of precipitation regimes over Turkey

1 *School of Geography, Earth and Environmental Sciences, University of Birmingham, Edgbaston, Birmingham B15 2TT, UK*

fxs720@bham.ac.uk

2 *Department of Geography, Faculty of Sciences and Arts, Çanakkale Onsekiz Mart University, Çanakkale 17020, Turkey*

Citation Sariş, F., Hannah, D. M. & Eastwood, W. J. (2010) Spatial variability of precipitation regimes over Turkey. *Hydrol. Sci. J.* **55**(2), 234-249

Abstract Turkish annual precipitation regimes are analysed to provide large-scale perspective and redefine precipitation regions. Monthly total precipitation data are employed for 107 stations (1963–2002). Precipitation regime shape (seasonality) and magnitude (size) are classified using a novel multivariate methodology. Six shape and five magnitude classes are identified, which exhibit clear spatial structure. A composite (shape and magnitude) regime classification reveals dominant controls on spatial variability of precipitation. Intra-annual timing and magnitude of precipitation is highly variable due to seasonal shifts in Polar and Subtropical zones and physiographic factors. Nonetheless, the classification methodology is shown to be a powerful tool that identifies physically-interpretable precipitation regions: (1) coastal regimes for Marmara, coastal Aegean, Mediterranean and Black Sea; (2) transitional regimes in continental Aegean and Southeast Anatolia; and (3) inland regimes across central and Eastern Anatolia. This research has practical implications for understanding water resources, which are under ever growing pressure in Turkey.

Key words precipitation climatology; rainfall; regimes; regionalization; classification; Turkey

Hydrological Sciences Journal is available online at: www.tandfonline.com

URL of Published Version: <http://dx.doi.org/10.1080/02626660903546142>

Identification Number/DOI: 10.1080/02626660903546142

APPENDIX II

Changes in precipitation and river flow in northeast Turkey: associations with the North Atlantic Oscillation

FAIZE SARIŞ^{1,2}, DAVID M. HANNAH¹ & WARREN J. EASTWOOD¹

¹*School of Geography, Earth and Environmental Sciences, University of Birmingham, Edgbaston, Birmingham B15 2TT, UK*
fxs720@bham.ac.uk

²*Department of Geography, Faculty of Sciences and Arts, Çanakkale Onsekiz Mart University, Çanakkale 17020, Turkey*

Abstract This paper explores the relationships between the North Atlantic Oscillation (NAO) index and precipitation and river flow over northeast Turkey. Precipitation totals and maximum, mean and minimum river flow are analysed at the seasonal scale for 12 and 10 stations, respectively. Pearson's and Mann-Kendall correlation tests are applied to assess relationships between the NAO index and precipitation and river flow metrics, and to detect trends in time-series. Autumn precipitation totals display significant increasing trends, especially for coastal stations, while inland stations show significant increasing trends for spring precipitation. Minimum and maximum river flow decreases significantly for spring and summer. This tendency implies varying conditions towards a drier regime. Seasonal precipitation patterns show a negative association with the NAO for December–January–February (DJF), March–April–May (MAM) and September–October–November (SON) for some stations. Positive associations between the NAO and winter-extended winter (December–March) river flows are detected for some stations in northeast Turkey.

Key words rainfall; runoff; time-series; trends; hydroclimatology; NAO; northeast Turkey

Global Change: Facing Risks and Threats to Water Resources (Proc. of the Sixth World FRIEND Conference, Fez, Morocco, October 2010). IAHS Publ. 340, 2010.

URL of Published Version: http://iahs.info/redbooks/a340/abs_340_0568.pdf

APPENDIX III

East Black Sea Basin



Photograph 1. 2218- Şimşirli station (İyidere River)



Photograph 2. 2218- Şimşirli station (İyidere River)



Photograph 3. Şimşirli River



Photograph 4. Tozköy River



Photograph 5. Tozköy River



Photograph 6. 2233- Tozköy station (Tozköy River)



Photograph 7. 2232- Topluca station (Firtına River)



Photograph 8. Firtina River



Photograph 9. Firtina River



Photograph 10. 2240- Eymür station (Harşit River)



Photograph 11. Harşit River



Photograph 12. 2272- Arili station (Arili River)



Photograph 13. Arili River



Photograph 14. 2240- Eymür station (Harşit River)



Photograph 15. 2271- Arili station (Arili River)



Photograph 16. Arili River

APPENDIX IV

Çoruh River Basin



Photograph 17. 2304- Bayburt station (Çoruh River)



Photograph 18. Çoruh River



Photograph 19. Çoruh River



Photograph 20. 2305- Peterek station (Çoruh River)



Photograph 21. 2305-Peterek station (Çoruh River)



Photograph 22. 2316 Ispir Statiton (Çoruh River)



Photograph 23. Çoruh River



Photograph 24. 2321 Duttdere Station (Barhal River)



Photograph 25. Ispir (Bridge) Station (Çoruh River)



Photograph 26. 2321 Dutturdere Station (Barhal River)



Photograph 27. 2323 Işhan Station (Oltu River)



Photograph 28. 2323 Işhan Station (Oltu River)



Photograph 29. 2328 Ferhatlı Station (Ardanuç River)



Photograph 30. 2328 Ferhatlı Station (Ardanuç River)



Photograph 31. Ardanuç River



Photograph 32. Çamlıkaya River



Photograph 33. Çamlıkaya River



Photograph 34. Çamlıkaya Station
(Çamlıkaya River)

LIST OF REFERENCES

- Akçar, N., Yavuz, V., Ivy-Ochs, S., Kubik, P. W., Vardar, M. & Schlüchter, C. (2007) Palaeoglacial records from Kavron Valley, NE Turkey: Field and cosmogenic exposure dating evidence. *Quaternary International*, 164-65: 170–183.
- Akkemik, Ü., D'Arrigo, R., Cherubini, P., Köse, N., Jacoby, G. C. (2008) Tree-ring reconstructions of precipitation and streamflow for north-western Turkey. *International Journal of Climatology*, 28 (2): 173-183.
- Akpınar, A., Komurcu, M.I., Kankal, M. & Filiz, M.H. (2009) Çoruh Havzasi'ndeki küçük hidroelektrik santrallerin durumu (*The situation of small hydroelectric power plants in Çoruh Basin*). Yenilenebilir Enerji Kaynakları Sempozyumu Bildiriler Kitabı. Diyarbakir, Turkey (In Turkish).
- Akpınar, A., Komurcu, M.I. & (2011) Development of hydropower energy in Turkey: The case of Çoruh river basin. *Renewable and Sustainable Energy Reviews*, 15: 1201–1209.
- Aksoy, H., Kaynar, L., Ünal, N. E. (2006) Structural characteristics of maximum flows in the Eastern Black Sea region, Turkey. In AMHY-FRIEND Group International Workshop on Hydrological Extremes “Observing and modelling exceptional floods and rainfalls” Rende (CS), 3 - 4 May 2006.
- Aksoy, H., Ünal, N. E., Alexandrov, V., Dakovab, S. & Yoonc, J. (2007) Hydrometeorological analysis of northwestern Turkey with links to climate change. *International Journal of Climatology*, 28(8):1047-1060.
- Alexander, L. V., Zhang, X., Peterson, T. C., Caesar, J., Gleason, B., Tank, M. Haylock, A., Collins, D., Trewin, B., Rahimzadeh, F., Tagipour, A., Kumar, K. R., Revadekar, J., Griffiths, G., Vincent, L., Stephenson, D. B., Burn, J., Aguilar, E., Brunet, M., Taylor, M., New, M., Zhai, P., Rusticucci, M. & Vazquez-Aguirre, J. L. (2006) Global observed changes in daily climate extremes of temperature and precipitation. *Journal of Geophysical Research-Atmospheres* 111 (5): 10.1029/2005JD006290.
- Alexandrov, V., Genev, M. & Aksoy, H. (2005) The impact of climate variability and change on water resources in the western coastal zone of the Black sea. *IAHS Publications*, 295: 62-71.
- Apak, G. & Ubay, B. (2007) First National Communication of Turkey on Climate Change. (Editors) the Ministry of environment and Forestry, Ankara.
- Atalay, I. & Mortan K. (2003) Türkiye Bölgesel Coğrafyası (*Regional Geography of Turkey*). İnkilap Kitabevi, Ankara (In Turkish).
- Aydinalp, C. & FitzPatrick, E.A. (2004) Classification of great soil groups in the east Black sea basin according to international soil classification systems, *Journal of Central European Agriculture*, 5(2): 119-126.
- Barnston, A. G. & Livezey, R. E. (1987) Classification, seasonality and persistence of low-frequency atmospheric circulation patterns. *Monthly Weather Review*, 115:1083-1126.
- Bartholy, J. & Pongrácz, R. (2007) Regional analysis of extreme temperature and precipitation indices for from 1946 to 2001. *Global and Planetary Change*, 57: 83-95.
- Berkun, M. (2010) Environmental evaluation of Turkey's transboundary rivers' hydropower systems. *Canadian Journal of Civil Engineering*, 37(5): 684-694.
- Belir Baykal, B., Tanık, A. & Gönenç, I. E. (2000) Water quality in the drinking water reservoirs of a megacity, Istanbul. *Environmental Management*, 26: 607–614.

- Bolle, H. J. (2002) Climate, Climate Variability and Impacts in the Mediterranean Area: An Overview (Editor). In Mediterranean Climate, Springer Verlag, Berlin.
- Bower, D. & Hannah, D. M. (2002) Spatial and temporal variability of UK river flow regimes. In Friend 2002-Regional Hydrology: Bridging the Gap between Research and Practice, 457-464.
- Bower, D. (2004) Western European climate and river flow regimes. PhD thesis, University of Birmingham, UK.
- Bower, D., Hannah, D. M. & McGregor, G. R. (2004) Techniques for assessing the climatic sensitivity of river flow regimes. Hydrological Processes, 18: 2515-2543.
- Brunetti, M., Buffoni, L., Mangianti, F., Maugeri, M. & Nanni, T. (2004) Temperature, precipitation and extreme events during the last century in Italy. Global and Planetary Change, 40: 141-149.
- Brunetti, M., Maugeri, M. & Nanni, T. (2001) Changes in total precipitation, rainy days and extreme events in northeastern Italy. International Journal of Climatology, 21: 861-871.
- Burn, D. H. & Elnur, M. A. H. (2002) Detection of hydrologic trends and variability. Journal of Hydrology, 255: 107-122.
- Ceylan A., & Kömüşçü, A. Ü. (2007a) Meteorolojik Karakterli Doğal Afetlerin Uzun Yıllar ve Mevsimsel Dağılımları (*Long-term and seasonal distributions of natural hazards in meteorological origin*). I. Türkiye İklim Değişikliği Kongresi Bildiriler Kitabı: 93-104. Istanbul, Turkey, (In Turkish).
- Ceylan A., Alan, I. & Ugurlu, A. (2007b) Causes and Effects of Flood Hazards in Turkey. In International Congress of River Basin Management, 22-24 March 2007, Gloria Golf Resort Hotel, Antalya-Turkey.
- Çiçek, İ., Türkoğlu, N., Ceylan, A. & Korkmaz, N. (2006) Seasonal Rainfall Intensity and Frequency in Turkey. In Proceedings Book of Conference on Water Observation and Information System for Decision Support, Ohrid, Republic of Macedonia, 23-26 May 2006.
- Cigizoglu, H. K., Bayazit, M. & Onoz, B. (2005) Trends in the maximum, mean, and low flows of Turkish rivers. Journal of Hydrometeorology, 6: 280-290.
- Climate Change (2007) Impacts, Adaptation and Vulnerability. Contribution of Working Group II to the Fourth Assessment Report of the IPCC (978 0521 88010-7 Hardback; 978 0521 70597-4 Paperback)
- Costa, A. C. & A. Soares (2009) Trends in extreme precipitation indices derived from a daily rainfall database for the South of Portugal. International Journal of Climatology, 29, 1956-1975.
- Cullen, H. M. & deMenocal, P. B. (2000) North Atlantic influence on Tigris-Euphrates streamflow. International Journal of Climatology, 20: 853-863.
- Cullen, H. M., Kaplan, A., Arkin, P. A. & deMenocal P. B. (2002) Impact of the North Atlantic Oscillation on Middle Eastern climate and streamflow. Climatic Change, 55: 315-338.
- Davie, T. (2002) Fundamentals of Hydrology. Routledge, London.
- Dixon, H., Lawler, D. M. & Shamseldin, A. Y. (2006) Streamflow trends in western Britain. Geophysical Research Letters, 33: 10.1029/2006gl027325.
- Douglas, E. M., Vogel, R. M. & Kroll, C.N. (2000) Trends in floods and low flows in the United States: impact of spatial correlation. Journal of Hydrology, 240: 90-105.
- Dunkeloh, A. & Jacobeit, J. (2003) Circulation dynamics of Mediterranean precipitation variability 1948-98. International Journal of Climatology, 23: 1843-1866.

- Easterling, D. R., Evans, J. L., Groisman, P. Y., Karl, T. R., Kunkel, K. E. & Ambenje P. (2000) Observed variability and trends in extreme climate events: A brief review. *Bulletin of the American Meteorological Society*, 81: 417-425.
- Ergünay, O. (2007) Türkiye'nin afet profili (*Hazard profile of Turkey*). TMMOB Afet Sempozyumu (5-7 Aralık 2007) Bildiriler Kitabı, Ankara (In Turkish).
- Fagherazzi, S., Fosser, G., D'Alpaos, L. & D'Odorico, P. (2005) Climatic oscillations influence the flooding of Venice. *Geophysical Research Letters*, 32: 10.1029/2005gl023758.
- Feldstein, S.B. (2000) The timescale, power-spectra, and climate noise properties of teleconnection patterns. *Journal of Climate*, 13: 4430-4440.
- Fischlin A., Midgley, G.F., Price, J.T., Leemans, R., Gopal, B., Turley C., Rounsevell, M.D.A., Dube, O.P., Tarazona, J. & Velichko, A.A. (2007) Ecosystems, their properties, goods, and services. *Climate Change 2007: Impacts, Adaptation and Vulnerability. Contribution of Working Group II to the Fourth Assessment Report of the Intergovernmental Panel on Climate Change*, M.L. Parry, O.F. Canziani, J.P. Palutikof, P.J. van der Linden and C.E. Hanson, Eds., Cambridge University Press, Cambridge, 211-272.
- Fleig, A. K., Tallaksen, L. M., Hisdal, H. & Demuth, S. (2006) A global evaluation of streamflow drought characteristics. *Hydrology and Earth System Sciences*, 10: 535–552.
- Fleming, S.W. (2004) Comparative statistical hydroclimatology of glacial and nival rivers in southwest Yukon and northwest British Columbia Canada. Ph.D Thesis, University of British Columbia, Canada.
- Founda, D. & van Loon, H. (2008) Circulation anomalies associated with winter temperature extremes in Athens during the period 1900-2004. *Meteorologische Zeitschrift*, 17: 55-59.
- Franzke, C. & Feldstein, S. B. (2005) The Continuum and Dynamics of Northern Hemisphere Teleconnection Patterns. *Journal of the Atmospheric Sciences*, 62: 3250-3267.
- Frederick, K. D. & Major, D. C. (1997) Climate change and water resources. *Climatic Change* 37, 7–23.
- Frich, P., Alexander, L. V., Della-Marta, P., Gleason, B., Haylock, M., Tank, A. & Peterson, T. (2002) Observed coherent changes in climatic extremes during the second half of the twentieth century. *Climate Research*, 19: 193-212.
- Garcia-Herrera, R., D. Paredes, R. M. Trigo, I. F. Trigo, E. Hernandez, D. Barriopedro & M. A. Mendes (2007) The outstanding 2004/05 drought in the Iberian Peninsula: Associated atmospheric circulation. *Journal of Hydrometeorology*, 8:483-498.
- Giorgi, F. & Lionello, P. (2008) Climate change projections for the Mediterranean region. *Global and Planetary Change*, 63: 90–104.
- Gokturk, O., Bozkurt, M. D., Sen, O. L., & Karaca, M. (2008) Quality control and homogeneity of Turkish precipitation data. *Hydrological Processes*, 22: 3210-3218.
- Gottschalk, L. (1985) Hydrological regionalization of Sweden. *Hydrological Sciences Journal*, 30(1): 65-83.
- Griffith, D. A. & Amrhein, C. G. (1997) *Multivariate Statistics for Geographers*. Prentice-Hall, New Jersey, USA.
- Groisman, P. Y., Knight, R. W., Easterling, D. R., Karl, T. R., Hegerl, G. C. & Razuvaev, V. A. N. (2005) Trends in intense precipitation in the climate record. *Journal of Climate*, 18: 1326-1350.

- Gustard, A. & Gross R. (1989) Low flow regimes of Northern and Western Europe. In: FRIENDS in Hydrology (A. Gustard and R. Gross (Eds.)). IAHS Press, Wallingford, ISBN: 0-947-57127-2, pp: 516.
- Haines, A. T., Finlayson, B. L. & McMahon, T. A. (1988) A global classification of river regimes. *Applied Geography*, 8(1): 255-272.
- Hannaford, J. & Marsh, T.J. (2008) High-flow and flood trends in a network of undisturbed catchments in the UK. *International Journal of Climatology*, 28(10): 1325-1338.
- Hannah, D. M., Smith, B. P. G., Gurnell, A. M. & McGregor, G. R. (2000) An approach to hydrograph classification. *Hydrological Processes*, 14: 317-338.
- Hannah, D. M., Kansakar, S. R., Gerrard, A. J. & Rees, G. (2005a) Flow regimes of Himalayan rivers of Nepal: their nature and spatial patterns. *Journal of Hydrology*, 308: 18–32.
- Hannah, D. M., Kansakar, S. R. & Gerrard, A. J. (2005b) Identifying potential hydrological impacts of climatic variability and change for Himalayan basins of Nepal. *Regional Hydrological Impacts of Climatic Change - Impact Assessment and Decision Making*, 295, 120-130.
- Hannah, D. M., Brown, L. E., Milner, A. M., Gurnell, A. M., McGregor G. R., Petts, G. E., Smith, B. P. G. & Snook, D. L. (2007a) Integrating climate-hydrology-ecology for alpine river systems. *Aquatic Conservation-Marine and Freshwater Ecosystems*, 17: 636-656.
- Hannah, D. M., Sadler, J. P. & Wood, P. J. (2007b) Hydroecology and ecohydrology: a potential route forward?. *Hydrological Processes*, 21: 3385-3390.
- Harding, A. E. (2006) Changes in Mediterranean climate extremes: patterns, causes, and impacts of change. PhD Thesis, University of East Anglia, Norwich, UK.
- Harris, N. M., Gurnell, A. M., Hannah, D. M. & Petts, G. E. (2000) Classification of river regimes: a context for hydroecology. *Hydrological Processes* 14: 2831–2848.
- Hatzaki, M., Flocas, H. A., Giannakopoulos, C. & Maheras, P. (2009) The Impact of the Eastern Mediterranean Teleconnection Pattern on the Mediterranean Climate. *Journal of Climate*, 22: 977-992.
- Helsel, D.R. & Hirsh, R. M. (2002) Statistical methods in water resources. U.S. Geological Survey, Techniques of Water-Resources Investigations Book 4, 510 pp.
- Hertig, E., Seubert, S. & Jacobeit, J. (2010) Temperature extremes in the Mediterranean area: trends in the past and assessments for the future. *Natural Hazards and Earth System Sciences*, 10: 2039-2050.
- Hirschi, M. & Seneviratne, S. I. (2010) Intra-annual link of spring and autumn precipitation over France. *Climate Dynamics*, 35: 1207-1218.
- Hodgkins G. A., Dudley, R. W. & Huntington, T. G. (2005) Summer low flows in New England during the 20th century. *Journal of the American Water Resources Association*, 41(2): 403-412.
- Houssos, E. E. & Bartzokas, A. (2006) Extreme precipitation events in NW Greece. *Advances in Geosciences*, 7: 91–96.
- <http://climate.geog.udel.edu/~wimp/>. The Web-based, Water-Budget, Interactive, Modeling Program. Centre for Climatic Research, Delaware, USA.
- <http://www.cgd.ucar.edu/cas/jhurrell/indices.html>. The NAO Index Data. The Climate Analysis Section of the NCAR. Boulder, Colorado, USA.
- <http://www.cpc.ncep.noaa.gov/data/teledoc/telecontents.shtml>. Northern Hemisphere Teleconnection Indices. Climate Prediction Center, National Weather Service, USA.

- http://cccma.seos.uvic.ca/ETCCDI/list_27_indices.shtml. ETCCDI/CRD Climate Change Indices.
- Hurrell, J. W. (1995) Decadal trends in the North Atlantic Oscillation: regional temperatures and precipitation. *Science*, 269: 676-679.
- Hurrell, J. W. & VanLoon, H. (1997) Decadal variations in climate associated with the north Atlantic oscillation. *Climatic Change*, 36: 301-326.
- IPCC. (2007) Summary for Policymakers. In: *Climate Change 2007: The Physical Science Basis. Contribution of Working Group I to the Fourth Assessment Report of the Intergovernmental Panel on Climate Change* [Solomon, S., D. Qin, M. Manning, Z. Chen, M. Marquis, K.B. Averyt, M. Tignor and H.L. Miller (eds.)]. Cambridge University Press, Cambridge, United Kingdom and New York, NY, USA.
- Isik, S. & Singh, V. P (2008) Hydrologic regionalization of watersheds in Turkey. *Journal of Hydrologic Engineering*, 13: 824-834.
- Kadioglu, M., Ozturk, N., Erdun, H. & Sen Z. (1999a) On the precipitation climatology of Turkey by harmonic analysis. *International Journal of Climatology*, 19: 1717-1728.
- Kadioglu, M., Tulunay, Y. & Borhan, Y. (1999b) Variability of Turkish precipitation compared to El Niño events. *Geophysical Research Letters*, 26(11): 1597-1600.
- Kadioglu, M. (2000) Regional variability of seasonal precipitation over Turkey. *International Journal of Climatology*, 20: 1743-1760.
- Kadiogullari, A. I. & Baskent, E. Z. (2008) Spatial and temporal dynamics of land use pattern in Eastern Turkey: a case study in Gumushane. *Environmental Monitoring and Assessment*, 138: 289-303.
- Kadiogullari, A. I., Keles, S., Baskent, E. Z. & Gunlu, A. (2008) Spatiotemporal Changes in Landscape Pattern in Response to Afforestation in Northeastern Turkey: A Case Study of Torul. *Scottish Geographical Journal*, 124: 259-273.
- Kahya, E. & M. C. Karabork (2001) The analysis of El Nino and La Nina signals in streamflows of Turkey. *International Journal of Climatology*, 21, 1231-1250.
- Kahya, E. & Kalayci, S. (2004) Trend analysis of streamflow in Turkey. *Journal of Hydrology*, 289: 128-144.
- Kahya, E., Kalayci, S. & Piechota, T. C. (2008a) Streamflow regionalization: Case study of Turkey. *Journal of Hydrologic Engineering*, 13: 205-214.
- Kahya, E., Demirel, M. C. & Beg, O. A. (2008b) Hydrologic Homogeneous Regions Using Monthly Streamflow In Turkey. *Earth Sciences Research Journal*, 12: 181-193.
- Kalayci, S. & Kahya, E. (2006) Assessment of streamflow variability modes in Turkey: 1964-1994. *Journal of Hydrology*, 324: 163-177.
- Kansakar, S.R., Hannah, D. M., Gerrard, A. J. & Rees, G. (2004) Spatial pattern in the precipitation regime of Nepal. *International Journal of Climatology*, 24: 1645-1659.
- Karabork, M. C. & Kahya, E. (2003) The teleconnections between the extreme phases of the southern oscillation and precipitation patterns over Turkey. *International Journal of Climatology*, 23: 1607-1625.
- Karabork, M. C., Kahya, E. & Karaca, M. (2005) The influences of the Southern and North Atlantic Oscillations on climatic surface variables in Turkey. *Hydrological Processes*, 19: 1185-1211.
- Karabork, M. C., Kahya, E. & Komuscu, A. U. (2007) Analysis of Turkish precipitation data: homogeneity and the Southern Oscillation forcings on frequency distributions. *Hydrological Processes*, 21: 3203-3210.

- Karabork, M. C. & Kahya, E. (2009) The links between the categorised Southern Oscillation indicators and climate and hydrologic variables in Turkey. *Hydrological Processes*, 23: 1927-1936.
- Karaca, M., Deniz, A. & Tayanç, M. (2000) Cyclone track variability over Turkey in association with regional climate. *International Journal of Climatology*, 20: 1225–1236.
- Karagiannidis, A., Karacostas, T., Maheras, P. & Makrogiannis, T. (2009) Trends and seasonality of extreme precipitation characteristics related to mid-latitude cyclones in Europe. *Advances in Geosciences*, 20: 39-43.
- Keles, S., Sivrikaya, F., Cakir, G., Baskent, E. Z. & Kose, S. (2008) Spatial and temporal changes in forest cover in Turkey's Artvin Forest, 1972-2002. *Polish Journal of Environmental Studies*, 17: 491-501.
- Kingston, D. G., Lawler, D. M. & McGregor, G. R. (2006a) Linkages between atmospheric circulation, climate and streamflow in the northern North Atlantic: research prospects. *Progress in Physical Geography*, 30(2): 143–174.
- Kingston, D. G., McGregor, G. R., Hannah, D. M. & Lawler, D. M. (2006b) River flow teleconnections across the northern North Atlantic region. *Geophysical Research Letters*, 33: 10.1029/2006GL026574.
- Kingston, D. G., McGregor, G. R., Hannah, D. M. & Lawler, D. M. (2007) Large-Scale Climatic Controls on New England River Flow. *Journal of Hydrometeorology*, 8: 367-379.
- Kingston, D. G., Hannah, D. M., Lawler, D. M. & McGregor, G. R. (2009) Climate-river flow relationships across montane and lowland environments in northern Europe. *Hydrological Processes*, 23: 985-996.
- Kioutsoukis, I., Melas, D. & Zerefos, C. (2010) Statistical assessment of changes in climate extremes over Greece (1955-2002). *International Journal of Climatology*, 30: 1723-1737.
- Klein-Tank, A. M. G. & Können, G. P. (2003) Trends in Indices of Daily Temperature and Precipitation Extremes in Europe, 1946-1999. *Journal of Climate*, 16: 3665-3680.
- Kletti, L. L. & Stefan, H. G. (1997) Correlations of climate and streamflow in three Minnesota streams. *Climatic Change*, 37: 575–600.
- Kömüşçü, A. Ü. (1998) An analysis of the fluctuations in the long-term annual mean air temperature data of Turkey. *International Journal of Climatology*, 18: 199-213.
- Kostopoulou, E. & Jones, P. D. (2007) Comprehensive analysis of the climate variability in the eastern Mediterranean. Part I: map-pattern classification. *International Journal of Climatology*, 27: 1189-1214.
- Krichak, S. O., Kishcha, P. & Alpert, P. (2002) Decadal trends of main Eurasian oscillations and the Eastern Mediterranean precipitation. *Theoretical and Applied Climatology*, 72: 209-220.
- Krichak, S. O. & Alpert, P. (2005) Decadal trends in the east Atlantic-west Russia pattern and Mediterranean precipitation. *International Journal of Climatology*, 25: 183-192.
- Kundzewicz, Z.W., Mata, L.J., Arnell, N.W., Döll, P., Kabat, P., Jiménez, B., Miller, K.A., Oki, T., Sen, Z. & Shiklomanov, I.A., (2007) Freshwater resources and their management. *Climate Change 2007: Impacts, Adaptation and Vulnerability. Contribution of Working Group II to the Fourth Assessment Report of the Intergovernmental Panel on Climate Change*, M.L. Parry, O.F. Canziani, J.P. Palutikof, P.J. van der Linden and C.E. Hanson, Eds., Cambridge University Press, Cambridge, UK, 173-210.

- Kutiel, H., Maheras, P. & Guika, S. (1996) Circulation and extreme rainfall conditions in the eastern Mediterranean during the last century. *International Journal of Climatology*, 16: 73-92.
- Kutiel, H., Hirsch-Eshkol, T. R. & Türkeş, M. (2001) Sea level pressure patterns associated with dry or wet monthly rainfall conditions in Turkey. *Theoretical and Applied Climatology*, 69: 39–67.
- Kutiel, H., Maheras, P., Turkes, M. & Paz, S. (2002) North Sea Caspian Pattern (NCP) - an upper level atmospheric teleconnection affecting the eastern Mediterranean - implications on the regional climate. *Theoretical and Applied Climatology*, 72: 173-192.
- Kutiel, H. & Türkeş, M. (2005) New evidence for the role of the North Sea – Caspian Pattern on the temperature and precipitation regimes in continental central Turkey. *Geographiska Annaler*, 87 A(4): 501–513.
- Laize, C. & Hannah, D. M. (2010) Modification of climate-river flow associations by basin properties. *Journal of Hydrology*, 389(1-2): 186-204.
- Luterbacher, J., Dietrich, D., Xoplaki, E., Grosjean, M. & Wanner, H. (2004) European seasonal and annual temperature variability, trends, and extremes since 1500. *Science*, 303: 1499-1503.
- Luterbacher, J., Liniger, M. A., Menzel, A., Estrella, N., Della-Marta, P. M., Pfister, C., Rutishauser, T. & Xoplaki, E. (2007) Exceptional European warmth of autumn 2006 and winter 2007: Historical context, the underlying dynamics, and its phenological impacts. *Geophysical Research Letters*, 34: 10.1029/2007gl029951.
- Mailier, P. J., Stephenson, D. B., Ferro, C. A. T. & Hodges, K. I. (2006) Serial Clustering of Extratropical Cyclones. *Monthly Weather Review*, 134(8): 2224-2240.
- Mather, J. R. (1978) *The climatic water balance in environmental analysis*. Lexington, Mass., D.C. Heath and Company, 239 p.
- Mather, J. R. (1979) Use of the climatic water budget to estimate streamflow, in Mather, J.R., ed., *Use of the climatic water budget in selected environmental water problems: Elmer, N.J., C.W. Thornthwaite Associates, Laboratory of Climatology, Publications in Climatology*, v. 32, no. 1, p. 1–52.
- Middelkoop, H., Daamen, K., Gellens, D., Grabs, W., Kwadijk, J. C. J., Lang, H., Parmet, W. A. H., Schadler, B., Schulla, J. & Wilke, K. (2001) Impact of climate change on hydrological regimes and water resources management in the Rhine Basin. *Climatic Change*, 49: 105–128.
- Moberg, A., Jones, P. D., Lister, D., Walther, A., Brunet, M., Jacobeit, J., Alexander, L. V., Della-Marta, P. M., Luterbacher, J., Yiou, P., Chen, D. L., Tank, A., Saladie, O., Sigro, J., Aguilar, E., Alexandersson, H., Almarza, C., Auer, I., Barriendos, M., Begert, M., Bergstrom, H., Bohm, R., Butler, C. J., Caesar, J., Drebs, A., Founda, D., Gerstengarbe F. W., Micela, G., Maugeri, M., Osterle, H., Pandzic, K., Petrakis, M., Srncic, L., Tolasz, R., Tuomenvirta, H., Werner, P. C., Linderholm, H., Philipp, A., Wanner, H. & Xoplaki, E. (2006) Indices for daily temperature and precipitation extremes in Europe analyzed for the period 1901-2000. *Journal of Geophysical Research-Atmospheres*, 111: 10.1029/2006dj007103.
- Mosley, M. P. (1981) Delimitation of New Zealand hydrologic regions. *Journal of Hydrology*, 49: 173-192.
- Mudelsee, M., Börngen, M., Tetzlaff, G. & Grünwald, U. (2003) No upward trend in the occurrence of extreme floods in central Europe. *Nature*, 425: 166–169.

- Murphy, S. J. & Washington, R. (2001) United Kingdom and Ireland precipitation variability and the North Atlantic sea-level pressure field. *International Journal of Climatology*, 21: 939-959.
- Nastos, P. T. & Zerefos, C.S. (2007) On extreme daily precipitation totals at Athens, Greece. *Advances in Geosciences*, 10: 59–66.
- Nesterov, E. S. (2009) East Atlantic oscillation of the atmospheric circulation. *Russian Meteorology and Hydrology*, 34: 794-800.
- Nilsson, C. & Malm Renöfält, B. (2008) Linking flow regime and water quality in rivers: a challenge to adaptive catchment management. *Ecology and Society*, 13(2): 18.
- Norrrant, C. & Douguédroit, A. (2006) Monthly and daily precipitation trends in the Mediterranean (1950–2000). *Theoretical and Applied Climatology*, 83: 89–106
- Odemis, B. & Evrendilek F. (2007) Monitoring water quality and quantity of national watersheds in Turkey. *Environmental Monitoring and Assessment*, 133: 215-229.
- Oguntunde, P. G., Friesen, J., van de Giesen, N. & Sevenije, H. H. G. (2006) Hydroclimatology of the Volta River Basin in West Africa: Trends and variability from 1901 to 2002. *Physics and Chemistry of the Earth* 31: 1180–1188.
- Oikonomou, C., Flocas, H. A., Hatzaki, M., Asimakopoulos, D. N. & Giannakopoulos C. (2008) Future changes in the occurrence of extreme precipitation events in Eastern Mediterranean. *Global Nest Journal*, 10: 255-262.
- Osborn, T. J., Hulme, M., Jones, P. D. & Basnett, T. A. (2000) Observed trends in the daily intensity of United Kingdom precipitation. *International Journal of Climatology* 20: 347-364.
- Paeth, H., Hense, A., Glowienka-Hense, R., Voss, R. & Cubasch, U. (1999) The North Atlantic Oscillation as an indicator for greenhouse-gas induced regional climate change. *Climate Dynamics*, 15: 953-960.
- Panagiotopoulos, F., Shahgedanova, M., Hannachi, A. & Stephenson, D. B. (2005). Observed trends and teleconnections of the Siberian High: A recently declining center of action. *Journal of Climate* 18: 1411–1422.
- Partal, T. & Kahya, E. (2006) Trend analysis in Turkish precipitation data. *Hydrological Processes*, 20: 2011–2026.
- Peterson, T. C., Folland, C., Gruza, G., Hogg, W., Mokssit, A. & Plummer, N. (2001) Report on the activities of the Working Group on Climate Change Detection and Related Rapporteurs 1998–2001. World Meteorological Organisation Rep. WCDMP-47, WMO-TD 1071, Geneva, Switzerland, 143 pp.
- Poff, N. L., Allen, J. D., Bain, M.B., Karr, J. R., Prestegard, K. L., Richter, B. D., Sparks, R.E. & Stromberg, J. C. (1997) The natural flow regime: a paradigm for river conservation and restoration. *BioScience*, 47: 769-784.
- Pujol, N., Neppel, L. & Sabatier, R. (2007) Regional tests for trend detection in maximum precipitation series in the French Mediterranean region. *Hydrological Sciences Journal*, 52 (5): 956 – 973.
- Ramos, M. C. & Martínez-Casasnovas, J. A. (2006) Trends in precipitation concentration and extremes in the Mediterranean Penedès-Anoia Region, Ne Spain. *Climatic Change*, 74: 457–474.
- Rango, A. & Vankatwijk, V. F. (1990) Climate change effects on the snowmelt hydrology of Western North-American mountain basins. *IEEE Transactions on Geoscience and Remote Sensing*, 28: 970-974.
- Raghunath, H. M. (2006) *Hydrology: principles, analysis, design*. New Age International (P) Ltd., Publishers, New Delhi.

- Regonda, S.K., Rajagopalan, B., Clark, M. & Pitlick, J. (2005) Seasonal cycle shifts in hydroclimatology over the Western United States. *Journal of Climate*, 18: 372-384.
- Reis, S. (2008) Analyzing Land Use/Land Cover Changes Using Remote Sensing and GIS in Rize, North-East Turkey. *Sensors*, 8: 6188-6202.
- Robson, A. J., Jones, T. K., Reed, D. W. & Bayliss, A. C. (1998) A study of national trend and variation in UK Floods. *International Journal of Climatology*, 18: 165-182.
- Rodriguez-Puebla, C., Encinas, A. H., Nieto, S. & Garmendia, J. (1998) Spatial and temporal patterns of annual precipitation variability over the Iberian Peninsula. *International Journal of Climatology*, 18: 299-316.
- Rogers, J. C. (1997) North Atlantic Storm Track Variability and Its Association to the North Atlantic Oscillation and Climate Variability of Northern Europe. *Journal of Climate*, 7(10): 1635-1647.
- Rogerson, P. A. (2001) *Statistical Methods for Geography*. Sage Publications, London.
- Rosenzweig, C., Iglesias, A., Yang, X.B., Epstein, P.R. & Chivian, E. (2001) Climate Change and Extreme Weather Events; Implications for Food Production, Plant Diseases, and Pests. *Global Change & Human Health*, 2(2) :90-104.
- Sahin, S. & Cigizoglu, H. K. (2010) Homogeneity analysis of Turkish meteorological data set. *Hydrological Processes*, 24: 981-992.
- Sancar, C., Turan, S. O. & Kadiogullari, A. L. (2009) Land use-cover change processes in Urban fringe areas: Trabzon case study, Turkey. *Scientific Research and Essays*, 4: 1454-1462.
- Sariş, F. (2006) Spatial and temporal variation of precipitation intensity over Turkey. MSc Thesis, Çanakkale Onsekiz Mart University, Turkey.
- Sariş, F., Hannah, D. M. & Eastwood, W. J. (2010) Spatial variability of precipitation regimes over Turkey. *Hydrological Sciences Journal*, 55: 234-249.
- Sen, Z. & Habib, Z. (2000) Spatial analysis of monthly precipitation in Turkey. *Theoretical and Applied Climatology*, 67: 81-96.
- Sensoy, S., Demircan, M. & Alan, I. (2008) Trends in Turkey Climate Extreme Indices from 1971 to 2004. In *Third International Conference BALWOIS 2008*, Ohrid, Republic of Macedonia, 27 -31 May.
- Sivrikaya, F., Cakir, G., Kadiogullari, A. I., Keles, S., Baskent, E. Z. & Terzioglu S. (2007) Evaluating land use/land cover changes and fragmentation in the camili forest planning unit of northeastern Turkey from 1972 to 2005. *Land Degradation & Development*, 18: 383-396.
- Sneyers, R. (1990) On the Statistical Analysis of Series of Observations. World Meteorological Organization (WMO), Technical Note No. 143, Geneva, 192 pp.
- Spanos, S., Maheras, P., Karacostas, T. & Pennas, P. (2003) Objective climatology of 500-hPa cyclones in central and east Mediterranean region during warm-dry period of the year. *Theoretical and Applied Climatology*, 75: 167-178.
- Stahl, K. & Demuth, S. (1999) Method for Regional Classification of Streamflow Drought Series: Cluster Analysis. *ARI DE Technical Report no. 1*. Institute of Hydrology, University of Freiburg, Germany.
- Stone, R.C. (1989) Weather types at Brisbane, Queensland: an example of the use of principal components and cluster analysis. *International Journal of Climatology*, 9: 3-32.
- Sümer, V. (2011) EU's water framework directive implementation in Turkey: the draft national implementation plan. In *ORSAM Water Research Programme Report no. 1*, Ankara, Turkey.

- Svensson, C., Kundzewicz, Z. W., Maurer, T. (2005) Trend detection in river flow series: 2. Flood and low-flow index series. *Hydrological Sciences Journal*, 50(5): 811-824.
- Tank, A. & Konnen, G. P. (2003) Trends in indices of daily temperature and precipitation extremes in Europe, 1946-99. *Journal of Climate*, 16: 3665-3680.
- Tatli, H., Dalfes, N. H. & Menteş, S. (2004) A statistical downscaling method for monthly total precipitation over Turkey. *International Journal of Climatology*, 24: 161–180.
- Tatli, H., Dalfes, N. H. & Mentes, S. (2005) Surface air temperature variability over Turkey and its connection to large-scale upper air circulation via multivariate techniques. *International Journal of Climatology*, 25: 331-350.
- Tatli, H. (2007) Synchronization between the North Sea-Caspian pattern (NCP) and surface air temperatures in NCEP. *International Journal of Climatology*, 27: 1171-1187.
- Tayanç, M., Karaca, M. & Yenigün, O. (1997) Annual and seasonal air temperature trend patterns of climate change and urbanization effects in relation to air pollutants in Turkey. *Journal of Geophysical Research*, 102(D2): 1909-1920.
- Tayanç, M., Dalfes, N. H., Karaca, M. & Yenigun, O. (1998) A comparative assessment of different methods for detecting inhomogeneities in Turkish temperature data set. *International Journal of Climatology*, 18: 561-578.
- Tecer, H.L. & Cerit, O. (2009) Temperature Trends and Changes in Rize, Turkey, for the Period 1975 to 2007. *Clean*, 37 (2):150-159.
- Thornthwaite, C. W. (1948) An Approach toward a Rational Classification of Climate. *Geographical Review*, 38 (1): 55-94.
- Topaloğlu, F. (2006a) Regional trend detection of Turkish river flows. *Nordic Hydrology*, 37, 165-182.
- Topaloğlu, F. (2006b) Trend detection of streamflow variables in Turkey. *Fresenius Environmental Bulletin*, 15: 644-653.
- TGM. (1984) Çoruh Havzası Toprakları (*Soils of the Çoruh Basin*). Toprak Su Genel Müdürlüğü Yayınları, 756, Ankara (In Turkish).
- Toreti, A., Xoplaki, E., Maraun, D., Kuglitsch, F. G., Wanner, H. & Luterbacher, J. (2010) Characterisation of extreme winter precipitation in Mediterranean coastal sites and associated anomalous atmospheric circulation patterns. *Natural Hazards and Earth System Sciences*, 10: 1037-1050.
- Trigo, I. F., Davies, T. D. & Bigg, G. R. (1999) Objective climatology of cyclones in the Mediterranean region. *Journal of Climate*, 12: 1685–1696.
- Trigo, R., Zezere, J. L., Rodrigues, M. L. & Trigo, I. F. (2005) The influence of the North Atlantic Oscillation on rainfall triggering of landslides near Lisbon. *Natural Hazards*, 36(3): 331-354.
- Tümertekin, E. & Cöntürk, H. (1958) Türkiye’de günlük maksimum yağışlar (*Daily maximum precipitations in Turkey*). *Coğrafya Enstitüsü Dergisi*, 9: 115-121 (In Turkish).
- Türkeş, M., Sumer, U. M. & Kilic, G. (1995) Variations and trends in annual mean air temperatures in Turkey with respect to climatic variability. *International Journal of Climatology*, 15: 557-569.
- Türkeş, M., Sumer, U. M. & Kilic, G. (1996) Observed changes in maximum and minimum temperatures in Turkey. *International Journal of Climatology*, 16: 463-477.
- Türkeş, M. (1996) Spatial and temporal analysis of annual rainfall variations in Turkey. *International Journal of Climatology*, 16: 1057-1076.
- Türkeş, M. (1998) Influence of geopotential heights, cyclone frequency and southern oscillation on rainfall variations in Turkey. *International Journal of Climatology*, 18: 649-680.

- Türkeş, M. (1999) Vulnerability of Turkey to desertification with respect to precipitation and aridity conditions. *Turkish Journal of Engineering & Environmental. Sciences*, 23: 363–380.
- Türkeş, M., Sumer, U. M. & Demir, I. (2002a) Re-evaluation of trends and changes in mean, maximum and minimum temperatures of Turkey for the period 1929-1999. *International Journal of Climatology*, 22, 947-977.
- Türkeş M., Sumer U. M. & Kilic, G. (2002b) Persistence and periodicity in the precipitation series of Turkey and associations with 500 hPa geopotential heights. *Climate Research*, 21: 59-81.
- Türkeş, M. & Erlat, E. (2003) Precipitation changes and variability in turkey linked to the North Atlantic oscillation during the period 1930-2000. *International Journal of Climatology*, 23: 1771-1796.
- Türkeş, M. (2003b) Küresel iklim degisikligi ve gelecekteki iklimimiz (*Global Climate Change and the Future Climate*) 23 Mart Dünya Meteoroloji Günü Kutlaması Gelecekteki İklimimiz Paneli (23 Mart 2003), Bildiriler Kitabı: 12-37. T.C. Çevre ve Orman Bakanlığı DMI Genel Müdürlüğü, Ankara (In Turkish).
- Türkeş M. & Sumer, U. M. (2004) Spatial and temporal patterns of trends and variability in diurnal temperature ranges of Turkey. *Theoretical and Applied Climatology*, 77: 195–227.
- Türkeş, M. & Erlat, E. (2005a) Climatological responses of winter precipitation in Turkey to variability of the North Atlantic Oscillation during the period 1930-2001. *Theoretical and Applied Climatology*, 81: 45-69.
- Türkeş, M. & Erlat, E. (2005b) Signatures of the NAO in the atmospheric circulation during wet winter months over the Mediterranean region. *Theoretical and Applied Climatology*, 82: 27-39.
- Türkeş, M. & Erlat, E. (2006) Influences of the North Atlantic oscillation on precipitation variability and changes in Turkey. *Nuovo Cimento Della Societa Italiana Di Fisica C-Geophysics and Space Physics*, 29: 117-135.
- Türkeş, M. & Erlat, E. (2008) Influence of the Arctic Oscillation on the variability of winter mean temperatures in Turkey. *Theoretical and Applied Climatology*, 92: 75-85.
- Türkeş, M. & Erlat, E. (2009) Winter mean temperature variability in Turkey associated with the North Atlantic Oscillation. *Meteorology and Atmospheric Physics*, 105: 211-225.
- Türkeş, M., Koç, T. & Sariş, F. (2009) Spatiotemporal variability of precipitation total series over Turkey. *International Journal of Climatology*, 29: 1056-1074.
- Türkeş, M. (2010) Küresel İklim Değişikliği: Başlıca Nedenleri, Gözlenen ve Öngörülen Değişiklikler ve Etkileri (*Global Climate Change: Principal Causes, Observed and Predicted Changes and Their Impacts*). Çağrılı Bildiri (*Invited Paper*), Uluslararası Katılımlı 1. Meteoroloji Sempozyumu Bildiri Kitabı, 27-28 Mayıs 2010, Devlet Meteoroloji İşleri Genel Müdürlüğü, 9-38, Ankara (In Turkish).
- Türkeş, M. & Akgündüz, S. (2011) Assessment of the desertification vulnerability of the Cappadocian district (Central Anatolia, Turkey) based on aridity and climate-process system. *International Journal of Human Sciences*, 8(1): 1234-1268.
- Ulbrich, U. & Christoph, M. (1999) A shift of the NAO and increasing storm track activity over Europe due to anthropogenic greenhouse gas forcing. *Climate Dynamics*, 15: 551-559.
- Uzlu, E., Filiz, M. H., Komurcu, M., Akpınar, A. & Yavuz, O. (2008) Doğu Karadeniz Havzası'ndaki küçük hidroelektrik santrallerin durumu (*The situation of small*

- hydroelectric power plants in East Black Sea Basin*). VII. Ulusal Temiz Enerji Sempozyumu (17-19 Aralık 2008) Bildiriler Kitabı: 459, Istanbul, (In Turkish).
- Ünal Y., Kindap, T. & Karaca, M. (2003) Redefining the climate zones of Turkey using cluster analysis. *International Journal of Climatology*, 23: 1045-1055.
- von Storch, H. & Navarra, A. (eds) (1995) *Analysis of Climate Variability*. Springer-Verlag, New York, USA.
- Wanner, H., Bronnimann, S., Casty, C., Gyalistras, D., Luterbacher, J., Schmutz, C., Stephenson, D. B. & Xoplaki, E. (2001) North Atlantic Oscillation - Concepts and studies. *Surveys in Geophysics*, 22: 321-382.
- Whitfield, P. H. (2001) Linked hydrologic and climate variations in British Columbia and Yukon. *Monitoring and Assessment*, 67: 217-238.
- Willmott, C. J. (1977) WATBUG: A Fortran IV Algorithm for Calculating the Climatic Water Budget. Water Resources Center, Delaware University, Contribution No. 23, Report No. 1, and Publications in Climatology, No. 2.
- Willmott, C. J., Rowe, C. M. & Mintz Y. (1985) Climatology of the terrestrial seasonal water cycle. *International Journal of Climatology*, 5 (6): 589-606.
- Wilson, D., Hisdal, H. & Lawrence, D. (2010) Has streamflow changed in the Nordic countries? - Recent trends and comparisons to hydrological projections. *Journal of Hydrology*, 394(3-4): 334-346.
- WMO. (1966) *Climatic Change*. World Meteorological Organization (WMO), Technical Note No. 79, Geneva, 79 pp.
- World Water Assessment Programme, (2009) *The United Nations World Water Development Report 3: Water in a Changing World*. Paris: UNESCO, and London: Earthscan.
- Xoplaki, E. (2002) *Climate variability over the Mediterranean*. PhD Thesis, University of Bern, Switzerland.
- Xoplaki, E., Gonzalez-Rouco, J. F., Luterbacher, J. & Wanner, H. (2004) Wet season Mediterranean precipitation variability: influence of large-scale dynamics and trends. *Climate Dynamics*, 23: 63-78.
- Xoplaki, E., Luterbacher, J., Paeth, H., Dietrich, D., Steiner, N., Grosjean, M. & Wanner, H. (2005) European spring and autumn temperature variability and change of extremes over the last half millennium. *Geophysical Research Letters*, 32(15): 10.1029/2005gl023424.
- Xoplaki, E., Luterbacher, J. & Gonzalez-Rouco, J. F. (2006) Mediterranean summer temperature and winter precipitation, large-scale dynamics, trends. *Nuovo Cimento Della Societa Italiana Di Fisica C-Geophysics and Space Physics*, 29: 45-54.
- Yang D., Ye, B. & Kane, D. L. (2004) Streamflow changes over Siberian Yenisei River Basin. *Journal of Hydrology*, 296: 59-80.
- Yarnal, B. (1992) *Synoptic Climatology in Environmental Analysis: A Primer*. Belhaven Press: London.
- Yue, S. & Wang, C. Y. (2002) Regional streamflow trend detection with consideration of both temporal and spatial correlation. *International Journal of Climatology*, 22: 51-63.
- Yue, S., Pilon, P., Phinney, B. & Cavadias, G. (2002) The influence of autocorrelation on the ability to detect trend in hydrological series. *Hydrological Processes*, 16: 1807-1829.
- Yue, S., Pilon, P. & Phinney, B. (2003) Canadian streamflow trend detection: impacts of serial and cross-correlation. *Hydrological Sciences Journal*, 48(1): 51-63.
- Yue, S. & Pilon, P. (2004) A comparison of the power of the t test, Mann-Kendall and bootstrap tests for trend detection. *Hydrological Sciences Journal*, 49: 21-37.

- Zaidman, M. D., Rees, H. G. & Young, A. R. (2001) Spatio-temporal development of streamflow droughts in northwest Europe. *Hydrology and Earth System Sciences*, 5(4): 733-751.
- Zhang, Q., Liu, C., Xu, C., Xu, Y. & Jiang, T. (2006) Observed trends of annual maximum water level and streamflow during past 130 years in the Yangtze River basin, China. *Journal of Hydrology*, 324: 255–265.
- Zhang, X. B., Aguilar, E., Sensoy, S., Melkonyan, H., Tagiyeva, U., Ahmed, N., Kotaladze, N., Rahimzadeh, F., Taghipour, A., Hantosh, T. H., Albert, P., Semawi, M., Ali, M. K., Al-Shabibi, M. H. S., Al-Oulan, Z., Zadari, T., Khelet, I. A., Hamoud, S., Sagir, R., Demircan, M., Eken, M., Adiguzel, M., Alexander, L., Peterson, T. C. & Wallis T. (2005) Trends in Middle East climate extreme indices from 1950 to 2003. *Journal of Geophysical Research-Atmospheres*, 110: 10.1029/2005jd006181.
- Zveryaev, I. (2009) Interdecadal changes in the links between European precipitation and atmospheric circulation during boreal spring and fall. *Tellus Series a-Dynamic Meteorology and Oceanography*, 61: 50-56.